

PROJECT ADMINISTRATION DATA SHEET

☒ ORIGINAL ☐ REVISION NO. _____

Project No. E-23-658

DATE 9/9/81

Project Director: Dr. George J. Simitzes School/Lab XXXX ESM

Sponsor: Air Force Office of Scientific Research (AFOSR)

Type Agreement: Grant No. AFOSR-81-0227

Award Period: From 6/30/81 To 6/29/82 (Performance) 8/29/82 (Reports)

Sponsor Amount: \$60,176 Contracted through: _____

Cost Sharing: \$5,492 (E-23-346) GTRI/ST

Title: Analysis of the Nonlinear Large Deformation Behavior of Composite Cylindrical Shells

ADMINISTRATIVE DATA

OCA Contact Faith G. Costello

1) Sponsor Technical Contact:

Dr. Anthony K. Amos
Program Manager
Department of the Air Force
AFOSR/NA
Bolling AFB, DC 20332

2) Sponsor Admin/Contractual Matters:

Jeffrey P. Parsons, 1Lt., USAF
Contracting Officer
AFOSR/PKD
Bldg. 410
Bolling AFB, D.C. 20332

PH; 202-767-4878

Defense Priority Rating: N/A

Security Classification: N/A

RESTRICTIONS

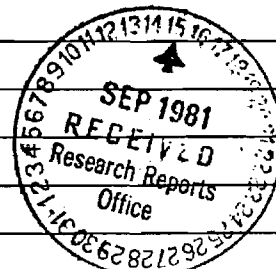
See Attached AFOSR Supplemental Information Sheet for Additional Requirements.

Travel: Foreign travel must have prior approval - Contact OCA in each case. Domestic travel requires sponsor approval where total will exceed greater of \$500 or 125% of approved proposal budget category.

Equipment: Title vests with GIT; items costing \$1,000 or more must have prior approval.

AFOSR retains the right to direct transfer of title to the Gov't within 120 days of completion of grant (reference Article II of Supplement).

COMMENTS:



COPIES TO:

Administrative Coordinator
Research Property Management
Accounting
Procurement/EES Supply Services
FORM OCA 4-781

Research Security Services
Reports Coordinator (OCA)
Legal Services (OCA)
Library

EES Public Relations (2)
Computer Input
Project File
Other _____

SPONSORED PROJECT TERMINATION SHEETDate 8/17/83

Project Title: Analysis of the Nonlinear Large Deformation Behavior of Composite Cylindrical Shells

Project No: E-23-658

Project Director: Dr. George J. Simitses

Sponsor: Air Force Office of Scientific Research

Effective Termination Date: 6/29/83Clearance of Accounting Charges: 8/29/83

Grant/Contract Closeout Actions Remaining:

- ☐ Final Invoice and Closing Documents
- ☒ Final Fiscal Report
- ☒ Final Report of Inventions
- ☐ Govt. Property Inventory & Related Certificate
- ☐ Classified Material Certificate
- ☐ Other _____

Assigned to: ESM (~~School~~/Laboratory)COPIES TO:

Administrative Coordinator
Research Property Management
Accounting
Procurement/EES Supply Services

Research Security Services
~~Reports Coordinator (OCA)~~
Legal Services (OCA)
Library

EES Public Relations (2)
Computer Input
Project File
Other Simitses



PREPRINT 82-509

\$2.00

ASCE CONVENTION AND EXHIBIT

RESPONSE OF SUDDENLY- LOADED STRUCTURAL CONFIGURATIONS

Jorge Simitzes

CE

New Orleans, LA

October 25-29, 1982



This preprint has been provided for the purpose of convenient distribution of information at the convention. To defray, in part, the cost of printing, a convention price of \$2.00 to all registrants has been established. The post-convention price, when ordered from ASCE headquarters will be \$2.00 while the supply lasts. For bulk orders (of not less than 200 copies of one preprint) please write for prices.

No acceptance or endorsement by the American Society of Civil Engineers is implied; the Society is not responsible for any statement made or opinion expressed in its publications.

Reprints may be made on condition that the full title, name of author, and date of preprinting by the Society are given.

Cover photo: Superdome Stadium, New Orleans, LA.

RESPONSE OF SUDDENLY-LOADED STRUCTURAL CONFIGURATIONS

by

G. J. Simitses

Introduction

Dynamic stability or instability of elastic structures has drawn considerable attention in the past thirty years. The beginning of the subject can be traced to the investigation of Koning and Taub [24], who considered the response of an imperfect (half-sine wave), simply supported column subjected to a sudden axial load of specified duration. Since then, several studies have been conducted by various investigators on structural systems, which are either suddenly loaded or subjected to time-dependent loads (periodic or non-periodic) and several attempts have been made to find common response features and to define critical conditions for these systems.

As a result of this, the term "Dynamic Stability" encompasses many classes of problems, many different physical phenomena and in some instances the term is used for two distinctly different responses for the same configuration subjected to the same dynamic loads. Therefore, it is not surprising that there exist several uses and interpretations of the term.

In general, problems which deal with stability of motion have concerned researchers for many years in many fields of engineering. Definitions for stability and for the related criteria and estimates of critical conditions, as developed through the years, are given by J. J. Stoker [50]. In particular, the contributions of Thomson and Tait [53] and Routh [37] deserve particular attention. Some of these criteria find wide uses in problems of control theory [30], stability and control of aircraft [40], and other areas [9]. The emphasis, in this paper, is placed on structural configurations, which are subjected to sudden loads. As already mentioned, even for just structural systems the diversity is extremely large.

The class of problems falling in the category of parametric excitation, or parametric resonance are the best defined, conceived and understood problems of dynamic stability. An excellent treatment and bibliography can be found in the book of V. V. Bolotin [4]. Another reference on the subject is J. J. Stoker's book [49]. For more recent works on the subject see [10, 26, 38, 5, 22, 28, 32].

The problem of parametric excitation is best defined in terms of an example. Consider an Euler column, which is loaded at one end by a periodic axial force. The other end is immovable. It can be shown that, for certain relationships between the exciting frequency and the column natural frequency of transverse vibration, transverse vibrations occur with rapidly increasing amplitudes. This is called parametric resonance and the system is said to be dynamically unstable. Moreover, the loading is called parametric loading, and the phenomenon parametric excitation.

Other examples of parametric excitation include (a) a parametrically loaded thin flat plate by in-plane forces, which may cause transverse plate vibrations, (b) parametrically loaded shallow arches (symmetric loading) which under certain conditions vibrate asymmetrically with increasing amplitude, and (c) long cylindrical, thin shells (or thin rings) under uniform but periodically applied pressure, which can excite vibrations in an asymmetric mode. Thus it is seen that, in

parametric excitation, the loading is parametric with respect to certain deflection forms. This makes parametric resonance different from the usual forced vibration resonance. In addition, from these few examples of parametric excitation one realizes that systems that exhibit bifurcational buckling under static conditions (regardless of whether the bifurcating static equilibrium branch is stable or unstable) are subject to parametric excitation.

Moreover, there exists a large class of problems, for which the load is applied statically but the system is nonconservative. An elastic system is conservative when subjected to conservative loads [45]; the reader is also referred to Ziegler's book [57] for a classification of loads and reactions. An excellent review of the subject of stability of elastic systems under nonconservative forces is given by Herrmann [13]. He classifies all problems of nonconservative systems into three groups. The first group deals with follower-force problems, the second with problems of rotating shafts (whirling), and the third with aeroelasticity (fluid interaction; flutter). All of these groups, justifiably or not, are called problems of dynamic stability. In the opinion of the author, justification is needed for the first group. Ziegler [56] has shown that critical conditions for this class of nonconservative systems can only be obtained through the use of the dynamic kinetic approach to static stability problems. The question of applicability of the particular approach was clearly presented by Herrmann and Bungay [14] through a two-degree-of-freedom model. They showed that in some nonconservative systems there exist two instability mechanisms, one of divergence (large deflection may occur) and one of flutter (oscillations of increasing amplitude). They further showed that the critical load for which "flutter" type of instability occurs can only be determined through the kinetic approach, while the "divergence" type of critical load can be determined by employing any one of the three approaches (classical potential energy or kinetic [45]). It is understandable then why many authors refer to the problem of follower-forced systems as dynamic stability problems. Some of the more recent works are those of [34, 12, 31, 51, 25, 27]. Furthermore, flow-induced vibrations in elastic pipes is another fluid-solid interaction problem that also falls under the general heading of dynamic stability. The establishment of stability concepts, as well as of estimates for critical conditions is an area of great practical importance. A few references [35, 3, 2] are provided for the interested reader. In addition, a few studies have been reported that deal with the phenomenon of parametric resonance in a fluid-structure interaction problem [3]. For completeness one should refer to a few studies of aeroelastic flutter [54].

Finally, a large class of structural problems, that has received attention recently and does qualify as a category of dynamic stability, is that of impulsively loaded configurations and configurations which are suddenly loaded with loads of constant magnitude and infinite duration. These configurations under static loading, are subject to either limit-point instability or bifurcational instability with unstable post-buckling branch (violent buckling). The two types of loads may be thought of as mathematical idealizations of blast loads of (a) large decay times and (b) small decay rates and large decay times respectively. For these loads, the concept of dynamic stability is related with the observation that for sufficiently small values of the loading, the system simply oscillates about the near static equilibrium point and the corresponding amplitudes of oscillation are sufficiently small. If the loading is increased, some systems will experience large amplitude oscillations or, in general, divergent type of motion. For this phenomenon to happen, the configuration (turns out) must possess two or more static equilibrium positions and escaping motion occurs by having trajectories that can pass through an unstable static equilibrium point. Consequently, the methodologies developed by the various investigators are for structural configurations that exhibit snap-through buckling when loaded quasistatically.

Solutions to such problems started appearing in the open literature in the 1950's. Hoff and Bruce [16] considered the dynamic stability of a pinned half-sine arch under a half-sine distributed load. Budiansky and Roth [8] in studying the axisymmetric behavior of a shallow spherical cap under suddenly applied loads

led the load to be critical when the transient response increases suddenly with little increase in the magnitude of the load. This concept was adopted by many investigators [46, 52, 7] in the subsequent years because it is tractable to other solutions. Finally, the concept was generalized in a subsequent paper by Hsu [6] in attempting to predict critical conditions for imperfection-sensitive structures under time-dependent loads.

Conceptually, one of the best efforts in the area of dynamic buckling, under only applied loads, is the work of Hsu and his collaborators [18-21]. In his studies, he defined sufficiency conditions for stability and sufficiency conditions for instability, thus finding upper and lower bounds for the critical impulse or critical sudden load. Independently, Simitses [43] in dealing with the dynamic buckling of shallow arches and spherical caps termed the lower bound as a minimum impermissible critical load (MPCL) and the upper bound as a minimum guaranteed critical load (MGCL). Finally, there exist a few reported investigations for the case of suddenly loaded systems with constant loads and finite duration [58, 44]. Note that this entire class of problems falls in the category of dynamic analysis of conservative systems.

The totality of concepts and methodologies used by the various investigators estimating critical conditions for suddenly loaded elastic systems (of the last category) can be classified in the following three groups:

(a) The Equations of Motion Approach (Budiansky-Roth [13]). The equations of motion are (numerically) solved for various values of the load parameter (ideal impulse, or sudden load), thus obtaining the system response. The load parameter, at which there exists a large (finite) change in the response, is called critical.

(b) The Total Energy - Phase Plane Approach (Hoff-Hsu [16, 18-21]). Critical conditions are related to characteristics of the system phase-plane, and the emphasis is on establishing sufficient conditions for stability (lower bounds) and sufficient conditions for instability (upper bounds).

(c) Total Potential Energy Approach (Hoff-Simitses [16, 43, 44, 48]). Critical conditions are related to characteristics of the system total potential. Through this approach also, lower and upper bounds of critical conditions are established. The last approach is applicable to conservative systems only. The concepts and procedure related to the last approach are next explained, with some detail.

Total Potential Energy Approach; Concepts and Procedure.

The concept of dynamic stability is best explained through a single-degree-of-freedom system. First the case of ideal impulse is treated and then the case of constant load of infinite duration.

(a) Ideal Impulse

Consider a single-degree-of-freedom system for which the total potential (under no load) curve is plotted versus the generalized coordinate (independent variable) (see Fig. 1). Clearly, points A, B, C denote static equilibrium points and point D denotes the initial position ($\theta = 0$) of the system.

Since the system is conservative, the sum of the total potential, \bar{U}_T^0 (under no load) and the kinetic energy, T^0 is a constant, C, or

$$\bar{U}_T^0 + T^0 = C \quad (1)$$

Moreover (see Fig. 1), since \bar{U}_T^0 is zero at the initial position ($\theta = 0$), the constant C, can be related to some initial kinetic energy, T_1^0 . Then

$$\bar{U}_T^0 + T^0 = T_1^0 \quad (2)$$

Next, consider an ideal impulse applied to the system. Through the impulse-momentum theorem, the impulse is related to the initial kinetic energy T_1^0 . Clearly, if T_1^0

is equal to D (see Fig. 1), or \bar{U}_T^0 (θ_{II}), the system will simply oscillate between θ_{II} and θ_{II} . On the other hand, if the initial kinetic energy, T_1^0 , is equal to

the value of the total potential at the unstable static equilibrium point C, then the system can reach point C with zero velocity ($T^0 = 0$), and there exists possibility of motion escaping (passing position C) or becoming unbounded. This motion is termed "buckled motion" in [43]. In the case for which motion is limited and the path may include the initial point (B), the motion is termed "unbuckled motion" in [43]. Through this, both a concept of dynamic stability is presented and the necessary steps for estimating critical impulses are suggested. Note that the unstable static equilibrium positions (pts. A and C) are established, the critical initial kinetic energy is estimated by

$$T_{I\text{cr}}^0 = \bar{U}_T^0(C) \quad (3)$$

Moreover, since $T_{I\text{cr}}^0$ is related to the ideal impulse, then the critical impulse is estimated through Eq. (3). Observe that an instability of this type can occur only when the system, under zero load, possesses unstable static equilibrium. Furthermore, if position C corresponds to a very large and thus unacceptable θ (from physical considerations), one may still use this concept and estimate the maximum allowable (and therefore critical) ideal impulse. For instance, if one restricts motion to the region between θ_I and θ_{II} , then the maximum allowable ideal impulse is obtained from Eq. (3), but with D or $\bar{U}_T^0(\theta_{II})$ replacing $\bar{U}_T^0(C)$. Because of a critical or an allowable ideal impulse can be obtained for all systems (including those that are not subject to buckling under static conditions such as beams, etc.).

For multi-degree-of-freedom systems, it is possible to use the same concept of dynamic stability and procedure for estimating critical conditions, but with a modification. For these systems, critical conditions can be bracketed between lower and upper bounds (see [16, 46, 19, 43, 48]). One final comment for the case of an ideal impulse: Note from Fig. 1, in the absence of damping (as assumed), the direction of the ideal impulse is immaterial. If the system is loaded in one direction such that the resulting motion corresponds to positive θ then a critical condition occurs when the system reaches position C with zero kinetic energy. If the system is loaded in the opposite direction, then some negative θ position will be reached with zero kinetic energy, after that the direction of the motion will reverse, and finally the system will reach position C with zero kinetic energy. Both of these phenomena occur for the same value of the ideal impulse.

(b) Constant Load of Infinite Duration

Consider again a single-degree-of-freedom system. Total potential curves are plotted versus the generalized coordinate θ on Fig. 2. Note that the various curves correspond to different load values, P_i . The index i varies from one to five as the magnitude of the load increases with increasing index value. These curves are typical of systems that, for each load value, contain at least two static equilibrium points, A_i and B_i . This is the case, when the system is subject to limit point instability and/or bifurcational buckling with unstable branching, under the application of the load (shallow arches and spherical caps, perfect or imperfect cylindrical and spherical shells, two-bar frames, etc.).

Given such a system, one applies a given load suddenly with constant magnitude and infinite duration. For a conservative system,

$$\bar{U}_T^P + T^P = C \quad (4)$$

The potential may be defined in such a way that it is zero at the initial position ($\theta = 0$). In such case, the constant is zero, or

$$\bar{U}_T^P + T^P = 0 \quad (5)$$

Since the kinetic energy is a positive definite function of the generalized velocity, then motion is possible when the total potential is non-positive (shaded area, on Fig. 2, for P_2). From this it is clear that for small values of the applied load, the system simply oscillates about the near (point A_2) static equilibrium

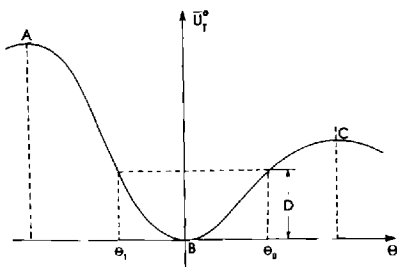


Fig. 1 Total Potential Curve (zero load)

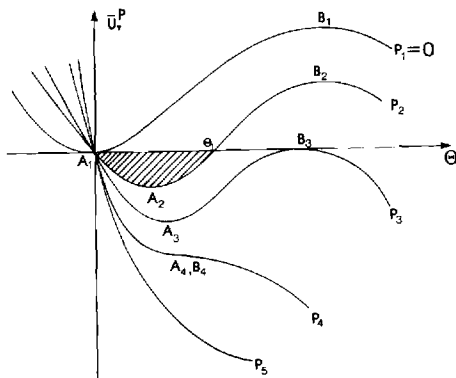


Fig. 2 Total Potential Curves

ems the upper and lower bounds are one and note true critical conditions.

Finally, this concept of dynamic stability has been extended to the case of suddenly loaded systems with constant load and finite duration [43] and to actual structures [42, 47, 48] rather than finite-degree-of-freedom models. The effect of static preloading on the critical dynamic conditions has been investigated [44], by this concept.

Extension of the Dynamic Stability Concept

The concept of dynamic stability, discussed in the previous article, is developed primarily for structural configurations, which are subject to violent buckling under static loading. It is also observed that, the concept can be extended, even for these systems, when one limits the maximum allowable deflection resulting from the sudden loads. This being the case then, the extended and modified concept can be used for all structural configurations (at least in theory).

This is demonstrated in this section through a simple model. First, though, some clarifying remarks are in order.

All structural configurations, when acted upon by quasi-static loads, respond in a manner described in one of the four figures, Figs. 3-6. These figures characterize equilibrium positions (structural response) as plots of a load parameter, P ,

position. This is also an observed physical phenomenon. As the load increases, the total potential at the unstable point, B_1 , decreases, it becomes zero (point B_3), and then it increases negatively until points A_1 and B_1 (A_4 , B_4) coincide (the corresponding load, P_4 , denotes the limit point under static loading). For loads higher than this (P_4), the stationary points (static equilibrium positions) disappear from the neighborhood. When the sudden load reaches the value corresponding to P_3 , a critical condition exists, because the system can reach position B_3 with zero kinetic energy and then move towards larger θ -values ("buckled motion" can occur). Thus, P_3 is a measure of the critical condition. Note that the value P_3 is smaller than the value of the limit point, P_4 . This implies that the critical load under sudden application (infinite duration) is smaller than the corresponding static critical load.

In this case, also, one may wish to limit the dynamic response of the system to a value smaller than B_2 (see Fig. 2), say θ_1 . Then the maximum allowable (critical dynamic) load corresponds to P_2 .

Note that in multi-degree-of-freedom systems, one may easily establish upper and lower bounds for the critical dynamic load (see [16, 19, 20, 21, 43, 47]). Moreover, it is clear that for single-degree-of-freedom sys-

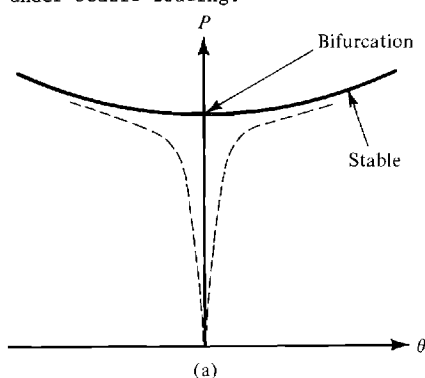
the same and therefore, the estimates de-

versus some characteristic displacement, θ . The solid curves denote the response of systems which are free of imperfections and the dashed-line curves denote the response of the corresponding imperfect configuration.

Fig. 3 shows the response of such structural elements as columns, plates, and unbraced portal frames. The perfect configuration is subject to bifurcational buckling, while the imperfect configuration is characterized by stable equilibrium (unique), for elastic material behavior.

Fig. 4 typifies the response of some simple trusses and two-bar frames. The perfect configuration is subject to bifurcational buckling, but smooth (stable) in one direction of the response and violent (unstable) in the other. Correspondingly the response of the imperfect configuration is characterized by stable equilibrium (and unique) for increasing load in one direction, while in the other the system is subject to limit point instability.

Fig. 5 typifies the response of troublesome structural configurations such as cylindrical shells (especially under uniform axial compression and of isotropic construction), pressure-loaded spherical shells and some simple two-bar frames. These systems are imperfection-sensitive systems and are subject to violent buckling under static loading.



----- : Imperfect geometry

Fig. 3 Bifurcated Equilibrium Paths with Stable Branching

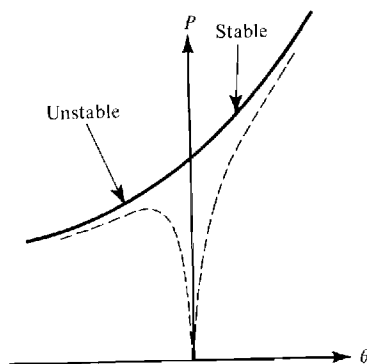


Fig. 4 Bifurcated Equilibrium Paths with Stable and Unstable Branches

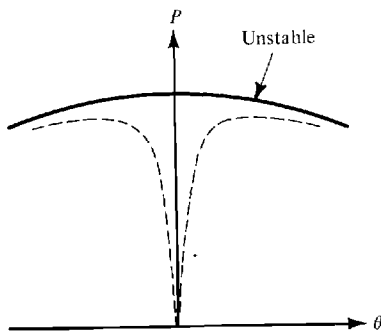


Fig. 5 Bifurcated Equilibrium Paths with Unstable Branching

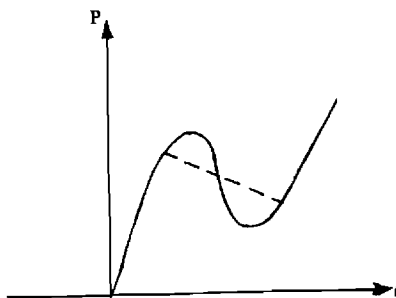


Fig. 6 Snapthrough Buckling Paths (Limit Pt. or Unstable Branching)

A large class of structural elements is subject to limit point instability. In cases, unstable bifurcation is present in addition to the limit point. The response of such systems is shown on Fig. 6. Two structural elements that behave in this manner are the shallow spherical cap and the low arch. Both elements have been examined extensively, in practice.

Finally, there is a very large class of structural elements, which are always in stable equilibrium for elastic behavior and for all levels of the applied loads. These elements are not subject to instability under static conditions. Typical members of this class are beams, and transversely loaded plates. For this class of structural elements, the load-displacement curve is unique and monotonically increasing. The concept of dynamic stability, as developed and discussed [16, 8, 18-21, 43], is always with reference to systems which under static loading are subject to limit buckling. This implies that dynamic buckling has been discussed for systems with static behavior shown in Figs. 4 (to the left), 5 and 6.

In developing concepts and the related criteria and estimates for dynamic buckling it is observed that, even for systems which are subject to violent (static) buckling, critical dynamic loads can be associated with limitations in deflectional response rather than escaping motion through a static unstable point. This is especially applicable to the design of structural members and configurations, which deflection is limited. From this point of view then, the concept of dynamic stability can be extended to all structural systems.

The extended concepts are demonstrated through the simple mass-spring (linear) system, shown on Fig. 7. Consider a suddenly applied load, $P(t)$, applied at $t = 0$. This load may, in general, include the weight (mg). In the case of finite duration, weight is considered to be negligibly small. First, the case of constant load, suddenly applied with infinite duration, is considered.

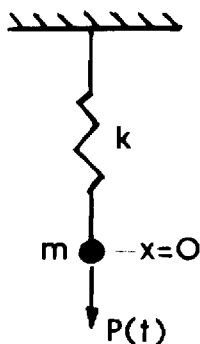


Fig. 7 The Mass-Spring System

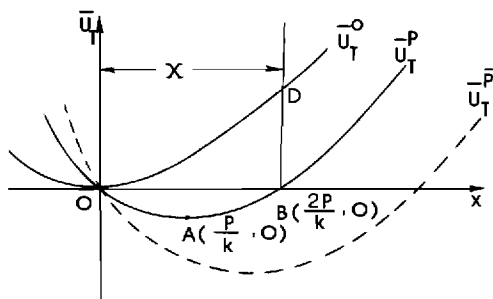


Fig. 8 Total Potential Curves

The problem is viewed from energy considerations. First, the total potential, and kinetic energy, T , for the system are given by

$$U_T = \frac{1}{2} kx^2 - Px; \quad T = \frac{1}{2} m (\dot{x})^2 \quad (6)$$

Note that the system is conservative, the kinetic energy is a positive definite function of the velocity (for all t), and that $U_T = 0$, when $x = 0$. Then, $U_T + I$ and motion is possible only in the range of x -values for which U_T is nonpositive (Fig. 8). It is also seen from Eq. (6) that the maximum x -value corresponds to 2. Note that the static deflection is equal to P/k (pt. A on Fig. 8). Therefore, the maximum dynamic response and maximum static deflection are to be equal to X , the $P_{st} = 2 P_{dyn}$.

Now, one may develop a different viewpoint for this same problem. Suppose that a load P is to be applied suddenly to the mass-spring system with the condition that the maximum deflectional response cannot be larger than a specified value X . If the magnitude of the load is such that $2P/k < X$, we shall call the load dynamically subcritical. When the inequality becomes an equality, we shall call the corresponding load dynamically critical. This implies that the system cannot withstand a dynamic load $P > kX/2$ without violating the kinematic constraint. Therefore, $P_{dyn,cr} = kX/2$.

Moreover, on the basis of this concept, one may find a critical ideal impulse. The question, in this load case, is to find the ideal impulse such that the system response does not exceed a prescribed value X . From Fig. 8 and conservation of

$$U_T^0 + T = T_i \quad (7)$$

and T_i is critical if the system can reach position D with zero velocity (zero kinetic energy). Thus,

$$T_{i,cr} = U_T^0(D) = U_T^0(X) \quad (8)$$

From the impulse-momentum theorem, the ideal impulse, Imp , is related to the initial velocity and consequently to the initial kinetic energy,

$$Imp = \lim_{t \rightarrow 0} (Pt_0) = m\dot{x}_i \quad (9)$$

where \dot{x}_i is the initial velocity magnitude (unidirectional case) and t_0 is the duration time of a square pulse.

From Eqs. (8) and (9)

$$Imp_{cr} = (mk)^{1/2} X \quad (10)$$

Suddenly-Loaded Imperfect Columns

As already mentioned, the field of dynamic stability of structural configurations started with the treatment of a suddenly-loaded imperfect column [24]. The imperfect column, under sudden application of an axial load, typifies structural systems with static behavior shown on Fig. 3. Such a system, when of perfect geometry, is subject to bifurcational buckling with stable post-buckling behavior (smooth buckling). On the other hand, if there exists an initial geometric imperfection (small initial curvature), the system exhibits a unique stable equilibrium path. Moreover, this system has received the most attention, as far as dynamic buckling is concerned and loaded axially either by sudden loads or by time-dependent loads. Two complete reviews (with respect to their date of publication) of this problem may be found in [23, 1]. As mentioned in these references, the problem dates back to 1933 with the pioneering work of Koning and Taub [24], who considered a simply supported, imperfect (half-sine wave) column subjected to an axial sudden load of specified duration. In their analysis, they neglected the effects of longitudinal inertia, and they state that for loads higher than the static (Euler load) the lateral deflection increases exponentially, while the column is loaded, and after the release of the load, the column simply oscillates freely with an amplitude equal to the maximum deflection. Many investigations followed this work with several variations. Some included inertia effects, others added effect of transverse shear, etc. The real difficulty

the problem, though, lies in the fact that there was no clear understanding by the investigators of the concept of dynamic stability and the related criteria.

According to [1], definition of a dynamic buckling load is possible only if there are initial small lateral imperfections in the column. Instability stems then from the growth of these imperfections. "Buckling occurs when the dynamic load reaches a critical value, associated with a maximum acceptable deformation, the magnitude of which is defined in most studies quite arbitrarily." There is some truth in this, primarily because the elastic column does not exhibit limit point instability or any other violent type of buckling under static application of the load. There is need for a cautioning remark to the above statement, though. Analytically, it has been shown [55] that, if a perfect column is suddenly loaded in the axial direction, the fundamental state is one of axial wave propagation (longitudinal oscillations). For some combination of the structural parameters, this state can become unstable and transverse vibrations of increasing amplitude are possible. Therefore, for this perfect column, there exists a possibility of parametric resonance, which is one form of dynamic instability. In spite of this, mostly all columns are geometrically imperfect and therefore, it is reasonable to investigate the dynamic behavior of imperfect columns including all variations of different effects as reported in [23, 1, 12, 17, 41, 33, 41]. These effects include: lateral inertia, rotatory inertia, transverse shear, and various loading mechanisms. Moreover, experimental results have been generated to test the various theories and effects.

Finally, the criterion employed in [1] is the one developed by Budiansky and Roth [8], and it is applicable only to imperfection sensitive structural systems, such as shallow arches, shallow spherical caps, and axially-loaded, imperfect, cylindrical shells. The reason that the application of the Budiansky-Roth criterion can possibly yield results for imperfect columns lies in the fact that the corresponding perfect configuration (column) possesses a very flat post-buckling branch. This means that the corresponding imperfect column can experience, at some level of a sudden load or impulse, very large amplitude oscillations (change from small to large amplitude oscillations). Note that the static curve for the imperfect column (static equilibrium), if the load is plotted versus the maximum lateral deflections, yields small values for the maximum deflection for small levels of the load. As the load approaches the Euler load, the value of the corresponding maximum deflection increases rapidly. On the other hand, if the criterion were to be applied to an imperfect flat plate, it is rather doubtful that reasonable answers could be obtained.

cluding Remarks

It is clearly seen from the material presented so far that some suddenly load-structural configurations are subject to parametric resonance and escaping motion means of a trajectory that passes through an unstable static equilibrium point. This is the case of system, which under static loading are subject to violent buckling.

On the other hand, these systems which under static loading are prone to bifurcational buckling with stable postbuckling branches (such as columns and plates), they are subject to parametric resonance, but there is no question of escaping motion type of dynamic instability. This is true, because an unstable static equilibrium point does not exist. Finally, systems that do not buckle under static loading are neither subject to parametric resonance nor to escaping motion type of instability. In all systems though, because of the modified dynamic stability concept, one might say that when sudden loads are applied, the problem is one of dynamic response. By this, one means that one needs only find the motion of the system resulting from the sudden loads. Note that for systems which exhibit violent static buckling, the deflectional limit imposed in the modified concept must include (be smaller than) the unstable static equilibrium position(s).

Please note that the above remarks are based on various mathematical models, some of which allow imperfection (geometric or loading type) and some of which do not. If one considers real world type of structural configurations, which do possess imperfections, one is inclined to discard parametric resonance for suddenly

loaded systems. For instance, if a perfect column is impacted, see Wauer [55] in-plane motion is accounted for, only then parametric resonance is possible. the other hand, if there exists a small initial curvature, the impacted column vibrate in a nonlinearly combined mode, and there is no parametric resonance other type of dynamic instability. Similarly, if a symmetric low arch is symmetrically loaded by a sudden load, the possibility of parametric resonance exists it is virtually impossible to expect both the arch and the loading to be perfectly symmetric. In the presence of imperfections, the arch is expected to become locally unstable only through escaping motion type of instability.

Finally, one should clearly address one more point. If the sudden loads present the extreme cases of either the ideal impulse, or constant load of infinite duration, elastic dynamic instability of the escaping motion type is possible means that the level of the internal loads (stresses) is below the proportional limit of the material. On the other hand, for constant sudden loads of relatively short duration, what might be more important is a material-type of instability cause of the possibly large level of internal loads [58, 48].

Acknowledgements

This work is supported by the U.S.A.F., Aeronautical Systems Division (AFS) Wright-Patterson A.F. Base under Contract No. F33 615-79-C-3221 and by the Air Force Office of Scientific Research, under AFOSR Grant No. AFOSR-81-0227. This support is gratefully acknowledged.

References

1. Ari-Gur, J., Weller, T., and Singer, J., "Experimental Studies of Columns under Axial Impact," TAE No. 346, December 1978, Dept. of Aeronautical Engineering Technion-Israel Institute of Technology.
2. Au-Yang, M. K., Brown, S. J., Jr., (editors), Fluid Structure Interaction Phenomena in Pressure Vessel and Piping Systems, Published, by ASME, PVT-PB-026 New York, N. Y., 1977.
3. Bohn, M. P., Herrmann, G., "The Dynamic Behavior of Articulated Pipes Conveying Fluid with Periodic Flow Rate", J. Appl. Mech., Vol. 41, No. 1, 1974, pp. 5-11.
4. Bolotin, V. V., The Dynamic Stability of Elastic Systems, (Translated by V. Weingarten et al.) Holden Day, San Francisco, 1964.
5. Briley, R. P., Carlson, R. L., "Investigation of the Parametric Excitation of an Eccentrically Tensioned Bar", Exp. Mech., Vol. 17, No. 9, 1977, pp. 354-358.
6. Budiansky, B., "Dynamic Buckling of Elastic Structures: Criteria and Estimates in Dynamic Stability of Structures (Edited by G. Herrmann), Pergamon Press, New York, 1967.
7. Budiansky, B., and Hutchinson, J. W., "Dynamic Buckling of Imperfection-Sensitive Structures", Proceedings of XI International Congress of Applied Mechanics, Munich, 1964.
8. Budiansky, B., and Roth, R. S., "Axisymmetric Dynamic Buckling of Clamped Spherical Shells", "Collected Papers on Instability of Shell Structures", NACA TN D-1510, 1962.
9. Crocco, L., and Cheng, S. I., Theory of Combustion Instability in Liquid Rocket Motors, AGARD Monograph No. 8, Butterworths Scientific Publ., Ltd., 1956.
10. Dugundji, J., and Mukhopadhyay, W., "Lateral Bending-Torsion Vibrations of a Thin Beam Under Parametric Excitation", J. Appl. Mech., Trans. ASME, Vol. 40, Ser. E., No. 3, Sept. 1973, pp. 693-698.
11. Grybos, R., "Impact Stability of a Bar", Int. J. Eng. Sci., Vol. 13, No. 5, 1975, pp. 463-478.
12. Hauger, W., "Stability of a Compressible Rod Subjected to Nonconservative Forces", J. Appl. Mech., Vol. 42, Ser. E. No. 4, December 1975, pp. 887-888.

Herrmann, G., "Stability of Equilibrium of Elastic Systems Subjected to Non-conservative Forces", J. Appl. Mech., Vol. 31, No. 3, 1964, pp. 435-440.

Herrmann, G., and Bungay, R. W., "On the Stability of Elastic Systems Subjected to Nonconservative Forces", J. Appl. Mech., Vol. 31, No. 3, 1964, pp. 435-550.

Off, N. J., "The Dynamics of the Buckling of Elastic Columns", J. Appl. Mech., Vol. 18, No. 1, 1951 pp. 69-74.

Off, N. J., and Bruce, V. C., "Dynamic Analysis of the Buckling of Laterally Loaded Flat Arches", J. Math and Phys., Vol. 32, 1954, pp. 276-288.

Busner, G. W., and Tso, W. K., "Dynamic Behavior of Supercritically Loaded Trusses", J. Eng. Mech. Div., ASCE, Vol. 88, No. EM5, 1962, pp. 41-65.

Su, C. S., "On Dynamic Stability of Elastic Bodies with Prescribed Initial Conditions", Int'l J. of Nonlinear Mech., Vol. 4, 1968, pp. 1-21.

Su, C. S., "The Effects of Various Parameters on the Dynamic Stability of a Hollow Arch", J. Appl. Mech., Vol. 34, No. 2, 1967, pp. 349-356.

Su, C. S., "Equilibrium Configurations of a Shallow Arch of Arbitrary Shape and Their Dynamic Stability Character", Int'l J. of Nonlinear Mech., Vol. 3, 1968, pp. 113-136.

Su, C. S., Kuo, C. T., and Lee, S. S., "On the Final States of Shallow Arches on Elastic Foundations Subjected to Dynamic Loads", J. Appl. Mech., Vol. 35, No. 4, 1968, pp. 713-723.

Su, C. S., Cheng, W. H., Yee, H. G., Steady State Response of a Non-linear System Under Impulsive Periodic Parametric Excitation, J. Sound Vib., Vol. 50, No. 1, Jan. 1977, pp. 95-116.

Wuffington, N. J., Jr., "Response of Elastic Columns to Axial Pulse Loading", IAA J., Vol. 1, No. 9, 1963, pp. 2099-2104.

Young, C., and Taub, J., "Impact Buckling of Thin Bars in the Elastic Range Loaded at Both Ends", Luftfahrtforschung, Vol. 10, No. 2, 1933, pp. 55-64, translated as NACA TM 748 in 1934).

Zounadis, A. N., Katsikadelis, J. T., "Coupling Effects on a Cantilever Subjected to a Follower Force", J. Sound Vibr., Vol. 62, No. 1, 1979, pp. 131-139.

Zounadis, A. N., Belbas, S., "On the Parametric Resonance of Columns Carrying Concentrated Masses", J. of Struct. Mech. Division, ASCE Vol. 5, No. 4, 1977, p. 383-394.

Zounadis, A. N., "Stability of Elastically Restrained Timoshenko Cantilevers with Attached Masses Subjected to a Follower Force", J. Appl. Mech., Vol. 44, No. 4, 1977, pp. 731-736.

Rajcinovic, D., and Herrmann, G., "Parametric Resonance of Straight Bars subjected to Repeated Impulsive Compression", AIAA J., Vol. 6, No. 10, 1968, pp. 1527-1532.

Ugo, G. C., Morino, L., Dugundji, J., "Perturbation and Harmonic Balance Methods of Nonlinear Panel Flutter", AIAA J., Vol. 10, No. 11, November 1972, pp. 1479-1484.

Wefschetz, S., Stability of Nonlinear Control Systems, Academic Press, New York, 1965.

Weipholz, H. H. E., Madan O. M. P., "On the Solution of the Stability Problem of Elastic Rods Subjected to Uniformly Distributed Tangential Follower Forces", Eng-Arch, Vol. 44, No. 5, 1975, pp. 347-357.

Wovell, E. G., and McIvor, J. K., "Nonlinear Response of a Cylindrical Shell to an Impulsive Pressure", J. Appl. Mech., Vol. 36, No. 2, 1969, pp. 277-284.

McIvor, J. K., and Bernard, J. E., "The Dynamic Response of Columns under Short Duration Axial Loads", J. Appl. Mech., Vol. 40, No. 3, 1973, pp. 688-692.

Zemat-Nassar, S., On Elastic Stability Under Nonconservative Loads, University of Waterloo, Waterloo-Ontario, 1972.

Zaidoussis, M. P., DeKnis, B. E., "Articulated Models of Cantilevers Conveying Fluid: The Study of a Paradox", J. Mech. Eng. Sci., Vol. 42, No. 14, 1970, pp. 288-300.

Zaidoussis, M. P., and Issid, N. T., "Experiments on Parametric Resonance of Pipes Containing Pulsatile Flow", J. Appl. Mech., Vol. 43, No. II, 1976, pp. 198-202.

37. Routh, E. J., Stability of Motion, (ed. by A. T. Guller) Taylor and Francis Ltd., Halsted Press, New York, 1975. (originally it appeared in 1877).
38. Sankar, T. S., Rajan G., Dynamic Response of Elastic Rods Under Parametric Excitations, Journal Eng. Ind. Trans. ASME, Vol. 99, Ser. B., No. 1, Feb. 1977
39. Sawyer, J. W., "Flutter and Buckling of General Laminated Plates", J. Aircraft Vol. 14, No. 4, April 1977, pp. 387-393.
40. Seckel, E., Stability and Control of Airplanes and Helicopters, New York, 19
41. Sevin, E., "On the Elastic Bending of Columns due to Dynamic Axial Forces including Effects of Axial Inertia," J. Appl. Mech., Vol. 27, No. 6, 1960.
42. Simites, G. J. et al, "Dynamic Buckling of Simple Frames under a Step-Load" J. of the EM Division, ASCE, EM 5, 1979, pp. 896-900.
43. Simites, G. J., "Dynamic Snap-Through Buckling of Low Arches and Shallow Ca Ph.D. Dissertation, Department of Aeronautics and Astronautics, Stanford University, June 1965.
44. Simites, G. J., "Effect of Static Preloading on the Dynamic Stability of Structures", Proceedings of the AIAA/ASME/ASCE/AHS Structures, Structural Dynamic Materials Conference, New Orleans, La., May 10-12, 1982, Part 2, pp. 299-307
45. Simites, G. J., Elastic Stability of Structures, Prentice-Hall, Inc., Englewood Cliffs, N. J., 1976.
46. Simites, G. J., "On the Dynamic Buckling of Shallow Spherical Caps", J. Appl. Mech., Vol. 41, No. 1, 1974, pp. 299-300.
47. Simites, G. J., and Blackmon, C. M., "Snapthrough Buckling of Eccentrically Stiffened Shallow Spherical Caps", Int'l J. Solids and Structures, Vol. 11, No. 9, 1975, pp. 1035-1049.
48. Simites, G. J., and Sheinman, I., "Dynamic Stability of Structures: Application to Frames, Cylindrical Shells and Other Systems", AFWAL-TR-81-3155, Fluid Dynamics Laboratory, Wright-Patterson AF Base, Ohio, 1981.
49. Stoker, J. J., Non-Linear Vibrations in Mechanical and Electrical Systems, Vol. II, Interscience Publishers Ltd., London, 1950.
50. Stoker, J. J., "On the Stability of Mechanical Systems", Communications on Pure and Applied Math., Vol. VIII, 1955, pp. 132-142.
51. Sundarajan, C., "Bounds for the Critical Load of Certain Elastic Systems Under Follower Forces", AIAA J., Vol. 14, No. 5, May 1976, pp. 690-692.
52. Tamura, Y. S. and Babcock, C. D., "Dynamic Stability of Cylindrical Shells under Step Loading", J. Appl. Mech., Vol. 42, No. 1, 1975, pp. 190-194.
53. Thompson, W., and Tait, P. G., Treatise on Natural Philosophy: Part I., Cambridge University Press, Cambridge, England, 1923 (It was first published in 1857).
54. Ventres, C., Dowell, E., "Comparison of Theory and Experiment for Non-linear Flutter of Loaded Plates, AIAA J. Vol. 8, No. 11, November 1970, pp. 2022-2030.
55. Wauer, J., "Über Kinetische Verzweigungs Problem Elastischer Strukturen unter Stossbelastung", Ingenieur-Archiv, Vol. 49, 1980, pp. 227-233.
56. Ziegler, H., "On the Concept of Elastic Stability", Advances in Applied Mechanics Vol. 4, Academic Press, 1956, pp. 351-403.
57. Ziegler, H., Principles of Structural Stability, Blaisdell Publishing Co., Waltham, Massachusetts, 1968.
58. Zimcik, D. G., and Tennyson, R. C., "Stability of Circular Cylindrical Shells Under Transient Axial Impulsive Loading," Proceedings, AIAA/ASME/ASCE/AHS 20th Structures, Structural Dynamics and Materials Conference, St. Louis, Missouri, April 4-6, 1979, pp. 275-281.

STABILITY OF LAMINATED COMPOSITE SHELLS SUBJECTED TO UNIFORM AXIAL COMPRESSION AND TORSION

**George J. Simitzes
Izhak Sheinman
and
Dein Shaw**



**School of Engineering Science and Mechanics
GEORGIA INSTITUTE OF TECHNOLOGY
A Unit of the University System of Georgia
Atlanta, Georgia 30332**

REPORT DOCUMENTATION PAGE		READ INSTRUCTIONS BEFORE COMPLETING FORM
1. REPORT NUMBER AFOSR TR-	2. GOVT ACCESSION NO.	3. RECIPIENT'S CATALOG NUMBER
4. TITLE (and Subtitle) STABILITY OF LAMINATED COMPOSITE SHELLS SUBJECTED TO UNIFORM AXIAL COMPRESSION AND TORSION		5. TYPE OF REPORT & PERIOD COVERED Interim June 30, 1981 - June 29, 1982
		6. PERFORMING ORG. REPORT NUMBER
7. AUTHOR(s) George J. Simitzes Izhak Sheinman and Dein Shaw		8. CONTRACT OR GRANT NUMBER(s) AFOSR 81-0227
9. PERFORMING ORGANIZATION NAME AND ADDRESS Georgia Institute of Technology School of Engineering Science and Mechanics 225 North Ave., N.W. Atlanta, GA 30332		10. PROGRAM ELEMENT, PROJECT, TASK AREA & WORK UNIT NUMBERS 612300 2307/B1 61102F
11. CONTROLLING OFFICE NAME AND ADDRESS Air Force Office of Scientific Research/NA Bldg. 410 Bolling AFB, D.C. 20332		12. REPORT DATE 1982
		13. NUMBER OF PAGES 174
14. MONITORING AGENCY NAME & ADDRESS (if different from Controlling Office)		15. SECURITY CLASS. (of this report) Unclassified
		15a. DECLASSIFICATION/DOWNGRADING SCHEDULE
16. DISTRIBUTION STATEMENT (of this Report) Approved for public release; distribution unlimited		
17. DISTRIBUTION STATEMENT (of the abstract entered in Block 20, if different from Report)		
18. SUPPLEMENTARY NOTES		
19. KEY WORDS (Continue on reverse side if necessary and identify by block number) Composite Cylinders Axial Compression Laminated Shells Torsion Stability Dynamic Buckling Stiffened Shells		
20. ABSTRACT (Continue on reverse side if necessary and identify by block number) The governing equations for the nonlinear analysis of imperfect, stiffened, laminated, circular, cylindrical, thin shells, subjected to uniform axial compression and torsion, and supported in various ways, are derived and presented. Two types of formulations have been developed; one (w,F - Formulation) is based Donnell-type nonlinear kinematic relations; and the other (u,v,w - formulation) is based on Sanders'-type of nonlinear kinematic relations (small strains, moderate rotations about in-plane axes).		

A solution methodology is developed and presented. Numerical results are generated for certain special geometries, and these serve as bench marks for the solution scheme. Parametric studies are performed for composite cylinders. The scope of these studies is to assess the effect of (a) geometric imperfections, (b) lamina stacking, (c) in-plane and transverse boundary conditions, and (d) load eccentricity on the critical condition. Moreover, dynamic (suddenly applied) critical loads are obtained for certain configurations under axial compression.

STABILITY OF LAMINATED COMPOSITE SHELLS
SUBJECTED TO UNIFORM AXIAL COMPRESSION
AND TORSION*

by

George J. Simitzes⁺, Izhak Sheinman⁺⁺

and

Dein Shaw⁺⁺⁺
Georgia Institute of Technology

*This work was supported by the United States Air Force Office of Scientific Research under Grant AFOSR-81-0227.

⁺Professor of Engineering Science and Mechanics.

⁺⁺Visiting Scholar; on leave from Israel Institute of Technology, Haifa, Israel.

⁺⁺⁺Graduate Student, School of Engineering Science and Mechanics.

Qualified requestors may obtain additional copies from the Defense Documentation Center, all others should apply to the National Technical Information Service.

Conditions of Reproduction

Reproduction, translation, publication, use and disposal in whole or in part by or for the United States Government is permitted.

TABLE OF CONTENTS

	<u>Page</u>
NOMENCLATURE	ii
SUMMARY	v
CHAPTER	
I. INTRODUCTION	1
II. MATHEMATICAL FORMULATION AND SOLUTION METHODOLOGY	4
III. DESCRIPTION OF STRUCTURAL GEOMETRY	7
III.1 Laminated Geometry	7
III.2 Isotropic Geometry	8
III.3 Orthotropic Geometry	8
III.4 Imperfection Shapes	9
IV. NUMERICAL RESULTS AND DISCUSSION	10
IV.1.0 Axial Compression	10
IV.1.1 Effect of Lamina Stacking	11
IV.1.2 Effect of Boundary Condition	18
IV.1.3 Effect of In-plane Load Eccentricity	21
IV.2.0 Torsion with and without Axial Compression	27
IV.3.0 Conclusion	35
APPENDIX A MATHEMATICAL FORMULATION AND SOLUTION METHODOLOGY	37
APPENDIX B COMPUTER PROGRAM	146
APPENDIX C MODIFICATION AND GENERALIZATION OF POTTER'S METHOD	147
APPENDIX D INSTABILITY OF LAMINATED CYLINDERS IN TORSION	155
REFERENCES	166

NOMENCLATURE

A_{ij}	$= \sum_{k=1}^N Q_{ij}^k (z_k - z_{k-1})$
B_{ij}	$= \frac{1}{2} \sum_{k=1}^N Q_{ij}^k (z_k^2 - z_{k-1}^2)$
D_{ij}	$= \frac{1}{3} \sum_{k=1}^N Q_{ij}^k (z_k^3 - z_{k-1}^3)$
F	= Airy Stress Function
L	= Length of Shell
M_{xx}, M_{xy}, M_{yy}	= Moment Resultants
N_{xx}, N_{xy}, N_{yy}	= Stress Resultants
Q_{ij}	= Material Elastic Constant
\bar{Q}_x	= Shearing Force at Boundary
R	= Radius of Shell
U_T	= Total Potential
U_i	= Strain Energy
U_P	= Potential of External Forces
h_n, h_o	= Z Coordinate of Extreme Surfaces of the Shell
q	= Pressure Force in Z direction
u, v, w	= Displacement Components
w^o	= Initial Geometric Imperfection
x, y, z	= Coordinates
δ_1	= 0 for Donell's Approximation = 1 for Sanders' Approximation
$\epsilon_{xx}^o, \epsilon_{xy}^o, \epsilon_{yy}^o$	= Reference Surface Strain Components

NOMENCLATURE

(Continued)

$\kappa_{xx}, \kappa_{yy}, \kappa_{xy}$ = Changes of Curvatures and Torsion of Reference Surface

ξ = Imperfection Amplitude Parameter

$\sigma_{xx}, \sigma_{yy}, \sigma_{xy}$ = Stress Components

Summary

An imperfect, laminated, circular, cylindrical, thin shell, simply supported or clamped at the boundaries, and subjected to a uniform axial compression and torsion (individually applied or in combination) is analyzed. The analysis is based on nonlinear kinematic relations, linearly elastic material behavior, and the usual lamination theory. The laminate consists of orthotropic laminae, which typically characterize fiber reinforced composites. Two types of formulation have been developed; one is referred to as the w, F -formulation, based on Donnell-type of kinematic relations. The governing equations consist of the transverse equilibrium equation and the in-plane compatibility equation. These two equations are expressed in terms of the transverse displacement, w , and an airy stress resultant function, F . The other, referred to as the u, v, w -formulation, is based on Sanders'-type of kinematic relations. The governing equations for this case consist of the three equilibrium equations. These three equations are expressed in terms of two in-plane displacement components u, v , and the transverse displacement component, w . Donnell's type of shell theory approximation can be treated as a special case in the u, v, w -formulation.

Some results are generated for certain geometries (isotropic and laminated) and these serve as bench marks for the solution scheme. Results are also generated for composite cylinders by changing several parameters. The scope of these parametric studies is to establish the effect of (a) geometric imperfections, (b) lamina stacking, (c) in-plane and transverse boundary conditions and (d) load eccentricity on the critical conditions. Moreover, dynamic critical loads are obtained for certain configurations under axial load (suddenly applied).

CHAPTER I INTRODUCTION

Shell-like structural configurations find wide uses in complicated aerospace structural systems. Their use requires sophisticated analyses in order to answer questions associated with their behavioral response to external loads and extreme temperature environments. In the past forty years or so, numerous investigations addresses themselves to several specific questions of shell behavior, and the answers to these questions have tremendously enhanced our understanding of their behavior. All of this was done primarily for metallic construction of these configurations. In particular, attention was paid to the degree of approximation involved in the use of various kinematic relations (which led to several linear and nonlinear shell theories), to the discrepancy between theory and experiment for the buckling of shells (post-buckling analyses and imperfection-sensitivity studies), to the use of stiffening for shell configurations (including eccentricity effects) to the effect of support conditions, cutouts, foreign inclusions and others. Moreover, as the size of shell-like structures increased and as the computational capability improved, large computer codes became available, for the analysis of the configurations.

In the recent few years, the constant demand for lightweight efficient structures led the structural engineer to the use of nonconventional materials, such as fiber-reinforced composites. The correct and effective use of these materials requires good understanding of the system response characteristics to external causes (loads, properties of the environment, etc.). Several research programs have been initiated in order to evaluate the physical properties of such materials. The main emphasis in these studies is placed on the characterization of physical properties (finding the constants in the

constitutive relations and how the environment affects them). In addition, there are several efforts related to failure criteria and failure-related effects, such as scissoring and delamination.

In 1975, R. C. Tennyson (1) made a review of previous studies on the buckling of laminated cylinders. According to Tennyson's (1) review, perhaps one of the earliest stability analyses of homogeneous orthotropic cylindrical shells was published by March et al. (2) in 1945. After that time, several theoretical analyses limited to orthotropic shell configurations were performed by Schnell and Bruhl (3), Thielemann et al. (4), and Hess (5). In these studies, simply supported end conditions were partially satisfied. The general linear theoretical solutions to anisotropic cylinders were presented by Cheng and Ho (6) (7), Jones and Morgan (8), Jones and Hennemann (9) and Hirano (10). Several papers were involved in the comparison of the efficiency and accuracy between Flugge's linear shell theory, which was employed by Cheng and Ho (6) (7), and other shell theories (such as the work done by Tasi (11), Martin and Drew (12) whose theory was based on Donnell's equations, and the work done by Chao (13), whose analysis was based on Timoshenko's buckling equations). Stiffened composite cylindrical shells have been analyzed by Jones (14). Terebushdo (15) and Cheng and Card (16). Theoretical analyses of the effect of initial geometric imperfection based on anisotropic shell theory have been published for the loading cases of pure torsion (17) axial compression (18) and combined loads (19) (20). Moreover, several computer codes (21-32) (based on finite elements and/or differences) that deal with the analysis of stiffened shell configurations have been modified in order to account for laminated shell construction. These codes do serve their purpose, and that is that they are very good analytical tools. On the other hand, it is very difficult, if not

possible, to use these codes for parametric studies or for evaluating the applicability and limitations of various shell theories. In this report, the following are presented:

(1) The mathematical formulation and derivation of the governing equations, based on Donnell-type (33) nonlinear kinematic relations and in terms of the transverse displacement component and an Airy stress (resultant) function, defined in the text.

(2) The mathematical formulation and derivation of the governing equations, based on Sanders'-type (34) nonlinear kinematic relations and in terms of the three displacement components (small strains but moderate rotations about in-plane axes).

(3) Solution schemes for both formulations. The solution methodology for the first formulation includes post-limit point behavior, while the solution methodology for the second formulation refers only to the pre-limit point behavior and it is employed to estimate critical static conditions (limit point loads). The listing of the related computer codes are presented in the Appendices of this report.

(4) Some numerical results are generated (and presented herein) with two objectives in mind. (a) Some serve as bench marks for the solution schemes and (b) some limited parametric studies are performed in order to assess effects of boundary conditions and of the lamina stacking sequence, for axially-loaded laminated cylindrical shells.

In closing, this report should be viewed as the first in a series of reports dealing with the behavior of geometrically imperfect, stiffened and laminated, thin, circular, cylindrical shells, supported in various ways (all possible extreme cases of transverse and in-plane boundary conditions) and subjected to static, as well as suddenly applied, destabilizing loads.

CHAPTER II.

MATHEMATICAL FORMULATION AND SOLUTION METHODOLOGY

The governing equations are derived, with all necessary steps shown in detail, in Appendix A. The geometry is a thin, circular, geometrically imperfect cylindrical shell. The construction consists of an orthogonally and eccentrically stiffened laminate (each lamina is orthotropic). Note that a laminated geometry, an eccentrically stiffened metallic configuration and a metallic shell are all special cases of the construction used herein. The stiffeners are uniform in geometry and with constant close spacing, which allows one to employ the "smeared" technique. The boundary conditions can be of any transverse and in-plane variety. This includes free, simply-supported and clamped with all possible in-plane combinations.

The loading consists of transverse (uniform lateral pressure) and eccentric in-plane loads, such as uniform axial compression and shear. Eccentric means that the line of action of these loads (applied stress resultants) is not necessarily in the plane of the reference surface.

In the derivation of the governing equations, the usual lamination theory is employed. Moreover, thin shell theory (Kirchhoff - Love hypotheses with two different approximation) and linearly elastic material behavior are assumed. The primary assumptions are listed in Appendix A. On the basis of these general assumptions two sets of field equations are derived. One, referred to as the w,F formulation, is based upon Donnell-type of kinematic

relations. For this case, the governing equations consist of the transverse equilibrium equation and the in-plane compatibility equation. These two equations and the proper boundary conditions are expressed in terms of the transverse displacement component, w , and an Airy stress resultant function, F . The second, referred to as the u, v, w - formulations, is based on Sanders' type of kinematic relations, those corresponding to small rotations about the normal and moderate rotations about in-plane axes. The governing equations, for this case, consist of the three equilibrium equations, expressed in terms of the displacement components u, v , and w . Also, the proper boundary conditions are expressed in terms of u, v , and w . In this formulation, the Donnell approximation is a special case of the more general Sanders' kinematic relations.

The solution methodology is an improvement and modification of the one employed and described in Refs. 36 and 37. For details the reader is referred to Appendix A. A brief description of the solution scheme is given below and only for the w, F - formulation.

1). First, a separated form (fourier series type) is assumed for the dependent variables $w(x,y)$ and $F(x,y)$. In addition the initial geometric imperfection is also expressed in a similar form.

2). Next, these expressions are substituted into the compatibility equations. Use of trigonometric identities and use of the orthogonality of the trigonometric functions reduces this nonlinear partial differential equation (compatibility) into a system of $(4k + 1)$ nonlinear ordinary differential equations. Furthermore, use of the Galerkin procedure in connection with the equilibrium equation (in the circumferential direction) yields $(2k + 1)$ additional nonlinear ordinary differential equations in the $(6k + 2)$

dependent (on x) functions needed to describe the response of the system. Thus, through these steps the two nonlinear partial differential equations are reduced to a set of nonlinear ordinary differential equations.

3). The nonlinear ordinary differential equations are reduced to a sequence of linear systems by employing the generalized Newton's method (Ref. 38). Iteration equations are derived, through this, based on the premise that a solution to the nonlinear set can be achieved by small corrections to an approximate solution.

4). Finally, the field equations (linearized iteration equations) and the corresponding boundary terms (linear set of equations) are cast into finite difference form by employing the usual central difference formula.

Finally, a computer program has been written (see Appendix B for Flow Charts and Program Listings) for generation of results. The solution algorithm is a modification of the one described in Ref. 43. This modification is fully described in Appendix C.

CHAPTER III

DESCRIPTION OF STRUCTURAL GEOMETRY

Three basic configurations are used in generating results. They consist of a four-ply laminated cylinder, an isotropic cylinder and an orthotropic cylinder. All configurations are geometrically imperfect but the imperfection is either symmetric or (virtually) axisymmetric.

The laminated geometries considered in the present study are variations of the one employed in (44). This reference reports experimental results for a symmetric angle-ply laminate, subjected to uniform axial compression and torsion. In addition some isotropic and orthotropic configurations are also used.

III.1 Laminated Geometry

For the laminated geometries, five different stacking combinations of the 4-ply laminate are used in the study.

First, the common geometric and structural features are: each lamina is orthotropic (Boron/Epoxy; AVCO 5505) with properties

$$E_{11} = 2.0690 \times 10^8 \text{ kN/m}^2 (30 \times 10^6 \text{ psi}); \nu_{12} = 0.21;$$

$$E_{22} = 0.1862 \times 10^8 \text{ kN/m}^2 (2.7 \times 10^6 \text{ psi}); R = 190.5 \text{ cm. (7.5 in.)};$$

$$G_{12} = 0.04482 \times 10^8 \text{ kN/m}^2 (0.65 \times 10^6 \text{ psi}); L = 381 \text{ cm. (15 in.)};$$

$$h_{ply} = 0.013462 \text{ cm (0.0053 in.)}$$

$$(h_{ply} = h_k - h_{k-1}; \text{ for } k = 1, 2, 3, 4; \text{ four plies}) \quad (1)$$

The five different stacking combinations are denoted by I - i, i = 1, 2..5, and correspond to

$$I-1: 45^{\circ}/-45^{\circ}/-45^{\circ}/45^{\circ} ; I-2: 45^{\circ}/-45^{\circ}/45^{\circ}/-45^{\circ} ; I3 = - I2$$

$$I-4: 90^{\circ}/60^{\circ}/30^{\circ}/0^{\circ} ; I-5: 0^{\circ}/30^{\circ}/60^{\circ}/90^{\circ} \quad (2)$$

Where the first number denotes the orientation of the fibers of the out-most ply with respect to x, and the last of the innermost. Geometry I-1 is a symmetric one and it corresponds to that of (44). Geometries I-2 and I-3 denote antisymmetric regular angle-ply laminates, while geometries I-4 and I-5 are completely asymmetric.

III.2 Isotropic Geometry

The isotropic cylinder has the following geometric and structural features (aluminum alloy)

$$E = 7.24 \times 10^7 \text{ kN/m}^2 (10.5 \times 10^6 \text{ psi}) ; \nu = 0.3$$

$$R = 10.16 \text{ cm. (4in)} ; L/R = 1 ; R/h = 1000 \quad (3)$$

III.3 Orthotropic Geometry

Finally, the properties of the orthotropic configuration are (single 0° - ply shell made of the Boron/Epoxy material)

$$E_{xx} = 2.069 \times 10^8 \text{ kN/m}^2 (30 \times 10^6 \text{ psi}) ; \nu_{xy} = 0.21$$

$$E_{yy} = 0.1862 \times 10^8 \text{ kN/m}^2 (2.7 \times 10^6 \text{ psi})$$

$$G_{xy} = 0.04482 \times 10^8 \text{ kN/m}^2 (0.65 \times 10^6 \text{ psi}) ; R = 190.5 \text{ cm. (7.5in.)}$$

$$L = 381.0 \text{ cm. (15in.)} ; t = 0.05385 \text{ cm. (0.0212in.)} \quad (4)$$

III.4 Imperfection Shapes

Two imperfection shapes are used in the study, one which is symmetric, and one which is virtually axisymmetric

$$\text{Symmetric: } w^0(x,y) = \xi h \sin \frac{\pi x}{L} \cos \frac{\pi y}{R} \quad (5)$$

$$\text{axisymmetric: } w^0(x,y) = \xi h \left(-\cos \frac{2\pi x}{L} + 0.1 \sin \frac{\pi x}{L} \cos \frac{\pi y}{R} \right) \quad (6)$$

where ξ is a measure of the imperfection amplitude. Note that for the symmetric imperfection, Eq. (5), $\xi = w_{\max}^0/h$, while for the (virtually) axisymmetric imperfection, Eq. (6), $\xi = w_{\max}^0/1.1h$.

CHAPTER IV

NUMERICAL RESULTS AND DISCUSSION

Numerical results are generated, for the geometries described in the preceeding chapter, using the W-F formulation, for two load cases: (a) uniform axial compression and (b) torsion. The loads are applied individually and in combination. The results consist of finding pre- and post-limits point behavior, as well as critical, conditions for static and dynamic (sudden-some results) application of the loads.

The generated results serve a multitude of purpose. Some results serve as bench marks for the solution methodology and the computer code. These results are compared with already known and accepted numbers. Some results correspond to parametric studies, which are performed in order to enhance our understanding of the behavior of laminated shells. The effects of lamina stacking on critical conditions is studied. Furthermore, the effect of in-plane and transverse boundary conditions on critical loads is evaluated for some geometries. Moreover, the imperfection sensitivity is fully assessed for all geometries. Dynamic critical loads are obtained for very few geometries. Most of the generated results are presented in tabular and graphical form. All generated results are not presented, herein, for the sake of brevity. The conclusions, though, are based on all generated data.

IV. 1.0 Axial Compression

Several studies are performed for this load case. Each one of these studies is described and discussed separately.

IV. 1.1 Effect of Lamina Stacking (Static and Dynamic)

For this study, the load is applied through the reference surface (which is the midsurface of the laminate) and the boundary conditions are SS-3 (classical simply supported). The imperfection shape is symmetric, Eq. (5).

Table 4-1 shows critical loads, \bar{N}_{xx}^l (limit point loads), for each geometry and various values of the imperfection amplitude parameter, ξ . It also presents the range of n-values used in finding critical loads, and the n-value corresponding to the critical condition. These results are also presented graphically on Fig. 4.1.

Geometry I-1 is the one reported in (44). According to this reference, the classical (linear theory) critical load is 165 lbs./in ($\bar{N}_{xx_{cl}}$) and the experimental value is 106 lbs./in. Note from Fig. 4.1 that through extrapolation \bar{N}_{xx}^l at $\xi = 0$ is approximately equal to 148 lbs./in., which is 10% lower than the reported [44] classical value.

The results for geometries I-2 and I-3 are identical. Both geometries are antisymmetric. This is reasonable since (a) the imperfection shape is symmetric with respect to a diametral plane and (b) the axially-loaded cylinder does not distinguish between a positive 45° direction and a negative 45° direction.

Moreover, for virtually the entire range of ξ -values considered, the I-2(3) geometry seems to be the weakest configuration, while the asymmetric configuration corresponding to I-5 is the strongest. The order of going from the weakest to the strongest is I-2(3), I-1, I-4 and I-5. Note that I-5 is a geometry for which the 0° -ply is on the outside. Now since buckling occurs in an inward transverse displacement mode (w is positive), then the outside layer is in compression and it is reasonable to expect the strongest configuration to correspond to I-5, the fibers of the outer ply are in the longitudinal direction.

Table 4.1 Critical Loads

Geometry	ξ	\bar{N}_{xx}^{ℓ} lbs/in	n-Range	n at \bar{N}_{xx}^{ℓ}
I-1	0.05	145.55	5-7	6
	0.50	136.0		6
	1.00	123.0		6
	2.00	98.3		6
I-2,3	0.05	138.80	5-7	6
	0.50	130.0		6
	1.00	118.7		6
	2.00	92.2		6
I-4	0.01	243.1	7-9	8
	0.05	232.03		8
	0.50	178.0		8
	1.00	137.2		8
	2.00	90.0		8
I-5	0.05	233.25	7-9	8
	0.50	191.0		8
	1.00	150.0		8
	2.00	109.5		8

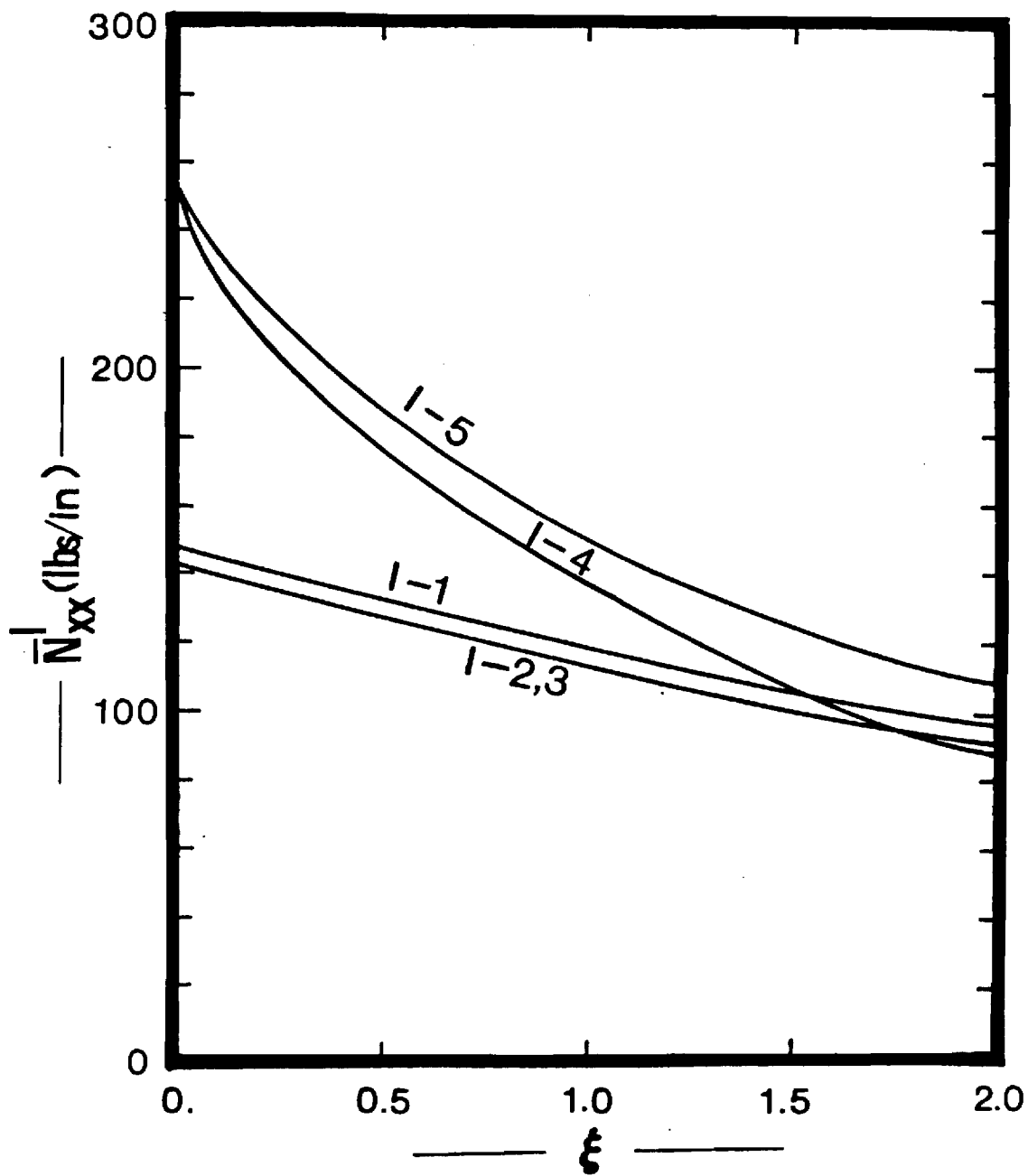


Fig. 4.1 Imperfection Sensitivity of the various Configurations

Furthermore, the difference between I-4 and I-5 geometries is the order of stacking (one is the reverse of the other). Their behavior, then, can be compared to the behavior of orthogonally stiffened metallic shells with outside and inside stiffening. Geometry I-5 is comparable to outside stiffening, while geometry I-4 to inside.

Figs. 4.2 and 4.3 present typical equilibrium paths for all geometries. Fig. 4.2 corresponds to geometry I-1, while Fig. 4.3 to geometry I-4. As seen, the response is in terms of plots of applied load \bar{N}_{xx} versus average end shortening, e_{AV} . It includes, pre-limit point behavior, limit points and post-limit point behavior, for each ξ -value. The entire curves correspond to the same wave number, n . This n -value is the one that yields critical conditions (the one at the instant of buckling). If a clear picture of post-limit point behavior is desired, one should show the plots that correspond to other wave numbers. This would possibly reveal that the post-limit point curves cross each other, as in the case of isotropic shells (46).

Finally, for the two asymmetric configurations, I-4 and I-5, critical dynamic loads are calculated of the entire ξ -range (see Fig. 4.4). These are obtained by employing the criteria described in (46, 39), and they correspond to lower bounds of critical conditions when the axial compression is applied suddenly with infinite duration. According to this criterion and methodology for estimating critical dynamic conditions, when $\xi = 0$ (perfect geometry) the static and dynamic critical loads are the same. As the imperfection amplitude increases the dynamic loads are smaller than the static loads. For these geometries, I-4 and I-5, and $0 \leq \xi < 2.0$, the dynamic critical load, \bar{N}_{xx}^d is never smaller than 60% of the corresponding static load, \bar{N}_{xx}^s .

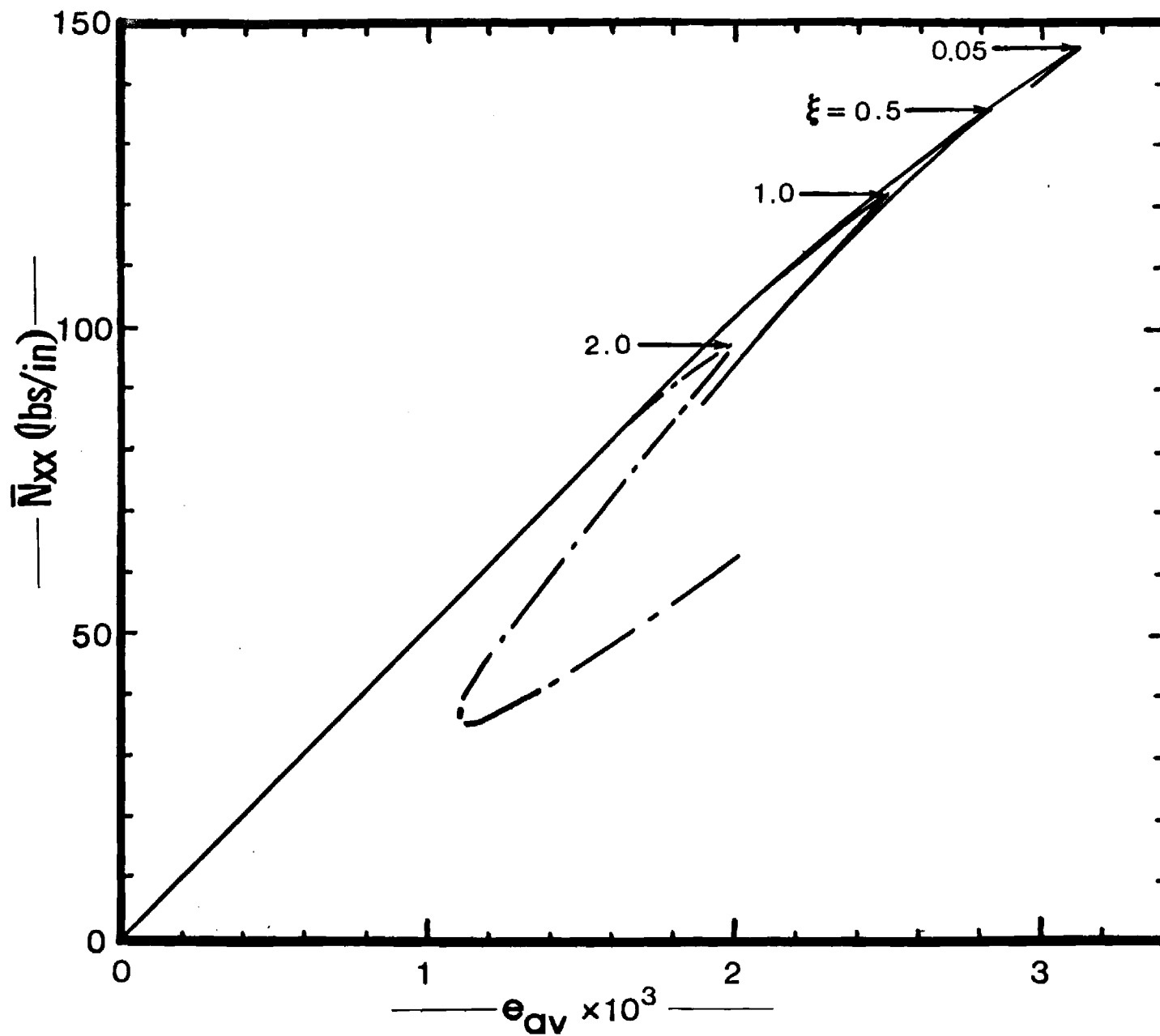


Fig. 4.2 Axial load, N_{xx} , Versus Average End Shortening, e_{av} (Conf. I-1)

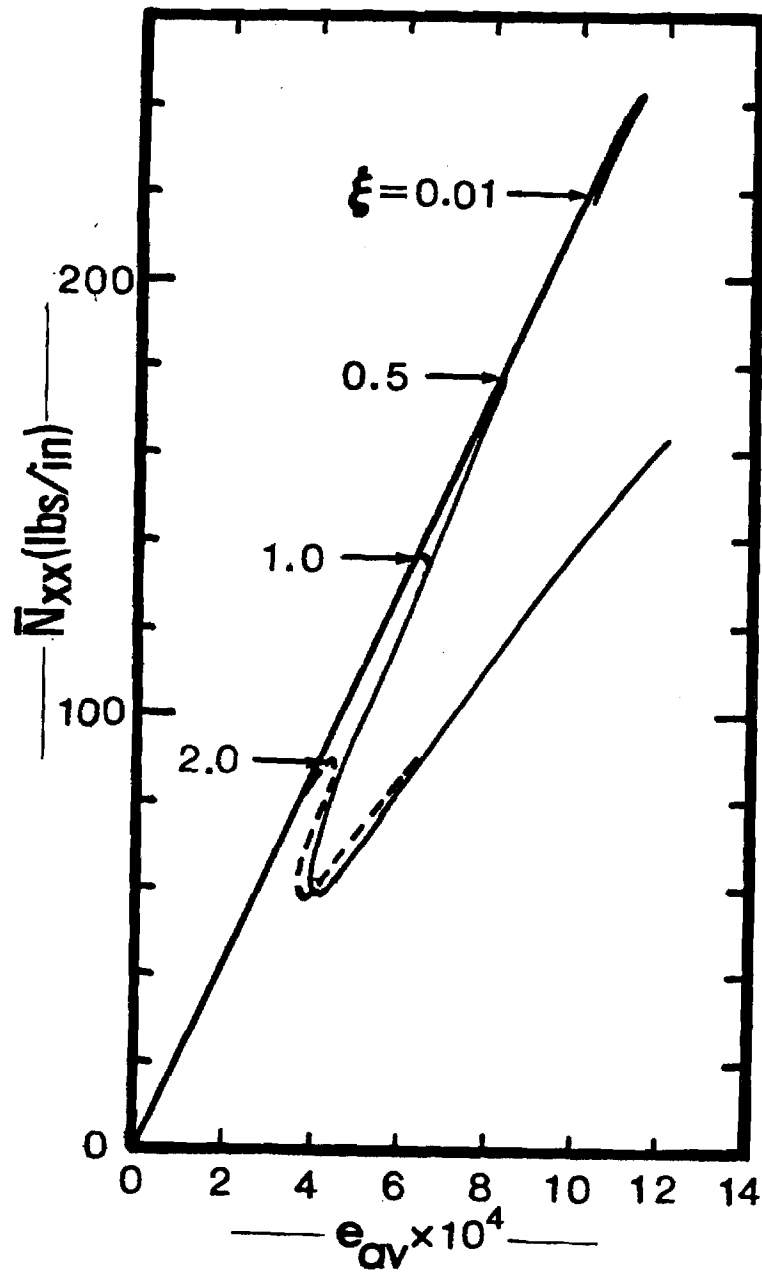


Fig. 4.3 Axial load , N_{xx} , Versis Average End shortening, e_{av} (Conf. I-4)

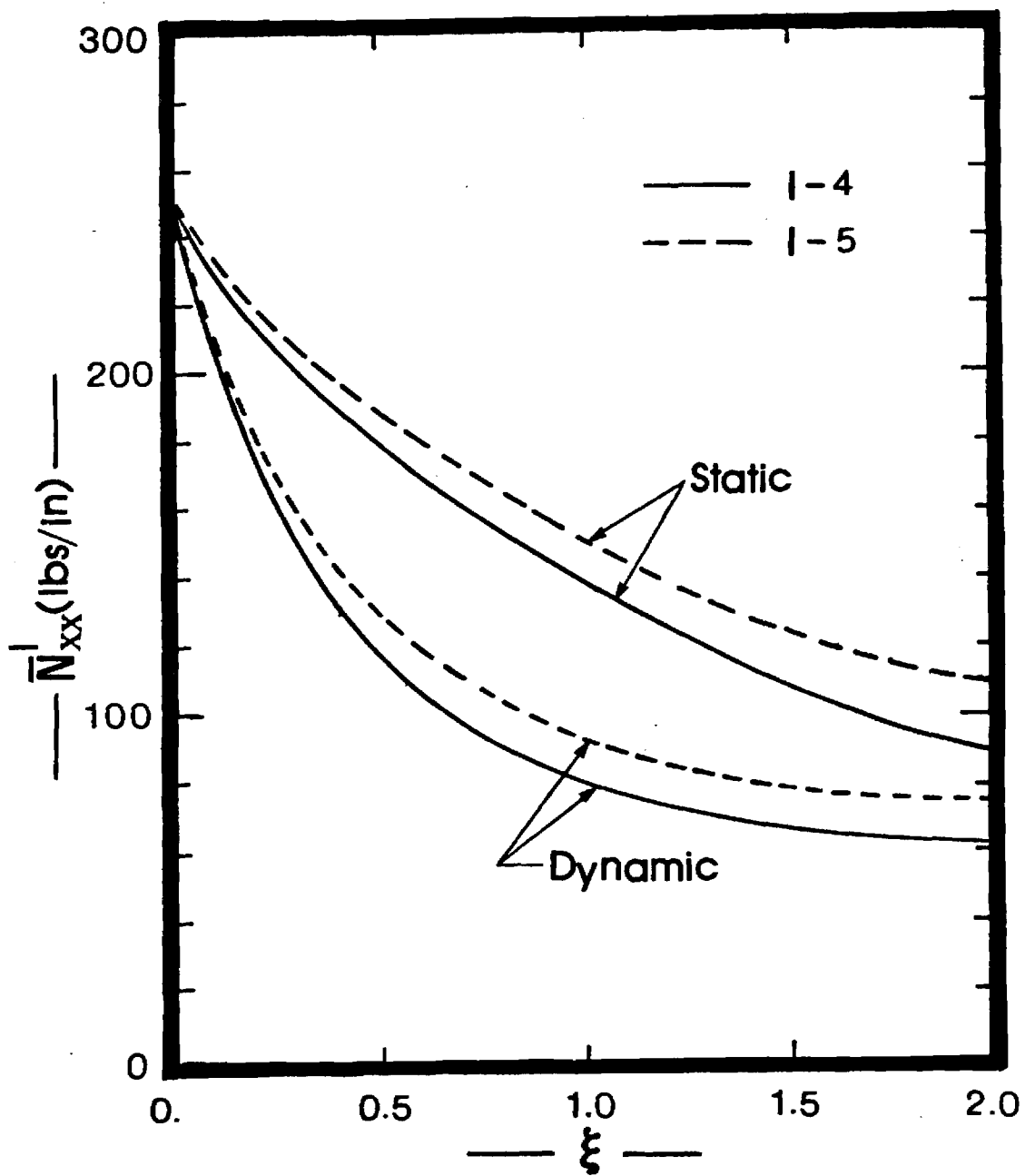


Fig. 4.4 Static and Dynamic critical loads versus Imperfection Amplitude ξ (Conf. I-4 and I-5).

IV. 1.2 Effect of Boundary Conditions

The effect of both transverse and in-plane boundary conditions are assessed.

Results are also generated for the isotropic geometry (aluminum alloy) and various in-plane boundary conditions. These serve as bench marks for the solution scheme, and the results are presented, in part, on Table 4.2 and Fig. 4.5. For this geometry the shape of the imperfection is taken to be axisymmetric, Eq. (6). On Table 4.2, the n -value that corresponds to the critical load is given in brackets. Note that for small ξ -values (see Fig. 4.5), the trend is exactly that suggested by Hoff and Ohira, independently (see (47)), i.e., the weakest configuration is SS-1, the next one SS-2, while SS-3 and SS-4 yield the classical results. Note also that, through extrapolation, (as $\xi \rightarrow 0$), the present results agree with those of (47). For SS-1 the ratio of critical load to classical load is 0.55, for SS-2 0.68, and for SS-3 and SS-4 0.98. Clearly here (isotropic case) the geometry for boundary conditions SS-1 and SS-2, is not very sensitive to geometric imperfection, while for SS-3 (primarily) and SS-4, it is. Note that, for small ξ -values, the $v = \text{const.}$ in-plane boundary conditions (SS-3 and SS-4) yield a stronger configuration. For higher ξ -values the stronger configuration corresponds to $u = \text{const.}$ in-plane boundary conditions (SS-2 and SS-4).

Table 4.2 Effect of In-Plane Boundary Condition on Critical Load (Isotropic Geometry, Simply Supported Case).

ξ	$\frac{l}{N_{xx}}, \text{ kN/m}^2 \text{ (lbs/in.)}$			
	SS-1	SS-2	SS-3	SS-4
.10	2.52 (14.40) [n=12]	3.05 (17.40) [n=15]	3.973 (22.69) [n=13]	4.307 (24.60) [n=15]
.50	2.45 (13.98) [n=12]	2.89 (16.50) [n=15]	2.905 (16.59) [n=13]	4.027 (23.00) [n=15]
1.00	2.36 (13.50) [n=12]	2.68 (15.30) [n=15]	1.985 (11.34) [n=13]	3.192 (18.23) [n=15]

Note that, no attempt is made here to find the shape of the imperfection that yields the lowest critical load. For the case of the laminated shell, the imperfection amplitude parameter, ξ , is varied from 0.05 to two. The first number, 0.05, corresponds to a virtually perfect geometry shell, while the second number (two) denotes an amplitude in the neighborhood of two shell thicknesses (this is considered very large for thin construction).

In order to establish the imperfection sensitivity of the laminated shell and the effect of boundary conditions on the limit point load (critical load), geometry I-5 is employed, along with a symmetric type of imperfection, Eq. (5). As already established, geometry I-5 yields the strongest configuration for SS-3, by comparison to all other geometries (I-1, $i = 1, 2, 3, 4$).

Table 4.3 Effect of Boundary Conditions on Critical Loads. (Laminated Geometry I-5).

ξ	$\frac{l}{N_{xx}}, \text{ kN/m (lbs/in)}$							
	SS-1 n=7	SS-2 n=8	SS-3 n=8	SS-4 n=9	CC-1 n=8	CC-2 n=9	CC-3 n=8	CC-4 n=9
0.05	27.32 (156.0)	32.39 (185.70)	40.84 (233.25)	46.79 (267.26)	41.88 (239.20)	46.32 (264.46)	41.97 (239.70)	—
0.50	26.76 (152.83)	31.78 (181.51)	33.43 (190.90)	40.15 (229.3)	37.10 (211.86)	40.75 (232.70)	37.22 (212.59)	41.44 (236.71)
1.00	25.84 (147.55)	30.04 (171.58)	26.27 (150.00)	32.92 (188.00)	29.53 (168.62)	33.62 (192.00)	29.51 (168.57)	34.63 (197.80)
2.00	20.44 (116.74)	23.21 (132.55)	13.67 (106.62)	21.20 (121.10)	19.65 (108.88)	21.27 (121.50)	19.04 (108.75)	21.95 (125.37)

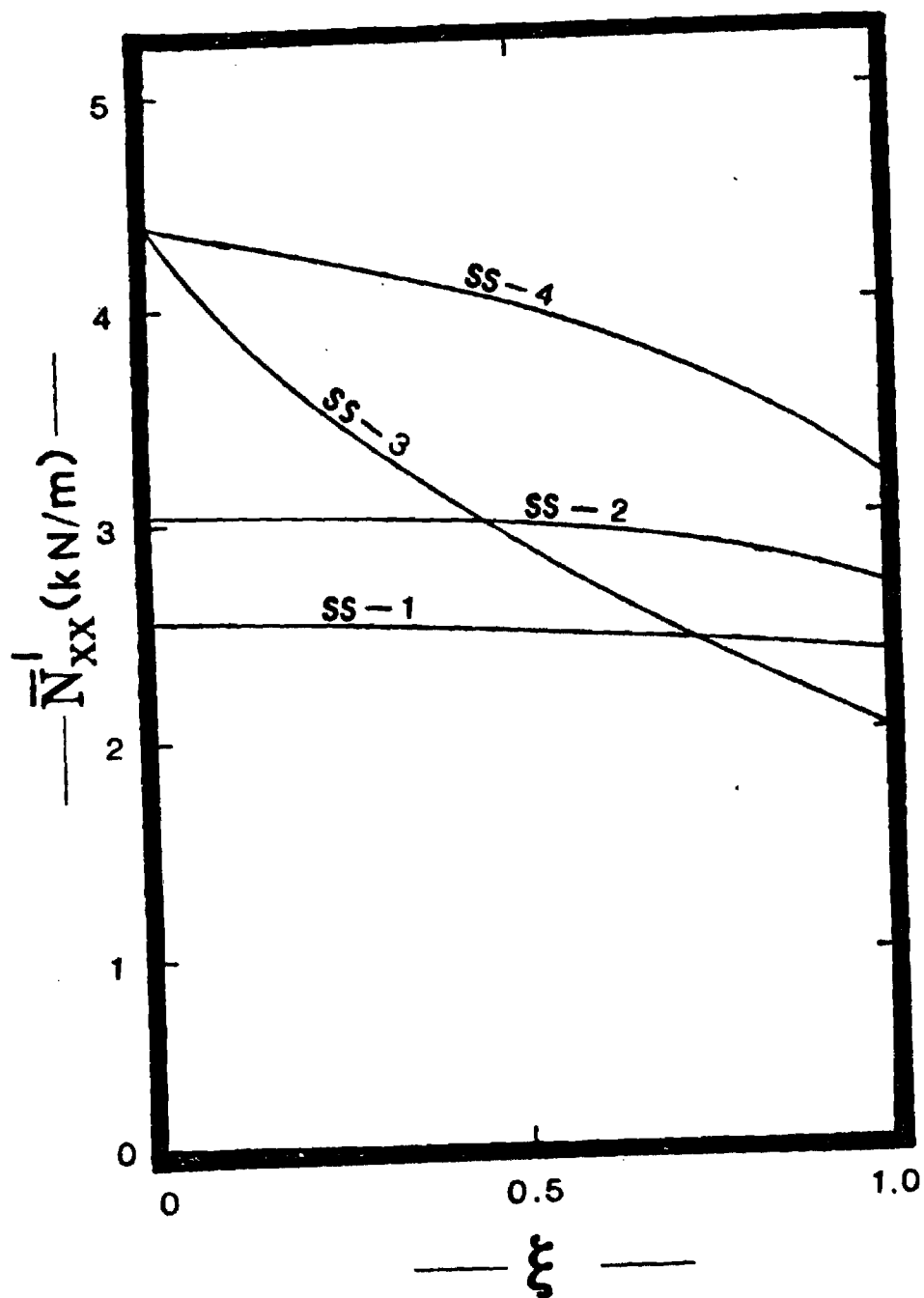


Fig. 4.5 Effect of In-plane Boundary Conditions on the Imperfection Sensitivity of Isotropic Geometry (SS-1)

Table 4.3 lists critical loads for various boundary conditions and ξ -values ($\xi = w_{\max}^0/h$; for this case). The value of n denotes the number of full waves around the circumference at the instant of buckling. These results are shown graphically on Figs. 4.6 and 4.7. A number of observations are made. First, for low ξ -values (see Fig 4.6) SS-3 and SS-4 yield stronger configurations than SS-1 and SS-2. For higher values of ξ , SS-2 and SS-4 yield stronger configurations than SS-1 and SS-3. Another way of stating the same thing is that for low ξ -values the $v = \text{const.}$ in-plane boundary condition yields a stronger configuration, while for higher ξ -values the $u = \text{const.}$ in-plane boundary condition yields higher critical loads. This conclusion is the same for isotropic geometries. On the other hand, for the clamped case, CC-2 and CC-4 ($u = \text{const.}$) yield stronger configurations than CC-1 and CC-3 for the entire ξ -range considered. Another observation is that for SS-1 and SS-2 the geometry is not as sensitive to initial geometric imperfections as it is for SS-3, SS-4, and CC-1 ($i = 1, 2, 3, 4$) [see Figs. 4.6 and 4.7]. It is also worth mentioning that a comparison between the values at $\xi = 0$ between SS-1 and SS-4 is reminiscent of what happens in the isotropic case (the critical load for SS-1 is virtually half the value of that for SS-4).

IV. 1.3 Effect of In-plane Load Eccentricity

Next, the effect of load eccentricity is assessed. In all configurations for which results are generated, the shell midsurface is taken as the reference surface. Then it is assumed that the uniform axial compression is applied eccentrically, which induces a bending moment at the boundary, $\bar{M} = \bar{E} \bar{N}_{xx}$ [see Eqs A-35 & A-36]. Note that this load eccentricity affects only the simply supported boundary conditions.

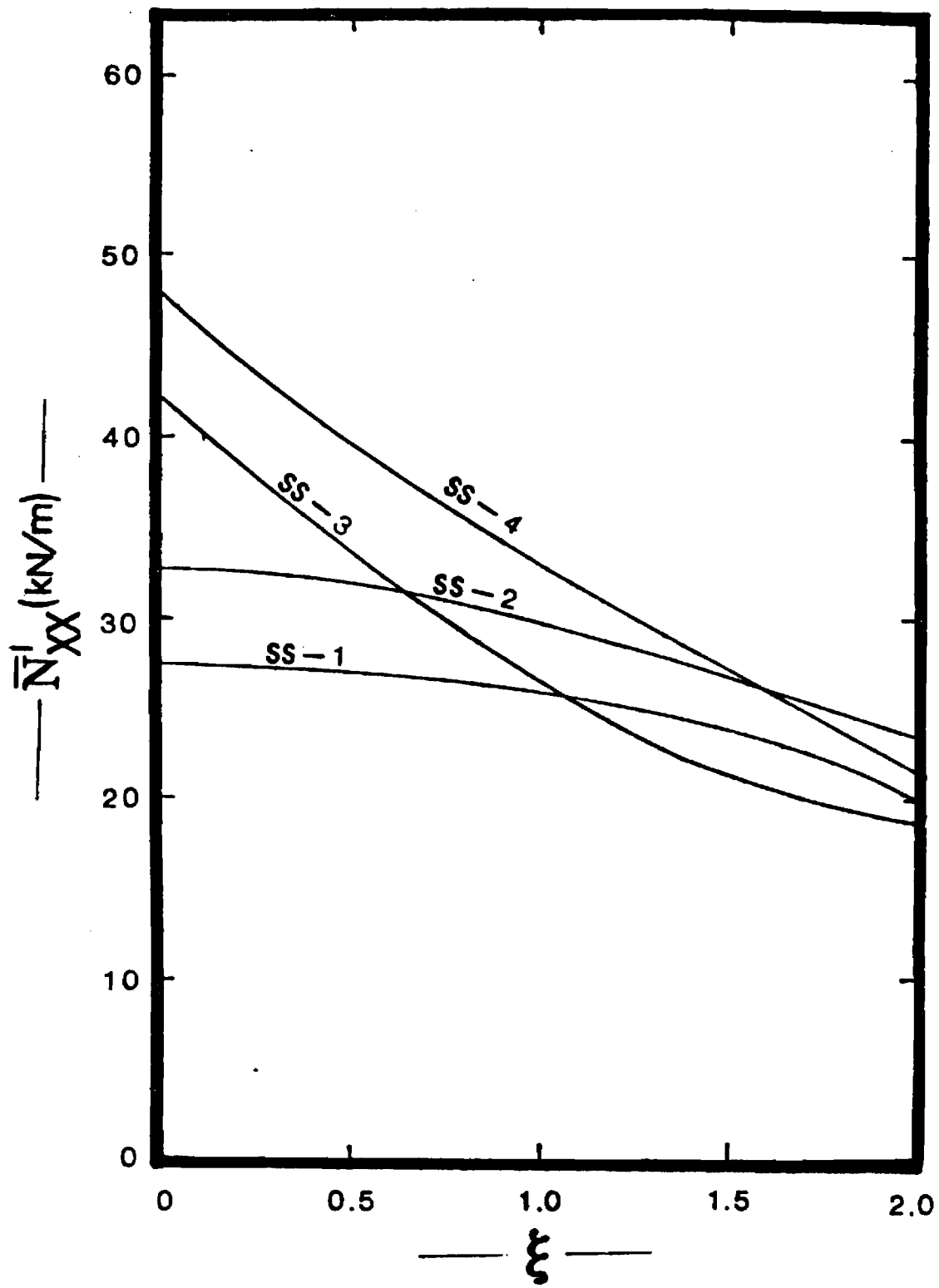


Fig. 4.6 Effect of In-plane Boundary Conditions on the imperfection Sensitivity of Geometry I-5 (ss-1)

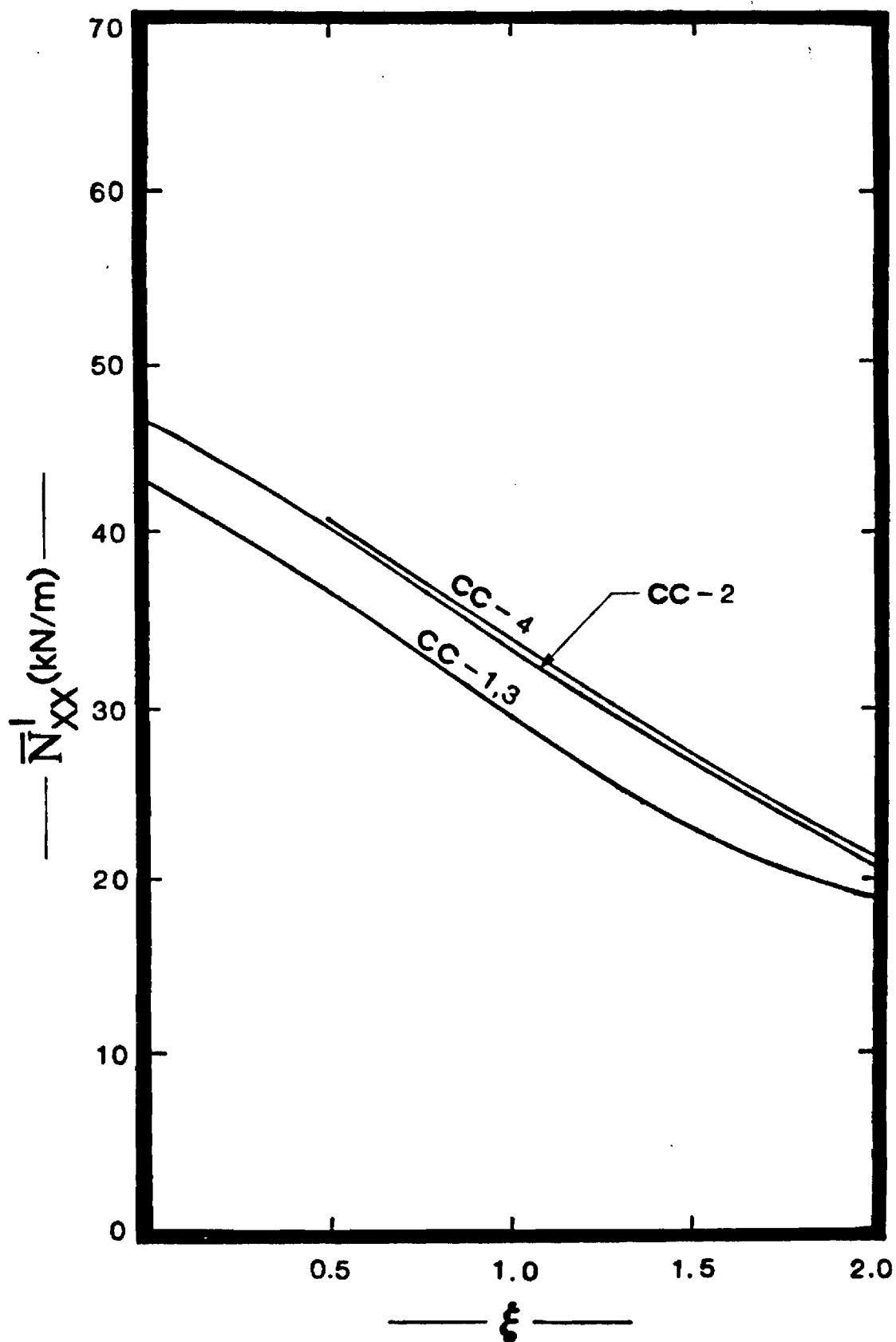


Fig. 4.7 Effect of In-plane Boundary Conditions on the Imperfection Sensitivity of Geometry (cc-1)

Results are generated and presented for the isotropic geometry, orthotropic geometry, and laminated I-1, I-4 and I-5 geometries, using a symmetric imperfection shape Eq. (5), and classical simply supported boundary conditions SS-3.

These results are, in part, presented on Tables 4.4-4.6.

One might expect a negative edge moment (corresponding to positive load eccentricity) to have a stabilizing effect on an axially-load cylindrical shell, regardless of the construction. Contrary to this, the generated results do not support the expectation. For small eccentricities ($-0.5 < e/h < 0.5$) and isotropic geometry (see Table 4.4) the response seems to be insensitive to the eccentric application of the load. This is true for both imperfection shapes [axisymmetric and symmetric, Eq. (5) & (6)].

Table 4.4 Effect of Load Eccentricity (Isotropic & Orthotropic)

Imperf. Shape & Geometry	$\frac{e}{h}$ \downarrow	\bar{N}_{xx} in kN/m (lbs/in.)						
		12.5	2.5	0.5	0	-0.5	-2.5	-12.5
Axisym. Eq.(23)	0.5	3.08 (17.57)	2.40 (13.72)	2.84 (16.20)	2.90 (16.59)	2.92 (16.68)	2.99 (17.07)	2.47 (14.01)
Isotropic	1.0			1.98 (11.336)	1.99 (11.342)	1.98 (11.337)		
Sym, Eq. (22) Isotropic	0.5			3.026 (17.284)	3.097 (17.686)	3.100 (17.704)		
Axisym. Orthotropic	1.0			12.41 (70.89)	12.39 (70.74)	12.36 (70.57)		

Table 4.5 Effect of Load Eccentricity (Laminated I-1 Geometry)

ξ	\bar{N}_{xx}^l in kN/m (lbs/in.)					
	$\bar{E}/h = 0.5$		$\bar{E}/h = 0$		$\bar{E}/h = -0.5$	
	Axisym. Eq. (23)	Sym. Eq. (22)	Axisym. Eq. (23)	Sym. Eq. (22)	Axisym. Eq. (23)	Sym. Eq. (22)
0.5	22.21 (126.85)	21.75 (124.2)	23.58 (134.71)	22.85 (130.49)	26.52 (151.48)	23.35 (133.34)
1.0	19.89 (113.61)	20.31 (115.98)	20.46 (116.85)	20.88 (119.25)	20.78 (118.7)	21.82 (124.6)
2.0	13.10 (74.83)	17.07 (97.46)	13.12 (74.91)	17.21 (98.30)	13.17 (75.22)	17.33 (99.00)

SS-4 boundary conditions and $n = 6$

Table 4.6 Effect of Load Eccentricity (Laminated I-4 and I-5 Geometries; Symmetric Imperfection; SS-3 boundary conditions).

ξ	\bar{N}_{xx}^l in kN/m (lbs/in.); $n = 8$					
	I - 4 geometry			I - 5 geometry		
	$\bar{E}/h = 0.2569$	$\bar{E}/h = 0$	$\bar{E}/h = -0.2569$	$\bar{E}/h = 0.2569$	$\bar{E}/h = 0$	$\bar{E}/h = -0.2569$
0.5	30.61. (174.70)	30.66 (175.08)	30.67 (175.18)	33.00 (188.49)	33.44 (191.00)	36.16 (206.52)
1.0	24.07 (137.45)	24.02 (137.18)	24.08 (137.50)	28.76 (164.27)	26.27 (150.00)	29.18 (166.62)
2.0	15.78 (90.10)	15.76 (90.00)	15.75 (89.93)	18.90 (107.96)	18.67 (106.62)	18.90 (107.85)

For very large eccentricities ($|\bar{E}/h| > 12$), positive eccentricity has a stabilizing effect, while negative eccentricity has a destabilizing effect. In the intermediate range an irregularity is observed. It was suspected that one possible reason for this behavior may be attributed to the Poisson effect. As the load is applied, quasistatically, the midportion of the shell moves outward because of the Poisson effect; it reaches a maximum expansion, before the load reaches its critical value, and then an inward motion takes place, and finally at and after collapse this inward motion continues. This sequence of events and the corresponding stabilization or destabilization of the load eccentricity is heavily dependent on the value of Poisson's ratio or the A_{12} term in the extensional stiffness matrix. For instance, some data are generated, for the isotropic geometry ($\xi = 0.5$; SS-3 and axisymmetric imperfection) but with $\nu = 0.1$. The limit point loads, N_{xx}^l , (critical load) for three values of eccentricity (\bar{E}/h) are: 3.305 kN/m (18.88 lbs/in) for $\bar{E}/h = +0.5$; 2.76 kN/m (15.81 lbs/in.) for $\bar{E}/h = 0$; and 2.745 kN/m (15.68 lbs/in) for $\bar{E}/h = -0.5$. This clearly shows that positive eccentricity has a stabilizing effect. This observation is also true for the orthotropic geometry (see Table 4.4) for which the value of A_{12} is small by comparison to A_{11} . On the other hand, for $\nu = 0.3$ and the laminated geometries for which the values of A_{12} are of the same order of magnitude as A_{11} , it cannot be said that positive eccentricity has a stabilizing effect (see Tables 4.5 and 4.6). In reality, for these geometries no definite conclusion should be drawn regarding stabilization through load eccentricity (or applied edge moment). It is worth observing, though, that for all laminated geometries (see Tables 4.5 and 4.6), whatever the effect is, it does diminish with increasing amplitude of imperfection.

IV. 2.0 Torsion with and without Axial Compression

For this particular load case, in addition to the axisymmetric shape for the geometric imperfection, two additional shapes are employed in the studies. These additional shapes correspond to approximations of the linear theory (see Appendix D) buckling modes for positive and negative torsion for all five geometries.

In particular, Appendix C deals with solutions to the linearized buckling equations for the case of pure torsion. To this end, the Galerkin procedure is employed and the following approximation is employed for the buckling modes

$$W' = \sum_{n=1}^N \sum_{i=1}^M (A_{in} \cos \frac{nY}{R} + B_{in} \sin \frac{nY}{R}) \left[\frac{L}{i\pi} \sin \frac{i\pi X}{L} - \frac{L}{(i+2)\pi} \sin \frac{(i+2)\pi X}{L} \right] \quad (7)$$

Because of orthogonality, only one n-value is needed. In Appendix D, a ten-term approximation (M=5) is obtained for all five geometries. By studying the results, one two-term approximation for positive torsion, $w^0(+)$, and one two-term approximation for negative torsion, $w^0(-)$, for all five geometries are used in this study. The various coefficients are first normalized with respect to B_{2n} , Eq. (7), and then adjusted such that the maximum amplitude is ξh .

$$W^0(+) = \xi h \left[0.536769 \cos \frac{\pi y}{R} \left(\sin \frac{\pi x}{L} - \frac{1}{3} \sin \frac{3\pi x}{L} \right) - 0.670961 \sin \frac{\pi y}{R} \left(\sin \frac{2\pi x}{L} - \frac{1}{2} \sin \frac{4\pi x}{L} \right) \right] \quad (8)$$

$$W^0(-) = \xi h \left[0.583128 \cos \frac{\pi y}{R} \left(\sin \frac{\pi x}{L} - \frac{1}{3} \sin \frac{3\pi x}{L} \right) + 0.64792 \sin \frac{\pi y}{R} \left(\sin \frac{2\pi x}{L} - \frac{1}{2} \sin \frac{4\pi x}{L} \right) \right] \quad (9)$$

$$W_{max}^0/h = \xi \quad (10)$$

The generated results for this case are presented, in part, both in tabular and graphical forms. The discussion, though, and the related conclusions are based on all data.

First, Table 4.7 shows values of critical torsion, \bar{N}_{xy}^l , for the two asymmetric imperfection shapes, Eqs. (8) and (9) (corresponding perfect geometry buckling modes for positive and negative torsion) and several values of the imperfection amplitude parameter. The torsion is applied in both directions and the critical values are recorded. The corresponding minimizing value of n (number of full waves) is shown in parenthesis.

Note that the linear theory, perfect geometry critical values (from Appendix D) for geometry I-1 are 39.9 lbs./in. for positive torsion, and -75.5 lbs./in. for negative torsion. Moreover, the experimental results obtained from (44) for this geometry (I-1) are 26.5 lbs./in. for negative torsion.

Note that the construction (orientation of the plies) is such that the configuration is much weaker when loaded in the negative direction, regardless of which of the two imperfection shapes is used. Furthermore, when $w^0(+)$ is present the configuration is somewhat sensitive for positive torsion (see second column at $\xi = 0.10$, $\bar{N}_{xy} = 35.32$ sensitive for negative torsion (see third column). On the other hand, when $w^0(-)$ the reverse is true, i.e. the

Table 4.7 Critical Shear Stress Resultant
(Geometry I-1 ; Positive & Negative Torsion)

ξ	For $w^0(+)$; Eq. (8)		For $w^0(-)$; Eq. (9)	
	\bar{N}_{xy} lbs./in. (n)	$-\bar{N}_{xy}$ lbs./in. (n)	\bar{N}_{xy} lbs./in. (n)	$-\bar{N}_{xy}$ lbs./in. (n)
0.1	35.32 (11)	-93.94 (13)	36.83 (11)	-63.44 (9)
0.5	31.57 (11)	-92.80 (13)	36.06 (10)	-57.61 (8)
1.0	28.32 (11)	-92.00 (13)	35.17 (10)	-52.11 (8)

Table 4.8 Critical Shear Stress Resultant
[for all geometries and $w^0(+)$]

ξ	\bar{N}_{xx} in lbs./in. (n)				
	I-1	I-2	I-3	I-4	I-5
0.1	35.32 (11)	46.40 (9)	46.36 (9)	44.18 (12)	66.49 (12)
0.5	31.57 (11)	41.81 (9)	41.84 (9)	38.75 (12)	56.91 (12)
1.0	28.32 (11)	37.89 (9)	37.96 (9)	34.22 (12)	48.72 (12)

Table 4.9 Critical Axial Compression-Torsion
Interaction Data* (Geometry I-1;
Axisymmetric Imperfect)

$\xi \downarrow$	n	6	10	10	10	11
0.1	\bar{N}_{xx}	146.1	135.1	95.9	40.9	0.0
	\bar{N}_{xy}	0	10.0	20.0	30.0	36.7
0.5	n	6	10	11	11	11
	\bar{N}_{xx}	140.2	128.9	81.9	28.7	0.0
	\bar{N}_{xy}	0.0	10.0	20.0	30.0	35.3
1.0	n	6	6	10	10	11
	\bar{N}_{xx}	117.7	117.2	87.3	48.4	0.0
	\bar{N}_{xy}	0.0	2.0	16.0	24.0	33.8
1.5	n	6	6	10	10	11
	\bar{N}_{xx}	93.7	93.2	73.6	37.8	0.0
	\bar{N}_{xy}	0.0	2.0	16.0	24.0	32.5

*The unit of the stress resultant is lbs./in.

Table 4.10 Critical Axial Compression-Torsion
Interaction Data* [Geometry I-1;
 $w^0(+)$, Eq. (8)]

$\xi \downarrow$	n	11	12	11	11	11
0.1	\bar{N}_{xx}	141.5	132.1	87.5	31.0	0.0
	\bar{N}_{xy}	0.0	10.0	20.0	30.0	35.3
0.5	n	11	11	11	11	11
	\bar{N}_{xx}	137.4	123.0	87.4	43.2	0.0
	\bar{N}_{xy}	0.0	8.0	16.0	24.0	31.6
1.0	n	11	12	11	11	11
	\bar{N}_{xx}	126.8	102.9	73.1	40.4	0.0
	\bar{N}_{xy}	0.0	7.0	14.0	21.0	28.3
1.5	n	11	11	11	12	11
	\bar{N}_{xx}	105.7	80.9	63.8	26.2	0.0
	\bar{N}_{xy}	0	7.0	14.0	21.0	25.4

*The unit of the stress resultant is lbs./in.

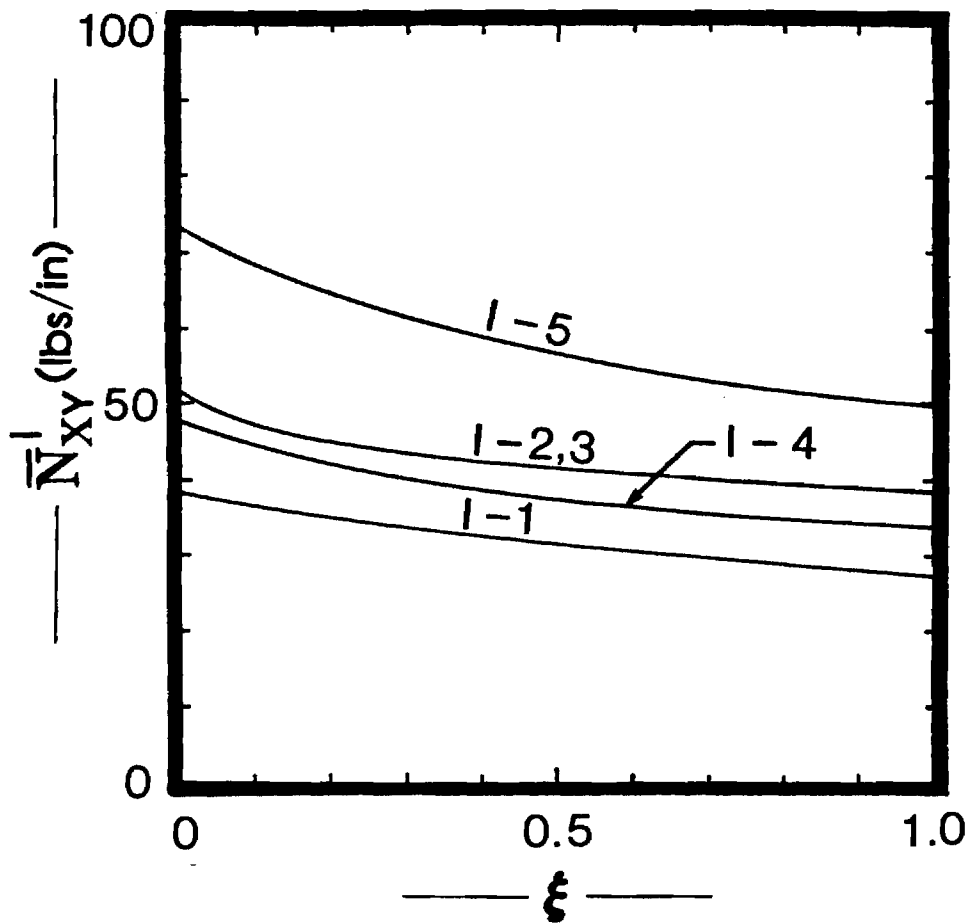


Fig. 4.8 Critical shear stress vs. Imperfection Amplitude [SS-3; $w^0(+)$. Eq. A-216]

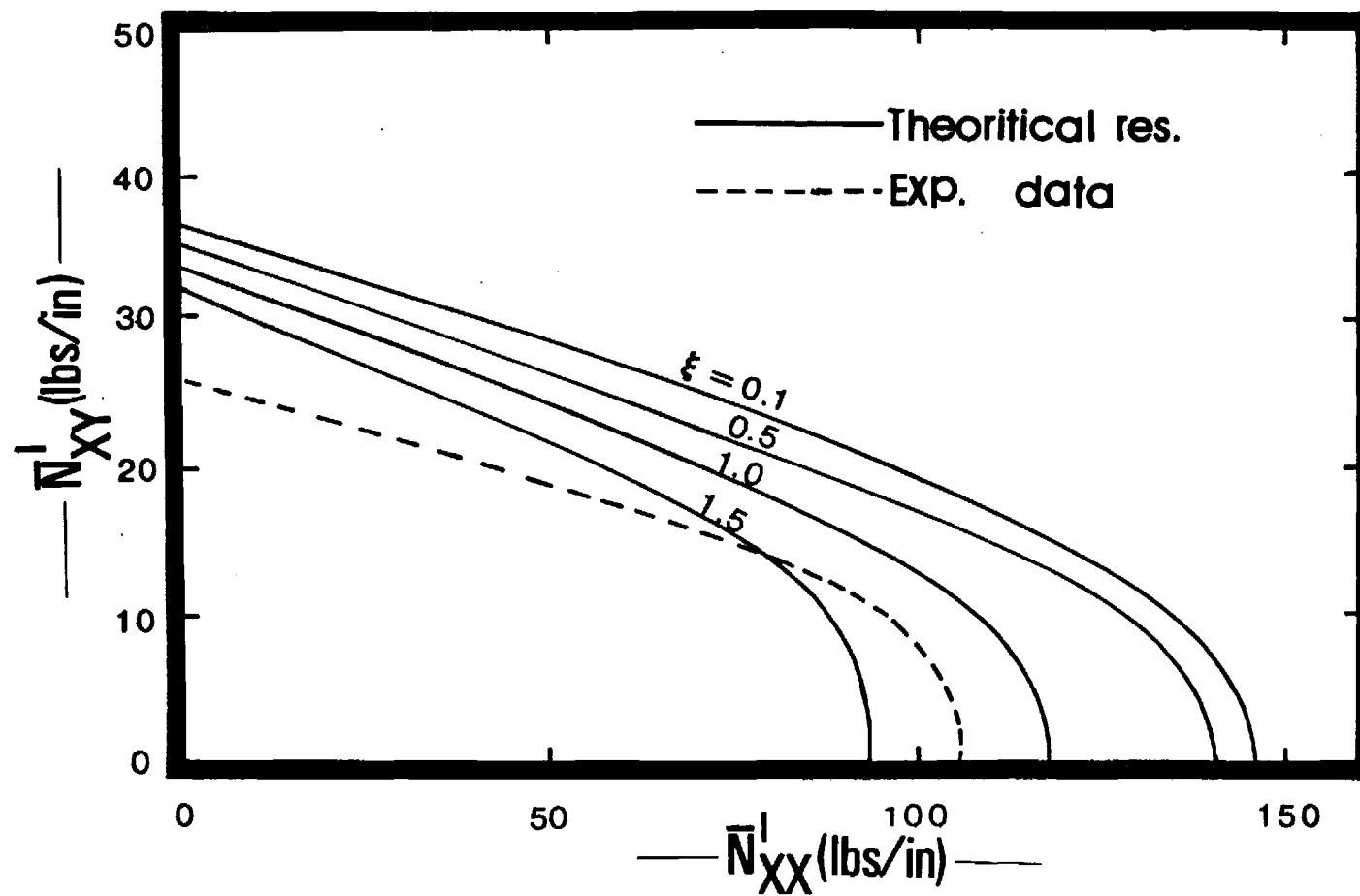


Fig. 4.9 Critical Interaction curves [Geometry I-1; Axisymmetric Imperfection, Eq. A-214,]

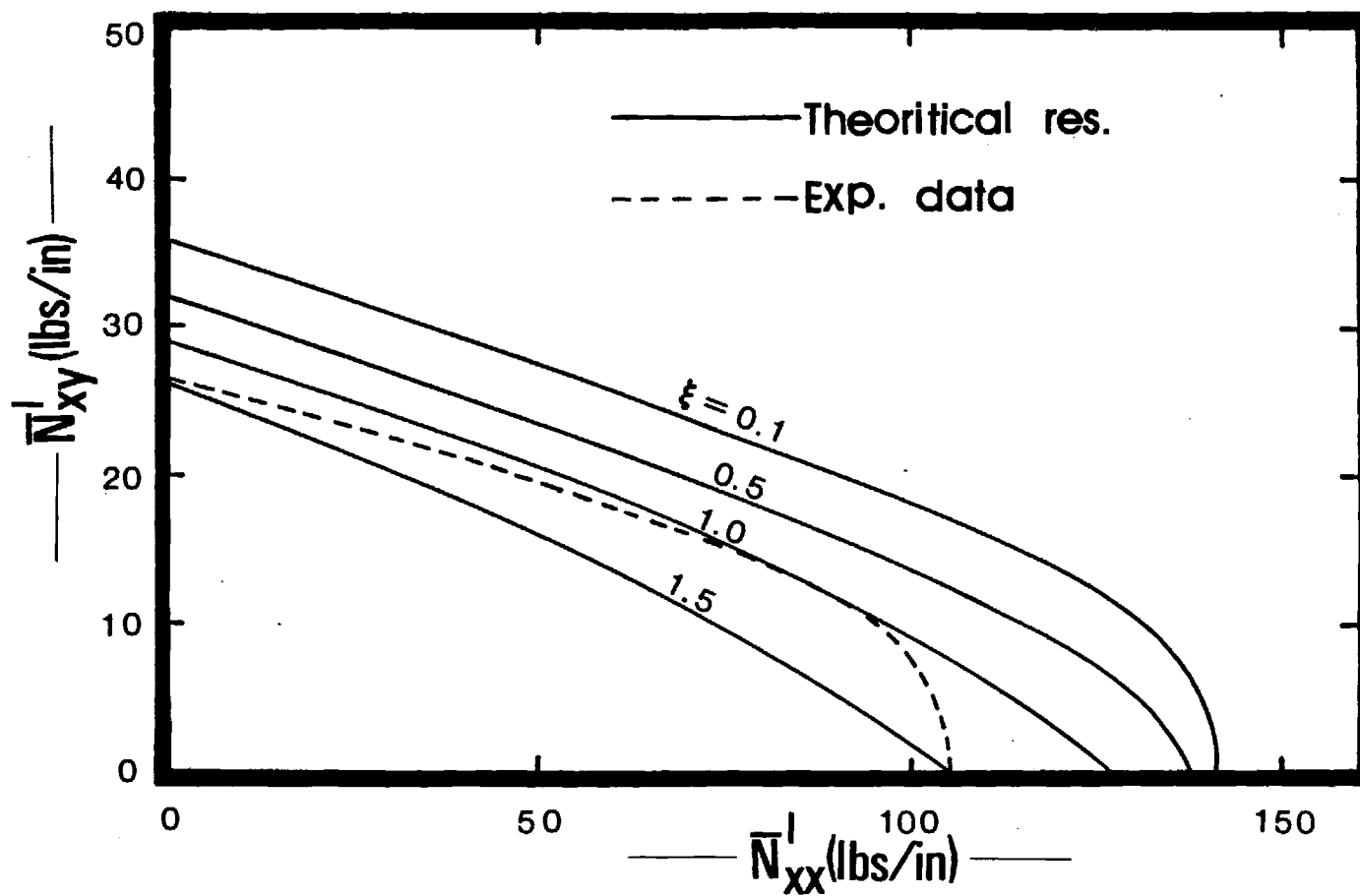


Fig. 4.10 Critical Interaction curves [Geometry I-1; Imperfection $w^0(+)$, Eq. A-216']

configuration is insensitive for positive torsion (fourth column) and rather sensitive for negative torsion (last column). Note that the experimental values (+ 26.5 lbs./in. and -65.72 lbs./in.), compare well with the theoretical values. Note that the tested specimen (44) is of unknown imperfection shape and amplitude.

Next, Table 4.8 presents critical shear stress resultants (and the minimizing n -value in parenthesis) for all five geometries and an imperfection shape similar to the positive torsion buckling mode of the perfect geometry, Eq. (8). These results are shown graphically on Fig. 4.8). Note that the strongest configuration corresponds to I-5, while the weakest to the symmetric geometry I-1. This conclusion holds true for the imperfection shape used, $w^0(+)$.

It is worth observing that the regular angle-ply antisymmetric geometries, I-2 and I-3, yield virtually the same strength for positive torsion and $w^0(+)$. Moreover, geometry I-4 is much weaker by comparison to the other asymmetric geometry (I-5) but not as weak as the symmetric geometry. These observations are reminiscent of the old external versus internal positioning of the orthogonal stiffeners controversy concerning metallic stiffened configurations. In relation to this, in the case of orthogonally stiffened complete spherical shells subjected to uniform pressure (see Ref. 48) it is observed that the weakest configuration corresponds to zero (or close to it) stiffener eccentricity, and the strength of the stiffened sphere increases as the eccentricity increases in either direction (inward or outward). Thus, one can conclude from Fig. 4.8 that all five configurations are imperfection sensitive, but not as sensitive as they are for the case of uniform axial compression (See Fig. 4.1). This conclusion is in line with the behavior of metallic cylindrical shells with or without stiffening members.

In Ref. 44, experiments are conducted for geometry I-1, to determine the interaction curve that separates the stable from the unstable region between uniform axial compression and torsion. Because of this, numerical results are obtained for geometry I-1 and two imperfection shapes. One is virtually axisymmetric, Eq. (6), and one similar to the (positive torsion) perfect geometry buckling mode, Eq. (8). The theoretical interaction curves are generated for several values of the imperfection amplitude parameter, ξ , by the following steps. First, the critical value for pure torsion is obtained. Then, starting with zero torsion and several values of the applied shear stress resultant, but smaller than the critical pure torsion the corresponding critical axial compression is obtained. In each combination a study of the effect of n is performed. The results are presented in tabular form on Tables 4.9 and 4.10 and graphically on Figs. 4.9 and 4.10.

The data of Table 4.9 are plotted on Fig. 4.9 and of Table 4.10 on Fig. 4.10. On both figures the experimental (44) interaction curve is shown by the dashed line. Not knowing what the imperfection shape and amplitude of the tested cylinder are, these plots may suggest a reasonable comparison between theory and test.

IV. 3.0 CONCLUSIONS

All of the conclusions are based on the generated results, which are obtained by the W, F-formulation. No results have, as yet, been generated by the u, v, w-formulation.

From all results, one may list the following as the most noteworthy conclusions.

1. Buckling, for all configurations, is of the violent type (snap through buckling through limit point instability).
2. For SS-3 boundary conditions and axial compression with zero eccentricity, the strongest configuration corresponds to the asymmetric configuration, I-5, while the weakest configuration corresponds to the antisymmetric configurations, I-2 and I-3.
3. Again for SS-3 and axial compression, the dynamic critical loads (lower bounds, when the corresponding static loads, but their values are never smaller than 60% of the static critical loads.
4. The average end shortening (for axial compression), corresponding to the limit point for the same ξ -value, is smaller for the asymmetric geometries (I-4, I-5) than for the symmetric (I-1) and antisymmetric (I-2 and I-3) geometries by almost a factor of three.
5. For the isotropic geometry (SS-i boundary conditions)
 - 5a: For the perfect configuration and very small imperfections, the effect of in-plane boundary conditions is such that SS-3 and SS-4 ($v = \text{const.}$) yield stronger configurations than SS-1 and SS-2 ($N_{xy} = -F_{,xy} = 0$)
 - 5b: For higher values of the imperfection amplitude, ξ , SS-2 and SS-4 ($u = \text{const.}$) yield stronger configurations than SS-1 and SS-3 ($N_{xx} = F_{,yy} - \bar{N}_{xx}$)

6. For the laminated geometry, the effect of in-plane boundary conditions for SS-i is the same as for the isotropic geometry. For clamped boundaries, CC-2 and CC-4 ($u = \text{const.}$) yield stronger configurations than CC-1 and CC-3, for the entire ξ -range.
7. For both geometries, I-5 and isotropic, the sensitivity to initial geometric imperfection is dependent upon the in-plane boundary conditions for SS-i. When $v = \text{const}$ (SS-1 and SS-2), the geometries are not very sensitive. On the other hand, when $u = \text{const}$ the geometries are very sensitive.
8. As far as the effect of load eccentricity on critical loads is concerned, no general conclusion can be drawn. But whatever the effect is (stabilizing or destabilizing for a given geometry), it diminishes with increasing value of the imperfection amplitude parameter (ξ -values).
9. When loaded in pure torsion, the strongest configuration corresponds to geometry I-5 (asymmetric), while the weakest corresponds to the symmetric geometry I-1, for the imperfection shape corresponding to the positive torsion buckling mode, $w^0(+)$.
10. Geometry I-1 is weaker when loaded in the positive direction than when loaded in the negative direction regardless of the imperfection shape (for all that were employed).
11. When loaded in pure torsion, laminated shell configurations are sensitive to initial geometric imperfections, but not as sensitive as when loaded in axial compression.
12. Comparison between theoretical predictions (corresponding to various imperfection amplitudes and shapes) and experimental results is reasonably good.

APPENDIX A

MATHEMATICAL FORMULATION

A. 1.0 Introduction

The governing equations are derived, in this section, for the following geometry and loading. The thin, circular, cylindrical shell is assumed to be geometrically imperfect. The construction is laminated (each lamina is orthotropic) and in addition, the shell is orthogonally and eccentrically stiffened. The stiffeners are uniform and with uniform close spacing, which allows one to employ the "smeared" technique. The boundary conditions can be of any transverse and in-plane variety. This includes free, simply-supported and clamped with all possible in-plane combinations. The loading consists of transverse (uniform lateral pressure) and eccentric in-plane loads, such as uniform axial compression and shear. Eccentric means that the line of action of these loads (applied stress resultants) is not necessarily in the plane of the reference surface. In the derivation of the governing equations, the usual lamination theory is employed. Moreover, thin shell theory (Kirchhoff-Love hypotheses) and linearly elastic behavior are assumed. The primary assumptions are listed below:

- (1) The shell is thin (total smeared thickness is much smaller than the initial average radius of curvature-cylinder radius).
- (2) Normals remain normal and inextensional.
- (3) The strains are small, the rotations about the normal are small and the rotations about in-plane axes are moderate.
- (4) The imperfection shape is such that the initial curvature is small $[R|w^0_{,ii} \ll 1; i = x, y]$.
- (5) The stiffness are along principal directions.
- (6) The stiffener-laminate connections are monolithic.

(7) The stiffeners do not carry shear; shear is entirely transmitted by the laminate .

(8) The stiffness are torsionally weak and thus they do not contribute to the shell twisting stiffness (the equations and related programs can easily be changed to accomodate the case of torsionally strong stiffeners).

On the basis of these general assumptions, two sets of field equations are derived. One, referred to as the w, F - formulation, is based on Donnell-type of kinematic relations. The governing equations consist of the transverse equilibrium equation and the in-plane compatibility equation. These two equations and the proper boundary conditions are expressed in terms of the transverse displacement component, w , and an Airy stress resultant function, F . The second, referred to as the u, v, w - formulation is based on Sanders' type of kinematic relations, those corresponding to small rotations about the normal and moderate rotations about in-plane axes. The governing equations for this case consist of the three equilibrium equations. These equations are expressed in terms of the three displacement components, u, v and w . Also, the proper boundary conditions are expressed in terms of u, v , and w . The corresponding Donnell approximation appears as a special case of the more general Sanders' kinematic relations. The derivation along with all necessary relations are presented separately for each formulation.

A. 2.0 The w, F - Formulation

The geometry and sign convention for this formulation are shown on Figs. A.1 and A.2.

The topics of kinematic relations, stress and moment resultants, governing equations, boundary conditions and solution procedure are treated separately.

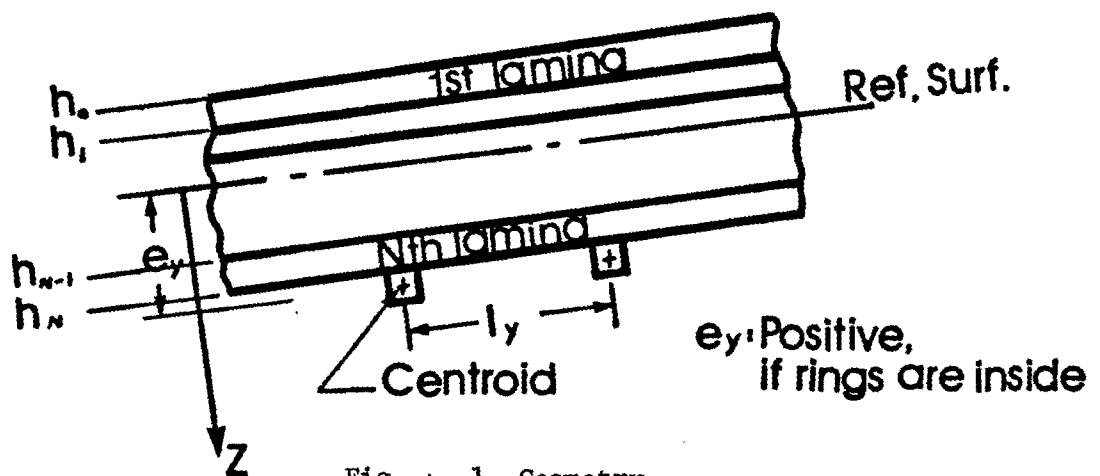
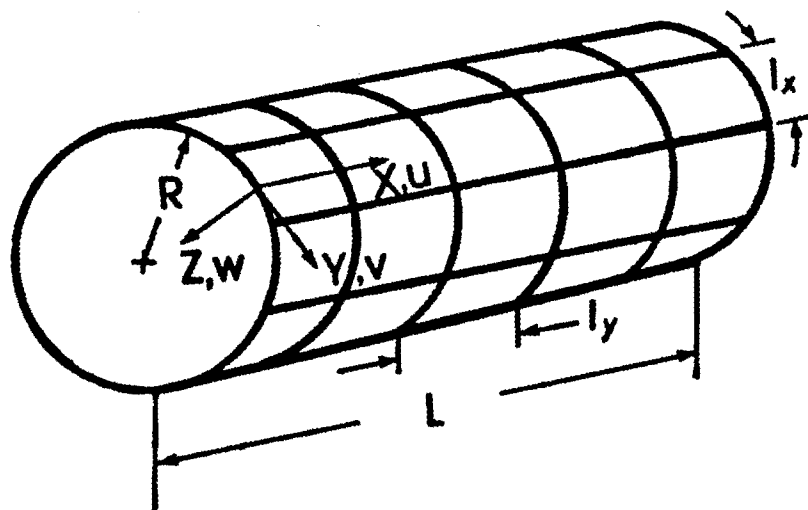
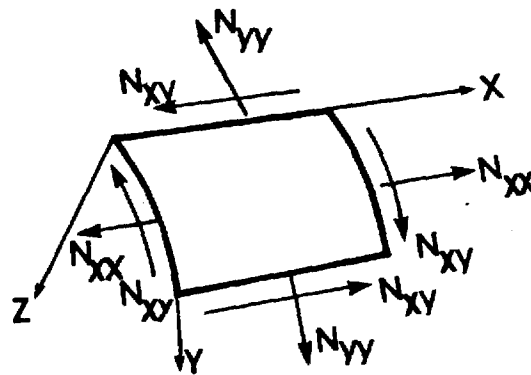
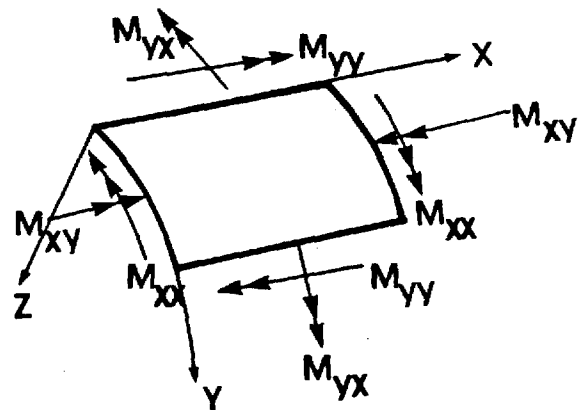


Fig. A. 1 Geometry



Stress Resultants



Moment Resultants

Fig. A.2 Sign Convention

A. 2.1 Kinematic Relations

Let w^0 be measured from the perfectly cylindrical surface to the refer surface of the laminated shell. Let w denote the transverse displacement component of reference surface material points and be measured from the undeformed surface. Let u and v denote the usual in-plane displacement components along the x and y directions respectively.

The Donnell-type (33) kinematic relations are given by

$$\begin{aligned}\epsilon_{xx} &= \epsilon_{xx}^0 - z \kappa_{xx} \\ \epsilon_{yy} &= \epsilon_{yy}^0 - z \kappa_{yy} \\ \gamma_{xy} &= \gamma_{xy}^0 - 2z \kappa_{xy}\end{aligned}\tag{A-1}$$

where the superscript "o" denotes reference surface strains and the κ 's denote the reference surface changes in curvature and torsion. Note that the positive z -direction is inward (see Fig. A.1).

According to Donnell the ϵ^0 's and κ 's are related to the displacement components by

$$\begin{aligned}\epsilon_{xx}^0 &= u_{,x} + \frac{1}{2} w_{,x}^2 + w_{,x} w_{,x}^0 \\ \epsilon_{yy}^0 &= v_{,y} - \frac{w}{R} + \frac{1}{2} w_{,y}^2 + w_{,y} w_{,y}^0 \\ \gamma_{xy}^0 &= u_{,y} + v_{,x} + w_{,x} w_{,y} + w_{,x} w_{,y}^0 + w_{,x}^0 w_{,y}\end{aligned}\tag{A-2}$$

$$\begin{aligned}\kappa_{xx} &= \varphi_{x,x} = (w_{,x})_{,x} = w_{,xx} \\ \kappa_{yy} &= \varphi_{y,y} = (w_{,y})_{,y} = w_{,yy} \\ \kappa_{xy} &= \varphi_{x,y} = \varphi_{y,x} = w_{,xy}\end{aligned}\tag{A-3}$$

A. 2.2 Stress-strain Relations

Each lamina is assumed to be orthotropic and the directions of orthotropy (1,2) make an angle θ with the in-plane axes (x,y) .

The orthotropic constitutive (it is assumed that the generalized Hooke's law holds) relations for the kth lamina are given below. Note that for an n-ply laminate k varies from one to n, and the first ply (or lamina) is on the outside, while the nth ply is on the inside (see Fig. A.1).

$$\begin{bmatrix} \sigma_{11} \\ \sigma_{22} \\ \sigma_{12} \end{bmatrix}^{(k)} = \begin{bmatrix} Q_{11} & Q_{12} & 0 \\ Q_{12} & Q_{22} & 0 \\ 0 & 0 & Q_{33} \end{bmatrix}^{(k)} \begin{bmatrix} \epsilon_{11} \\ \epsilon_{22} \\ 2\epsilon_{12} \end{bmatrix} \quad (A-4)$$

where $2\epsilon_{12} = \gamma_{12}$ and 1, 2 are the orthotropic directions.

Since one is interested in relating the stresses to the strains in the xy frame of axes, the usual transformation relation for second order tensors are employed (see Ref. 35 for details) and the transformed constitutive equations (for the kth ply) become

$$\begin{bmatrix} \sigma_{11} \\ \sigma_{22} \\ \sigma_{12} \end{bmatrix}^{(k)} = \begin{bmatrix} \bar{Q}_{11} & \bar{Q}_{12} & \bar{Q}_{13} \\ \bar{Q}_{12} & \bar{Q}_{22} & \bar{Q}_{23} \\ \bar{Q}_{13} & \bar{Q}_{23} & \bar{Q}_{33} \end{bmatrix}^{(k)} \begin{bmatrix} \epsilon_{xx} \\ \epsilon_{yy} \\ \epsilon_{xy} \end{bmatrix} \quad (A-5)$$

where

$$[\bar{Q}] = [T]^T [Q] [T] \quad (A-6)$$

and

$$[T] = \begin{bmatrix} \cos^2 \theta & \sin^2 \theta & \sin 2\theta \\ \sin^2 \theta & \cos^2 \theta & -\sin 2\theta \\ -\frac{1}{2} \sin 2\theta & \frac{1}{2} \sin 2\theta & \cos 2\theta \end{bmatrix} \quad (A-7)$$

Next, the stress-strain relations for the stiffeners are

$$\sigma_{xxst} = E_{st} \epsilon_{xx} \quad (A-8)$$

$$\sigma_{yyt} = E_r \epsilon_{yy}$$

where E_{st} and E_r denote the Young's moduli for stringer and ring material respectively. Note that according to the smeared technique assumptions, stiffeners do not transmit shear.

A. 2.3 Stress and Moment Resultants

Instead of dealing with stresses, it is more convenient in thin shell and plate theory to deal with integrated stresses. This leads to the introduction and definition of stress (N_{ij}) and moment (M_{ij}) resultants.

For a stiffened laminate these are

$$\begin{bmatrix} N_{xx} \\ N_{yy} \\ N_{xy} \end{bmatrix} = \int_{h_o}^{h_n} \begin{bmatrix} \sigma_{xx} \\ \sigma_{yy} \\ \sigma_{xy} \end{bmatrix} dz + \int_{A_i} \begin{bmatrix} \frac{\sigma_{xxst}}{\ell_x} dA_x \\ \frac{\sigma_{yyr}}{\ell_y} dA_y \\ 0 \end{bmatrix} \quad (A-9)$$

and

$$\begin{bmatrix} M_{xx} \\ M_{yy} \\ M_{xy} \end{bmatrix} = \int_{h_o}^{h_n} z \begin{bmatrix} \sigma_{xx} \\ \sigma_{yy} \\ \sigma_{xy} \end{bmatrix} dz + \int_{A_i} \begin{bmatrix} z \frac{\sigma_{xxst}}{\ell_x} dA_x \\ z \frac{\sigma_{yyr}}{\ell_y} dA_y \\ 0 \end{bmatrix} \quad (A-10)$$

where

ℓ_x and ℓ_y are the stringer and ring spacings (respectively), A_i denotes the proper stiffener cross-sectional area with A_x denoting stringer area and A_y ring area, and h_o h_n denote the outer surface and inner surface coordinate of the laminate (see Fig. A.1). Note also that the above definitions lead to the sign convention shown on Fig. A.2

Substitution of Eqs. A-5 and A-8 for the stresses in Eqs. A-9 and A-10 prior substitution of Eqs. A-1 for the strains in Eqs. A-5 and A-8 and performing some minor mathematical operations lead to

$$\begin{bmatrix} N_{xx} \\ N_{yy} \\ N_{xy} \end{bmatrix} = \sum_{k=1}^N [\bar{Q}]^{(k)} \int_{h_{k-1}}^{h_k} \left\{ \begin{bmatrix} \epsilon_{xx}^{\circ} \\ \epsilon_{yy}^{\circ} \\ \gamma_{xy}^{\circ} \end{bmatrix} - z \begin{bmatrix} \kappa_{xx} \\ \kappa_{yy} \\ 2\kappa_{xy} \end{bmatrix} \right\} dz$$

$$+ \begin{bmatrix} \frac{E_{st} A_x}{\ell_x} \epsilon_{xx}^{\circ} \\ \frac{E_r A_y}{\ell_y} \epsilon_{yy}^{\circ} \\ 0 \end{bmatrix} - \begin{bmatrix} \frac{E_{st} A_x}{\ell_x} e_x \kappa_{xx} \\ \frac{E_r A_y}{\ell_y} e_y \kappa_{yy} \\ 0 \end{bmatrix} \quad (A-11)$$

$$\begin{bmatrix} M_{xx} \\ M_{yy} \\ M_{xy} \end{bmatrix} = \sum_{k=1}^N [\bar{Q}]^{(k)} \int_{h_{k-1}}^{h_k} \left\{ z \begin{bmatrix} \epsilon_{xx}^{\circ} \\ \epsilon_{yy}^{\circ} \\ \gamma_{xy}^{\circ} \end{bmatrix} - z \begin{bmatrix} \kappa_{xx} \\ \kappa_{yy} \\ 2\kappa_{xy} \end{bmatrix} \right\} dz$$

$$+ \begin{bmatrix} \frac{E_{st} A_x}{\ell_x} e_x \epsilon_{xx}^{\circ} \\ \frac{E_r A_y}{\ell_y} e_y \epsilon_{yy}^{\circ} \\ 0 \end{bmatrix} - \begin{bmatrix} \frac{E_{st}}{\ell_x} (I_{xc} + A_x e_x^2) \\ \frac{E_r}{\ell_y} (I_{yc} + A_y e_y^2) \\ 0 \end{bmatrix} \quad (A-12)$$

where e_x e_y are the stiffener eccentricities (positive if on the side of

positive z) and I_{x_c} , I_{y_c} are the stiffener second moment of areas about centroidal axes.

After performing the indicated operation [Eqs. A-11 and A-12], one may write

$$\begin{bmatrix} N_{xx} \\ N_{yy} \\ N_{xy} \\ M_{xx} \\ M_{yy} \\ M_{xy} \end{bmatrix} = \begin{bmatrix} \bar{A}_{11} & \bar{A}_{12} & \bar{A}_{13} & -\bar{B}_{11} & -\bar{B}_{12} & -\bar{B}_{13} \\ \bar{A}_{12} & \bar{A}_{22} & \bar{A}_{23} & -\bar{B}_{12} & -\bar{B}_{22} & -\bar{B}_{23} \\ \bar{A}_{13} & \bar{A}_{23} & \bar{A}_{33} & -\bar{B}_{13} & -\bar{B}_{23} & -\bar{B}_{33} \\ \bar{B}_{11} & \bar{B}_{12} & \bar{B}_{23} & -\bar{D}_{11} & -\bar{D}_{12} & -\bar{D}_{13} \\ \bar{B}_{12} & \bar{B}_{22} & \bar{B}_{23} & -\bar{D}_{12} & -\bar{D}_{22} & -\bar{D}_{23} \\ \bar{B}_{13} & \bar{B}_{23} & \bar{B}_{33} & -\bar{D}_{13} & -\bar{D}_{23} & -\bar{D}_{33} \end{bmatrix} \begin{bmatrix} \epsilon_{xx}^0 \\ \epsilon_{yy}^0 \\ \gamma_{xy}^0 \\ \kappa_{xx} \\ \kappa_{yy} \\ \kappa_{xy} \end{bmatrix} \quad (A-13)$$

where

$$[\bar{A}_{ij}] = [A_{ij}] + \begin{bmatrix} \frac{E_{st} A_x}{l_x} & 0 & 0 \\ 0 & \frac{E_r A_y}{l_y} & 0 \\ 0 & 0 & 0 \end{bmatrix} \quad (A-14a)$$

$$[\bar{B}_{ij}] = [B_{ij}] + \begin{bmatrix} \frac{E_{st} A_x}{l_x} e_x & 0 & 0 \\ 0 & \frac{E_r A_y}{l_y} e_y & 0 \\ 0 & 0 & 0 \end{bmatrix} \quad (A-14b)$$

and

$$[\bar{D}_{ij}] = [D_{ij}] + \begin{bmatrix} \frac{E_{st}}{l_x} (I_{xc} + e_x^2 A_x) & 0 & 0 \\ 0 & \frac{E_r}{l_y} (I_{yc} + e_y^2 A_y) & 0 \\ 0 & 0 & 0 \end{bmatrix} \quad (A-14c)$$

with

$$\begin{aligned}
 A_{ij} &= \sum_{k=1}^N \bar{Q}_{ij}^{(k)} (h_k - h_{k-1}) \\
 B_{ij} &= \sum_{k=1}^N \bar{Q}_{ij}^{(k)} (h_k^2 - h_{k-1}^2) \\
 D_{ij} &= \sum_{k=1}^N \bar{Q}_{ij}^{(k)} (h_k^3 - h_{k-1}^3)
 \end{aligned} \tag{A-15}$$

Since, in the derivation of the field equation for this formulation, the dependent variable are, w and a stress function F (through which the stress resultants are derived), then it is convenient to express the moment resultants in terms of the N_{ij} 's and the ϵ 's.

Starting with Eqs. A-13, one may write

$$\begin{bmatrix} N_{xx} \\ N_{yy} \\ N_{xy} \end{bmatrix} = [\bar{A}_{ij}] \begin{bmatrix} \epsilon_{xx}^0 \\ \epsilon_{yy}^0 \\ \gamma_{xy}^0 \end{bmatrix} - [\bar{B}_{ij}] \begin{bmatrix} \kappa_{xx} \\ \kappa_{yy} \\ 2\kappa_{xy} \end{bmatrix} \tag{A-16}$$

From this, one can solve for the strain vector, or

$$\begin{bmatrix} \epsilon_{xx}^0 \\ \epsilon_{yy}^0 \\ \gamma_{xy}^0 \end{bmatrix} = [\bar{A}_{ij}]^{-1} \begin{bmatrix} N_{xx} \\ N_{yy} \\ N_{xy} \end{bmatrix} + [\bar{A}_{ij}]^{-1} [\bar{B}_{ij}] \begin{bmatrix} \kappa_{xx} \\ \kappa_{yy} \\ 2\kappa_{xy} \end{bmatrix} \tag{A-17}$$

Another form for this equation, Eq. (17), is the following

$$\begin{bmatrix} \epsilon_{xx}^0 \\ \epsilon_{yy}^0 \\ \gamma_{xy}^0 \end{bmatrix} = [a_{ij}] \begin{bmatrix} N_{xx} \\ N_{yy} \\ N_{xy} \end{bmatrix} + [\theta_{ij}] \begin{bmatrix} \kappa_{xx} \\ \kappa_{yy} \\ 2\kappa_{xy} \end{bmatrix} \tag{A-18}$$

where

$$[a_{ij}] = [\bar{A}_{ij}]^{-1} \quad [\theta_{ij}] = [\bar{A}_{ij}]^{-1} [\bar{B}_{ij}] \tag{A-19}$$

Next, substitution of Eqs. A-18 into the expression for the moment resultants, Eqs. A-13, yields

$$\begin{aligned}
 \begin{bmatrix} M_{xx} \\ M_{yy} \\ M_{xy} \end{bmatrix} &= [\bar{B}_{ij}] \begin{bmatrix} \epsilon_{xx}^0 \\ \epsilon_{yy}^0 \\ \gamma_{xy}^0 \end{bmatrix} - [\bar{D}_{ij}] \begin{bmatrix} \kappa_{xx} \\ \kappa_{yy} \\ 2\kappa_{xy} \end{bmatrix} \\
 &= [\bar{B}_{ij}][a_{ij}] \begin{bmatrix} N_{xx} \\ N_{yy} \\ N_{xy} \end{bmatrix} + [[\bar{B}_{ij}][b_{ij}] - [\bar{D}_{ij}]] \begin{bmatrix} \kappa_{xx} \\ \kappa_{yy} \\ 2\kappa_{xy} \end{bmatrix} \\
 &= [b_{ij}]^T \begin{bmatrix} N_{xx} \\ N_{yy} \\ N_{xy} \end{bmatrix} + [d_{ij}] \begin{bmatrix} \kappa_{xx} \\ \kappa_{yy} \\ 2\kappa_{xy} \end{bmatrix} \quad (A-20)
 \end{aligned}$$

where

$$[d_{ij}] = [\bar{B}_{ij}][b_{ij}] - [\bar{D}_{ij}] \quad (A-21)$$

Note that $[a_{ij}]$ and $[d_{ij}]$ are symmetric three by three matrices, while $[b_{ij}]$ is a nonsymmetric three by three matrix.

A. 2.4 Equilibrium Equations

The equilibrium equations are derived by employing the principle of the stationary value of the total potential.

According to the principle, for equilibrium

$$\delta U_T = 0 \quad (A-22)$$

where

$$U_T = U_i + U_p \quad (A-23)$$

the sum of the strain energy and the potential of the external forces.

From Eq. A-22 one may write

$$\begin{aligned}
\delta U_T &= \delta U_i + \delta U_p = 0 \\
&= \int_0^{2\pi R} \int_0^L (N_{xx} \delta \epsilon_{xx}^\circ + N_{yy} \delta \epsilon_{yy}^\circ + N_{xy} \delta \gamma_{xy}^\circ \\
&\quad - M_{xx} \delta \kappa_{xx} - M_{yy} \delta \kappa_{yy} - 2 M_{xy} \delta \kappa_{xy}) dx dy \\
&\quad - \int_0^{2\pi R} \int_0^L q \delta w dx dy - \int_0^{2\pi R} (-\bar{N}_{xx} \delta u + \bar{N}_{xy} \delta v \\
&\quad + \bar{Q}_x \delta w - \bar{M}_{xx} \delta w_{,x} - \bar{M}_{xy} \delta w_{,y}) \Big|_0^L dy \quad (A-24)
\end{aligned}$$

Where q denote the external pressure (positive in the positive z -direction) and the "bar" quantities denote external loads applied at the boundaries (\bar{N}_{xx} and \bar{N}_{xy} are in-plane loads, while Q_x is applied transverse shear load and \bar{M}_{xx} and \bar{M}_{xy} external moments). Note that \bar{M}_{xx} and \bar{M}_{xy} could represent moments arising from eccentrically applied \bar{N}_{xx} and \bar{N}_{xy} .

Use of Eqs. A-2 and A-3 for expressing the variations, in the reference surface strains and changes of curvature and torsion in terms of variations in displacement components yields

$$\begin{aligned}
\delta U_T &= \int_0^{2\pi R} \int_0^L \{ N_{xx} [\delta u_{,x} + w_{,x} \delta w_{,x} + w_{,x}^\circ \delta w_{,x}] \\
&\quad + N_{yy} [\delta v_{,y} - \frac{1}{R} \delta w + w_{,y} \delta w_{,y} + w_{,y}^\circ \delta w_{,y}] \\
&\quad + N_{xy} [\delta u_{,y} + \delta v_{,x} + w_{,x} \delta w_{,y} + w_{,y} \delta w_{,x} \\
&\quad + w_{,x}^\circ \delta w_{,y} + w_{,y}^\circ \delta w_{,x}] - M_{xx} \delta w_{,xx} - M_{yy} \delta w_{,yy} \\
&\quad - 2 M_{xy} \delta w_{,xy} \} dx dy - \int_0^{2\pi R} \int_0^L q \delta w dx dy \\
&\quad - \int_0^{2\pi R} \int_0^L [-\bar{N}_{xx} \delta u + \bar{N}_{xy} \delta v + \bar{Q}_x \delta w - \bar{M}_{xx} \delta \varphi_x \\
&\quad - \bar{M}_{xy} \delta \varphi_y] \Big|_0^L dy \quad (A-25)
\end{aligned}$$

Re-writing the above in a convenient form in order to use Green's theorem, one may write

$$\begin{aligned}
\delta U_T = & \int_0^{2\pi R} \int_0^L \left\{ [N_{xx} \delta u + N_{xx}(w_{,x} + w_{,x}^{\circ}) \delta w \right. \\
& + N_{xy}(w_{,y} + w_{,y}^{\circ}) \delta w - M_{xx} \delta w_{,x}]_{,x} \\
& + [N_{yy} \delta v + N_{yy}(w_{,y} + w_{,y}^{\circ}) \delta w + N_{xy} \delta u \\
& + N_{xy}(w_{,x} + w_{,x}^{\circ}) \delta w - M_{yy} \delta w_{,y}]_{,y} \\
& - [N_{xx,x} \delta u + [N_{xx}(w_{,x} + w_{,x}^{\circ})]_{,x} \delta w \\
& + N_{xy,x} \delta v + [N_{xy}(w_{,y} + w_{,y}^{\circ})]_{,x} \delta w \\
& - M_{xx,x} \delta w + N_{yy,y} \delta v + [N_{yy}(w_{,y} \\
& + w_{,y}^{\circ})]_{,y} \delta w + N_{xy,y} \delta u \\
& + [N_{xy}(w_{,x} + w_{,x}^{\circ})]_{,y} \delta w - M_{yy,y} \delta w_{,y}] \\
& \left. - \frac{N_{yy}}{R} \delta w - 2M_{xy} \delta w_{,xy} \right\} dx dy \\
& - \int_0^{2\pi R} \int_0^L q \delta w dx dy - \int_0^{2\pi R} [-\bar{N}_{xx} \delta u + \bar{N}_{xy} \delta v \\
& + \bar{Q}_x \delta w - \bar{M}_{xx} \delta \varphi_x - \bar{M}_{xy} \delta \varphi_y] \Big|_0^L dy
\end{aligned}$$

$$\begin{aligned}
&= \int_0^{2\pi R} \int_0^L \left\{ \left[N_{xx} \delta u + N_{xx} (w_{,x} + w_{,x}^{\circ}) \delta w + N_{xy} \delta v + N_{xy} (w_{,y} \right. \right. \\
&\quad \left. \left. + w_{,y}^{\circ}) \delta w - M_{xx} \delta w_{,x} + M_{xx,x} \delta w + 2M_{xy,y} \delta w \right]_{,x} \right. \\
&\quad \left. + \left[N_{yy} \delta v + N_{yy} (w_{,y} + w_{,y}^{\circ}) \delta w + N_{xy} \delta u \right. \right. \\
&\quad \left. \left. + N_{xy} (w_{,x} + w_{,x}^{\circ}) \delta w - M_{yy} \delta w_{,y} + M_{yy,y} \delta w \right. \right. \\
&\quad \left. \left. + 2M_{xy,x} \delta w \right]_{,y} - \left[N_{xx,x} \delta u + \left[N_{xx} (w_{,x} + w_{,x}^{\circ}) \right]_{,x} \delta w \right. \right. \\
&\quad \left. \left. + N_{xy,x} \delta v + \left[N_{xy} (w_{,y} + w_{,y}^{\circ}) \right]_{,x} \delta u \right. \right. \\
&\quad \left. \left. + M_{xx,xx} \delta w + N_{yy,y} \delta v + \left[N_{yy} (w_{,y} + w_{,y}^{\circ}) \right]_{,y} \delta w \right. \right. \\
&\quad \left. \left. + N_{xy,y} \delta u + \left[N_{xy} (w_{,x} + w_{,x}^{\circ}) \right]_{,y} \delta w \right. \right. \\
&\quad \left. \left. + M_{yy,yy} \delta w \right] - \frac{N_{yy}}{R} \delta w \right. \\
&\quad \left. - 2M_{xy,xy} \delta w \right\} dx dy \\
&\quad - \int_0^{2\pi R} \int_0^L q \delta w dx dy - \int_0^{2\pi R} \left[-\bar{N}_{xx} \delta u + \bar{N}_{xy} \delta v \right. \\
&\quad \left. + \bar{Q}_x \delta w - \bar{M}_{xx} \delta \varphi_x - \bar{M}_{xy} \delta \varphi_y \right] \Big|_0^L dy \tag{A-26}
\end{aligned}$$

By Green's theorem, one obtains the following equilibrium equations and associated boundary terms,

Equilibrium Equations

$$N_{xx,x} + N_{xy,y} = 0$$

$$N_{xy,x} + N_{yy,y} = 0$$

$$M_{xx,xx} + 2M_{xy,xy} + M_{yy,yy} + \frac{N_{yy}}{R} + N_{xx}(w_{,xx} + w_{,xx}^{\circ}) + 2N_{xy}(w_{,xy} + w_{,xy}^{\circ}) + N_{yy}(w_{,yy} + w_{,yy}^{\circ}) + q = 0 \quad (A-27)$$

Boundary Terms

either

$$N_{xx} = -\bar{N}_{xx}$$

$$N_{xy} = \bar{N}_{xy}$$

$$N_{xx}(w_{,x} + w_{,x}^{\circ}) + N_{xy}(w_{,y} + w_{,y}^{\circ})$$

$$+ M_{xx,x} + 2M_{xy,y} = \bar{Q}_x + \bar{M}_{xy,y}$$

$$M_{xx} = \bar{M}_{xx}$$

or

$$\delta U = 0$$

$$\delta V = 0$$

$$\delta W = 0$$

$$\delta W_{,x} = 0 \quad (A-28)$$

The first two equilibrium equations, Eqs. A-27 can be identically satisfied through the introduction of the following stress function

$$N_{xx} = F_{,yy} - \bar{N}_{xx}$$

$$N_{yy} = F_{,xx}$$

$$N_{xy} = -F_{,xy} + \bar{N}_{xy} \quad (A-29)$$

With the introduction of the stress function, F, the third equilibrium equation becomes

$$M_{xx,xx} + 2M_{xy,xy} + M_{yy,yy} + \frac{1}{R}F_{,xx} + F_{,yy}(w_{,xx} + w_{,xx}^{\circ}) + F_{,xx}(w_{,yy} + w_{,yy}^{\circ}) - 2F_{,xy}(w_{,xy} + w_{,xy}^{\circ}) - \bar{N}_{xx}(w_{,xy} + w_{,xy}^{\circ}) + 2\bar{N}_{xy}(w_{,xy} + w_{,xy}^{\circ}) + q = 0 \quad (A-30)$$

A. 2.5 Compatibility Equation

Since the in-plane equilibrium equations are identically satisfied with the introduction of the Airy stress function, F, then the governing equations

consist of the transverse equilibrium equation, Eq. A-30 and one more. This one more results from requiring compatibility of the in-plane displacement components u and v . From Eqs. A-2 one obtains

$$\begin{aligned}\epsilon_{xx,yy}^{\circ} &= \mathcal{U}_{,xyy} + \frac{1}{2} W_{,xyy} (W_{,x} + 2W_{,x}^{\circ}) + \frac{1}{2} W_{,x} (W_{,xyy} + 2W_{,xyy}^{\circ}) \\ \epsilon_{yy,xx}^{\circ} &= \mathcal{V}_{,yxx} - \frac{W_{,xx}}{R} + \frac{1}{2} (2W_{,y} W_{,yxx} + 2W_{,yxx} W_{,y}^{\circ} + 2W_{,y} W_{,yxx}^{\circ}) \\ \gamma_{xy,xy}^{\circ} &= \mathcal{U}_{,xyy} + \mathcal{V}_{,xxy} + W_{,xxy} W_{,y} + W_{,x} W_{,xyy} + W_{,xyy} W_{,x}^{\circ} \\ &\quad + W_{,y} W_{,xxy}^{\circ} + W_{,xxy} W_{,y}^{\circ} + W_{,x} W_{,xyy}^{\circ}\end{aligned}\quad (A-31)$$

Elimination of u and v leads to the following compatibility equation

$$\begin{aligned}\epsilon_{xx,yy}^{\circ} + \epsilon_{yy,xx}^{\circ} - \gamma_{xy,xy}^{\circ} &= -\frac{W_{,xx}}{R} + W_{,xy} (W_{,xy} + 2W_{,xy}^{\circ}) \\ &\quad - \frac{1}{2} W_{,xx} (W_{,yy} + 2W_{,yy}^{\circ}) - \frac{1}{2} W_{,yy} (W_{,xx} + 2W_{,xx}^{\circ})\end{aligned}\quad (A-32)$$

Substitution of Eqs. A-18 [Eqs. A-29 for the N 's and Eqs. A-3 for the n 's] into the compatibility equation, Eq. A-32, yields

$$\begin{aligned}& a_{11} F_{,yyyy} + a_{12} F_{,xxyy} - a_{13} F_{,xyyy} + \theta_{11} W_{,xxyy} + \theta_{12} W_{,yyyy} + 2\theta_{13} W_{,xyyy} \\ & + a_{12} F_{,xxyy} + a_{22} F_{,xxxx} - a_{23} F_{,xxxy} + \theta_{21} W_{,xxxx} + \theta_{22} W_{,xxyy} + 2\theta_{23} W_{,xxxy} \\ & - a_{13} F_{,xyyy} - a_{23} F_{,xxxy} + a_{33} F_{,xxyy} - \theta_{31} W_{,xxxy} - \theta_{32} W_{,xyyy} - 2\theta_{33} W_{,xxyy} \\ & = -\frac{W_{,xx}}{R} + W_{,xy} (W_{,xy} + 2W_{,xy}^{\circ}) - \frac{1}{2} W_{,xx} (W_{,yy} + 2W_{,yy}^{\circ}) - \frac{1}{2} W_{,yy} (W_{,xx} + 2W_{,xx}^{\circ})\end{aligned}\quad (A-33)$$

Similarly, substitution of Eqs. A-19 into the transverse equilibrium equation, Eq. A-30, yields

$$\begin{aligned}
& \theta_{11} F_{,xxyy} + \theta_{21} F_{,xxxx} - \theta_{31} F_{,xxyy} + d_{11} W_{,xxxx} + d_{12} W_{,xxy} + 2d_{13} W_{,xxx} \\
& + 2\theta_{13} F_{,xyyy} + 2\theta_{23} F_{,xxyy} - 2\theta_{33} F_{,xxyy} + 2d_{31} W_{,xxx} + 2d_{32} W_{,xyy} + 4d_{33} W_{,xxy} \\
& + \theta_{12} F_{,yyyy} + \theta_{22} F_{,xxyy} - \theta_{32} F_{,xyyy} + d_{21} W_{,xxy} + d_{22} W_{,yyy} + 2d_{23} W_{,xyy} \\
& + \frac{1}{R} F_{,xx} + F_{,yy} (W_{,xx} + W_{,xx}^{\circ}) - \bar{N}_{xx} (W_{,xx} + W_{,xx}^{\circ}) \\
& + 2 \bar{N}_{xy} (W_{,xy} + W_{,xy}^{\circ}) - 2F_{,xy} (W_{,xy} + W_{,xy}^{\circ}) + F_{,xx} (W_{,yy} + W_{,yy}^{\circ}) \\
& + \mathcal{G} = 0 \tag{A-34}
\end{aligned}$$

A. 2.6 Boundary Conditions

The boundary conditions, Eqs. A-28, can be designated according to transverse one (simply supported, clamped, free) and in-plane ones. Since all of the application to be considered deal with supported boundaries, only simply supported (ss-i; i = 1, 2, 3, 4) and clamped (cc-i) boundary conditions are listed. These are (at $x = 0, L$):

$$\begin{aligned}
SS-1: & \quad W = 0 ; M_{xx} = \bar{M}_{xx} ; N_{xx} = -\bar{N}_{xx} ; N_{xy} = \bar{N}_{xy} \\
SS-2: & \quad W = 0 ; M_{xx} = \bar{M}_{xx} ; u = \text{Const.} ; N_{xy} = \bar{N}_{xy} \\
SS-3: & \quad W = 0 ; M_{xx} = \bar{M}_{xx} ; N_{xx} = -\bar{N}_{xx} ; v = \text{Const.} \\
SS-4: & \quad W = 0 ; M_{xx} = \bar{M}_{xx} ; u = \text{Const.} ; v = \text{Const.} \tag{A-35}
\end{aligned}$$

and

$$CC-1: \quad W=0 \quad ; \quad W_{,x}=0 \quad ; \quad N_{xx}=-\bar{N}_{xx} \quad ; \quad N_{xy}=\bar{N}_{xy}$$

$$CC-2: \quad W=0 \quad ; \quad W_{,x}=0 \quad ; \quad u = \text{Const.} \quad ; \quad N_{xy}=\bar{N}_{xy}$$

$$CC-3: \quad W=0 \quad ; \quad W_{,x}=0 \quad ; \quad N_{xx}=-\bar{N}_{xx} \quad ; \quad v = \text{Const.}$$

$$CC-4: \quad W=0 \quad ; \quad W_{,x}=0 \quad ; \quad u = \text{Const.} \quad ; \quad v = \text{Const.} \quad (A-36)$$

The above boundary conditions may be written in terms of the dependent variables F , and w . The kinematic conditions $u = \text{const}$ and $v = \text{const}$ are first expressed in terms of equivalent conditions. This is shown below for each of the relevant conditions separately.

Note, first that the expressions for the M_{ij} 's and N_{ij} 's are given by Eqs. A-20 and A-29.

$$\underline{SS-1}: \quad W=0$$

$$\theta_{21}F_{,xx} + d_{11}W_{,xx} + 2d_{13}W_{,xy} = \bar{M}_{xx} + \theta_{11}\bar{N}_{xx} - \theta_{31}\bar{N}_{xy}$$

$$F_{,yy}=0 \quad \text{and} \quad F_{,xy}=0 \quad (A-37)$$

$$\underline{SS-2}: \quad W=0$$

$$\theta_{11}F_{,yy} + \theta_{21}F_{,xx} + d_{11}W_{,xx} + 2d_{13}W_{,xy} = \bar{M}_{xx} + \theta_{11}\bar{N}_{xx} - \theta_{31}\bar{N}_{xy}$$

$$F_{,yy}=0 \quad \text{and} \quad F_{,xy}=0 \quad (A-38)$$

The $u = \text{const.}$ condition is expressed in terms of an equivalent condition by employing the following steps.

The expressions for γ_{xy} from the kinematic relations, Eqs. A-2, and from the constitutive equations, Eqs. A-18, are first equated to each other,

or

$$\begin{aligned} \gamma_{xy}^0 &= u_{,y} + v_{,x} + w_{,x}w_{,y} + w_{,x}w_{,y}^0 + w_{,x}^0w_{,y} \\ &= a_{13}(F_{,yy} - \bar{N}_{xx}) + a_{23}F_{,xx} + a_{33}(\bar{N}_{xy} - F_{,xy}) \\ &\quad + \theta_{31}W_{,xx} + \theta_{32}W_{,yy} + 2\theta_{33}W_{,xy} \end{aligned} \quad (A-38a)$$

One differentiation with respect to y and use of the conditions $w = 0$ and $F_{,xy} = 0$ yields at $x = 0, L$

$$U_{,xy} + W_{,xy} W_{,y}^{\circ} + W_{,x} W_{,yy}^{\circ} = a_{13} F_{,yyy} + a_{23} F_{,xxy} + \theta_{31} W_{,xxy} + 2\theta_{33} W_{,xyy} \quad (A-38b)$$

Similarly,

$$\begin{aligned} E_{,yy} &= U_{,y} - \frac{W}{R} + \frac{1}{2} W_{,y}^2 + W_{,y} W_{,y}^{\circ} \\ &= a_{12} (F_{,yy} - \bar{N}_{xx}) + a_{22} F_{,xx} + a_{23} (\bar{N}_{xy} - F_{,xy}) \\ &\quad + \theta_{21} W_{,xx} + \theta_{22} W_{,yy} + 2\theta_{23} W_{,xy} \end{aligned} \quad (A-39a)$$

from which one differentiation with respect to x yields

$$\begin{aligned} U_{,yx} - \frac{W_{,x}}{R} + W_{,xy} W_{,y}^{\circ} &= a_{22} F_{,xxx} - a_{23} F_{,xxy} + 2\theta_{23} W_{,xxy} \\ &\quad + \theta_{21} W_{,xxx} + \theta_{22} W_{,xyy} \end{aligned} \quad (A-39b)$$

Elimination of $v_{,xy}$ and $v_{,yx}$ from Eqs. (A-38) and (A-39) yields the equivalent (to $u = \text{const}$) boundary term, which is:

$$\begin{aligned} a_{13} F_{,yyy} + 2a_{23} F_{,xxy} - a_{22} F_{,xxx} - \frac{W_{,x}}{R} - W_{,x} W_{,yy}^{\circ} - \theta_{21} W_{,xxx} \\ + (\theta_{31} - 2\theta_{23}) W_{,xxy} - (\theta_{22} - 2\theta_{33}) W_{,xyy} = 0 \end{aligned}$$

Note that because $F_{,xy} = 0$ for this boundary condition, the term containing $F_{,xy}$ has been dropped.

Thus, for SS-2 the final form of the boundary terms becomes

$$W = 0$$

$$\theta_{11} F_{,yy} + \theta_{21} F_{,xx} + \theta_{11} W_{,xx} + 2d_{13} W_{,xy} = \bar{M}_{xx} + \theta_{11} \bar{N}_{xx} - \theta_{31} \bar{N}_{xy}$$

$$F_{,xy} = 0$$

$$\begin{aligned} a_{13} F_{,yyy} + 2a_{23} F_{,xxy} - a_{22} F_{,xxx} - \frac{W_{,x}}{R} - W_{,x} W_{,yy}^{\circ} - \theta_{21} W_{,xxx} \\ + (\theta_{31} - 2\theta_{23}) W_{,xxy} - (\theta_{22} - 2\theta_{33}) W_{,xyy} = 0 \end{aligned} \quad (A-40)$$

SS-3

$$W = 0$$

$$\theta_{11} F_{,yy} + \theta_{21} F_{,xx} + d_{11} W_{,xx} + 2d_{13} W_{,xy} - \theta_{31} F_{,xy} = \bar{M}_{xx} + \theta_{11} \bar{N}_{xx} - \theta_{31} \bar{N}_{xy}$$

$$F_{,yy} = 0 \quad \text{and} \quad v = \text{Const.}$$

Similarly, as in the case of SS-2 ($u = \text{const}$), an equivalent condition is obtained for $v = \text{const}$. From Eq.A-39a., since $w = 0$ and $v_{,y} = 0$, then the equivalent condition becomes $\epsilon_{yy} = 0$ or

$$-a_{12} \bar{N}_{xx} + a_{22} F_{,xx} + a_{23} (\bar{N}_{xy} - F_{,xy}) + \theta_{21} W_{,xx} + 2\theta_{23} W_{,xy} = 0$$

Thus for SS-3 the final form of the boundary term becomes

$$W = 0$$

$$\theta_{21} F_{,xx} + d_{11} W_{,xx} + 2d_{13} W_{,xy} - \theta_{31} F_{,xy} = \bar{M}_{xx} + \theta_{11} \bar{N}_{xx} - \theta_{31} \bar{N}_{xy}$$

$$F_{,yy} = 0$$

$$a_{22} F_{,xx} - a_{23} F_{,xy} + \theta_{21} W_{,xx} + 2\theta_{23} W_{,xy} = a_{12} \bar{N}_{xx} - a_{23} \bar{N}_{xy} \quad (A-41)$$

SS-4

For this case the equivalent set of the boundary terms becomes

$$W = 0$$

$$\theta_{11} F_{,yy} + \theta_{21} F_{,xx} - \theta_{31} F_{,xy} + d_{11} W_{,xx} + 2d_{13} W_{,xy} = \bar{M}_{xx} + \theta_{11} \bar{N}_{xx} - \theta_{31} \bar{N}_{xy}$$

$$a_{22} F_{,xx} + a_{12} F_{,yy} - a_{23} F_{,xy} + \theta_{21} W_{,xx} + 2\theta_{23} W_{,xy} = a_{12} \bar{N}_{xx} - a_{23} \bar{N}_{xy}$$

$$a_{13} F_{,yyy} + 2a_{23} F_{,xxy} - (a_{12} + a_{33}) F_{,xyy} - a_{22} F_{,xxx} - \frac{W_{,x}}{R} - W_{,x} W_{,yy}^0 + (2\theta_{33} - \theta_{22}) W_{,xyy} + (\theta_{31} - 2\theta_{23}) W_{,xxy} - \theta_{21} W_{,xxx} = 0 \quad (A-42)$$

Following similar steps, boundary conditions CC-i, $i = 1, 2, 3$ and 4, are also expressed in terms of w and F only, or

CC-1

$$W = W_{,x} = F_{,yy} = F_{,xy} = 0 \quad (A-43)$$

CC-2

$$W = W_{,x} = F_{,xy} = 0$$

$$a_{13} F_{,yyy} + 2a_{23} F_{,xxy} - a_{22} F_{,xxx} - \theta_{21} W_{,xxx} + (\theta_{31} - 2\theta_{23}) W_{,xxy} = 0 \quad (A-44)$$

CC-3

$$W = W_{,x} = F_{,yy} = 0$$

$$a_{22} F_{,xx} - a_{23} F_{,xy} + \theta_{21} W_{,xx} = a_{12} \bar{N}_{xx} - a_{23} \bar{N}_{xy} \quad (A-45)$$

CC-4

$$W = W_{,x} = 0$$

$$a_{12} F_{,yy} + a_{22} F_{,xx} - a_{23} F_{,xy} + \theta_{21} W_{,xx} = a_{12} \bar{N}_{xx} - a_{23} \bar{N}_{xy}$$

$$a_{13} F_{,yyy} + 2a_{23} F_{,xxy} - (a_{12} + a_{33}) F_{,xyy} - a_{22} F_{,xxx} - \theta_{21} W_{,xxx} + (\theta_{31} - 2\theta_{23}) W_{,xxy} = 0 \quad (A-46)$$

II. 2.7 Solution Methodology - Field Equation

The solution methodology is an improvement and modification of the one employed and outlined in Refs. 36 and 37.

The separated form, shown below, is used for the two dependent variables $w(x, y)$ and $F(x, y)$.

$$F(x, y) = C_0(x) + \sum_{i=1}^{2K} \left[C_i(x) \cos \frac{iny}{R} + D_i(x) \sin \frac{iny}{R} \right]$$
$$W(x, y) = A_0(x) + \sum_{i=1}^K \left[A_i(x) \cos \frac{iny}{R} + B_i(x) \sin \frac{iny}{R} \right] \quad (A-47)$$

where n denotes the circumferential wave number.

In addition, similar expression can be employed for the imperfection parameter $w^0(x, y)$ and the external pressure $q(x, y)$. Note that in most applications the pressure is assumed uniform (q_0 only).

$$W^0(x, y) = A_0^0(x) + \sum_{i=1}^K \left[A_i^0(x) \cos \frac{iny}{R} + B_i^0(x) \sin \frac{iny}{R} \right]$$
$$q(x, y) = q_0'(x) + \sum_{i=1}^K \left[q_i^1(x) \cos \frac{iny}{R} + q_i^2(x) \sin \frac{iny}{R} \right] \quad (A-48)$$

Because of the nonlinearity of the field equations, Eqs. A-33 and A-34, substitution of Eqs. A-47, and A-48 into them yields double summations for the trigonometric functions. These double summations involve products of sine and cosine of iny/R in all four possible combinations (cosine-cosine, sine-cosine, cosine-sine, and sine-sine). Furthermore, these products have different origins. Some of them come from products of $W_{,xy}$, $W_{,xy}$, others from products of $F_{,xx}$, $W_{,yy}$ [see Eqs. A-33 and A-34]. In order to simplify the final expressions (and use single sums instead of double sums), and in order to cover all possible combinations of double sums, the following simplifying equations are presented. These are based on trigonometric identities involving products.

$$\sum_{i=0}^K \sum_{j=0}^L [j b_j \cos j\theta] a_i i \cos i\theta = \sum_{i=0}^{K+L} A_{IJ1(K)}^i(b, a) \cos i\theta$$

$$\sum_{i=0}^K \sum_{j=0}^L [j b_j \cos j\theta] a_i i \sin i\theta = \sum_{i=0}^{K+L} A_{IJ2(K)}^i(b, a) \sin i\theta$$

$$\sum_{i=0}^K \sum_{j=0}^L [j b_j \sin j\theta] a_i i \cos i\theta = \sum_{i=0}^{K+L} A_{IJ3(K)}^i(b, a) \sin i\theta$$

$$\sum_{i=0}^K \sum_{j=0}^L [j b_j \sin j\theta] a_i i \sin i\theta = \sum_{i=0}^{K+L} A_{IJ4(K)}^i(b, a) \cos i\theta \quad (A-49)$$

$$\sum_{i=0}^K \sum_{j=0}^L [b_j \cos j\theta] a_i i^2 \cos i\theta = \sum_{i=0}^{K+L} A_{I21(K)}^i(b, a) \cos i\theta$$

$$\sum_{i=0}^K \sum_{j=0}^L [b_j \cos j\theta] a_i i^2 \sin i\theta = \sum_{i=0}^{K+L} A_{I22(K)}^i(b, a) \sin i\theta$$

$$\sum_{i=0}^K \sum_{j=0}^L [b_j \sin j\theta] a_i i^2 \cos i\theta = \sum_{i=0}^{K+L} A_{I23(K)}^i(b, a) \sin i\theta$$

$$\sum_{i=0}^K \sum_{j=0}^L [b_j \sin j\theta] a_i i^2 \sin i\theta = \sum_{i=0}^{K+L} A_{I24(K)}^i(b, a) \cos i\theta \quad (A-50)$$

$$\sum_{i=0}^K \sum_{j=0}^L [j^2 b_j \cos j\theta] a_i \cos i\theta = \sum_{i=0}^{K+L} A_{J21(K)}^i(b, a) \cos i\theta$$

$$\sum_{i=0}^K \sum_{j=0}^L [j^2 b_j \cos j\theta] a_i \sin i\theta = \sum_{i=0}^{K+L} A_{J22(K)}^i(b, a) \sin i\theta$$

$$\sum_{i=0}^K \sum_{j=0}^L [j^2 b_j \sin j\theta] a_i \cos i\theta = \sum_{i=0}^{K+L} A_{J23(K)}^i(b, a) \sin i\theta$$

$$\sum_{i=0}^K \sum_{j=0}^L [j^2 b_j \sin j\theta] a_i \sin i\theta = \sum_{i=0}^{K+L} A_{J24(K)}^i(b, a) \cos i\theta \quad (A-51)$$

where

$$A_{IJ1(K)}^i(b, a) = \frac{1}{2} \sum_{j=0}^K [(i+j) b_{i+j} + (1 - \eta_{j-i}^2 + \eta_i) |i-j| b_{|i-j|}] j a_j$$

$$A_{IJ2(K)}^i(b, a) = \frac{1}{2} \sum_{j=0}^K [-(i+j) b_{i+j} + (1-\eta_{j-i}^2 + \eta_i)(i-j) b_{|i-j|}] j a_j$$

$$A_{IJ3(K)}^i(b, a) = \frac{1}{2} \sum_{j=0}^K [(i+j) b_{i+j} + (-1 + \eta_{i-j} + \eta_i)(i-j) b_{|i-j|}] j a_j$$

$$A_{IJ4(K)}^i(b, a) = \frac{1}{2} \sum_{j=0}^K [(i+j) b_{i+j} + (-1 - \eta_{i-j} + \eta_i)(i-j) b_{|i-j|}] j a_j \quad (A-52)$$

$$A_{IJ21(K)}^i(b, a) = \frac{1}{2} \sum_{j=0}^K [b_{i+j} + (1-\eta_{j-i}^2 + \eta_i) b_{|i-j|}] j^2 a_j$$

$$A_{IJ22(K)}^i(b, a) = \frac{1}{2} \sum_{j=0}^K [-b_{i+j} + (1-\eta_{j-i}^2 + \eta_i) b_{|i-j|}] j^2 a_j$$

$$A_{IJ23(K)}^i(b, a) = \frac{1}{2} \sum_{j=0}^K [b_{i+j} + (-1 + \eta_{i-j} + \eta_i) b_{|i-j|}] j^2 a_j$$

$$A_{IJ24(K)}^i(b, a) = \frac{1}{2} \sum_{j=0}^K [b_{i+j} + (-1 - \eta_{i-j} + \eta_i) b_{|i-j|}] j^2 a_j \quad (A-53)$$

$$A_{IJ21(K)}^i(b, a) = \frac{1}{2} \sum_{j=0}^K [(i+j)^2 b_{i+j} + (1-\eta_{j-i}^2 + \eta_i)(i-j)^2 b_{|i-j|}] a_j$$

$$A_{IJ22(K)}^i(b, a) = \frac{1}{2} \sum_{j=0}^K [-(i+j)^2 b_{i+j} + (1-\eta_{j-i}^2 + \eta_i)(i-j)^2 b_{|i-j|}] a_j$$

$$A_{IJ23(K)}^i(b, a) = \frac{1}{2} \sum_{j=0}^K [(i+j)^2 b_{i+j} + (-1 + \eta_{i-j} + \eta_i)(i+j)^2 b_{|i-j|}] a_j$$

$$A_{IJ24(K)}^i(b, a) = \frac{1}{2} \sum_{j=0}^K [(i+j)^2 b_{i+j} + (-1 - \eta_{i-j} + \eta_i)(i+j)^2 b_{|i-j|}] a_j \quad (A-54)$$

and

$$K \geq L \quad ; \quad \eta_l = \begin{cases} 1 & \text{if } l > 0 \\ 0 & \text{if } l = 0 \\ 1 & \text{if } l < 0 \end{cases}$$

Next, returning to the solution procedure, the expressions for F , w , w^0 and q , Eqs A-47 and A-48 are substituted into the equilibrium and compatibility Equations, Eqs A-33 and A-34. This substitution yields the following non-linear differential equations:

Equilibrium equation

$$\begin{aligned}
 & \sum_{i=0}^K \left[h_{40} \left(A_{i,xxx} \cos \frac{iny}{R} + B_{i,xxx} \sin \frac{iny}{R} \right) + h_{31} \left(\frac{in}{R} \right) \left(-A_{i,xx} \sin \frac{iny}{R} \right. \right. \\
 & \quad \left. \left. + B_{i,xx} \cos \frac{iny}{R} \right) - h_{22} \left(\frac{in}{R} \right)^2 \left(A_{i,xx} \cos \frac{iny}{R} + B_{i,xx} \sin \frac{iny}{R} \right) \right. \\
 & \quad \left. + h_{13} \left(\frac{in}{R} \right)^3 \left(A_{i,x} \sin \frac{iny}{R} - B_{i,x} \cos \frac{iny}{R} \right) + h_{40} \left(\frac{in}{R} \right)^4 \left(A_i \cos \frac{iny}{R} + B_i \sin \frac{iny}{R} \right) \right] \\
 & + \sum_{i=0}^K \left[g_{40} \left(C_{i,xxx} \cos \frac{iny}{R} + D_{i,xxx} \sin \frac{iny}{R} \right) + g_{31} \left(\frac{in}{R} \right) \left(-C_{i,xx} \sin \frac{iny}{R} \right. \right. \\
 & \quad \left. \left. + D_{i,xx} \cos \frac{iny}{R} \right) - g_{22} \left(\frac{in}{R} \right)^2 \left(C_{i,xx} \cos \frac{iny}{R} + D_{i,xx} \sin \frac{iny}{R} \right) \right. \\
 & \quad \left. + g_{13} \left(\frac{in}{R} \right)^3 \left(C_{i,x} \sin \frac{iny}{R} - D_{i,x} \cos \frac{iny}{R} \right) + g_{40} \left(\frac{in}{R} \right)^4 \left(C_i \cos \frac{iny}{R} + D_i \sin \frac{iny}{R} \right) \right] \\
 & + \frac{1}{R} \sum_{i=0}^{2K} \left(C_{i,xx} \cos \frac{iny}{R} + D_{i,xx} \sin \frac{iny}{R} \right) + L \left(F, W + W^0 \right) \\
 & - \bar{N}_{xx} \sum_{i=0}^K \left[\left(A_{i,xx} + A_{i,xx}^0 \right) \cos \frac{iny}{R} + \left(B_{i,xx} + B_{i,xx}^0 \right) \sin \frac{iny}{R} \right] \\
 & + 2 \bar{N}_{xy} \sum_{i=0}^K \left(\frac{in}{R} \right) \left[- \left(A_{i,x} + A_{i,x}^0 \right) \sin \frac{iny}{R} + \left(B_{i,x} + B_{i,x}^0 \right) \cos \frac{iny}{R} \right] \\
 & + \sum_{i=0}^K \left[g_i' \cos \frac{iny}{R} + g_i'' \sin \frac{iny}{R} \right] = 0 \quad (A-55)
 \end{aligned}$$

where

$$\begin{aligned}
 L(F, W + W^0) = & \left[\sum_{i=0}^{2K} C_{i,xx} \cos \frac{iny}{R} + D_{i,xx} \sin \frac{iny}{R} \right] \left[\sum_{i=0}^K \left(\frac{in}{R} \right)^2 \left\{ - \left(A_i + A_i^0 \right) \cos \frac{iny}{R} \right. \right. \\
 & \left. \left. - \left(B_i + B_i^0 \right) \sin \frac{iny}{R} \right\} \right] - 2 \left[\sum_{i=0}^{2K} \left(\frac{in}{R} \right) \left(-C_{i,x} \sin \frac{iny}{R} + D_{i,x} \cos \frac{iny}{R} \right) \right] \left[\sum_{i=0}^K \right. \\
 & \left. \left(\frac{in}{R} \right) \left\{ - \left(A_{i,x} + A_{i,x}^0 \right) \sin \frac{iny}{R} + \left(B_{i,x} + B_{i,x}^0 \right) \cos \frac{iny}{R} \right\} \right] + \left[\sum_{i=0}^{2K} - \left(\frac{in}{R} \right)^2 \left(C_i \cos \frac{iny}{R} \right. \right. \\
 & \left. \left. + D_i \sin \frac{iny}{R} \right) \right] \left[\sum_{i=0}^K \left\{ \left(A_{i,xx} + A_{i,xx}^0 \right) \cos \frac{iny}{R} + \left(B_{i,xx} + B_{i,xx}^0 \right) \sin \frac{iny}{R} \right\} \right] = 0 \quad (A-56 a)
 \end{aligned}$$

or

$$\begin{aligned}
L(F, W+W^0) = & \left(\frac{\pi}{R}\right)^2 \sum_{i=0}^{2K} \sum_{j=0}^K [-j^2 (A_j + A_j^0) \cos \frac{jny}{R}] C_{i,xx} \cos \frac{jny}{R} \\
& + \left(\frac{\pi}{R}\right)^2 \sum_{i=0}^{2K} \sum_{j=0}^K [-j^2 (A_j + A_j^0) \cos \frac{jny}{R}] D_{i,xx} \sin \frac{jny}{R} \\
& + \left(\frac{\pi}{R}\right)^2 \sum_{i=0}^{2K} \sum_{j=0}^K [-j^2 (B_j + B_j^0) \sin \frac{jny}{R}] C_{i,xx} \cos \frac{jny}{R} \\
& + \left(\frac{\pi}{R}\right)^2 \sum_{i=0}^{2K} \sum_{j=0}^K [-j^2 (B_j + B_j^0) \sin \frac{jny}{R}] D_{i,xx} \sin \frac{jny}{R} \\
& - \left(\frac{\pi}{R}\right)^2 \sum_{i=0}^{2K} \sum_{j=0}^K [(A_{j,xx} + A_{j,xx}^0) \cos \frac{jny}{R}] C_i i^2 \cos \frac{jny}{R} \\
& - \left(\frac{\pi}{R}\right)^2 \sum_{i=0}^{2K} \sum_{j=0}^K [(A_{j,xx} + A_{j,xx}^0) \cos \frac{jny}{R}] D_i i^2 \sin \frac{jny}{R} \\
& - \left(\frac{\pi}{R}\right)^2 \sum_{i=0}^{2K} \sum_{j=0}^K [(B_{j,xx} + B_{j,xx}^0) \sin \frac{jny}{R}] C_i i^2 \cos \frac{jny}{R} \\
& - \left(\frac{\pi}{R}\right)^2 \sum_{i=0}^{2K} \sum_{j=0}^K [(B_{j,xx} + B_{j,xx}^0) \sin \frac{jny}{R}] D_i i^2 \sin \frac{jny}{R} \\
& + 2 \left(\frac{\pi}{R}\right)^2 \sum_{i=0}^{2K} \sum_{j=0}^K [-j (A_{j,x} + A_{j,x}^0) \sin \frac{jny}{R}] C_{i,x} i \sin \frac{jny}{R} \\
& + 2 \left(\frac{\pi}{R}\right)^2 \sum_{i=0}^{2K} \sum_{j=0}^K [j (A_{j,x} + A_{j,x}^0) \sin \frac{jny}{R}] D_{i,x} i \cos \frac{jny}{R} \\
& + 2 \left(\frac{\pi}{R}\right)^2 \sum_{i=0}^{2K} \sum_{j=0}^K [j (B_{j,x} + B_{j,x}^0) \cos \frac{jny}{R}] C_{i,x} i \sin \frac{jny}{R} \\
& + 2 \left(\frac{\pi}{R}\right)^2 \sum_{i=0}^{2K} \sum_{j=0}^K [-j (B_{j,x} + B_{j,x}^0) \cos \frac{jny}{R}] D_{i,x} i \cos \frac{jny}{R} \quad (A-56b)
\end{aligned}$$

and

$$\begin{aligned}
h_{40} &= d_{11} & g_{40} &= \theta_{21} \\
h_{31} &= 2d_{31} + 2d_{13} & g_{31} &= -\theta_{31} + 2\theta_{23} \\
h_{22} &= d_{12} + 4d_{33} + d_{21} & g_{22} &= \theta_{11} - 2\theta_{33} + \theta_{22} \\
h_{13} &= 2d_{32} + 2d_{23} & g_{13} &= 2\theta_{13} - \theta_{32} \\
h_{04} &= d_{22} & g_{04} &= \theta_{12}
\end{aligned}$$

Note that the operator $L(F, w + w^0)$, Eqs A-56, can be written in terms of a single series, which is the most appropriate form, for use in Eq. A-55. This is accomplished through the use of Eqs. A-49-A-54.

$$\begin{aligned}
 L(F, W+W^0) = & -\left(\frac{\eta}{R}\right) \sum_{i=0}^{23K} [A_{J21(2K)}^i (A+A^0, C_{,xx}) + A_{J24(2K)}^i (B+B^0, D_{,xx}) \\
 & + A_{I21(2K)}^i (A_{,xx} + A_{,xx}^0, C) + A_{I24(2K)}^i (B_{,xx} + B_{,xx}^0, D) \\
 & + 2A_{IJ4(2K)}^i (A_{,x} + A_{,x}^0, C_{,x}) + 2A_{IJ1(2K)}^i (B_{,x} + B_{,x}^0, D_{,x})] \cos \frac{iny}{R} \\
 & - \left(\frac{\eta}{R}\right) \sum_{i=0}^{23K} [A_{J22(2K)}^i (A+A^0, D_{,xx}) + A_{J23(2K)}^i (B+B^0, C_{,xx}) \\
 & + A_{I22(2K)}^i (A_{,xx} + A_{,xx}^0, D) + A_{I23(2K)}^i (B_{,xx} + B_{,xx}^0, C) \\
 & - 2A_{IJ3(2K)}^i (A_{,x} + A_{,x}^0, D_{,x}) - 2A_{IJ2(2K)}^i (B_{,x} + B_{,x}^0, C_{,x})] \sin \frac{iny}{R} \\
 & \quad \quad \quad (A-57)
 \end{aligned}$$

Compatibility equation

$$\begin{aligned}
 & \sum_{i=0}^K [g_{40} (A_{i,xxxx} \cos \frac{iny}{R} + B_{i,xxxx} \sin \frac{iny}{R}) + g_{31} \frac{in}{R} (-A_{i,xxx} \sin \frac{iny}{R} + B_{i,xxx} \cos \frac{iny}{R}) \\
 & + g_{22} \left(\frac{in}{R}\right)^2 (-A_{i,xx} \cos \frac{iny}{R} - B_{i,xx} \sin \frac{iny}{R}) + g_{13} \left(\frac{in}{R}\right)^3 (A_{i,x} \sin \frac{iny}{R} - B_{i,x} \cos \frac{iny}{R}) \\
 & + g_{04} \left(\frac{in}{R}\right)^4 (A_i \cos \frac{iny}{R} + B_i \sin \frac{iny}{R})] \\
 & + \sum_{i=0}^K [a_{22} (C_{i,xxx} \cos \frac{iny}{R} + D_{i,xxx} \sin \frac{iny}{R}) + 2a_{23} \left(\frac{in}{R}\right) (C_{i,xx} \sin \frac{iny}{R} \\
 & - D_{i,xx} \cos \frac{iny}{R}) + (2a_{12} + a_{33}) \left(\frac{in}{R}\right)^2 (-C_{i,x} \sin \frac{iny}{R} - D_{i,x} \sin \frac{iny}{R})
 \end{aligned}$$

$$\begin{aligned}
& + 2A_{13} \left(\frac{in}{R} \right)^3 \left(-C_{i,x} \sin \frac{iny}{R} + D_{i,x} \cos \frac{iny}{R} \right) + A_{11} \left(\frac{in}{R} \right)^4 \left(C_i \cos \frac{iny}{R} + D_i \sin \frac{iny}{R} \right) \\
& + \sum_{i=0}^k \left(\frac{A_{i,xx}}{R} \cos \frac{iny}{R} + \frac{B_{i,xy}}{R} \sin \frac{iny}{R} \right) - \frac{1}{2} \left(\frac{n}{R} \right)^2 \sum_{i=0}^{2k} \left[A_{J21(k)}^i (A + 2A^\circ, A_{,xx}) \right. \\
& + A_{J24(k)}^i (B + 2B^\circ, B_{,xx}) + A_{I21(k)}^i (A_{,xx} + 2A_{,xx}^\circ, A) + A_{I24(k)}^i (B_{,xx} + 2B_{,xx}^\circ, B) \\
& + 2A_{IJ4(k)}^i (A_{,x} + 2A_{,x}^\circ, A_{,x}) + 2A_{IJ1(k)}^i (B_{,x} + 2B_{,x}^\circ, B_{,x}) \left. \right] \cos \frac{iny}{R} \\
& - \frac{1}{2} \left(\frac{n}{R} \right)^2 \sum_{i=0}^{2k} \left[A_{J22(k)}^i (A + 2A^\circ, B_{,xx}) + A_{J23(k)}^i (B + 2B^\circ, A_{,xx}) \right. \\
& + A_{I22(k)}^i (A_{,xx} + 2A_{,xx}^\circ, B) + A_{I23(k)}^i (B_{,xx} + 2B_{,xx}^\circ, A) \\
& - 2A_{IJ3(k)}^i (A_{i,x} + 2A_{i,x}^\circ, B_{,x}) - 2A_{IJ2(k)}^i (B_{,x} + 2B_{,x}^\circ, A_{,x}) \left. \right] \sin \frac{iny}{R} \\
& = 0 \tag{A-58}
\end{aligned}$$

Parenthesis

As far as the equilibrium equation is concerned, the summation starts from zero and goes up to $3k$ [see Eqs A-55 and A-57] because of the nonlinearity. The Galerkin procedure will be employed for this equation in the circumferential direction. This will yield $(2k + 1)$ nonlinear ordinary differential equations [from the vanishing of $(2k + 1)$ Galerkin integrals].

On the other hand the compatibility equation, Eq. A-58, is written in series form, from, zero to $2k$. Because of the orthogonality of the trigonometric functions $(4k + 1)$ nonlinear differential equations result, which relate the C's and D's to the A's and B's [see Eqs A-47]. This set of ordinary differential equations is shown in a complete form in the pages that follow. Before showing them, though, some simplification can be made.

For the case of $i = 0$, one obtains the following equation, from the compatibility equation, Eq A-58.

$$\begin{aligned}
 & g_{40} A_{0,xxxx} + \frac{1}{R} A_{0,xx} + a_{22} C_{0,xxxx} - \frac{1}{2} \left(\frac{\pi}{R} \right)^2 [A_{J21(k)}^i (A + 2A^\circ, A_{,xx}) \\
 & + A_{J24(k)}^i (B + 2B^\circ, B_{,xx}) + A_{I21(k)}^\circ (A_{,xx} + 2A_{,xx}^\circ, A) \\
 & + A_{I24(k)}^i (B_{,xx} + 2B_{,xx}^\circ, B) + 2 A_{IJ4(k)}^\circ (A_{,x} + 2A_{,x}^\circ, A_{,x}) \\
 & + 2 A_{IJ1(k)}^\circ (B_{,x} + 2B_{,x}^\circ, B_{,x})] = 0
 \end{aligned}$$

or

$$\begin{aligned}
 C_{0,xxxx} = \frac{1}{a_{22}} \{ & -g_{40} A_{0,xxxx} - \frac{1}{R} A_{0,xx} + \frac{1}{4} \left(\frac{\pi}{R} \right)^2 \sum_{j=1}^K [j^2 (A_j + 2A_j^\circ) A_{j,xx} \\
 & + j^2 (B_j + 2B_j^\circ) B_{j,xx} + j^2 (A_{j,xx} + 2A_{j,xx}^\circ) A_j + j^2 (B_{j,xx} + 2B_{j,xx}^\circ) B_j \\
 & + 2j^2 (A_{j,x} + 2A_{j,x}^\circ) A_{j,x} + 2j^2 (B_{j,x} + 2B_{j,x}^\circ) B_{j,x}] \} \quad (A-59)
 \end{aligned}$$

Moreover, the displacement component $v(x, y)$ is a continuous and single-valued function of y (and x), therefore

$$\int_0^{2\pi R} v_{,y} dy = v(x, 2\pi R) - v(x, 0) = 0 \quad (A-60)$$

From the second of Eqs A-2 one may write

$$v_{,y} = \epsilon_{yy}^\circ + w/R - w_{,y} (w_{,y} + 2w_{,y}^\circ)/2 \quad (A-61)$$

Furthermore, use of Eqs A-18 [relation between ϵ_{yy}^0 and N_{ij} , n_{ij}], of Eqs A-29 [definition of stress resultant function], and of Eqs A-47 and A-48 [assumed form for W , F and w^0] yields the following relation,

$$\begin{aligned} \int_0^{2\pi R} v_{,y} dy &= \int_0^{2\pi R} (-a_{12} \bar{N}_{xx} + a_{23} \bar{N}_{xy}) dy \\ &+ \int_0^{2\pi R} [a_{12} F_{,yy} + a_{22} F_{,xx} - a_{23} F_{,xy} + \theta_{23} W_{,xx} \\ &+ \theta_{22} W_{,yy} + 2\theta_{23} W_{,xy} + \frac{W}{R} - \frac{1}{2} W_{,y}(W_{,y} \\ &+ 2W_{,y}^0)] dy = 0 \end{aligned} \quad (A-62)$$

or

$$\begin{aligned} &\int_0^{2\pi R} (-a_{12} \bar{N}_{xx} + a_{23} \bar{N}_{xy}) dy + \int_0^{2\pi R} \left\{ a_{12} \sum_{i=0}^{2K} \left(\frac{i\pi}{R}\right)^2 [-C_i \cos \frac{i\pi y}{R} \right. \\ &\quad \left. - D_i \sin \frac{i\pi y}{R}] + a_{22} \sum_{i=0}^{2K} [C_{i,xx} \cos \frac{i\pi y}{R} + D_{i,xx} \sin \frac{i\pi y}{R}] \right. \\ &\quad \left. - a_{23} \sum_{i=0}^{2K} \left(\frac{i\pi}{R}\right) [-C_{i,x} \sin \frac{i\pi y}{R} + D_{i,x} \cos \frac{i\pi y}{R}] \right. \\ &\quad \left. + \theta_{21} \sum_{i=0}^K [A_{i,xx} \cos \frac{i\pi y}{R} + B_{i,xx} \sin \frac{i\pi y}{R}] + \theta_{22} \sum_{i=0}^K \left(\frac{i\pi}{R}\right)^2 \right. \\ &\quad \left. - A_i \cos \frac{i\pi y}{R} - B_i \sin \frac{i\pi y}{R} \right\} + 2\theta_{23} \sum_{i=0}^K \left(\frac{i\pi}{R}\right) [-A_{i,x} \sin \frac{i\pi y}{R} + B_{i,x} \cos \frac{i\pi y}{R}] \\ &\quad + \frac{1}{R} \sum_{i=0}^K (A_i \cos \frac{i\pi y}{R} + B_i \sin \frac{i\pi y}{R}) - \frac{1}{2} \sum_{i=0}^K \left(\frac{i\pi}{R}\right) [-A_i \sin \frac{i\pi y}{R} \\ &\quad + B_i \cos \frac{i\pi y}{R}] \cdot \sum_{j=0}^K \left(\frac{j\pi}{R}\right) [- (A_j + 2A_j^0) \sin \frac{j\pi y}{R} + (B_j + 2B_j^0) \cos \frac{j\pi y}{R}] dy \\ &= 0 \end{aligned} \quad (A-63)$$

This equation, Eq. A-63, after performing the indicated operations (integration, becomes

$$\int_0^{2\pi R} \left\{ -a_{12} \bar{N}_{xx} + a_{23} \bar{N}_{xy} + a_{22} C_{o,xx} - \theta_{21} A_{o,xx} + \frac{A_o}{R} \right. \\ \left. - \frac{\eta^2}{4R^3} \sum_{j=0}^K j^2 [(A_j + 2A_j^o) A_j + (B_j + 2B_j^o) B_j] \right\} dy = 0 \quad (A-64)$$

From which, one may write

$$C_{o,xx} = \frac{1}{a_{22}} \left\{ -\theta_{21} A_{o,xx} - \frac{A_o}{R} + \frac{\eta^2}{4R^3} \sum_{j=0}^K j^2 [(A_j + 2A_j^o) A_j \right. \\ \left. + (B_j + 2B_j^o) B_j] + a_{12} \bar{N}_{xx} - a_{23} \bar{N}_{xy} \right\} \quad (A-65)$$

The remaining compatibility (nonlinear, ordinary differential) equations are

For $i = 1, 2, \dots, 2k$ and cosine terms

$$a_{22} C_{i,xxxx} - 2a_{23} \left(\frac{i\eta}{R}\right) D_{i,xxx} - (2a_{12} + a_{33}) \left(\frac{i\eta}{R}\right)^2 C_{i,xx} + 2a_{13} \left(\frac{i\eta}{R}\right)^3 D_{i,x} \\ + a_{11} \left(\frac{i\eta}{R}\right)^4 C_i + \delta_i [g_{40} A_{i,xxxx} + g_{31} \left(\frac{i\eta}{R}\right) B_{i,xxx} - g_{22} \left(\frac{i\eta}{R}\right)^2 A_{i,xx} \\ - g_{13} \left(\frac{i\eta}{R}\right)^3 B_{i,x} + g_{04} \left(\frac{i\eta}{R}\right)^4 A_i + \frac{A_{i,xx}}{R} - \frac{1}{2} \left(\frac{\eta}{R}\right)^2 i^2 (A_i + 2A_i^o) A_{o,xx}] \\ - \left(\frac{\eta}{2R}\right)^2 \sum_{j=0}^K \left\{ [(i+j)^2 (A_{i+j} + 2A_{i+j}^o) + (2 - \eta_{j-i}^2) (i-j)^2 (A_{i-j} + 2A_{i-j}^o) \right. \\ \left. \right] A_{j,xx} + [(i+j)^2 (B_{i+j} + 2B_{i+j}^o) - \eta_{i-j}^2 (i-j)^2 (B_{i-j} + 2B_{i-j}^o)] B_{j,xx}$$

$$\begin{aligned}
& + [A_{itj,xx} + 2A_{itj,xx}^{\circ} + (2 - \gamma_{j-i}^2)(A_{|i-j|,xx} + 2A_{|i-j|,xx}^{\circ})] j^2 A_j \\
& + [B_{itj,xx} + 2B_{itj,xx}^{\circ} - \gamma_{i-j}(B_{|i-j|,xx} + 2B_{|i-j|,xx}^{\circ})] j^2 B_j \\
& + 2[(i+j)(A_{itj,x} + 2A_{itj,x}^{\circ}) - \gamma_{i-j}|i-j|(A_{|i-j|,x} + 2A_{|i-j|,x}^{\circ})] \\
& \cdot j A_{j,x} + 2[(i+j)(B_{itj,x} + 2B_{itj,x}^{\circ}) + (2 - \gamma_{j-i}^2)|i-j|(B_{|i-j|,x} \\
& + 2B_{|i-j|,x}^{\circ})] j B_{j,x} \} = 0 \quad (A-66)
\end{aligned}$$

For $i = 1, 2, \dots, 2k$ and Sine terms

$$\begin{aligned}
& a_{22} D_{i,xxx} + 2a_{23} \left(\frac{i\eta}{R}\right) C_{i,xxx} - (2a_{12} + a_{33}) \left(\frac{i\eta}{R}\right)^2 D_{i,xx} \\
& - 2a_{13} \left(\frac{i\eta}{R}\right)^3 C_{i,x} + a_{11} \left(\frac{i\eta}{R}\right)^4 D_i + \delta_i [g_{40} B_{i,xxx} \\
& - g_{31} \left(\frac{i\eta}{R}\right) A_{i,xxx} - g_{22} \left(\frac{i\eta}{R}\right)^2 B_{i,xx} + g_{13} \left(\frac{i\eta}{R}\right)^3 A_{i,x} + g_{04} \left(\frac{i\eta}{R}\right)^4 B_i \\
& + \frac{B_{i,xx}}{R} - \frac{1}{2} \left(\frac{\eta}{R}\right)^2 i^2 (B_i + B_i^{\circ}) A_{0,xx}] - \frac{1}{4} \left(\frac{\eta}{R}\right)^2 \sum_{j=1}^K \{ [-(i+j)^2 (A_{itj} + 2A_{itj}^{\circ}) \\
& + (2 - \gamma_{j-i}^2) (i-j)^2 (A_{|i-j|} + 2A_{|i-j|}^{\circ})] B_{j,xx} + [(i+j)^2 (B_{j+i} + 2B_{j+i}^{\circ}) \\
& + \gamma_{i-j} (i-j)^2 (B_{|i-j|} + 2B_{|i-j|}^{\circ})] A_{j,xx} + [-(A_{itj,xx} + 2A_{itj,xx}^{\circ}) \\
& + (2 - \gamma_{j-i}^2) (A_{|i+j|,xx} + 2A_{|i+j|,xx}^{\circ})] j^2 B_j + [(B_{itj,xx} + 2B_{itj,xx}^{\circ}) \\
& + \gamma_{i-j} (B_{|i-j|,xx} + 2B_{|i-j|,xx}^{\circ})] j^2 A_j - 2[(i+j)(A_{itj,x} + 2A_{itj,x}^{\circ}) + \gamma_{i-j}|i-j| \\
& \cdot (A_{|i-j|,x} + 2A_{|i-j|,x}^{\circ})] j B_{j,x} - 2[-(i+j)(B_{itj,x} + 2B_{itj,x}^{\circ}) + (2 - \gamma_{j-i}^2)|i-j| \\
& \cdot (B_{|i-j|,x} + 2B_{|i-j|,x}^{\circ})] j A_{j,x} \} = 0 \quad (A-67)
\end{aligned}$$

where

$$\delta_i = \begin{cases} 0 & i > K \\ 1 & i \leq K \end{cases}; \quad \eta_i = \begin{cases} -1 & l < 0 \\ 0 & l = 0 \\ 1 & l > 0 \end{cases}$$

As already mentioned, the Galerkin procedure is employed in connection with the equilibrium equation, Eq. A-54, in the circumferential direction. The vanishing of the $(2k + 1)$ Galerkin integrals yields the following set of nonlinear ordinary differential equations.

For $i = 0$

$$\begin{aligned} & h_{40} A_{0,xxxx} + g_{40} C_{0,xxxx} + \frac{1}{R} C_{0,xx} - (A_{0,xx} + A_{0,xx}^{\circ}) \bar{N}_{xx} \\ & - \left(\frac{\pi}{R}\right)^2 \frac{1}{2} \sum_{j=0}^{2K} [j^2 (A_j + A_j^{\circ}) C_{j,xx} + j^2 (B_j + B_j^{\circ}) D_{j,xx} + j^2 (A_{j,xx} \\ & + A_{j,xx}^{\circ}) C_j + j^2 (B_{j,xx} + B_{j,xx}^{\circ}) D_j + 2j^2 (A_{j,x} + A_{j,x}^{\circ}) C_{j,x} \\ & + 2j^2 (B_{j,x} + B_{j,x}^{\circ}) D_{j,x}] + g_0' = 0 \end{aligned} \quad (A-68)$$

By employing Eqs. A-59 and A-65 one obtains

$$\begin{aligned} & A_{0,xxxx} (d_{11} - \frac{b_{21}^2}{a_{22}}) - A_{0,xx} (\frac{2b_{21}}{Ra_{22}}) - \bar{N}_{xx} (A_{0,xx} + A_{0,xx}^{\circ}) - \frac{A_0}{a_{22}R^2} \\ & + \left(\frac{\pi}{2R}\right)^2 \sum_{j=1}^K j^2 \left\{ \frac{b_{21}}{a_{22}} [(A_j + 2A_j^{\circ}) A_{j,xx} + (A_{j,xx} + 2A_{j,xx}^{\circ}) A_j \right. \\ & + 2(A_{j,x} + 2A_{j,x}^{\circ}) A_{j,x} + (B_j + 2B_j^{\circ}) B_{j,xx} + (B_{j,xx} + 2B_{j,xx}^{\circ}) B_j \\ & + 2(B_{j,x} + 2B_{j,x}^{\circ}) B_{j,x}] + \frac{1}{a_{22}R} [(A_j + 2A_j^{\circ}) A_j + (B_j + 2B_j^{\circ}) B_j] \\ & \left. - 2[(A_j + A_j^{\circ}) C_{j,xx} + (B_j + B_j^{\circ}) D_{j,xx} + 2(A_{j,x} + A_{j,x}^{\circ}) C_{j,x} \right. \end{aligned}$$

$$\begin{aligned}
& + 2(B_{j,x} + B_{j,x}^{\circ}) D_{j,x} + (A_{j,xx} + A_{j,xx}^{\circ}) C_j + (B_{j,xx} + B_{j,xx}^{\circ}) D_j \} \\
& + \frac{a_{12}}{a_{22}R} \bar{N}_{xx} - \frac{a_{23}}{a_{22}R} \bar{N}_{xy} + \mathcal{G}'_0 = 0
\end{aligned} \tag{A-69}$$

For $i = 1, 2, \dots, K$ (when the weighting function is $\cos \frac{iny}{R}$)

$$\begin{aligned}
& d_{11} A_{i,xxxx} + 4d_{13} \left(\frac{in}{R}\right) B_{i,xxx} - (2d_{12} + 4d_{33}) \left(\frac{in}{R}\right)^2 A_{i,xx} \\
& - 4d_{23} \left(\frac{in}{R}\right)^3 B_{i,x} + d_{22} \left(\frac{in}{R}\right)^4 A_i + \theta_{21} C_{i,xxx} + (2\theta_{23} - \theta_{31}) \left(\frac{in}{R}\right) D_{i,xxx} \\
& - (\theta_{11} - 2\theta_{33} + \theta_{22}) \left(\frac{in}{R}\right)^2 C_{i,xx} - (2\theta_{13} - \theta_{32}) \left(\frac{in}{R}\right)^3 D_{i,x} \\
& + \theta_{12} \left(\frac{in}{R}\right)^4 C_i + \frac{1}{R} C_{i,xx} - \left(\frac{in}{R}\right)^2 \left(\frac{A_i + A_i^{\circ}}{a_{22}}\right) \left\{ -\theta_{21} A_{0,xx} - \frac{A_0}{R} \right. \\
& \left. + \left(\frac{n}{2R}\right)^2 \sum_{j=1}^K j^2 [(A_j + 2A_j^{\circ}) A_j + (B_j + 2B_j^{\circ}) B_j] \right\} \\
& - \left(\frac{in}{R}\right)^2 \left(\frac{A_i + A_i^{\circ}}{a_{22}}\right) (a_{12} \bar{N}_{xx} - a_{23} \bar{N}_{xy}) - (A_{i,xx} + A_{i,xx}^{\circ}) \bar{N}_{xx} \\
& + 2 \bar{N}_{xy} \left(\frac{in}{R}\right) (B_{i,x} + B_{i,x}^{\circ}) - \frac{1}{2} \left(\frac{n}{R}\right)^2 \sum_{j=1}^{2K} \{ [(i+j)^2 \delta_{ij} (A_{itj} + A_{itj}^{\circ}) \\
& + (2 - \gamma_{j-i}^2) (i-j)^2 \delta_{i-j} (A_{i-j} + A_{i-j}^{\circ})] C_{j,xx} \\
& + [(i+j)^2 \delta_{ij} (B_{itj} + B_{itj}^{\circ}) - \gamma_{i-j} (i-j)^2 \delta_{i-j} (B_{i-j} + B_{i-j}^{\circ})] D_{j,xx} \\
& + 2 [(i+j) \delta_{ij} (A_{itj,x} + A_{itj,x}^{\circ}) - \gamma_{i-j} |i-j| \delta_{i-j} (A_{i-j,x} \\
& + A_{i-j,x}^{\circ})] j C_{j,x} + 2 [(i+j) \delta_{ij} (B_{itj,x} + B_{itj,x}^{\circ}) \\
& + (2 - \gamma_{j-i}^2) |i-j| \delta_{i-j} (B_{i-j,x} + B_{i-j,x}^{\circ})] j D_{j,x} + [\delta_{ij} (A_{i+j,xx} + A_{i+j,xx}^{\circ}) \\
& + (2 - \gamma_{j-i}^2) \delta_{i-j} (A_{i-j,xx} + A_{i-j,xx}^{\circ})] j^2 C_j + [\delta_{ij} (B_{i+j,xx} + B_{i+j,xx}^{\circ}) \\
& - \gamma_{i-j} \delta_{i-j} (B_{i-j,xx} + B_{i-j,xx}^{\circ})] j^2 D_j \} + \mathcal{G}'_i = 0
\end{aligned} \tag{A-70}$$

For $i = 1, 2 \dots k$ (when the weighting function is $\sin \frac{iny}{R}$)

$$\begin{aligned}
& d_{11} B_{i,xxx} - 4 d_{13} \left(\frac{in}{R}\right) A_{i,xx} - (2d_{12} + 4d_{33}) \left(\frac{in}{R}\right)^2 B_{i,xx} + 4d_{23} \left(\frac{in}{R}\right)^3 A_{i,x} \\
& + d_{22} \left(\frac{in}{R}\right)^4 B_i + \theta_{21} D_{i,xxx} - (2\theta_{23} - \theta_{31}) \left(\frac{in}{R}\right) C_{i,xx} \\
& - (\theta_{11} - 2\theta_{33} + \theta_{22}) \left(\frac{in}{R}\right)^2 D_{i,xx} + (2\theta_{13} - \theta_{32}) \left(\frac{in}{R}\right)^3 C_{i,x} + \theta_{12} \left(\frac{in}{R}\right)^4 D_i \\
& + \frac{D_{i,xx}}{R} - \left(\frac{in}{R}\right)^2 \left(\frac{B_i + B_i^0}{a_{22}}\right) \left\{ -\theta_{21} A_{o,xx} - \frac{A_o}{R} + \left(\frac{n}{2R}\right)^2 \sum_{j=1}^K j^2 [(A_j + 2A_j^0) A_j \right. \\
& + (B_j + 2B_j^0) B_j] \right\} - \left(\frac{in}{R}\right)^2 \left(\frac{B_i + B_i^0}{a_{22}}\right) (a_{12} \bar{N}_{xx} - a_{23} \bar{N}_{xy}) - (B_{i,xx} + B_{i,xx}^0) \bar{N}_{xx} \\
& - 2 \bar{N}_{xy} \left(\frac{in}{R}\right) (A_{i,x} + A_{i,x}^0) - \frac{1}{2} \left(\frac{n}{R}\right)^2 \sum_{j=1}^{2K} \left\{ [(i+j)^2 \delta_{ij} (B_{itj} + B_{itj}^0) \right. \\
& + \gamma_{ij} (i-j)^2 \delta_{|i-j|} (B_{|i-j|} + B_{|i-j|}^0)] C_{i,xx} + [-(i+j)^2 \delta_{ij} (A_{itj} + A_{itj}^0) \\
& + (2 - \gamma_{j-i}^2) (i-j)^2 \delta_{|i-j|} (A_{|i-j|} + A_{|i-j|}^0)] D_{j,xx} - 2 [-(i+j) \delta_{ij} (B_{itj,x} + B_{itj,x}^0) \\
& + (2 - \gamma_{j-i}^2) (i+j) \delta_{|i-j|} (B_{|i-j|,x} + B_{|i-j|,x}^0)] j C_{j,x} \\
& - 2 [(i+j) \delta_{ij} (A_{itj,x} + A_{itj,x}^0) + \gamma_{ij} |i-j| \delta_{|i-j|} (A_{|i-j|,x} + A_{|i-j|,x}^0)] j D_{j,x} \\
& + [\delta_{ij} (B_{itj,xx} + B_{itj,xx}^0) + \gamma_{ij} \delta_{|i-j|} (B_{|i-j|,xx} + B_{|i-j|,xx}^0)] j^2 C_j \\
& + [-\delta_{ij} (A_{itj,xx} + A_{itj,xx}^0) + (2 - \gamma_{j-i}^2) \delta_{|i-j|} (A_{|i-j|,xx} + A_{|i-j|,xx}^0)] j^2 D_j \} \\
& + g_i^2 = 0 \tag{A-71}
\end{aligned}$$

Clearly the response of the configuration is known provided that one can solve the nonlinear ordinary differential equations. Their number is $(6k + 2)$ and the number of unknown dependent variables (functions of x) is also $(6k + 2)$. These are $(k + 1)$ A_i 's, (k) B_i 's, $(2k + 1)$ C_i 's and $(2k)$ D_i 's. Note that C_0 can and has been eliminated, through Eqs A-59 and A-65 and therefore both the number of equations and number of unknowns is reduced by one to $(6k + 1)$. In these equations there is one more undetermined parameter, the wave number n . This number is determined by requiring the total potential to be a minimum at a given level of the load. In other words the response is obtained for various n -values and, through comparison the true response (n -value and corresponding values for the dependent variables) is established.

So far, the partial differential equations are reduced to a set of $(6k + 1)$ nonlinear ordinary differential equations. Next, the generalized Newton's method (Ref. 38), applicable to differential equations is used to reduce the nonlinear field equations and boundary conditions to a sequence of linear systems. Iteration equations are derived by assuming that the solution to the nonlinear set can be achieved by small corrections to an approximate solution. The small corrections or the values of the variables at the $(m + 1)$ step in terms of the closely spaced state \underline{m} , can be obtained by solving the linearized differential equations. Note below the way that a typical nonlinear term (product of X and Y) in the differential equation is linearized.

$$\begin{aligned}
 X^{m+1} Y^{m+1} &= (X^m + dX^m)(Y^m + dY^m) \\
 &= X^m Y^m + X^m dY^m + Y^m dX^m + dX^m dY^m \\
 &\approx X^m Y^m + Y^m dX^m + X^m dY^m + dX^m dY^m - X^m Y^m \\
 &= X^m (Y^m + dY^m) + Y^m (X^m + dX^m) - X^m Y^m
 \end{aligned}$$

$$= X^m Y^{m+1} + Y^m X^{m+1} - X^m Y^m \quad (A-72)$$

where X & Y can be A_i , B_i , C_i or D_i

By making use of Eqs (72), the linearized set of governing equations (iteration equation) is obtained from Eqs A-66, A-67, A-69, A-71. These are:

1. Compatibility (i) [cosine terms, Eqs A-67]

For $i = 1, 2, \dots, K$

$$\begin{aligned} & a_{22} C_{i,XXX}^{m+1} - 2 a_{23} \left(\frac{i\eta}{R}\right) D_{i,XX}^{m+1} - (2 a_{12} + a_{33}) \left(\frac{i\eta}{R}\right)^2 C_{i,XX}^{m+1} \\ & + 2 a_{13} \left(\frac{i\eta}{R}\right)^3 D_{i,X}^{m+1} + a_{11} \left(\frac{i\eta}{R}\right)^4 C_i^{m+1} + \delta_i \{ \theta_{21} A_{i,XXX}^{m+1} \\ & + (2 \theta_{23} - \theta_{31}) \left(\frac{i\eta}{R}\right) B_{i,XX}^{m+1} - (\theta_{11} - 2 \theta_{33} + \theta_{22}) \left(\frac{i\eta}{R}\right)^2 A_{i,XX}^{m+1} \\ & - (2 \theta_{13} - \theta_{32}) \left(\frac{i\eta}{R}\right)^3 B_{i,X}^{m+1} + \theta_{12} \left(\frac{i\eta}{R}\right)^4 A_i^{m+1} + \frac{1}{R} A_{i,XX}^{m+1} \\ & - \frac{1}{2} \left(\frac{i\eta}{R}\right)^2 [A_i^{m+1} A_{0,XY}^m + (A_i^m + 2 A_i^0) A_{0,XY}^{m+1} - A_i^m A_{0,XX}^m] \} \\ & - \left(\frac{\eta}{2R}\right)^2 \sum_{j=1}^K \{ J_{ij}^{m+1} (A + 2A^0) A_{j,XX}^m + J_{ij}^m (A + 2A^0) A_{j,XX}^{m+1} - J_{ij}^m (A + 2A^0) A_{j,XX}^m \\ & + K_{ij}^{m+1} (B + 2B^0) B_{j,XX}^m + K_{ij}^m (B + 2B^0) B_{j,XX}^{m+1} - K_{ij}^m (B + 2B^0) B_{j,XX}^m \\ & + 2 [L_{ij}^{m+1} (A + 2A^0) A_{j,X}^m + L_{ij}^m (A + 2A^0) A_{j,X}^{m+1} - L_{ij}^m (A + 2A^0) A_{j,X}^m] \\ & + 2 [M_{ij}^{m+1} (B + 2B^0) B_{j,X}^m + M_{ij}^m (B + 2B^0) B_{j,X}^{m+1} - M_{ij}^m (B + 2B^0) B_{j,X}^m] \\ & + N_{ij}^{m+1} (A + 2A^0) A_j^m + N_{ij}^m (A + 2A^0) A_j^{m+1} - N_{ij}^m (A + 2A^0) A_j^m \\ & + O_{ij}^{m+1} (B + 2B^0) B_j^m + O_{ij}^m (B + 2B^0) B_j^{m+1} - O_{ij}^m (B + 2B^0) B_j^m \} \\ & = 0 \end{aligned} \quad (A-73)$$

where

$$J_{ij}^m(Y) = (i+j) \delta_{ij} Y_{itj}^m + (2 - \eta_{j-i}^2) (i-j)^2 \delta_{|i-j|} Y_{itj}^m$$

$$K_{ij}^m(Y) = (i+j)^2 \delta_{ij} Y_{itj}^m - \eta_{j-i}^2 (i-j)^2 \delta_{|i-j|} Y_{itj}^m$$

$$L_{ij}^m(Y) = [(i+j) \delta_{ij} Y_{ij,x}^m - \eta_{ij} |i-j| \delta_{|i-j|} Y_{|i-j|,x}^m] j$$

$$M_{ij}^m(Y) = [(i+j) \delta_{ij} Y_{ij,x}^m + (2-\eta_{j-i}) |i-j| \delta_{|i-j|} Y_{|i-j|,x}^m] j$$

$$N_{ij}^m(Y) = [\delta_{ij} Y_{ij,xx}^m + (2-\eta_{j-i}) \delta_{|i-j|} Y_{|i-j|,xx}^m] j^2$$

$$O_{ij}^m(Y) = [\delta_{ij} Y_{ij,xxx}^m - \eta_{ij} \delta_{|i-j|} Y_{|i-j|,xxx}^m] j^2$$

(ii) [sine terms, Eq A-68]

For $i = 1, 2, \dots, K$

$$\begin{aligned} & a_{22} D_{i,xxxx}^{m+1} + 2a_{23} \left(\frac{i\eta}{R}\right) C_{i,xxx}^{m+1} - (2a_{12} + a_{33}) \left(\frac{i\eta}{R}\right)^2 D_{i,xx}^{m+1} \\ & - 2a_{13} \left(\frac{i\eta}{R}\right)^3 C_{i,x}^{m+1} + a_{11} \left(\frac{i\eta}{R}\right)^4 D_i^{m+1} + \delta_i [\theta_{21} B_{i,xxx}^{m+1} - (2\theta_{23} - \theta_{31}) \\ & \cdot \left(\frac{i\eta}{R}\right) A_{i,xxx}^{m+1} - (\theta_{11} - 2\theta_{33} + \theta_{21}) \left(\frac{i\eta}{R}\right)^2 B_{i,xx}^{m+1} + (2\theta_{13} - \theta_{32}) \left(\frac{i\eta}{R}\right)^3 A_{i,x}^{m+1} \\ & + \theta_{12} \left(\frac{i\eta}{R}\right)^4 B_i^{m+1} + \frac{B_{i,xx}^{m+1}}{R} - \frac{1}{2} \left(\frac{i\eta}{R}\right)^2 [B_i^m A_{o,xx}^m + (B_i^m + 2B_i^o) A_{o,xx}^{m+1} \\ & - B_i^m A_{o,xx}^m] - \left(\frac{\eta}{2R}\right)^2 \sum_{l=0}^K \{ Q_{ij}^{m+1} (B + 2B^o) A_{j,xx}^m + Q_{ij}^m (B + 2B^o) A_{j,xx}^{m+1} \\ & - Q_{ij}^m (B + 2B^o) A_{j,xx}^m + R_{ij}^{m+1} (A + 2A^o) B_{j,xx}^m + R_{ij}^m (A + 2A^o) B_{j,xx}^{m+1} \\ & - R_{ij}^m (A + 2A^o) B_{j,xx}^{m+1} - 2 [S_{ij}^{m+1} (B + 2B^o) A_{j,x}^m + S_{ij}^m (B + 2B^o) A_{j,x}^{m+1} \\ & - S_{ij}^m (B + 2B^o) A_{j,x}^m] - 2 [T_{ij}^{m+1} (A + 2A^o) B_{j,x}^m + T_{ij}^m (A + 2A^o) B_{j,x}^{m+1} \\ & - T_{ij}^m (A + 2A^o) B_{j,x}^m] + U_{ij}^{m+1} (B + 2B^o) A_j^m + U_{ij}^m (B + 2B^o) A_j^{m+1} \\ & - U_{ij}^m (B + 2B^o) A_j^m + V_{ij}^{m+1} (A + 2A^o) B_j^m + V_{ij}^m (A + 2A^o) B_j^{m+1} \\ & - V_{ij}^m (A + 2A^o) B_j^m \} = 0 \end{aligned} \quad (A-74)$$

where

$$Q_{ij}^m(Y) = (i+j)^2 \delta_{ij} Y_{ij}^m + k_{ij} (i-j)^2 \delta_{|i-j|} Y_{|i-j|}^m$$

$$R_{ij}^m(Y) = -(i+j)^2 \delta_{ij} Y_{ij}^m + (2-k_{j-i}^2) (i-j)^2 \delta_{|i-j|} Y_{|i-j|}^m$$

$$S_{ij}^m(Y) = [-(i+j) \delta_{ij} Y_{ij,x}^m + (2-k_{j-i}^2) |i-j| \delta_{|i-j|} Y_{|i-j|,x}^m] j$$

$$T_{ij}^m(Y) = [(i+j) \delta_{ij} Y_{ij,x}^m + k_{ij} |i-j| \delta_{|i-j|} Y_{|i-j|,x}^m] j$$

$$U_{ij}^m(Y) = [\delta_{ij} Y_{ij,xx}^m + k_{ij} \delta_{|i-j|} Y_{|i-j|,xx}^m] j^2$$

$$V_{ij}^m(Y) = [-\delta_{ij} Y_{ij,xx}^m + (2-k_{j-i}^2) \delta_{|i-j|} Y_{|i-j|,xx}^m] j^2$$

(2) Equilibrium

(i) $[i = 0, \text{Eq. A-69}]$

$$\begin{aligned} & A_{0,xxx}^{m+1} (d_{11} - \frac{\theta_{21}}{a_{22}}) - A_{0,xx}^{m+1} (\frac{2\theta_{21}}{R a_{22}}) - A_0^{m+1} (\frac{1}{R^2 a_{22}}) - \bar{N}_{xx} (A_{0,xx}^{m+1} \\ & + A_{0,xx}^0) + (\frac{\kappa}{2R})^2 \sum_{j=1}^K j^2 \{ \frac{\theta_{21}}{a_{22}} [A_j^{m+1} A_{j,xx}^m + (A_j^m + 2A_j^0) A_{j,xx}^{m+1} \\ & - A_j^m A_{j,xx}^m + A_{j,xx}^{m+1} A_j^m + (A_{j,xx}^m + 2A_{j,xx}^0) A_j^{m+1} - A_{j,xx}^m A_j^m + 2A_{j,x}^{m+1} A_{j,x}^m \\ & + 2(A_{j,x}^m + 2A_{j,x}^0) A_{j,x}^{m+1} - 2A_{j,x}^m A_{j,x}^m + B_j^{m+1} B_{j,xx}^m \\ & + (B_j^m + 2B_j^0) B_{j,xx}^{m+1} - B_j^m B_{j,xx}^m + (B_{j,xx}^{m+1} + 2B_{j,xx}^0) B_j^m \\ & + (B_{j,xx}^m + 2B_{j,xx}^0) B_j^{m+1} - (B_{j,xx}^m + 2B_{j,xx}^0) B_j^m \\ & + 2B_{j,x}^{m+1} B_{j,x}^m + 2(B_{j,x}^m + 2B_{j,x}^0) B_{j,x}^{m+1} - 2B_{j,x}^m B_{j,x}^m] \\ & + \frac{1}{a_{22} R} [A_j^{m+1} A_j^m + (A_j^m + 2A_j^0) A_j^{m+1} - A_j^m A_j^m \end{aligned}$$

$$\begin{aligned}
& + B_j^{m+1} B_j^m + (B_j^m + 2 B_j^0) B_j^{m+1} - B_j^m B_j^m \} \\
& - \frac{1}{2} \left(\frac{\eta}{R} \right)^2 \sum_{j=1}^K \{ j^2 [A_j^{m+1} C_{j,xx}^m + (A_j^m + A_j^0) C_{j,xx}^{m+1} - A_j^m C_{j,xx}^m \\
& + B_j^{m+1} D_{j,xx}^m + (B_j^m + B_j^0) D_{j,xx}^{m+1} - B_j^m D_{j,xx}^m] \\
& + 2 A_{j,x}^{m+1} C_{j,x}^m + 2 (A_{j,x}^m + A_{j,x}^0) C_{j,x}^{m+1} - 2 A_{j,x}^m C_{j,x}^m \\
& + 2 B_{j,x}^{m+1} D_{j,x}^m + (B_{j,x}^m + B_{j,x}^0) D_{j,x}^{m+1} - 2 B_{j,x}^m D_{j,x}^m \\
& + A_{j,xx}^{m+1} C_j^m + (A_{j,xx}^m + A_{j,xx}^0) C_j^{m+1} - A_{j,xx}^m C_j^m \\
& + B_{j,xx}^{m+1} D_j^m + (B_{j,xx}^m + B_{j,xx}^0) D_j^{m+1} - B_{j,xx}^m D_j^m \} \\
& + \frac{a_{12}}{a_{22}R} \bar{N}_{xx} - \frac{a_{23}}{a_{22}R} \bar{N}_{xy} + g_0' = 0 \tag{A-75}
\end{aligned}$$

(ii) [i = 1, 2, ...K; weighting function is $\cos \frac{i\eta y}{R}$]

$$\begin{aligned}
& d_{11} A_{i,xxxx}^{m+1} + 4 d_{13} \left(\frac{i\eta}{R} \right) B_{i,xxx}^{m+1} - (2 d_{12} + 4 d_{33}) \left(\frac{i\eta}{R} \right)^2 A_{i,xx}^{m+1} \\
& - 4 d_{23} \left(\frac{i\eta}{R} \right)^3 B_{i,x}^{m+1} + d_{22} \left(\frac{i\eta}{R} \right)^4 A_i^{m+1} + \theta_{21} C_{i,xxxx}^{m+1} \\
& + (2 \theta_{23} - \theta_{31}) \left(\frac{i\eta}{R} \right) D_{i,xxx}^{m+1} - (\theta_{11} - 2 \theta_{33} + \theta_{22}) \left(\frac{i\eta}{R} \right)^2 C_{i,xx}^{m+1} \\
& - (2 \theta_{13} - \theta_{32}) \left(\frac{i\eta}{R} \right)^3 D_{i,x}^{m+1} + \theta_{12} \left(\frac{i\eta}{R} \right)^4 C_i^{m+1} + \frac{1}{R} C_{i,xx}^{m+1} \\
& - \left(\frac{i\eta}{R} \right) \frac{1}{a_{22}} \{ -\theta_{21} A_i^{m+1} A_{0,xx}^m - \theta_{21} (A_i^m + A_i^0) A_{0,xx}^{m+1} \\
& + \theta_{21} A_i^m A_{0,xx}^m - \frac{1}{R} A_i^{m+1} A_0^m - \frac{1}{R} (A_i^m + A_i^0) A_0^{m+1} + \frac{1}{R} A_i^m A_0^m \\
& + \left(\frac{\eta}{2R} \right)^2 \sum_{j=1}^K j^2 [(A_j^{m+1} + A_i^0) (A_j^m + 2 A_j^0) A_j^m + (A_i^m + A_i^0) (A_j^{m+1} + 2 A_j^0) A_j^m
\end{aligned}$$

$$\begin{aligned}
& + (A_i^m + A_i^0)(A_j^m + 2A_j^0)A_j^{m+1} - 2(A_i^m + A_i^0)(A_j^m + 2A_j^0)A_j^m \\
& + (A_i^m + A_i^0)(B_j^m + 2B_j^0)B_j^m + (A_i^m + A_i^0)(B_j^{m+1} + 2B_j^0)B_j^m \\
& + (A_i^m + A_i^0)(B_j^m + 2B_j^0)B_j^{m+1} - 2(A_i^m + A_i^0)(B_j^m + 2B_j^0)B_j^m \} \\
& - \left(\frac{i\eta}{R}\right)^2 \left(\frac{A_i^{m+1} + A_i^0}{a_{22}}\right) (a_{12}\bar{N}_{xx} - a_{23}\bar{N}_{xy}) \\
& - (A_{i,xx}^{m+1} + A_{i,xx}^0)\bar{N}_{xx} + 2\bar{N}_{xy}\left(\frac{i\eta}{R}\right)(B_{i,x}^{m+1} + B_{i,x}^0) \\
& - \frac{1}{2}\left(\frac{\eta}{R}\right)^2 \sum_{j=1}^{2K} j^2 \{ [J_{ij}^{m+1}(A)C_{j,xx}^m + J_{ij}^m(A+A^0)C_{j,xx}^{m+1} \\
& - J_{ij}^m(A)C_{j,xx}^m] + [K_{ij}^{m+1}(B)D_{j,xx}^m + K_{ij}^m(B+B^0)D_{j,xx}^{m+1} \\
& - K_{ij}^m(B)D_{j,xx}^m] + 2[L_{ij}^{m+1}(A)C_{j,x}^m + L_{ij}^m(A+A^0)C_{j,x}^{m+1} - L_{ij}^m(A)C_{j,x}^m] \\
& + 2[M_{ij}^{m+1}(B)D_{j,x}^m + M_{ij}^m(B+B^0)D_{j,x}^{m+1} - M_{ij}^m(B)D_{j,x}^m] \\
& + N_{ij}^{m+1}(A)C_j^m + N_{ij}^m(A+A^0)C_j^{m+1} - N_{ij}^m(A)C_j^m \\
& + O_{ij}^{m+1}(B)D_j^m + O_{ij}^m(B+B^0)D_j^{m+1} - O_{ij}^m(B)D_j^m \} + \delta_i' = 0 \quad (A-76)
\end{aligned}$$

(iii) [$i = 1, 2, \dots, K$; weighting function is $\sin \frac{i\eta y}{R}$; Eq A.71]

$$\begin{aligned}
& d_{11}B_{i,xxxx}^{m+1} - 4d_{13}\left(\frac{i\eta}{R}\right)A_{i,xxx}^{m+1} - (2d_{12} + 4d_{33})\left(\frac{i\eta}{R}\right)^2 B_{i,xx}^{m+1} + 4d_{23}\left(\frac{i\eta}{R}\right)^3 A_{i,x}^{m+1} \\
& + d_{22}\left(\frac{i\eta}{R}\right)^4 B_i^{m+1} + \theta_{21}D_{i,xxxx}^{m+1} - (2\theta_{23} - \theta_{31})\left(\frac{i\eta}{R}\right)C_{i,xxx}^{m+1} \\
& - (\theta_{11} - 2\theta_{33} + \theta_{22})\left(\frac{i\eta}{R}\right)^2 D_{i,xx}^{m+1} + (2\theta_{13} - \theta_{32})\left(\frac{i\eta}{R}\right)^3 C_{i,x}^{m+1} + \theta_{12}\left(\frac{i\eta}{R}\right)^4 D_i^{m+1} \\
& + \frac{D_{i,xxx}^{m+1}}{R} - \left(\frac{i\eta}{R}\right)^2 \frac{1}{a_{22}} \{ -\theta_{21}B_i^{m+1}A_{0,xx}^m - \theta_{21}(B_i^m + B_i^0)A_{0,xx}^{m+1}
\end{aligned}$$

$$\begin{aligned}
& + \theta_{21} B_i^m A_{o,xx}^m - \frac{1}{R} B_i^{m+1} A_o^m - \frac{1}{R} (B_i^m + B_i^o) A_o^{m+1} + \frac{1}{R} B_i^m A_o^m \\
& + \left(\frac{n}{2R}\right)^2 \sum_{j=1}^k j^2 \{ (B_i^{m+1} + B_i^o) (A_j^m + 2A_j^o) A_j^m + (B_i^m + B_i^o) (A_j^{m+1} + 2A_j^o) A_j^m \\
& + (B_i^m + B_i^o) (A_j^m + 2A_j^o) A_j^{m+1} - 2(B_i^m + B_i^o) (A_j^m + 2A_j^o) A_j^m \\
& + (B_i^{m+1} + B_i^o) (B_j^m + 2B_j^o) B_j^m + (B_i^m + B_i^o) (B_j^{m+1} + 2B_j^o) B_j^m \\
& + (B_i^m + B_i^o) (B_j^m + 2B_j^o) B_j^{m+1} - 2(B_i^m + B_i^o) (B_j^m + 2B_j^o) B_j^m \} \\
& - \left(\frac{in}{R}\right)^2 \left(\frac{B_i^{m+1} + B_i^o}{a_{i2}}\right) (a_{12} \bar{N}_{xx} - a_{23} \bar{N}_{xy}) - (B_{i,xx}^{m+1} + B_{i,xx}^o) \bar{N}_{xx} \\
& - 2\bar{N}_{xy} \left(\frac{in}{R}\right) (A_{i,x}^{m+1} + A_{i,x}^o) - \frac{1}{2} \left(\frac{n}{R}\right)^2 \sum_{j=1}^{2k} \{ Q_{ij}^{m+1}(B) C_{j,xx}^m \\
& + Q_{ij}^m (B + B^o) C_{j,xx}^{m+1} - Q_{ij}^m (B) C_j^m + R_{ij}^{m+1}(A) D_{j,xx}^m \\
& + R_{ij}^m (A + A^o) D_{j,xx}^{m+1} - R_{ij}^m (A) D_{j,xx}^m - 2(S_{ij}^{m+1}(B) C_{j,x}^m \\
& + S_{ij}^m (B + B^o) C_{j,x}^{m+1} - S_{ij}^m (A) C_{j,x}^m) - 2(T_{ij}^{m+1}(A) D_{j,x}^m \\
& + T_{ij}^m (A + A^o) D_{j,x}^{m+1} - T_{ij}^m (A) D_{j,x}^m) + U_{ij}^{m+1}(B) C_j^m + U_{ij}^m (B + B^o) C_j^{m+1} \\
& - U_{ij}^m (B) C_j^m + V_{ij}^{m+1}(A) D_j^m + V_{ij}^m (A + A^o) D_j^m - V_{ij}^m (A) D_j^m \} \\
& + \mathcal{G}_i^2 = 0 \tag{A-77}
\end{aligned}$$

Finally, the Boundary Conditions [SS-i, CC-i, Eqs A-37, and A-40 - A-46] are also expressed in terms of the dependent variables, through the use of Eqs A-47. They are:

$$\underline{SS-1} \quad A_0 = 0$$

$$A_{0,xx}(d_{11} - \frac{b_{21}^2}{a_{22}}) = \frac{\theta_{21}}{a_{22}}(-a_{12}\bar{N}_{xx} + a_{23}\bar{N}_{xy}) + \bar{M}_{xx} + \theta_{11}\bar{N}_{xx} - \theta_{31}\bar{N}_{xy}$$

$$A_i = B_i = 0 \quad ,$$

$$\left. \begin{aligned} d_{11}A_{i,xx} + \theta_{21}C_{i,xx} + 2d_{13}\left(\frac{i\eta}{R}\right)B_{i,x} &= 0 \\ d_{11}B_{i,xx} + \theta_{21}D_{i,xx} - 2d_{13}\left(\frac{i\eta}{R}\right)A_{i,x} &= 0 \end{aligned} \right\} i = 1, 2, \dots, k$$

$$C_i = D_{i,x} = D_i = C_{i,x} = 0 \quad ; \quad i = 1, 2, \dots, 2k \quad (A-78)$$

$$\underline{SS-2} \quad A_0 = 0$$

$$A_{0,xx}(d_{11} - \frac{\theta_{21}^2}{a_{22}}) = \frac{\theta_{21}}{a_{22}}(-a_{12}\bar{N}_{xx} + a_{23}\bar{N}_{xy}) + \bar{M}_{xx} + \theta_{11}\bar{N}_{xx} - \theta_{31}\bar{N}_{xy}$$

$$A_i = B_i = 0$$

$$\left. \begin{aligned} d_{11}A_{i,xx} + \theta_{21}C_{i,xx} - \theta_{11}\left(\frac{i\eta}{R}\right)^2 C_i + 2d_{13}\left(\frac{i\eta}{R}\right)B_{i,x} &= 0 \\ d_{11}B_{i,xx} + \theta_{21}D_{i,xx} - \theta_{11}\left(\frac{i\eta}{R}\right)^2 D_i - 2d_{13}\left(\frac{i\eta}{R}\right)A_{i,x} &= 0 \end{aligned} \right\} i = 1, 2, \dots, k$$

$$D_{i,x} = C_{i,x} = 0 \quad ; \quad i = 1, 2, \dots, 2k$$

$$a_{22}C_{i,xxx} - 2a_{23}\left(\frac{i\eta}{R}\right)D_{i,xx} + a_{13}\left(\frac{i\eta}{R}\right)^3 D_i + \theta_{21}A_{i,xxx} + (2\theta_{33} - \theta_{31})\frac{i\eta}{R}B_{i,xx}$$

$$+ (2\theta_{33} - \theta_{22})\left(\frac{i\eta}{R}\right)^2 A_i + \frac{A_{i,x}}{R} - \frac{\eta^2}{2R^3} \sum_{j=0}^k \{ [(i+j)^2 A_{i+j}^0$$

$$+ (1 - \eta_{j-i}^2 + \eta_i)(i-j)^2 A_{i-j}^0] A_{j,x} + [(i+j)^2 B_{i+j}^0$$

$$+ (1 - \eta_{i-j}^2 + \eta_i)(i-j)^2 B_{i-j}^0] B_{j,x} \} = 0 \quad ; \quad i = 1, 2, \dots, 2k$$

$$a_{22}D_{i,xxx} + 2a_{23}\left(\frac{i\eta}{R}\right)C_{i,xx} - a_{13}\left(\frac{i\eta}{R}\right)^3 C_i + \theta_{21}B_{i,xxx}$$

$$- (2\theta_{23} - \theta_{31})\left(\frac{i\eta}{R}\right)A_{i,xx} + (2\theta_{33} - \theta_{21})\left(\frac{i\eta}{R}\right)^2 B_{i,x}$$

$$+ \frac{B_{i,x}}{R} - \frac{\eta^2}{2R^3} \sum_{j=0}^k \{ [- (i+j)^2 A_{i+j}^0$$

$$+ (1 - \eta_{i-j}^2 + \eta_i)(i-j)^2 A_{i-j,1}^\circ] B_{i,xx} + [(i+j)^2 B_{i+j}^\circ$$

$$+ (-1 + \eta_{i-j} + \eta_i)(i-j)^2 B_{i-j,1}^\circ] A_{j,x} \} = 0 ; i = 1, 2, \dots, 2K \quad (A-79)$$

SS-3 $A_0 = 0$

$$A_{0,xy} (d_{11} - \frac{\theta_{21}^2}{a_{22}}) = \frac{\theta_{21}}{a_{22}} [-a_{12} \bar{N}_{xx} + a_{23} \bar{N}_{xy}] + \bar{M}_{xx} + \theta_{11} \bar{N}_{xx} - \theta_{31} \bar{N}_{xy}$$

$$A_i = B_i = 0$$

$$\left. \begin{aligned} d_{11} B_{i,xx} + \theta_{21} D_{i,xx} + \theta_{31} (\frac{i\eta}{R}) C_{i,x} - 2d_{13} (\frac{i\eta}{R}) B_{i,x} &= 0 \\ d_{11} B_{i,xx} + \theta_{21} D_{i,xx} + \theta_{31} (\frac{i\eta}{R}) C_{i,x} - 2d_{13} (\frac{i\eta}{R}) A_{i,x} &= 0 \end{aligned} \right\} i = 1, 2, \dots, K$$

$$C_i = D_i = 0$$

$$\left. \begin{aligned} a_{22} C_{i,xx} - a_{23} (\frac{i\eta}{R}) D_{i,x} + \theta_{21} A_{i,xx} + 2\theta_{23} (\frac{i\eta}{R}) B_{i,x} &= 0 \\ a_{22} D_{i,xx} + a_{23} (\frac{i\eta}{R}) C_{i,x} + \theta_{21} B_{i,xx} - 2\theta_{23} A_{i,x} &= 0 \end{aligned} \right\} i = 1, 2, \dots, 2K \quad (A-80)$$

SS-4 $A_0 = 0$

$$A_{0,xx} (d_{11} - \frac{\theta_{21}^2}{a_{22}}) = \frac{\theta_{21}}{a_{22}} [-a_{12} \bar{N}_{xx} + a_{23} \bar{N}_{xy}] + \bar{M}_{xx} + \theta_{11} \bar{N}_{xx} - \theta_{31} \bar{N}_{xy}$$

$$A_i = B_i = 0$$

$$\left. \begin{aligned} \theta_{21} C_{i,xx} - \theta_{11} (\frac{i\eta}{R})^2 C_i - \theta_{31} (\frac{i\eta}{R}) D_{i,x} + d_{11} A_{i,xx} + 2d_{13} (\frac{i\eta}{R}) B_{i,x} &= 0 \\ \theta_{21} D_{i,xx} - \theta_{11} (\frac{i\eta}{R})^2 D_i + \theta_{31} (\frac{i\eta}{R}) D_{i,x} + d_{11} B_{i,xx} - 2d_{13} (\frac{i\eta}{R}) B_{i,x} &= 0 \end{aligned} \right\} i = 1, 2, \dots, K$$

$$-a_{12}\left(\frac{i\eta}{R}\right)^2 C_i + a_{22} C_{i,xx} - a_{23}\left(\frac{i\eta}{R}\right) D_{i,x} + \theta_{21} A_{i,xx} + 2\theta_{23}\left(\frac{i\eta}{R}\right) B_{i,x} = 0$$

$$-a_{13}\left(\frac{i\eta}{R}\right)^3 D_i + 2a_{23}\left(\frac{i\eta}{R}\right) D_{i,xx} + (a_{33} + a_{12}) C_{i,x}\left(\frac{i\eta}{R}\right)^2 - a_{22} C_{i,xxx}$$

$$+ (\theta_{31} - 2\theta_{23})\left(\frac{i\eta}{R}\right) B_{i,xx} - (2\theta_{33} - \theta_{22})\left(\frac{i\eta}{R}\right)^2 A_{i,x} - \theta_{21} A_{i,xxx} - \frac{A_{i,x}}{R}$$

$$+ \frac{\eta^2}{2R^2} \sum_{j=0}^K \left\{ [(i+j)^2 A_{i+j}^\circ + (1 - \eta_{j-i}^2 + \eta_i)(i-j)^2 A_{|i-j|}^\circ] A_{j,x} \right.$$

$$\left. + [(i+j)^2 B_{i+j} + (-1 - \eta_{i-j} + \eta_i)(i-j)^2 B_{|i-j|}^\circ] B_{j,x} \right\} = 0$$

$i=1, 2, \dots, 2K$

$$-a_{12}\left(\frac{i\eta}{R}\right)^2 D_i + a_{22} D_{i,xx} + a_{23}\left(\frac{i\eta}{R}\right) C_{i,x} + \theta_{21} B_{i,xx} - 2\theta_{23}\left(\frac{i\eta}{R}\right) A_{i,x} = 0$$

$$a_{13}\left(\frac{i\eta}{R}\right)^3 C_i - 2a_{23}\left(\frac{i\eta}{R}\right) C_{i,xx} + (a_{33} + a_{12}) D_{i,x}\left(\frac{i\eta}{R}\right)^2 - a_{22} D_{i,xxx}$$

$$- (\theta_{31} - 2\theta_{23})\left(\frac{i\eta}{R}\right) A_{i,xx} - (2\theta_{33} - \theta_{22})\left(\frac{i\eta}{R}\right)^2 B_{i,x} - \theta_{21} B_{i,xxx} - \frac{B_{i,x}}{R}$$

$$+ \frac{\eta^2}{2R^2} \sum_{j=0}^K \left\{ [-(i+j)^2 A_{i+j}^\circ + (1 - \eta_{j-i}^2 + \eta_i)(i-j)^2 A_{|i-j|}^\circ] B_{j,x} \right.$$

$$\left. + [(i+j)^2 B_{i+j}^\circ + (-1 + \eta_{i-j} + \eta_i)(i-j)^2 B_{|i-j|}^\circ] A_{j,x} \right\} = 0$$

(A-81)

CC-1

$$A_0 = A_{0,x} = 0$$

$$A_i = A_{i,x} = B_i = B_{i,x} = 0 \quad ; \quad i = 1, 2, \dots, K$$

$$C_i = D_{i,x} = D_i = C_{i,x} = 0 \quad ; \quad i = 1, 2, \dots, 2K$$

(A-82)

CC-2

$$A_0 = A_{0,x} = 0$$

$$A_i = A_{i,x} = B_i = B_{i,x} = 0 \quad ; \quad i = 1, 2, \dots, k$$

$$D_{i,x} = C_{i,x} = 0$$

$$\left. \begin{aligned} & -a_{13} \left(\frac{i\eta}{R}\right)^3 D_i + 2a_{23} \left(\frac{i\eta}{R}\right) D_{i,xx} - a_{22} C_{i,xxx} - \theta_{21} A_{i,xxx} \\ & + (\theta_{31} - 2\theta_{23}) \left(\frac{i\eta}{R}\right) B_{i,xx} = 0 \\ & a_{13} \left(\frac{i\eta}{R}\right)^3 C_i - 2a_{23} \left(\frac{i\eta}{R}\right) C_{i,xx} - a_{22} D_{i,xxx} - \theta_{21} B_{i,xxx} \\ & - (\theta_{31} - 2\theta_{23}) \left(\frac{i\eta}{R}\right) A_{i,xx} = 0 \end{aligned} \right\} i = 1, 2, \dots, 2k \quad (A-83)$$

CC-3

$$A_0 = A_{0,x} = 0$$

$$A_i = A_{i,x} = B_i = B_{i,x} = 0 \quad ; \quad i = 1, 2, \dots, k$$

$$\left. \begin{aligned} & C_i = D_i = a_{22} C_{i,xx} - a_{23} \left(\frac{i\eta}{R}\right) D_{i,x} + \theta_{21} A_{i,xx} = 0 \\ & a_{22} D_{i,xx} + a_{23} \left(\frac{i\eta}{R}\right) C_{i,x} + \theta_{21} B_{i,xx} = 0 \end{aligned} \right\} i = 1, 2, \dots, 2k \quad (A-84)$$

CC-4

$$A_0 = A_{0,x} = 0$$

$$A_i = A_{i,x} = B_i = B_{i,x} \quad ; \quad i = 1, 2, \dots, k$$

$$\left. \begin{aligned} & -a_{12} \left(\frac{i\eta}{R}\right)^2 C_i + a_{22} C_{i,xx} - a_{23} \left(\frac{i\eta}{R}\right) D_{i,x} + \theta_{21} A_{i,xx} = 0 \\ & -a_{13} \left(\frac{i\eta}{R}\right)^2 D_i + 2a_{23} \left(\frac{i\eta}{R}\right) D_{i,xx} + (a_{33} + a_{12}) \left(\frac{i\eta}{R}\right)^2 C_{i,x} \end{aligned} \right\}$$

$$\begin{aligned}
& -a_{22}C_{i,xyx} - \theta_{21}A_{i,xyx} + (\theta_{31} - 2\theta_{23})\left(\frac{i\eta}{R}\right)B_{i,xy} = 0 \\
& -a_{12}\left(\frac{i\eta}{R}\right)^2 D_i + a_{22}D_{i,xx} + a_{23}\left(\frac{i\eta}{R}\right)C_{i,x} + \theta_{21}B_{i,xx} = 0 \\
& a_{13}\left(\frac{i\eta}{R}\right)^3 C_i - 2a_{23}\left(\frac{i\eta}{R}\right)C_{i,xx} + (a_{33} + a_{12})\left(\frac{i\eta}{R}\right)^2 D_{i,x} \\
& - a_{22}D_{i,xyx} - \theta_{21}B_{i,xyx} - (\theta_{31} - 2\theta_{23})\left(\frac{i\eta}{R}\right)A_{i,xx} = 0
\end{aligned}
\quad \left. \vphantom{\begin{aligned} & -a_{22}C_{i,xyx} - \theta_{21}A_{i,xyx} + (\theta_{31} - 2\theta_{23})\left(\frac{i\eta}{R}\right)B_{i,xy} = 0 \\ & -a_{12}\left(\frac{i\eta}{R}\right)^2 D_i + a_{22}D_{i,xx} + a_{23}\left(\frac{i\eta}{R}\right)C_{i,x} + \theta_{21}B_{i,xx} = 0 \\ & a_{13}\left(\frac{i\eta}{R}\right)^3 C_i - 2a_{23}\left(\frac{i\eta}{R}\right)C_{i,xx} + (a_{33} + a_{12})\left(\frac{i\eta}{R}\right)^2 D_{i,x} \\ & - a_{22}D_{i,xyx} - \theta_{21}B_{i,xyx} - (\theta_{31} - 2\theta_{23})\left(\frac{i\eta}{R}\right)A_{i,xx} = 0 \end{aligned}} \right\} i = 1, 2, \dots, 2K \quad (A-85)$$

A. 2.8 Solution Methodology-Finite Difference Equations

Before casting the field equations into finite difference form, the linearized ordinary differential equations of compatibility and equilibrium, Eqs (73) - (77), can be written in matrix form.

$$\begin{aligned}
& [M_1]\{X_{,xxxx}\} + [M_2]\{X_{,xxx}\} + [M_3]\{X_{,xx}\} \\
& + [M_4]\{X_{,x}\} + [M_5]\{X\} + \{M_6\} = 0 \quad (A-86)
\end{aligned}$$

where

$$\{X\} = [A_0^{m+1}, \dots, A_k^{m+1}, B_1^{m+1}, \dots, B_k^{m+1}, C_1^{m+1}, \dots, C_{2K}^{m+1}, D_1^{m+1}, \dots, D_{2K}^{m+1}]^T \quad (A-87)$$

is the column matrix of the unknown function of position x , and $[M_j]$, $j = 1, 2, \dots, 5$ are square matrices $[(6k + 1) \text{ by } (6k + 1)]$; see Eqs A-73-A-77 with elements composed of known parameters (applied loads, geometry, and values of the unknowns evaluated at the previous step, m and therefore known).

$\{M_6\}$ is a column matrix of known elements.

Next, transformation equations are introduced in order to reduce the order of the linearized differential equations. This step increases (doubles) the number of equations, but it is introduced for convenience, because it is easier to deal with low order equations when employing the finite difference scheme. These transformation equations are

$$\{\eta\} = \{X_{,xx}\}$$

and they are used in only in connection with the third and fourth derivatives.

By this transformation, Eq. A-87 Eq. A-86 becomes

$$[R] \begin{Bmatrix} \{X_{,xx}\} \\ \{\eta_{,xx}\} \end{Bmatrix} + [S] \begin{Bmatrix} \{X_{,x}\} \\ \{\eta_{,x}\} \end{Bmatrix} + [T] \begin{Bmatrix} \{X\} \\ \{\eta\} \end{Bmatrix} = \{G\} \quad (A-88)$$

where

$$[R] = \begin{bmatrix} [0] & [M_1] \\ [I] & [0] \end{bmatrix} ; [S] = \begin{bmatrix} [M_4] & [M_2] \\ [0] & [0] \end{bmatrix}$$

$$[T] = \begin{bmatrix} [M_5] & [M_3] \\ [0] & -[I] \end{bmatrix} ; \{G\} = \begin{Bmatrix} -[M_6] \\ \{0\} \end{Bmatrix} \quad (A-89)$$

The governing equations (linearized ordinary differential equations) shown in matrix form, Eqs A-88, are next cast into finite difference form. The usual central difference formula is employed and the equation become

$$\left(\frac{1}{h^2} [R]^{(j)} + \frac{1}{2h} [S]^{(j)} \right) \begin{Bmatrix} \{X\}^{(j+1)} \\ \{\eta\}^{(j+1)} \end{Bmatrix} + \left(-\frac{1}{2h} [R]^{(j)} \right. \\ \left. + [T]^{(j)} \right) \begin{Bmatrix} \{X\}^{(j)} \\ \{\eta\}^{(j)} \end{Bmatrix} + \left(\frac{1}{h^2} [R]^{(j)} - \frac{1}{2h} [S]^{(j)} \right) \begin{Bmatrix} \{X\}^{(j-1)} \\ \{\eta\}^{(j-1)} \end{Bmatrix} = \{G\}^{(j)} \quad (A-90)$$

where j denotes the j th node of the finite difference grid. At each end (x = 0 and L) one more fictitious point is used. This requires (12k + 2) additional equations at each end [the total number is (24k + 4)]. These needed additional equations are the boundary conditions at each end, Eqs A-78- A-79, (whichever set applies from SS-i or CC-i) and their number is (12k + 2). The boundary conditions may also be, first, expressed in matrix form and then cast into finite difference form.

at either $x = 0$ or L

$$[N_1]\{X_{xxx}\} + [N_2]\{X_{xx}\} + [N_3]\{X_x\} + [N_4]\{X\} + \{N_5\} = 0 \quad (A-91)$$

where $[N_j]$, $j = 1, 2, 3, 4$, are matrices $[(12k + 2) \text{ by } (6k + 1)]$ with known element, and $\{N_5\}$ in a column matrix $[(12k + 2) \text{ by one}]$ with, also, known elements.

Use of the transformation equations, Eq A-87, yields

$$[BS] \begin{Bmatrix} \{X_x\} \\ \{\eta_x\} \end{Bmatrix} + [BT] \begin{Bmatrix} \{X\} \\ \{\eta\} \end{Bmatrix} = [BG] \quad (A-92)$$

where

$$[BS] = [[N_3][N_1]]$$

$$[BT] = [[N_4][N_2]]$$

and

$$[BG] = - \{N_5\} \quad (A-93)$$

Note that $[BS]$ and $[BT]$ are square matrices $[(12k + 2) \text{ by } (12k + 2)]$. In finite difference form, Eq. A-92, becomes

$$\frac{1}{2h} [BS]^j \begin{Bmatrix} \{X\} \\ \{\eta\} \end{Bmatrix}^{j+1} + [BT]^j \begin{Bmatrix} \{X\} \\ \{\eta\} \end{Bmatrix}^j - \frac{1}{2h} [BS]^j \begin{Bmatrix} \{X\} \\ \{\eta\} \end{Bmatrix}^{j-1} = \{BG\}^j \quad (A-94)$$

where j is the node number at $x = 0$ and $x = L$ (1 or N)

A. 2.9 End Shortening, Average Shear Strain and Total Potential

Before outlining in detail the numerical scheme of the solution methodology, it is necessary to write the expressions for the average end shortening, average shear strain and the total potential in terms of the dependent variables, A_i , B_i , C_i and D_i .

The average end shortening and shear strain are defined by

$$e_{AV} = -\frac{1}{2\pi RL} \int_0^{2\pi R} \int_0^L \frac{\partial u}{\partial x} dx dy$$

$$\gamma_{AV} = \frac{1}{2\pi RL} \int_0^{2\pi R} \int_0^L \left(\frac{\partial u}{\partial y} + \frac{\partial v}{\partial x} \right) dx dy \quad (A-95)$$

In terms of the variables $w(x, y)$ and $F(x, y)$, the above expressions become:

$$e_{AV} = a_{11} \bar{N}_{xx} - a_{13} \bar{N}_{xy} - \frac{1}{2\pi RL} \int_0^{2\pi R} \int_0^L \left[a_{11} F_{,yy} + a_{12} F_{,xx} - a_{13} F_{,xy} \right. \\ \left. + \theta_{11} W_{,xx} + \theta_{12} W_{,yy} + 2\theta_{23} W_{,xy} - \frac{1}{2} W_{,x} (W_{,x} + 2W_{,x}^0) \right] dx dy \quad (A-96)$$

$$\gamma_{AV} = -a_{13} \bar{N}_{xx} + a_{33} \bar{N}_{xy} + \frac{1}{2\pi RL} \int_0^{2\pi R} \int_0^L \left[a_{13} F_{,yy} + a_{23} F_{,xx} - a_{33} F_{,xy} \right. \\ \left. + \theta_{31} W_{,xx} + \theta_{32} W_{,yy} + 2\theta_{33} W_{,xy} - \frac{1}{2} W_{,x} (W_{,y} + 2W_{,y}^0) \right. \\ \left. - \frac{1}{2} W_{,y} (W_{,x} + 2W_{,x}^0) \right] dx dy \quad (A-97)$$

Finally, if the expressions for w and F are substituted into Eqs. A-96 and A-97 these equations become:

$$e_{AV} = a_{11} \bar{N}_{xx} - a_{13} \bar{N}_{xy} - \frac{1}{2} \int_0^L \left\{ \frac{a_{12}}{a_{22}} \left\{ -\theta_{21} A_0'' - A_0/R + a_{12} \bar{N}_{xx} \right. \right. \\ \left. \left. - a_{23} \bar{N}_{xy} + \left(\frac{\pi}{2R} \right)^2 \sum_{j=1}^K j^2 [(A_j + 2A_j^0) A_j + (B_j + 2B_j^0) B_j] \right\} \right. \\ \left. + \theta_{11} A_0'' - \frac{1}{2} (A_0' + 2A_0^0) A_0' - \frac{1}{4} [A_j' (A_j' + 2A_j^0') + B_j' (B_j' + 2B_j^0')] \right\} dx \quad (A-98)$$

$$\gamma_{AV} = -a_{13} \bar{N}_{xx} + a_{33} \bar{N}_{xy} + \frac{1}{2} \int_0^L \left\{ \frac{a_{23}}{a_{22}} \left\{ -\theta_{21} A_0'' - A_0/R \right. \right. \\ \left. \left. + a_{12} \bar{N}_{xx} - a_{23} \bar{N}_{xy} + \left(\frac{\pi}{2R} \right)^2 \sum_{j=1}^K j^2 [(A_j + 2A_j^0) A_j \right. \right.$$

$$\begin{aligned}
& + (B_j + 2B_j^\circ) B_j \} + \theta_{31} A_0'' - \sum_{j=1}^K \left(\frac{j\pi}{2R} \right)^2 [A_j' (B_j + B_j^\circ) \\
& - B_j' (A_j + A_j^\circ) + A_j^\circ B_j - B_j^\circ A_j] \} dx
\end{aligned} \tag{A-99}$$

Similarly, the expression for the total potential is:

$$\begin{aligned}
U_T = & \frac{1}{2} \int_0^{2\pi R} \int_0^L (N_{xx} \epsilon_{xx}^\circ + N_{yy} \epsilon_{yy}^\circ + N_{xy} \gamma_{xy}^\circ - M_{xx} \kappa - M_{yy} \kappa_{yy} \\
& - 2M_{xy} \kappa_{xy}) dx dy - \int_0^{2\pi R} \int_0^L g w dx dy - \int_0^{2\pi R} [-\bar{N}_{xx} u \\
& + \bar{N}_{xy} v] \Big|_0^L dy + \int_0^{2\pi R} (\bar{M}_{xx} w_{,x}) \Big|_0^L dy
\end{aligned} \tag{A-100}$$

where $\bar{M}_{xx} = -\bar{E} N_{xx}$ and \bar{E} is the load eccentricity measured positive in the positive z-direction and

$$u \Big|_0^L = \int_0^L \frac{\partial u}{\partial x} dx \quad \& \quad v \Big|_0^L = \int_0^L \frac{\partial v}{\partial x} dx$$

Thus, the contribution of the in-plane loads to the total potential becomes

$$-\int_0^{2\pi R} [-\bar{N}_{xx} u + \bar{N}_{xy} v] \Big|_0^L dy = -\int_0^{2\pi R} [-\bar{N}_{xx} \int_0^L \frac{\partial u}{\partial x} dx + \bar{N}_{xy} \int_0^L \frac{\partial v}{\partial x} dx] dy$$

In terms of w and F the expression for U_T becomes

$$\begin{aligned}
U_T = & \frac{1}{2} \int_0^{2\pi R} \int_0^L [a_{11} F_{,yy}^2 + a_{22} F_{,xx}^2 + a_{33} F_{,xy}^2 + 2a_{12} F_{,xx} F_{,yy} \\
& - 2a_{13} F_{,yy} F_{,xy} - 2a_{23} F_{,xx} F_{,xy}] dx dy - \frac{1}{2} \int_0^{2\pi R} \int_0^L (d_{11} w_{,xx}^2 \\
& + d_{22} w_{,yy}^2 + 4d_{33} w_{,xy}^2 + 2d_{12} w_{,xx} w_{,yy} + 4d_{13} w_{,xx} w_{,xy} \\
& + 4d_{23} w_{,yy} w_{,xy}) dx dy - \bar{N}_{xx} \int_0^{2\pi R} \int_0^L (a_{11} F_{,yy} + a_{12} F_{,xx} \\
& - a_{13} F_{,xy}) dx dy + \bar{N}_{xy} \int_0^{2\pi R} \int_0^L (a_{23} F_{,xx} - a_{33} F_{,xy}
\end{aligned}$$

$$\begin{aligned}
& + a_{13} F_{,yy}) dx dy - \int_0^{2\pi R} \int_0^L g w dx dy + \pi R L (a_{11} \bar{N}_{xx}^2 \\
& + a_{33} \bar{N}_{xy} - 2\pi R L (e_{Av} \bar{N}_{xx} + \gamma_{Av} \bar{N}_{xy}) - 2\pi R L a_{13} \bar{N}_{xx} \bar{N}_{xy} \\
& - \int_0^{2\pi R} (\bar{E} \bar{N}_{xx} w_{,x}) \Big|_0^L dy \quad (A-101)
\end{aligned}$$

Finally, the expression for the total potential in terms of A_i , B_i , C_i and D_i becomes

$$\begin{aligned}
U_T = & \pi R \int_0^L \left\{ \frac{1}{a_{22}} \left\{ -\theta_{21} A_0'' - A_0/R + \left(\frac{\pi}{2R}\right)^2 \sum_{j=1}^K j^2 [(A_j + 2A_j^0) A_j \right. \right. \\
& + (B_j + 2B_j^0) B_j] + a_{12} \bar{N}_{xx} - a_{23} \bar{N}_{xy} \Big\}^2 + 2(a_{23} \bar{N}_{xy} - a_{12} \bar{N}_{xy}) \\
& \cdot \frac{1}{a_{22}} \left\{ -\theta_{21} A_0'' - A_0/R + \left(\frac{\pi}{2R}\right)^2 \sum_{j=1}^K j^2 [(A_j + 2A_j^0) A_j \right. \\
& + (B_j + 2B_j^0) B_j] + a_{12} \bar{N}_{xx} - a_{23} \bar{N}_{xy} \Big\} - d_{11} (A_0'')^2 \\
& + \frac{1}{2} \sum_{i=1}^{2K} \left\{ a_{11} \left(\frac{i\pi}{R}\right)^4 (C_i^2 + D_i^2) + a_{22} [(C_i'')^2 + (D_i'')^2] \right. \\
& + a_{33} \left(\frac{i\pi}{R}\right)^2 [(C_i')^2 + (D_i')^2] - 2a_{12} \left(\frac{i\pi}{R}\right)^2 (C_i'' C_i + D_i'' D_i) \\
& - 2a_{13} \left(\frac{i\pi}{R}\right)^3 (-C_i D_i' + D_i C_i') - 2a_{23} \left(\frac{i\pi}{R}\right) (C_i'' D_i - D_i'' C_i) \Big\} \\
& - \frac{1}{2} \sum_{i=1}^K \left\{ d_{11} [(A_i'')^2 + (B_i'')^2] + d_{22} \left(\frac{i\pi}{R}\right)^4 (A_i^2 + B_i^2) \right. \\
& + 4d_{33} \left(\frac{i\pi}{R}\right)^2 [(A_i')^2 + (B_i')^2] - 2d_{12} \left(\frac{i\pi}{R}\right)^2 (A_i'' A_i + B_i'' B_i)
\end{aligned}$$

$$\begin{aligned}
& -4d_{13}\left(\frac{i\eta}{R}\right)(-A_i''B_i' + B_i''A_i') - 4d_{33}\left(\frac{i\eta}{R}\right)^3(A_iB_i' - B_iA_i') \} \} dx \\
& - \pi R \int_0^L \{ 2g_0' A_0 + \sum_{j=1}^K [g_j' A_j + g_j' B_j] \} dx - 2\pi RL (e_{Av} \bar{N}_{xx} \\
& + \gamma_{Av} \bar{N}_{xy}) + \pi RL (a_{11} \bar{N}_{xx}^2 - 2a_{13} \bar{N}_{xx} \bar{N}_{xy} + a_{33} \bar{N}_{xy}^2) \\
& - 4\pi \bar{E} \bar{N}_{xy} R A_0'
\end{aligned} \tag{A-102}$$

Before leaving this section, it is important to give the expression for the modified potential an expression needed in the estimation of dynamic critical loads. As explained in Ref. 39 the modification is associated with the deflectional response of the system. When an axial load is applied, an axial motion will result (with some related transverse motion). If an instability of the type described in Refs. 40-43 and 37 is to take place, under sudden application of the axial load, it should not be expected to occur through the primary axial node, but through the existence of transverse deflectional nodes, unrelated to the axial node. Because of this and since the governing equation for dynamic buckling is (though conservation of energy)

$$U_{T_{Mod.}} + T = 0 \tag{A-103}$$

where T is the kinetic energy (unrelated to transverse deflectional modes), then the modified potential must not contain in plane node terms, when suddenly applied in-plane loads, \bar{N}_{xx} and \bar{N}_{xy} , are considered. In the case of lateral pressure, the modification is different, therefore the expression, given below for the modified total potential, applies only to in-plane loads. This expression is obtained by excluding strictly load-dependent terms and those terms related to $F(x, y)$, $[C_0'']$, which correspond to in-plane motion.

$$U_{T \text{ Mod}} = U_T + \pi R L [\bar{N}_{xx}^2 (a_{11} - a_{12}^2/a_{22}) + \bar{N}_{xy} (a_{33} - a_{23}^2/a_{22}) + 2\bar{N}_{xx}\bar{N}_{xy} (a_{12} a_{33}/a_{22} - a_{13})] \quad (A-104)$$

A. 2.9 Solution Methodology - Numerical Scheme

A computer program has been written (see Appendix A for flow charts and Program Listing) for data generation. The linearized finite difference equations are solved by an algorithm which is a modification of the one described in Ref. 43. The modification, which consists of a generalization of the algorithm of Ref. 43 is fully described in Appendix B. The solution procedure used for the problem, herein, is based on the algorithm described in Appendix B.

The field equations, Eq. A-90, can be written as

$$[\bar{C}_k] \{ \bar{Z}_{k-1} \} + [\bar{B}_k] \{ \bar{Z}_k \} + [\bar{A}_k] \{ \bar{Z}_{k+1} \} = \{ G_k \} \quad (A-105)$$

where $k = 1, 2, \dots, N$ and

$$[\bar{C}_k] = \frac{1}{h^2} [R]^k - \frac{1}{2h} [S]^k ; [\bar{B}_k] = -\frac{1}{2h^2} [\bar{R}]^k + [T]^k$$

$$[\bar{A}_k] = \frac{1}{h^2} [R]^k + \frac{1}{2h} [S]^k ; \{ \bar{Z}_k \} = \left\{ \begin{matrix} \{X\} \\ \{Y\} \end{matrix} \right\}^k \quad (A-106)$$

Note that there are $(12k + 2)$ elements in the $\{ \bar{Z}_k \}$ vector.

In addition, the boundary conditions, Eqs. A-94 can be written in a similar [to Eqs A.105] form.

at $x = 0$ ($k = 1$)

$$-[\bar{C}_1]\{\bar{Z}_0\} + [\bar{B}_1]\{\bar{Z}_1\} + [\bar{A}_1]\{\bar{Z}_2\} = \{BG_1\} \quad (A-107)$$

and at $x = L (K = N)$

$$-[\bar{C}_N]\{\bar{Z}_{N-1}\} + [\bar{B}_N]\{\bar{Z}_N\} + [\bar{A}_N]\{\bar{Z}_{N+1}\} = \{BG_N\} \quad (A-108)$$

where

$$[\bar{C}_i] = \frac{1}{2h}[BS]^i; [\bar{B}_i] = [BT]^i; [\bar{A}_i] = \frac{1}{2h}[BS]^i \quad i = 1, N \quad (A-109)$$

Note that $\{\bar{Z}_0\}$ and $\{\bar{Z}_{N+1}\}$ denote the vectors of the unknowns at the fictitious points ($k = 0$ and $k = N + 1$).

By properly arranging Eqs. A-105, A-107 and A-108 for the entire cylinder, the following matrix representation is obtained.

$$\begin{bmatrix} \bar{C}_1 & \bar{B}_1 & \bar{A}_1 & & & \\ \bar{C}_1 & \bar{B}_1 & \bar{A}_1 & & & \\ & \bar{C}_2 & \bar{B}_2 & \bar{A}_2 & & \\ & & \bar{C}_3 & \bar{B}_3 & \bar{A}_3 & \\ & & & \ddots & \ddots & \ddots \\ & & & & \bar{C}_{i-1} & \bar{B}_{i-1} & \bar{A}_{i-1} \\ & & & & & \bar{C}_i & \bar{B}_i & \bar{A}_i \\ & & & & & & \bar{C}_{i+1} & \bar{B}_{i+1} & \bar{A}_{i+1} \\ & & & & & & & \ddots & \ddots & \ddots \\ & & & & & & & & \bar{C}_{N-2} & \bar{B}_{N-2} & \bar{A}_{N-2} \\ & & & & & & & & & \bar{C}_{N-1} & \bar{B}_{N-1} & \bar{A}_{N-1} \\ & & & & & & & & & & \bar{C}_N & \bar{B}_N & \bar{A}_N \\ & & & & & & & & & & & \bar{C}_N & \bar{B}_N & \bar{A}_N \end{bmatrix} \begin{Bmatrix} \bar{Z}_0 \\ \bar{Z}_1 \\ \bar{Z}_2 \\ \bar{Z}_3 \\ \vdots \\ \bar{Z}_{i-1} \\ \bar{Z}_i \\ \bar{Z}_{i+1} \\ \vdots \\ \bar{Z}_{N-2} \\ \bar{Z}_{N-1} \\ \bar{Z}_N \\ \bar{Z}_{N+1} \end{Bmatrix} = \begin{Bmatrix} BG_1 \\ G_1 \\ G_2 \\ G_3 \\ \vdots \\ G_{i-1} \\ G_i \\ G_{i+1} \\ \vdots \\ G_{N-2} \\ G_{N-1} \\ G_N \\ GB_N \end{Bmatrix} \quad (A-110)$$

Eq. A.110 can be put in the form of Fig C.1 (Appendix C) and it will be a special case of this form, by the following changes. First, there is no common unknown vector Z_i and thus all the $\{d_i\}$ vectors are zero (tridiagonal matrix). Next,

$$[B_i] = \begin{bmatrix} [\bar{C}_i] & [\bar{B}_i] \\ [\bar{C}_i] & [\bar{B}_i] \end{bmatrix} \quad (24k+4) \text{ by } (24k+4)$$

$$\{Z_i\} = \begin{bmatrix} \{\bar{Z}_0\} \\ \{\bar{Z}_i\} \end{bmatrix} \quad (24k+4) \text{ by one}$$

$$[A_i] = \begin{bmatrix} [\bar{A}_i] \\ [\bar{A}_i] \end{bmatrix} \quad (24k+4) \text{ by } (12k+2)$$

$$[Q_i] = \begin{bmatrix} \{BG_i\} \\ \{G_i\} \end{bmatrix} \quad (24k+4) \text{ by one}$$

$$[C_2] = [(0) \quad [\bar{C}_2]] \quad (12k+2) \text{ by } (24k+4)$$

$$[C_j] = [\bar{C}_j] \quad j = 3, 4, \dots, N-1$$

$$[B_j] = [\bar{B}_j] \quad j = 2, 3, \dots, N-1$$

$$[A_j] = [\bar{A}_j] \quad j = 2, 3, \dots, N-2$$

$$\{z_j\} = \{\bar{z}_j\}$$

$$j = 2, 3, \dots, N-1$$

$$\{q_j\} = \{\bar{q}_j\}$$

$$[A_{N-1}] = \left[[\bar{A}_{N-1}], [0] \right] \quad (12k+2) \text{ by } (24k+4)$$

$$[C_N] = \begin{bmatrix} [\bar{C}_N] \\ [\bar{\bar{C}}_N] \end{bmatrix} \quad (24k+4) \text{ by } (12k+2)$$

$$[B_N] = \begin{bmatrix} [\bar{B}_N] & [\bar{A}_N] \\ [\bar{\bar{B}}_N] & [\bar{\bar{A}}_N] \end{bmatrix} \quad (24k+4) \text{ by } (24k+4)$$

$$\{z_N\} = \begin{Bmatrix} \{\bar{z}_N\} \\ \{\bar{\bar{z}}_{N+1}\} \end{Bmatrix} \quad (24k+4) \text{ by one}$$

$$\{q_N\} = \begin{Bmatrix} \{G_N\} \\ \{BG_N\} \end{Bmatrix} \quad (24k+4) \text{ by one}$$

Note that $m_1 = m_N = 24k + 4$, while $m_i = 12k + 2$ for $i = 2, 3, 4, \dots, N - 1$.

Note also that Eqs. A-110 represents equilibrium and compatibility equations in which displacement components (A_i, B_i) and stress resultant components (C_i, D_i) [see Eq. A-86a] are the

unknown functions, while the geometry and the loading (taken in increments) are taken on known parameters (assigned everytime the equations are solved). Thus, this special case of the algorithm, Eqs A-110, is employed for finding pre-limit point response. When approaching the critical load, the increment in the applied load parameter is kept small and the sign of the determinant of the coefficients [D in Eq.(C - 19)] must be checked. If convergence fails, the load level is over the limit point. But if convergence does not fail and the sign of the determinant changes from what it was at the previous load level, then the load level is also over the limit point. Desired accuracy can be achieved by taking smaller and smaller increments in the load parameter. It is also observed that by employing this procedure (special case of the algorithm in which the load parameter is known), no solution can be obtained past the limit point. Because of this, the more general algorithm, described in Appendix B, is employed at this point of the solution procedure. The new and more general algorithm simply changes the role of one of the displacement terms with that of the applied load parameter. By so doing the form of the equations changes and the matrix of the coefficients of the unknown ceases to be tridiagonal. Depending on the position of the particular term that replaces the load parameter [which one of the $(6k + 2)$ terms, and at which node (x-position)] column matrices appear all along the column corresponding to the vector $\{Z_L\}$ and the new equations assume exactly the form shown on Fig. C-1. Thus, at some level before, the limit point, the procedure is switched to the more general algorithm (Appendix C), in which one of the displacement parameters (A_I or B_I) at some specified node is taken as known (specified increments) and the load parameter is the unknown. This solution procedure is continued until the desired portion of the post-limit point response is obtained.

Finally, in generating data, numerical integration is used to find the values of the total potential, the average end shortening and the average shear [see Eqs A-102, A-98, and A-99].

A.3.0 The u, v, w - Formulation

The geometry and sign convention for this formulation are shown on Figs A.3 and A.4. Note that for this case the x-axis (and therefore the transverse displacement component w) is taken as positive outward.

In this formulation two distinctly different kinematic relations (different shell theories) are employed. One is due to Sanders (Ref 34) and one due to Donnell (Ref 33). In the case of Sanders' equations, it is assumed that the reference surface strains are small, the rotation about the normal is negligibly small and the rotations about in-plane axes are moderate.

One of the reasons for expressing the governing equations in terms of u, v, and w, is that it is not possible to define a stress resultant function, in order to satisfy the in-plane equilibrium equation identically, when using the Sanders' kinematic relations. The case of using Donnell-type kinematic relations is a special case of the Sanders case.

A. 3.1 Kinematic Relations

The kinematic relations derived by Sanders assume a perfect reference surface. These kinematic relations (Ref 34) are modified to include the effect of an initial geometric imperfection $w^0(x,y)$ as shown below.

$$\epsilon_{xx} = \epsilon_{xx}^0 + z \kappa_{xx}$$

$$\epsilon_{yy} = \epsilon_{yy}^0 + z \kappa_{yy}$$

$$\gamma_{xy} = \gamma_{xy}^0 + 2z \kappa_{xy} \quad (A-111)$$

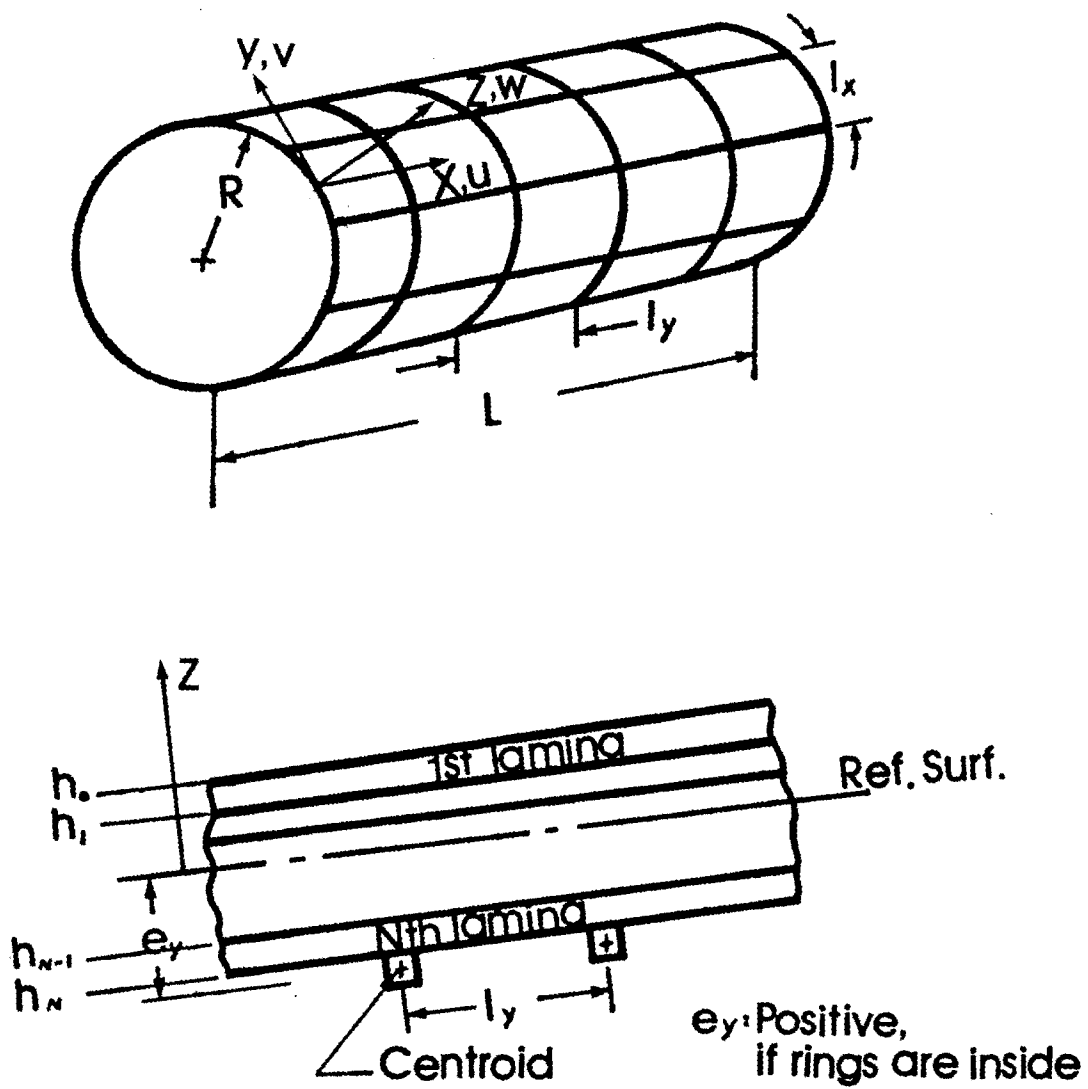
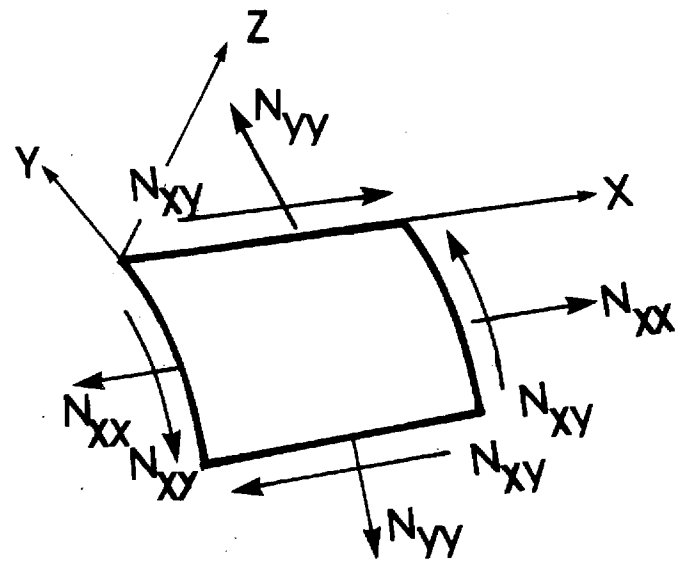
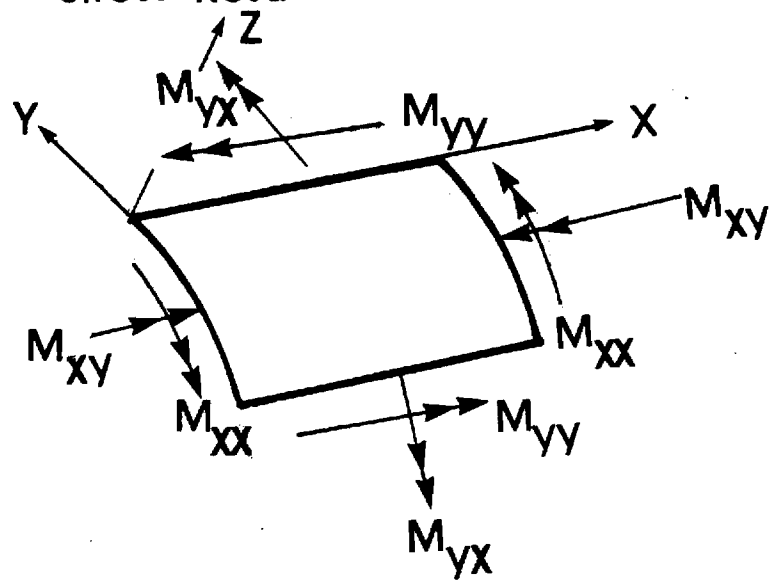


Fig. A.3 Geometry



Stress Resultants



Moment Resultants

Fig. A.4 Sign Convention

where

$$\begin{aligned}
\epsilon_{xx}^0 &= u_{,x} + \frac{1}{2} w_{,x}^2 + w_{,x} w_{,x}^0 \\
\epsilon_{yy}^0 &= v_{,y} + \frac{w}{R} + \frac{1}{2} w_{,y}^2 + w_{,y} w_{,y}^0 + \frac{\delta_1}{2} \left[\frac{v^2}{R^2} - 2 \frac{v}{R} (w_{,y} + w_{,y}^0) \right] \\
\gamma_{xy}^0 &= u_{,y} + v_{,x} + w_{,x} w_{,y} + w_{,x}^0 w_{,y} + w_{,x} w_{,y}^0 - \delta_1 \frac{v}{R} (w_{,x} + w_{,x}^0) \\
\phi_x &= -w_{,x} \quad ; \quad \phi_y = -w_{,y} + \delta_1 \frac{v}{R} \\
K_{xx} &= -w_{,xx} \quad ; \quad K_{yy} = -w_{,yy} + \delta_1 \frac{v_{,y}}{R} \\
K_{xy} &= -w_{,xy} + \frac{1}{2} \delta_1 \frac{v_{,x}}{R}
\end{aligned} \tag{A-113}$$

where

$$\delta_1 = \begin{cases} 1 & \text{for Sanders' kinematic relations} \\ 0 & \text{for Donnell's kinematic relations} \end{cases} \tag{A-114}$$

A. 3.2 Stress-Strain Relations

The constitutive equations are the same as in the w , F -formulation. Because of the different sign convention the relations between the stress and moment resultants on one hand and the reference surface strains and changes in curvature and torsions on the other, these equations are

$$\begin{Bmatrix} N_{xx} \\ N_{yy} \\ N_{xy} \\ M_{xx} \\ M_{yy} \\ M_{xy} \end{Bmatrix} = \begin{bmatrix} \bar{A}_{11} & \bar{A}_{12} & \bar{A}_{13} & \bar{B}_{11} & \bar{B}_{12} & \bar{B}_{13} \\ \bar{A}_{12} & \bar{A}_{22} & \bar{A}_{23} & \bar{B}_{12} & \bar{B}_{22} & \bar{B}_{23} \\ \bar{A}_{13} & \bar{A}_{23} & \bar{A}_{33} & \bar{B}_{13} & \bar{B}_{23} & \bar{B}_{33} \\ \bar{B}_{11} & \bar{B}_{12} & \bar{B}_{13} & \bar{D}_{11} & \bar{D}_{12} & \bar{D}_{13} \\ \bar{B}_{12} & \bar{B}_{22} & \bar{B}_{23} & \bar{D}_{12} & \bar{D}_{22} & \bar{D}_{23} \\ \bar{B}_{13} & \bar{B}_{23} & \bar{B}_{33} & \bar{D}_{13} & \bar{D}_{23} & \bar{D}_{33} \end{bmatrix} \begin{Bmatrix} \epsilon_{xx}^0 \\ \epsilon_{yy}^0 \\ \gamma_{xy}^0 \\ K_{xx} \\ K_{yy} \\ 2K_{xy} \end{Bmatrix} \tag{A-115}$$

where the expressions for \bar{A}_{ij} , \bar{B}_{ij} and \bar{D}_{ij} are given by Eqs A-14 and A-15.

A. 3.3 Equilibrium Equations

Following the same procedure as the one described in section A.2.3, the equilibrium equations and associated boundary conditions are:

Equilibrium Equations

$$N_{xx,x} + N_{xy,y} = 0$$

$$N_{xy,x} + N_{yy,y} - \delta_1 \frac{N_{yy}}{R} \left(\frac{U}{R} - (W_{,x} + W_{,x}^0) \right) + \delta_1 N_{xy} \frac{(W_{,x} + W_{,x}^0)}{R} \\ + \delta_1 \frac{M_{xy,x}}{R} + \delta_1 \frac{M_{yy,y}}{R} = 0$$

$$[N_{xx}(W_{,x} + W_{,x}^0)]_{,x} + [N_{xy}(W_{,y} + W_{,y}^0)]_{,x} + [N_{xy}(W_{,x} + W_{,x}^0)]_{,y} \\ + [N_{yy}(W_{,y} + W_{,y}^0)]_{,y} - \frac{N_{yy}}{R} - \frac{\delta_1}{R} [(N_{xy}U)_{,x} + (N_{yy}U)_{,y}] \\ + M_{xx,xx} + 2M_{xy,xy} + M_{yy,yy} + \mathcal{G} = 0 \quad (A-116)$$

Boundary Conditions (at $x = 0, L$)

Either

$$N_{xx} = \bar{N}_{xx}$$

$$N_{xy} + \frac{M_{xy}}{R} \delta_1 = \bar{N}_{xy} + \frac{\bar{M}_{xy}}{R} \delta_1$$

$$N_{xx}(W_{,x} + W_{,x}^0) + N_{xy}(W_{,y} + W_{,y}^0)$$

$$- \delta_1 \frac{N_{xy}}{R} U + M_{xx,x} + 2M_{xy,y} = \bar{Q}_x + \bar{M}_{xy,y} \delta W = 0$$

$$M_{xx} = \bar{M}_{xx}$$

Or

$$\delta U = 0$$

$$\delta U = 0$$

$$\delta W_{,x} = 0$$

(A-117)

Use of the first equilibrium equation in the third yields

$$\begin{aligned}
 & (w_{,y} + w_{,y}^0) (N_{xy,x} + N_{yy,y}) + N_{xx} (w_{,xx} + w_{,xx}^0) + 2N_{xy} (w_{,xy} + w_{,xy}^0) \\
 & + N_{yy} (w_{,yy} + w_{,yy}^0) - \frac{N_{yy}}{R} - \frac{\delta_1}{R} [U (N_{xy,x} + N_{yy,y}) + N_{xy} U_{,x} + N_{yy} U_{,y}] \\
 & + M_{xx,xx} + 2M_{xy,xy} + M_{yy,yy} + q = 0
 \end{aligned} \tag{A-118}$$

A.3.4 Solution Methodology-Field Equations

The solution procedure for this formulation is as follows: assume a separated solution for u , v , and w ; express the known (assigned) parameters w^0 (imperfection) and q (pressure) in a similar form; find expressions for reference surface strains, changes in curvature and torsion and stress and moment resultants; substitute these expressions into the equilibrium equations and use the Galerkin procedure in the circumferential direction (this changes the nonlinear partial differential equations to a set of nonlinear ordinary differential equations); use Newton's method, applicable to differential equations, to reduce the nonlinear field equations to a sequence of linear systems; finally cast equations into finite difference form.

All of these steps are shown herein, in detail. Then, once this step is completed, the solution scheme of Appendix B is used to solve the final set of equations.

The dependent variables are the three displacement components $u(x,y)$, $v(x,y)$ and $w(x,y)$. A separated series form is assumed for each of them

$$\begin{aligned}
 u(x,y) &= \sum_{i=0}^K \left[U_{1i}(x) \cos \frac{iny}{R} + U_{2i}(x) \sin \frac{iny}{R} \right] \\
 v(x,y) &= \sum_{i=0}^K \left[V_{1i}(x) \cos \frac{iny}{R} + V_{2i}(x) \sin \frac{iny}{R} \right] \\
 w(x,y) &= \sum_{i=0}^K \left[W_{1i}(x) \cos \frac{iny}{R} + W_{2i}(x) \sin \frac{iny}{R} \right]
 \end{aligned} \tag{A-119}$$

Thus, the number of unknown functions of x is $(2k + 2)$ for each variable.

The total number is $(6k + 6)$ subject to the condition that

$$U_{20} = V_{20} = W_{20} = 0 \quad (A-120)$$

Note that the true number of unknown functions is $(6k + 3)$.

Similarly the expressions for w^0 and the pressure $q(x, y)$ are:

$$W_{(x,y)}^0 = \sum_{i=0}^K [W_{1i}^0(x) \cos \frac{iny}{R} + W_{2i}^0(x) \sin \frac{iny}{R}] \quad (A-121)$$

$$q(x,y) = \sum_{i=0}^K [g_{1i} \cos \frac{iny}{R} + g_{2i} \sin \frac{iny}{R}] \quad (A-122)$$

In this case also, the condition $w_{20}^0 = q_{20} = 0$ is imposed.

In order to express the equilibrium equations in terms of the parameters of Eqs A-119 -A-122, one needs to first find the expressions for the stress resultants and therefore reference surface strains and changes in curvature and torsion.

Use of Eqs A-119 and A-120 in the expression for ϵ_{ij} and κ_{ij} , Eqs A-112 and A-113 yields

$$\begin{aligned} \epsilon_{xx}^0 = & \sum_{i=0}^{2K} [(\delta_i U_{1i,x} + t_{x1i}^L + t_{x1i}^N) \cos \frac{iny}{R} \\ & + (\delta_i U_{2i,x} + t_{x2i}^L + t_{x2i}^N) \sin \frac{iny}{R}] \end{aligned} \quad (A-123)$$

where

$$t_{x1i}^L = A_{1(K)}^i(W_{1,x}^0, W_{1,x}) + A_{4(K)}^i(W_{2,x}^0, W_{2,x})$$

$$t_{x2i}^L = A_{2(K)}^i(W_{1,x}^0, W_{2,x}) + A_{3(K)}^i(W_{2,x}^0, W_{1,x})$$

$$t_{x1i}^N = \frac{1}{2} \{ A_{1(K)}^i(W_{1,x}, W_{1,x}) + A_{4(K)}^i(W_{2,x}, W_{2,x}) \}$$

$$t_{x2i}^N = \frac{1}{2} \{ A_{2(K)}^i(W_{1,x}, W_{2,x}) + A_{3(K)}^i(W_{2,x}, W_{1,x}) \} \quad (A-123a)$$

$$\epsilon_{yy}^0 = \sum_{i=0}^{2K} \left\{ \left[\left(\frac{i\pi}{R} u_{2i} + \frac{w_{2i}}{R} \right) \delta_i + t_{y1i}^L + t_{y1i}^N \right] \cos \frac{i\pi y}{R} \right. \\ \left. + \left[\left(-\frac{i\pi}{R} u_{1i} + \frac{w_{1i}}{R} \right) \delta_i + t_{y2i}^L + t_{y2i}^N \right] \sin \frac{i\pi y}{R} \right\} \quad (A-124)$$

where

$$t_{y1i}^L = \left(\frac{\pi}{R} \right)^2 \left[A_{IJ4(k)}^i(w_1^0, w_1) + A_{IJ1(k)}^i(w_2^0, w_2) \right] \\ + \frac{\delta_1 \pi}{R^2} \left[-A_{J1(k)}^i(w_2^0, v_1) + A_{J4(k)}^i(w_1^0, v_2) \right] \\ t_{y2i}^L = -\left(\frac{\pi}{R} \right)^2 \left[A_{IJ2(k)}^i(w_2^0, w_1) + A_{IJ3(k)}^i(w_1^0, w_2) \right] \\ + \frac{\delta_1 \pi}{R^2} \left[A_{J3(k)}^i(w_1^0, v_1) - A_{J2(k)}^i(w_2^0, v_2) \right] \\ t_{y1i}^N = \frac{1}{2} \left(\frac{\pi}{R} \right)^2 \left(A_{IJ4(k)}^i(w_1, w_2) + A_{IJ1(k)}^i(w_2, w_2) \right) \\ + \frac{\delta_1}{2R^2} \left(A_{1(k)}^i(v_1, v_1) + A_{4(k)}^i(v_2, v_2) \right) \\ + \frac{\delta_1 \pi}{R^2} \left(A_{J4(k)}^i(w_1, v_2) - A_{J1(k)}^i(w_2, v_1) \right) \\ t_{y2i}^N = -\frac{1}{2} \left(\frac{\pi}{R} \right)^2 \left(A_{IJ2(k)}^i(w_2, w_1) + A_{IJ3(k)}^i(w_1, w_2) \right) \\ + \frac{\delta_1}{2R^2} \left(A_{3(k)}^i(v_2, v_1) + A_{2(k)}^i(v_1, v_2) \right) \\ + \frac{\delta_1 \pi}{R^2} \left(A_{J3(k)}^i(w_1, v_1) - A_{J1(k)}^i(w_2, v_2) \right) \quad (A-124a)$$

$$\gamma_{xy}^0 = \sum_{i=0}^{2K} \left\{ \left[\left(\frac{i\pi}{R} u_{2i} + v_{1i,x} \right) \delta_i + t_{xy1i}^L + t_{xy1i}^N \right] \cos \frac{i\pi y}{R} \right. \\ \left. + \left[\left(-\frac{i\pi}{R} u_{1i} + v_{2i,x} \right) \delta_i + t_{xy2i}^L + t_{xy2i}^N \right] \sin \frac{i\pi y}{R} \right\} \quad (A-125)$$

where

$$t_{xy1i}^L = \frac{\pi}{R} \left[A_{J1(k)}^i(w_2^0, w_{1,x}) - A_{J4(k)}^i(w_1^0, w_{2,x}) \right]$$

$$\begin{aligned}
& - A_{I4(k)}^i (W_{2,x}^0, W_1) + A_{I1(k)}^i (W_{1,x}^0, W_2)] \\
& - \frac{\delta_1}{R} [A_{1(k)}^i (U_1, W_{1,x}^0) + A_{4(k)}^i (U_2, W_{2,x}^0)] \\
t_{xyzi}^L = & \frac{n}{R} [A_{J2(k)}^i (W_2^0, W_{2,x}) - A_{J3(k)}^i (W_1^0, W_{1,x}) \\
& - A_{I2(k)}^i (W_{1,x}^0, W_1) + A_{I3(k)}^i (W_{2,x}^0, W_2)] \\
& - \frac{\delta_1}{R} [A_{3(k)}^i (U_2, W_{1,x}^0) + A_{2(k)}^i (U_1, W_{2,x}^0)] \\
t_{xyzi}^n = & \frac{n}{2R} [A_{J1(k)}^i (W_2, W_{1,x}) - A_{J4(k)}^i (W_1, W_{2,x}) \\
& - A_{I4(k)}^i (W_{2,x}^0, W_1) + A_{I1(k)}^i (W_{1,x}^0, W_2)] \\
& - \frac{\delta_1}{R} [A_{1(k)}^i (U_1, W_{1,x}) + A_{4(k)}^i (U_2, W_{2,x})] \\
t_{xyzi}^n = & \frac{n}{2R} [A_{J2(k)}^i (W_2, W_{2,x}) - A_{J3(k)}^i (W_1, W_{1,x}) \\
& - A_{I2(k)}^i (W_{1,x}, W_1) + A_{I3(k)}^i (W_{2,x}, W_2)] \\
& - \frac{\delta_1}{R} [A_{3(k)}^i (U_2, W_{1,x}) + A_{2(k)}^i (U_1, W_{2,x})] \quad (A-125a)
\end{aligned}$$

and

$$K_{xx} = - \sum_{i=0}^k [W_{1i,xx} \cos \frac{iny}{R} + W_{2i,xx} \sin \frac{iny}{R}] \quad (A-126)$$

$$\begin{aligned}
K_{yy} = & \frac{1}{R^2} \sum_{i=0}^k [in (in W_{1i} + \delta_1 U_{2i}) \cos \frac{iny}{R} \\
& + in (in W_{2i} - \delta_1 U_{1i}) \sin \frac{iny}{R}] \quad (A-127)
\end{aligned}$$

$$\begin{aligned}
K_{xy} = & \sum_{i=0}^k [(-\frac{in}{R} W_{2i,x} + \frac{\delta_1}{2R} U_{1i,x}) \cos \frac{iny}{R} \\
& + (\frac{in}{R} W_{1i,x} + \frac{\delta_1}{2R} U_{2i,x}) \sin \frac{iny}{R}] \quad (A-128)
\end{aligned}$$

Note that δ_i and η_l are the same as before, or

$$\delta_i = \begin{cases} 0 & i > k \\ 1 & i \leq k \end{cases}; \quad \eta_l = \begin{cases} -1 & l < 0 \\ 0 & l = 0 \\ 1 & l > 0 \end{cases} \quad (A-129)$$

The symbols $A_{j(k)}^{(i)}$ ($i = 1, 2, 3, 4$), $A_{Jj(k)}^{(i)}$ ($j = 1, 2, 3, 4$), $A_{Ij(k)}$ ($j = 1, 2, 3, 4$), $A_{IJj(k)}$ ($j = 1, 2, 3, 4$) and $A_{J2j(k)}$ ($j = 1, 2, 3, 4$) result from the use of trigonometric identities, which are employed to change double to single sums [similar to Eqs A-49 - A-51 and symbols defined by Eqs A-52 - A-54; note that some are common]. The needed trigonometric identities and definition of symbols are given below.

$$\begin{aligned} \sum_{i=0}^K \sum_{j=0}^L [\theta_j \cos j\theta] a_i \cos i\theta &= \sum_{i=0}^{K+L} A_{1(k)}^i(b, a) \cos i\theta \\ \sum_{i=0}^K \sum_{j=0}^L [\theta_j \cos j\theta] a_i \sin i\theta &= \sum_{i=0}^{K+L} A_{2(k)}^i(b, a) \sin i\theta \\ \sum_{i=0}^K \sum_{j=0}^L [\theta_j \sin j\theta] a_i \cos i\theta &= \sum_{i=0}^{K+L} A_{3(k)}^i(b, a) \sin i\theta \\ \sum_{i=0}^K \sum_{j=0}^L [\theta_j \sin j\theta] a_i \sin i\theta &= \sum_{i=0}^{K+L} A_{4(k)}^i(b, a) \cos i\theta \end{aligned} \quad (A-130)$$

$$\begin{aligned} \sum_{i=0}^K \sum_{j=0}^L [j \theta_j \cos j\theta] a_i \cos i\theta &= \sum_{i=0}^{K+L} A_{J1(k)}^i(b, a) \cos i\theta \\ \sum_{i=0}^K \sum_{j=0}^L [j \theta_j \cos j\theta] a_i \sin i\theta &= \sum_{i=0}^{K+L} A_{J2(k)}^i(b, a) \sin i\theta \\ \sum_{i=0}^K \sum_{j=0}^L [j \theta_j \sin j\theta] a_i \cos i\theta &= \sum_{i=0}^{K+L} A_{J3(k)}^i(b, a) \sin i\theta \\ \sum_{i=0}^K \sum_{j=0}^L [j \theta_j \sin j\theta] a_i \sin i\theta &= \sum_{i=0}^{K+L} A_{J4(k)}^i(b, a) \cos i\theta \end{aligned} \quad (A-131)$$

$$\begin{aligned}
\sum_{i=0}^K \sum_{j=0}^L [\theta_j \cos j\theta] a_{ii} \cos i\theta &= \sum_{i=0}^{K+L} A_{I1(\kappa)}^i(\theta, a) \cos i\theta \\
\sum_{i=0}^K \sum_{j=0}^L [\theta_j \cos j\theta] a_{ii} \sin i\theta &= \sum_{i=0}^{K+L} A_{I2(\kappa)}^i(\theta, a) \sin i\theta \\
\sum_{i=0}^K \sum_{j=0}^L [\theta_j \sin j\theta] a_{ii} \cos i\theta &= \sum_{i=0}^{K+L} A_{I3(\kappa)}^i(\theta, a) \sin i\theta \\
\sum_{i=0}^K \sum_{j=0}^L [\theta_j \sin j\theta] a_{ii} \sin i\theta &= \sum_{i=0}^{K+L} A_{I4(\kappa)}^i(\theta, a) \cos i\theta \quad (A-132) \\
\sum_{i=0}^K \sum_{j=0}^L [j \theta_j \cos j\theta] a_{ii} \cos i\theta &= \sum_{i=0}^{K+L} A_{IJ1(\kappa)}^i(\theta, a) \cos i\theta \\
\sum_{i=0}^K \sum_{j=0}^L [j \theta_j \cos j\theta] a_{ii} \sin i\theta &= \sum_{i=0}^{K+L} A_{IJ2(\kappa)}^i(\theta, a) \sin i\theta \\
\sum_{i=0}^K \sum_{j=0}^L [j \theta_j \sin j\theta] a_{ii} \cos i\theta &= \sum_{i=0}^{K+L} A_{IJ3(\kappa)}^i(\theta, a) \sin i\theta \\
\sum_{i=0}^K \sum_{j=0}^L [j \theta_j \sin j\theta] a_{ii} \sin i\theta &= \sum_{i=0}^{K+L} A_{IJ4(\kappa)}^i(\theta, a) \cos i\theta \quad (A-133) \\
\sum_{i=0}^K \sum_{j=0}^L [j^2 \theta_j \cos j\theta] a_{ii} \cos i\theta &= \sum_{i=0}^{K+L} A_{J21(\kappa)}^i(\theta, a) \cos i\theta \\
\sum_{i=0}^K \sum_{j=0}^L [j^2 \theta_j \cos j\theta] a_{ii} \sin i\theta &= \sum_{i=0}^{K+L} A_{J22(\kappa)}^i(\theta, a) \sin i\theta \\
\sum_{i=0}^K \sum_{j=0}^L [j^2 \theta_j \sin j\theta] a_{ii} \cos i\theta &= \sum_{i=0}^{K+L} A_{J23(\kappa)}^i(\theta, a) \sin i\theta \\
\sum_{i=0}^K \sum_{j=0}^L [j^2 \theta_j \sin j\theta] a_{ii} \sin i\theta &= \sum_{i=0}^{K+L} A_{J24(\kappa)}^i(\theta, a) \cos i\theta \quad (A-134)
\end{aligned}$$

where

$$\begin{aligned}
A_{I1(\kappa)}^i(\theta, a) &= \frac{1}{2} \sum_{j=0}^K [\theta_{i+j} + (1 - \eta_{j-i}^2 + \eta_i) \theta_{i-j}] a_j \\
A_{I2(\kappa)}^i(\theta, a) &= \frac{1}{2} \sum_{j=0}^K [-\theta_{i+j} + (1 - \eta_{j-i}^2 + \eta_i) \theta_{i-j}] a_j \\
A_{I3(\kappa)}^i(\theta, a) &= \frac{1}{2} \sum_{j=0}^K [\theta_{i+j} + (-1 + \eta_{i-j} + \eta_i) \theta_{i-j}] a_j \\
A_{I4(\kappa)}^i(\theta, a) &= \frac{1}{2} \sum_{j=0}^K [-\theta_{i+j} + (-1 - \eta_{i-j} + \eta_i) \theta_{i-j}] a_j \quad (A-135) \\
A_{IJ1(\kappa)}^i(\theta, a) &= \frac{1}{2} \sum_{j=0}^K [(i+j) \theta_{i+j} + (1 - \eta_{j-i}^2 + \eta_i) |i-j| \theta_{i-j}] a_j \\
A_{IJ2(\kappa)}^i(\theta, a) &= \frac{1}{2} \sum_{j=0}^K [-(i+j) \theta_{i+j} + (1 - \eta_{j-i}^2 + \eta_i) |i-j| \theta_{i-j}] a_j \\
A_{IJ3(\kappa)}^i(\theta, a) &= \frac{1}{2} \sum_{j=0}^K [(i+j) \theta_{i+j} + (-1 + \eta_{i-j} + \eta_i) |i-j| \theta_{i-j}] a_j \\
A_{IJ4(\kappa)}^i(\theta, a) &= \frac{1}{2} \sum_{j=0}^K [-(i+j) \theta_{i+j} + (-1 - \eta_{i-j} + \eta_i) |i-j| \theta_{i-j}] a_j \quad (A-136) \\
A_{J1(\kappa)}^i(\theta, a) &= \frac{1}{2} \sum_{j=0}^K [\theta_{i+j} + (1 - \eta_{j-i}^2 + \eta_i) \theta_{i-j}] j a_j
\end{aligned}$$

$$A_{I21(k)}^i(\theta, a) = \frac{1}{2} \sum_{j=0}^k [\theta_{i+j} + (1 - \eta_{j-i}^2 + \eta_i) \theta_{i-j}] a_j$$

$$A_{I31(k)}^i(\theta, a) = \frac{1}{2} \sum_{j=0}^k [\theta_{i+j} + (-1 + \eta_{i-j} + \eta_i) \theta_{i-j}] a_j$$

$$A_{I41(k)}^i(\theta, a) = \frac{1}{2} \sum_{j=0}^k [\theta_{i+j} + (-1 - \eta_{i-j} + \eta_i) \theta_{i-j}] a_j \quad (A-137)$$

$$A_{IJ1(k)}^i(\theta, a) = \frac{1}{2} \sum_{j=0}^k [(i+j) \theta_{i+j} + (1 - \eta_{j-i}^2 + \eta_i) |i-j| \theta_{i-j}] a_j$$

$$A_{IJ2(k)}^i(\theta, a) = \frac{1}{2} \sum_{j=0}^k [-(i+j) \theta_{i+j} + (1 - \eta_{j-i}^2 + \eta_i) |i-j| \theta_{i-j}] a_j$$

$$A_{IJ3(k)}^i(\theta, a) = \frac{1}{2} \sum_{j=0}^k [(i+j) \theta_{i+j} + (-1 + \eta_{i-j} + \eta_i) |i-j| \theta_{i-j}] a_j$$

$$A_{IJ4(k)}^i(\theta, a) = \frac{1}{2} \sum_{j=0}^k [(i+j) \theta_{i+j} + (-1 - \eta_{i-j} + \eta_i) |i-j| \theta_{i-j}] a_j \quad (A-138)$$

$$A_{J21(k)}^i(\theta, a) = \frac{1}{2} \sum_{j=0}^k [(i+j)^2 \theta_{i+j} + (1 - \eta_{j-i}^2 + \eta_i) (i-j)^2 \theta_{i-j}] a_j$$

$$A_{J22(k)}^i(\theta, a) = \frac{1}{2} \sum_{j=0}^k [-(i+j)^2 \theta_{i+j} + (1 - \eta_{j-i}^2 + \eta_i) (i-j)^2 \theta_{i-j}] a_j$$

$$A_{J23(k)}^i(\theta, a) = \frac{1}{2} \sum_{j=0}^k [(i+j)^2 \theta_{i+j} + (-1 + \eta_{i-j} + \eta_i) (i-j)^2 \theta_{i-j}] a_j$$

$$A_{J24(k)}^i(\theta, a) = \frac{1}{2} \sum_{j=0}^k [(i+j)^2 \theta_{i+j} + (-1 - \eta_{i-j} + \eta_i) (i-j)^2 \theta_{i-j}] a_j \quad (A-139)$$

In order to write the strain-displacement relations in matrix form the following definitions of column matrices (vectors) are needed.

$$\begin{pmatrix} \epsilon_{xx}^0 \\ \epsilon_{yy}^0 \\ \gamma_{xy}^0 \\ k_{xx} \\ k_{yy} \\ 2k_{xy} \end{pmatrix} = \sum_{i=0}^{2k} [(\{\epsilon_{1i}\} + \{t_{1i}^L\} + \{t_{1i}^N\}) \cos \frac{i\pi y}{R} + (\{\epsilon_{2i}\} + \{t_{2i}^L\} + \{t_{2i}^N\}) \sin \frac{i\pi y}{R}] \quad (A-140)$$

where

$$\begin{aligned}
 \{\epsilon_{1i}\} &= {}^L \begin{bmatrix} \epsilon_{xx1}^0, \epsilon_{yy1}^0, \gamma_{xy1}^0, \kappa_{xx1}, \kappa_{yy1}, 2\kappa_{xy1} \end{bmatrix}_i^T \\
 \{\epsilon_{2i}\} &= {}^L \begin{bmatrix} \epsilon_{xx2}^0, \epsilon_{yy2}^0, \gamma_{xy2}^0, \kappa_{xx2}, \kappa_{yy2}, 2\kappa_{xy2} \end{bmatrix}_i^T \\
 \{t_{1i}^L\} &= {}^L \begin{bmatrix} t_{x1}^L, t_{y1}^L, t_{xy1}^L, 0, 0, 0 \end{bmatrix}_i^T \\
 \{t_{2i}^L\} &= {}^L \begin{bmatrix} t_{x2}^L, t_{y2}^L, t_{xy2}^L, 0, 0, 0 \end{bmatrix}_i^T \\
 \{t_{1i}^n\} &= {}^L \begin{bmatrix} t_{x1}^n, t_{y1}^n, t_{xy1}^n, 0, 0, 0 \end{bmatrix}_i^T \\
 \{t_{2i}^n\} &= {}^L \begin{bmatrix} t_{x2}^n, t_{y2}^n, t_{xy2}^n, 0, 0, 0 \end{bmatrix}_i^T
 \end{aligned} \tag{A-141}$$

Note that t^L and t^n elements are given by Eqs A-123a, A-124a and A-125a, while the ϵ_{ij} and κ_{ij} elements are:

$$\begin{aligned}
 \epsilon_{xx1}^0 &= \delta_i u_{1i,x} & ; \quad \kappa_{xx1} &= -w_{1i,x} \delta_i \\
 \epsilon_{xx2}^0 &= \delta_i u_{2i,x} & ; \quad \kappa_{xx2} &= -w_{2i,x} \delta_i \\
 \epsilon_{yy1}^0 &= \left(\frac{i\eta}{R} u_{1i} + \frac{w_{1i}}{R}\right) \delta_i & ; \quad \kappa_{yy1} &= \left[\frac{i\eta}{R} (i\eta w_{1i} + \delta_i u_{1i})\right] \delta_i \\
 \epsilon_{yy2}^0 &= \left(-\frac{i\eta}{R} u_{1i} + \frac{w_{2i}}{R}\right) \delta_i & ; \quad \kappa_{yy2} &= \left[\frac{i\eta}{R} (i\eta w_{1i} + \delta_i u_{1i})\right] \delta_i \\
 \gamma_{xy1}^0 &= \left(\frac{i\eta}{R} u_{2i} + u_{1i,x}\right) \delta_i & ; \quad \kappa_{xy1} &= \left[-\frac{i\eta}{R} w_{2i} + \frac{\delta_i}{2R} u_{1i,x}\right] \delta_i \\
 \gamma_{xy2}^0 &= \left(-\frac{i\eta}{R} u_{1i} + u_{2i,x}\right) \delta_i & ; \quad \kappa_{xy2} &= \left[\frac{i\eta}{R} w_{1i,x} + \frac{\delta_i}{2R} u_{2i,x}\right] \delta_i
 \end{aligned} \tag{A-142}$$

Substitution of the expressions for reference surface strains and changes in curvature and torsion into the stress-strain relations, Eqs A-115, yields

$$\begin{Bmatrix} N_{xx} \\ N_{yy} \\ N_{xy} \\ M_{xx} \\ M_{yy} \\ M_{xy} \end{Bmatrix} = \sum_{i=0}^{2K} \begin{bmatrix} \bar{A} & \bar{B} \\ \bar{B} & \bar{D} \end{bmatrix} \left[(\{\epsilon_{,i}\} + \{t_{,i}^L\} + \{t_{,i}^N\}) \cos \frac{iny}{R} \right. \\ \left. + (\{\epsilon_{,i}\} + \{t_{,i}^L\} + \{t_{,i}^N\}) \sin \frac{iny}{R} \right] \quad (A-143)$$

or

$$= \sum_{i=0}^{2K} \left[(\{\eta_{,i}\} + \{\eta_{,i}^L\} + \{\eta_{,i}^N\}) \cos \frac{iny}{R} \right. \\ \left. + (\{\eta_{,i}\} + \{\eta_{,i}^L\} + \{\eta_{,i}^N\}) \sin \frac{iny}{R} \right] \quad (A-144)$$

where

$$\{\eta_{,i}\} = \begin{Bmatrix} \eta_{xx,i} \\ \eta_{yy,i} \\ \eta_{xy,i} \\ \eta_{xx,i} \\ \eta_{yy,i} \\ \eta_{xy,i} \end{Bmatrix} = \begin{bmatrix} \bar{A} & \bar{B} \\ \bar{B} & \bar{D} \end{bmatrix} \{\epsilon_{,i}\} \quad (A-145)$$

$$\{\mathcal{N}_2\}_i = \begin{Bmatrix} \mathcal{N}_{xx2} \\ \mathcal{N}_{yy2} \\ \mathcal{N}_{xy2} \\ \mathcal{M}_{xx2} \\ \mathcal{M}_{yy2} \\ \mathcal{M}_{xy2} \end{Bmatrix} = \begin{bmatrix} \bar{A} & \bar{B} \\ \bar{B} & \bar{D} \end{bmatrix} \{\epsilon_{2i}\} \quad (A-146)$$

$$\{\mathcal{N}_1^L\}_i = \begin{Bmatrix} \mathcal{N}_{xx1}^L \\ \mathcal{N}_{yy1}^L \\ \mathcal{N}_{xy1}^L \\ \mathcal{M}_{xx1}^L \\ \mathcal{M}_{yy1}^L \\ \mathcal{M}_{xy1}^L \end{Bmatrix} = \begin{bmatrix} \bar{A} & \bar{B} \\ \bar{B} & \bar{D} \end{bmatrix} \{t_{1i}^L\} \quad (A-147)$$

$$\{\mathcal{N}_2^L\}_i = \begin{Bmatrix} \mathcal{N}_{xx2}^L \\ \mathcal{N}_{yy2}^L \\ \mathcal{N}_{xy2}^L \\ \mathcal{M}_{xx2}^L \\ \mathcal{M}_{yy2}^L \\ \mathcal{M}_{xy2}^L \end{Bmatrix} = \begin{bmatrix} \bar{A} & \bar{B} \\ \bar{B} & \bar{D} \end{bmatrix} \{t_{2i}^L\} \quad (A-148)$$

$$\{\mathcal{N}_1^n\} = \begin{Bmatrix} \mathcal{N}_{xx1}^n \\ \mathcal{N}_{yy1}^n \\ \mathcal{N}_{xy1}^n \\ \mathcal{M}_{xx1}^n \\ \mathcal{M}_{yy1}^n \\ \mathcal{M}_{xy1}^n \end{Bmatrix} = \begin{bmatrix} \bar{A} & \bar{B} \\ \bar{B} & \bar{D} \end{bmatrix} \{t_{1i}^n\} \quad (A-149)$$

$$\{\mathcal{N}_2^n\} = \begin{Bmatrix} \mathcal{N}_{xx2}^n \\ \mathcal{N}_{yy2}^n \\ \mathcal{N}_{xy2}^n \\ \mathcal{M}_{xx2}^n \\ \mathcal{M}_{yy2}^n \\ \mathcal{M}_{xy2}^n \end{Bmatrix} = \begin{bmatrix} \bar{A} & \bar{B} \\ \bar{B} & \bar{D} \end{bmatrix} \{t_{2i}^n\} \quad (A-150)$$

Note that the $\{\epsilon_{1i}\}$ and $\{\epsilon_{2i}\}$ vectors result from linear portion of the kinematic relations; the $\{t_{1i}^L\}$ and $\{t_{2i}^L\}$ from the coupling between the imperfection parameter, w^0 , and the displacement components v and w (thus, in a sense, nonlinear relations); and the $\{t_{1i}^n\}$ and $\{t_{2i}^n\}$ vectors from the nonlinear terms of the kinematic relations (v and w coupling).

Substitution of all the derived expressions into the equilibrium equations, Eqs A-116, yields in-plane equilibrium

$$\begin{aligned} & \sum_{i=0}^{2K} \left[(N_{xx2i,x} + \frac{i\eta}{R} N_{xy2i} + N_{xx1i,x}^L + \frac{i\eta}{R} N_{xy2i}^L + N_{xx1i,x}^n + \frac{i\eta}{R} N_{xy2i}^n) \cos \frac{i\eta y}{R} \right. \\ & \quad \left. + (N_{xx2i,x} - \frac{i\eta}{R} N_{xy2i} + N_{xx2i,x}^L - \frac{i\eta}{R} N_{xy2i}^L + N_{xx2i,x}^n - \frac{i\eta}{R} N_{xy2i}^n) \sin \frac{i\eta y}{R} \right] \\ & = 0 \end{aligned} \quad (A-151)$$

$$\begin{aligned} & \sum_{i=0}^K \xi_{ii}^1 \cos \frac{i\eta y}{R} + \sum_{i=0}^{2K} (\xi_{ii}^2 + \xi_{ii}^3) \cos \frac{i\eta y}{R} + \sum_{i=0}^{3K} (\xi_{ii}^3 + \xi_{ii}^3) \cos \frac{i\eta y}{R} \\ & + \sum_{i=0}^K \xi_{ii}^1 \sin \frac{i\eta y}{R} + \sum_{i=0}^{2K} (\xi_{ii}^2 + \xi_{ii}^3) \sin \frac{i\eta y}{R} + \sum_{i=0}^{3K} (\xi_{ii}^3 + \xi_{ii}^3) \sin \frac{i\eta y}{R} = 0 \end{aligned} \quad (A-152)$$

where

$$\begin{aligned} \xi_{ii}^1 &= \frac{i\eta}{R} N_{yy2i} + N_{xy1i,x} + \frac{\delta_1}{R} M_{xy1i,x} + \frac{i\eta\delta_1}{R} M_{yy2i} \\ \xi_{ii}^1 &= -\frac{i\eta}{R} N_{yy2i} + N_{xy1i,x} + \frac{\delta_1}{R} M_{xy1i,x} - \frac{i\eta\delta_1}{R} M_{yy2i} \\ \xi_{ii}^2 &= \frac{\delta_1}{R^2} N (A_{J1(k)}^i (W_1^0, N_{yy1}) - A_{J4(k)}^i (W_1^0, N_{yy2})) \\ & + \frac{\delta_1}{R} (A_{1(k)}^i (W_{1,x}^0, N_{xy1}) + A_{4(k)}^i (W_{2,x}^0, N_{xy2})) \\ & + \frac{i\eta}{R} N_{yy2i}^L + N_{xy1i,x}^L + \frac{\delta_1}{R} M_{xy1i,x}^L + \frac{i\eta}{R} \delta_1 M_{yy2i} \end{aligned} \quad (A-153)$$

$$\begin{aligned}\Xi_{jil}^2 &= \frac{\delta_1}{R^2} \mathcal{N} [A_{J2(K)}^i(W_2^0, \mathcal{N}_{yy2}) - A_{J3(K)}^i(W_1^0, \mathcal{N}_{yy1})] \\ &\quad + \frac{\delta_1}{R} [A_{3(K)}^i(W_{2,x}^0, \mathcal{N}_{xy}) + A_{2(K)}^i(W_{1,x}^0, \mathcal{N}_{xy2})] \\ &\quad - \frac{i\mathcal{N}}{R} \mathcal{N}_{yy1i}^L + \mathcal{N}_{xy2i,x}^L + \frac{\delta_1}{R} \mathcal{M}_{xy2i,x}^L - \frac{i\mathcal{N}}{R^2} \delta_1 \mathcal{M}_{yy1i}^L\end{aligned}$$

$$\begin{aligned}\Xi_{lin}^2 &= \frac{i\mathcal{N}}{R} \mathcal{N}_{yy2i}^n + \mathcal{N}_{xy1i,x}^n + \frac{\delta_1}{R} \mathcal{M}_{xy1i,x}^n + \frac{i\mathcal{N}}{R^2} \delta_1 \mathcal{M}_{yy2i}^n \\ &\quad + \frac{\delta_1}{R^2} \mathcal{N} [A_{J1(K)}^i(W_2, \mathcal{N}_{yy1}) - A_{J4(K)}^i(W_1, \mathcal{N}_{yy2})] \\ &\quad - \frac{\delta_1}{R^2} A_{1(K)}^i(V_1, \mathcal{N}_{yy1}) - \frac{\delta_1}{R^2} A_{4(K)}^i(V_2, \mathcal{N}_{yy2}) \\ &\quad + \frac{\delta_1}{R} [A_{1(K)}^i(W_{1,x}, \mathcal{N}_{xy1}) + A_{4(K)}^i(W_{2,x}, \mathcal{N}_{xy2})]\end{aligned}$$

$$\begin{aligned}\Xi_{2in}^2 &= -\frac{i\mathcal{N}}{R} \mathcal{N}_{yy1i}^n + \mathcal{N}_{xy2i,x}^n + \frac{\delta_1}{R} \mathcal{M}_{xy2i,x}^n - \frac{i\mathcal{N}}{R^2} \delta_1 \mathcal{M}_{yy1i}^n \\ &\quad + \frac{\delta_1}{R^2} \mathcal{N} [A_{J2(K)}^i(W_2, \mathcal{N}_{yy2}) - A_{J3(K)}^i(W_1, \mathcal{N}_{yy1})] \\ &\quad - \frac{\delta_1}{R^2} [A_{3(K)}^i(V_2, \mathcal{N}_{yy1}) + A_{2(K)}^i(V_1, \mathcal{N}_{yy2})] \\ &\quad + \frac{\delta_1}{R} [A_{3(K)}^i(W_{2,x}, \mathcal{N}_{xy1}) + A_{2(K)}^i(W_{1,x}, \mathcal{N}_{xy2})]\end{aligned}\tag{A-154}$$

$$\begin{aligned}\Xi_{ilu}^3 &= \frac{\delta_1 \mathcal{N}}{R^2} [A_{J1(2K)}^i(W_2^0, \mathcal{N}_{yy1}^L) - A_{J4(2K)}^i(W_1^0, \mathcal{N}_{yy1}^L)] \\ &\quad + \frac{\delta_1}{R} [A_{1(2K)}^i(W_{1,x}^0, \mathcal{N}_{xy1}^L) + A_{4(2K)}^i(W_{2,x}^0, \mathcal{N}_{xy2}^L)]\end{aligned}$$

$$\begin{aligned}\Xi_{2lu}^3 &= \frac{\delta_1 \mathcal{N}}{R^2} [-A_{J3(2K)}^i(W_1^0, \mathcal{N}_{xy1}^L) + A_{J2(2K)}^i(W_2^0, \mathcal{N}_{yy2}^L)] \\ &\quad + \frac{\delta_1}{R} [A_{3(2K)}^i(W_{2,x}^0, \mathcal{N}_{xy1}^L) + A_{2(2K)}^i(W_{1,x}^0, \mathcal{N}_{xy2}^L)]\end{aligned}$$

$$\begin{aligned}\Xi_{lin}^3 &= \frac{\delta_1 \mathcal{N}}{R} [A_{J1(2K)}^i(W_2 + W_2^0, \mathcal{N}_{yy1}^n) - A_{J4(2K)}^i(W_1 + W_1^0, \mathcal{N}_{yy2}^n)] \\ &\quad - \frac{\delta_1}{R^2} [A_{1(2K)}^i(V_1, \mathcal{N}_{yy1}^n) + A_{4(2K)}^i(V_2, \mathcal{N}_{yy2}^n)] \\ &\quad + \frac{\delta_1}{R} [A_{1(2K)}^i(W_{1,x} + W_{1,x}^0, \mathcal{N}_{xy1}^n) + A_{4(2K)}^i(W_{2,x} + W_{2,x}^0, \mathcal{N}_{xy2}^n)]\end{aligned}$$

$$\begin{aligned}
& + \frac{\delta_1 \pi}{R^2} [A_{J1(2K)}^i(W_2, \mathcal{N}_{yy1}^L) - A_{J4(2K)}^i(W_1, \mathcal{N}_{yy2}^L)] \\
& - \frac{\delta_1}{R^2} [A_{1(2K)}^i(U_1, \mathcal{N}_{yy1}^L) + A_{4(2K)}^i(U_2, \mathcal{N}_{yy2}^L)] \\
& + \frac{\delta_1}{R} [A_{1(2K)}^i(W_{1,x}, \mathcal{N}_{xy1,x}^L) + A_{4(2K)}^i(W_{2,x}, \mathcal{N}_{xy2,x}^L)] \\
\Xi_{21n}^3 = & \frac{\delta_1 \pi}{R^2} [-A_{J3(2K)}^i(W_1 + W_1^0, \mathcal{N}_{yy1}^n) + A_{J2(2K)}^i(W_2 + W_2^0, \mathcal{N}_{yy2}^n)] \\
& - \frac{\delta_1}{R^2} [A_{2(2K)}^i(U_1, \mathcal{N}_{yy2}^n) + A_{3(2K)}^i(U_2, \mathcal{N}_{yy1}^n)] \\
& + \frac{\delta_1}{R} [A_{3(2K)}^i(W_{2,x} + W_{2,x}^0, \mathcal{N}_{xy1}^n) + A_{2(2K)}^i(W_{1,x} + W_{1,x}^0, \mathcal{N}_{xy2}^n)] \\
& + \frac{\delta_1 \pi}{R^2} [-A_{J3(2K)}^i(W_1, \mathcal{N}_{yy1}^L) + A_{J2(2K)}^i(W_2, \mathcal{N}_{yy2}^L)] \\
& - \frac{\delta_1}{R^2} [A_{2(2K)}^i(U_1, \mathcal{N}_{yy2}^L) + A_{3(2K)}^i(U_2, \mathcal{N}_{yy1}^L)] \\
& + \frac{\delta_1}{R} [A_{3(2K)}^i(W_{2,x}, \mathcal{N}_{xy1}^L) + A_{2(2K)}^i(W_{1,x}, \mathcal{N}_{xy2}^L)] \tag{A-155}
\end{aligned}$$

Transverse equilibrium

$$\begin{aligned}
& \sum_{i=0}^K (\eta_{ii}^1 \cos \frac{i\pi y}{R} + \eta_{ii}^1 \sin \frac{i\pi y}{R}) + \sum_{i=0}^{2K} [(\eta_{iil}^2 + \eta_{iin}^2) \cos \frac{i\pi y}{R} + (\eta_{iil}^2 + \eta_{iin}^2) \sin \frac{i\pi y}{R}] \\
& + \sum_{i=0}^{3K} [(\eta_{iil}^3 + \eta_{iin}^3) \cos \frac{i\pi y}{R} + (\eta_{iil}^3 + \eta_{iin}^3) \sin \frac{i\pi y}{R}] + \sum_{i=0}^K (\delta_{ii} \cos \frac{i\pi y}{R} + \delta_{ii} \sin \frac{i\pi y}{R}) = 0 \tag{A-156}
\end{aligned}$$

where

$$\begin{aligned}
\eta_{ii}^1 &= \mathcal{M}_{xxil,xx} + 2\mathcal{M}_{xy2i,x}(\frac{i\pi}{R}) - (\frac{i\pi}{R})^2 \mathcal{M}_{yyii} - \frac{\mathcal{N}_{yyii}}{R} \\
\eta_{2i}^1 &= \mathcal{M}_{xx2i,xx} - 2\mathcal{M}_{xyii,x}(\frac{i\pi}{R}) - (\frac{i\pi}{R})^2 \mathcal{M}_{yy2i} - \frac{\mathcal{N}_{yy2i}}{R} \\
\eta_{iil}^2 &= \mathcal{M}_{xxil,xx}^L + 2\mathcal{M}_{xy2i,x}^L(\frac{i\pi}{R}) - (\frac{i\pi}{R})^2 \mathcal{M}_{yyii}^L - \frac{\mathcal{N}_{yyii}^L}{R} \\
& + \frac{\pi}{R} [A_{J1(K)}^i(W_2^0, \mathcal{N}_{xy1,x}) - A_{J4(K)}^i(W_1^0, \mathcal{N}_{xy2,x})] \\
& + (\frac{\pi}{R})^2 [A_{J1(K)}^i(W_2^0, \mathcal{N}_{yy2}) + A_{J4(K)}^i(W_1^0, \mathcal{N}_{yy1})]
\end{aligned} \tag{A-157}$$

$$\begin{aligned}
& + [A_{1(k)}^i(W_{1,xx}, \mathcal{N}_{xx1}) + A_{4(k)}^i(W_{2,xx}, \mathcal{N}_{xx2})] \\
& + \frac{2\eta}{R} [A_{J1(k)}^i(W_{2,x}, \mathcal{N}_{xy1}) - A_{J4(k)}^i(W_{1,x}, \mathcal{N}_{xy2})] \\
& + \left(\frac{\eta}{R}\right)^2 [-A_{J21(k)}^i(W_1^0, \mathcal{N}_{yy1}) - A_{J24(k)}^i(W_2^0, \mathcal{N}_{yy2})] \quad (A-158a)
\end{aligned}$$

$$\begin{aligned}
\eta_{2il}^2 = & \mathcal{M}_{xx2l,xx}^L - 2\left(\frac{i\eta}{R}\right)\mathcal{M}_{xyil,x}^L - \left(\frac{i\eta}{R}\right)^2\mathcal{M}_{yyil}^L - \frac{\mathcal{N}_{yy2}^L}{R} \\
& + \left(\frac{\eta}{R}\right) [A_{J2(k)}^i(W_2^0, \mathcal{N}_{xy2,x}) - A_{J3(k)}^i(W_1^0, \mathcal{N}_{xy1,x})] \\
& + \left(\frac{\eta}{R}\right)^2 [-A_{IJ2(k)}^i(W_2^0, \mathcal{N}_{yy1}) - A_{IJ3(k)}^i(W_1^0, \mathcal{N}_{yy2})] \\
& + A_{2(k)}^i(W_{1,xx}, \mathcal{N}_{xx2}) + A_{3(k)}^i(W_{2,xx}, \mathcal{N}_{xx1}) \\
& + \frac{2\eta}{R} (A_{J2(k)}^i(W_{2,x}, \mathcal{N}_{xy2}) - A_{J3(k)}^i(W_{1,x}, \mathcal{N}_{xy1})) \\
& + \left(\frac{\eta}{R}\right)^2 [-A_{J22(k)}^i(W_1^0, \mathcal{N}_{yy2}) - A_{J23(k)}^i(W_2^0, \mathcal{N}_{yy1})] \quad (A-158b)
\end{aligned}$$

$$\begin{aligned}
\eta_{1il}^2 = & \mathcal{M}_{xyil,xx}^n + 2\mathcal{M}_{xy2l,x}^n\left(\frac{i\eta}{R}\right) - \left(\frac{i\eta}{R}\right)^2\mathcal{M}_{yyil}^n - \frac{\mathcal{N}_{yy1}^n}{R} \\
& + \frac{\eta}{R} [A_{J1(k)}^i(W_2, \mathcal{N}_{xy1,x}) - A_{J4(k)}^i(W_1, \mathcal{N}_{xy2,x})] \\
& + \left(\frac{\eta}{R}\right)^2 [A_{IJ1(k)}^i(W_2, \mathcal{N}_{yy2}) + A_{IJ4(k)}^i(W_1, \mathcal{N}_{yy1})] \\
& + \frac{\delta_1}{R} [-A_{1(k)}^i(V_1, \mathcal{N}_{xy1,x}) - A_{4(k)}^i(V_2, \mathcal{N}_{xy2,x})] \\
& + \frac{\delta_1\eta}{R^2} [-A_{21(k)}^i(V_1, \mathcal{N}_{yy2}) + A_{24(k)}^i(V_2, \mathcal{N}_{yy1})] \\
& + A_{1(k)}^i(W_{1,xx}, \mathcal{N}_{xx1}) + A_{4(k)}^i(W_{2,xx}, \mathcal{N}_{xx2}) \\
& + \frac{2\eta}{R} [A_{J1(k)}^i(W_{2,x}, \mathcal{N}_{xy1}) - A_{J4(k)}^i(W_{1,x}, \mathcal{N}_{xy2})] \\
& - \frac{\delta_1}{R} [A_{1(k)}^i(V_{1,x}, \mathcal{N}_{xy1}) + A_{4(k)}^i(V_{2,x}, \mathcal{N}_{xy2})] \\
& + \left(\frac{\eta}{R}\right)^2 [-A_{J21(k)}^i(W_1, \mathcal{N}_{yy1}) - A_{J24(k)}^i(W_2, \mathcal{N}_{yy2})] \\
& + \frac{\delta_1\eta}{R^2} [-A_{J1(k)}^i(V_2, \mathcal{N}_{yy1}) + A_{J4(k)}^i(V_1, \mathcal{N}_{yy2})] \quad (A-158c)
\end{aligned}$$

$$\begin{aligned}
\eta_{212}^2 = & \mathcal{M}_{xx2i,xy}^n - 2\mathcal{M}_{xy1i,x}^n \left(\frac{i\eta}{R}\right) - \left(\frac{i\eta}{R}\right)^2 \mathcal{M}_{yy2i}^n - \frac{\mathcal{M}_{yy2}^n}{R} \\
& + \left(\frac{\eta}{R}\right) [A_{J2(K)}^i(W_2, \mathcal{N}_{xy2,x}) - A_{J3(K)}^i(W_1, \mathcal{N}_{xy1,x})] \\
& + \left(\frac{\eta}{R}\right)^2 [-A_{J2(K)}^i(W_2, \mathcal{N}_{yy1}) - A_{J3(K)}^i(W_1, \mathcal{N}_{yy2})] \\
& + \frac{\delta_1}{R} [-A_{J2(K)}^i(V_1, \mathcal{N}_{xy2,x}) - A_{J3(K)}^i(V_2, \mathcal{N}_{xy1,x})] \\
& + \frac{\delta_1 \eta}{R^2} [A_{J2(K)}^i(V_1, \mathcal{N}_{yy1}) - A_{J3(K)}^i(V_2, \mathcal{N}_{yy2})] \\
& + A_{J2(K)}^i(W_{1,xx}, \mathcal{N}_{xx2}) + A_{J3(K)}^i(W_{2,xx}, \mathcal{N}_{xx1}) \\
& + \frac{2\eta}{R} [A_{J2(K)}^i(W_{2,x}, \mathcal{N}_{xy2}) - A_{J3(K)}^i(W_{1,x}, \mathcal{N}_{xy1})] \\
& + \frac{\delta_1}{R} [-A_{J2(K)}^i(V_{1,x}, \mathcal{N}_{xy2}) - A_{J3(K)}^i(V_{2,x}, \mathcal{N}_{xy1})] \\
& + \left(\frac{\eta}{R}\right)^2 [-A_{J22(K)}^i(W_1, \mathcal{N}_{yy2}) - A_{J23(K)}^i(W_2, \mathcal{N}_{yy1})] \\
& + \frac{\delta_1 \eta}{R^2} [-A_{J2(K)}^i(V_2, \mathcal{N}_{yy2}) + A_{J3(K)}^i(V_1, \mathcal{N}_{yy1})] \quad (A-158d)
\end{aligned}$$

$$\begin{aligned}
\eta_{12L}^3 = & \frac{\eta}{R} [A_{J1(2K)}^i(W_2^0, \mathcal{N}_{xy1,x}^L) - A_{J4(2K)}^i(W_1^0, \mathcal{N}_{xy2,x}^L) \\
& + 2A_{J1(2K)}^i(W_{2,x}^0, \mathcal{N}_{xy1}^L) - 2A_{J4(2K)}^i(W_{1,x}^0, \mathcal{N}_{xy2}^L)] \\
& + \left(\frac{\eta}{R}\right)^2 [A_{J31(2K)}^i(W_2^0, \mathcal{N}_{yy2}^L) + A_{J34(2K)}^i(W_1^0, \mathcal{N}_{yy1}^L) \\
& - A_{J21(2K)}^i(W_1^0, \mathcal{N}_{yy1}^L) - A_{J24(2K)}^i(W_2^0, \mathcal{N}_{yy2}^L)] \\
& + A_{J1(2K)}^i(W_{1,xx}^0, \mathcal{N}_{xx1}^L) + A_{J4(2K)}^i(W_{2,xx}^0, \mathcal{N}_{xx2}^L) \quad (A-159a)
\end{aligned}$$

$$\begin{aligned}
\eta_{21L}^3 = & \frac{\eta}{R} [A_{J2(K)}^i(W_2^0, \mathcal{N}_{xy2,x}^L) - A_{J3(2K)}^i(W_1^0, \mathcal{N}_{xy1,x}^L) \\
& + 2A_{J2(2K)}^i(W_{2,x}^0, \mathcal{N}_{xy2}^L) - 2A_{J3(2K)}^i(W_{1,x}^0, \mathcal{N}_{xy1}^L)] \\
& + \left(\frac{\eta}{R}\right)^2 [-A_{J22(2K)}^i(W_2^0, \mathcal{N}_{yy1}^L) - A_{J23(2K)}^i(W_1^0, \mathcal{N}_{yy2}^L)]
\end{aligned}$$

$$\begin{aligned}
& - A_{J22(2K)}^i (W_1^0, \mathcal{N}_{yy2}^L) - A_{J23(2K)}^i (U_2, \mathcal{N}_{yy1}^L) \\
& + A_{2(2K)}^i (W_{1,xx}^0, \mathcal{N}_{xx2}^L) + A_{3(2K)}^i (W_{2,xx}^0, \mathcal{N}_{xx1}^L)
\end{aligned} \tag{A-159b}$$

$$\begin{aligned}
\eta_{lin}^3 = \frac{\eta}{R} [& A_{J1(2K)}^i (W_2 + W_2^0, \mathcal{N}_{xy1,x}^\eta) - A_{J4(2K)}^i (W_1 + W_1^0, \mathcal{N}_{xy2,x}^\eta) \\
& + A_{J1(2K)}^i (W_2, \mathcal{N}_{xy1,x}^L) - A_{J4(2K)}^i (W_1, \mathcal{N}_{xy2,x}^L) \\
& + 2 A_{J1(2K)}^i (W_{2,x} + W_{2,x}^0, \mathcal{N}_{xy1}^\eta) - 2 A_{J4(2K)}^i (W_{1,x} + W_{2,x}^0, \mathcal{N}_{xy2}^\eta) \\
& + 2 A_{J1(2K)}^i (W_{2,x}, \mathcal{N}_{xy1}^L) - 2 A_{J4(2K)}^i (W_{1,x}, \mathcal{N}_{xy2}^L)] \\
& + \left(\frac{\eta}{R}\right)^2 [A_{J1(2K)}^i (W_2 + W_2^0, \mathcal{N}_{yy2}^\eta) + A_{J4(2K)}^i (W_1 + W_1^0, \mathcal{N}_{yy1}^\eta) \\
& - A_{J21(2K)}^i (W_1 + W_1^0, \mathcal{N}_{yy1}^\eta) - A_{J24(2K)}^i (W_2 + W_2^0, \mathcal{N}_{yy2}^\eta) \\
& + A_{J1(2K)}^i (W_2, \mathcal{N}_{yy2}^L) + A_{J4(2K)}^i (W_1, \mathcal{N}_{yy1}^L) - A_{J21(2K)}^i (W_1, \mathcal{N}_{yy1}^L) \\
& - A_{J24(2K)}^i (W_2, \mathcal{N}_{yy2}^L)] + \frac{\delta_1}{R} [- A_{1(2K)}^i (U_1, \mathcal{N}_{xy1,x}^\eta) - A_{4(2K)}^i (U_2, \mathcal{N}_{xy2,x}^\eta) \\
& - A_{1(2K)}^i (U_{1,x}, \mathcal{N}_{xy1}^\eta) - A_{4(2K)}^i (U_{2,x}, \mathcal{N}_{xy2}^\eta) - A_{1(2K)}^i (U_1, \mathcal{N}_{xy1,x}^L) \\
& - A_{4(2K)}^i (U_2, \mathcal{N}_{xy2,x}^L) - A_{1(2K)}^i (U_{1,x}, \mathcal{N}_{xy1}^L) - A_{4(2K)}^i (U_{2,x}, \mathcal{N}_{xy2}^L)] \\
& + \frac{\delta_1 \eta}{R^2} [- A_{J1(2K)}^i (U_1, \mathcal{N}_{yy2}^\eta) + A_{J4(2K)}^i (U_2, \mathcal{N}_{yy1}^\eta) - A_{J1(2K)}^i (U_2, \mathcal{N}_{yy1}^\eta) \\
& + A_{J4(2K)}^i (U_1, \mathcal{N}_{yy2}^\eta) - A_{J1(2K)}^i (U_1, \mathcal{N}_{yy2}^L) + A_{J4(2K)}^i (U_2, \mathcal{N}_{yy1}^L) \\
& - A_{J1(2K)}^i (U_2, \mathcal{N}_{yy1}^L) + A_{J4(2K)}^i (U_1, \mathcal{N}_{yy2}^L)] \\
& + A_{1(2K)}^i (W_{1,xx} + W_{1,xx}^0, \mathcal{N}_{xx1}^\eta) + A_{4(2K)}^i (W_{2,xx} + W_{2,xx}^0, \mathcal{N}_{xx2}^\eta) \\
& + A_{1(2K)}^i (W_{1,xx}, \mathcal{N}_{xx1}^L) + A_{4(2K)}^i (W_{2,xx}, \mathcal{N}_{xx2}^L)
\end{aligned} \tag{A-159c}$$

$$\begin{aligned}
\gamma_{2i\pi}^3 = & \left(\frac{\pi}{R}\right) [A_{J2(2k)}^i(W_2+W_2^0, \mathcal{N}_{xy2,x}^\pi) - A_{J3(2k)}^i(W_1+W_1^0, \mathcal{N}_{xy1,x}^\pi) \\
& + 2A_{J2(2k)}^i(W_{2,x}+W_{2,x}^0, \mathcal{N}_{xy2}^\pi) - 2A_{J3(2k)}^i(W_{1,x}+W_{1,x}^0, \mathcal{N}_{xy1}^\pi) \\
& + A_{J2(2k)}^i(W_2, \mathcal{N}_{xy2,x}^L) - A_{J3(2k)}^i(W_1, \mathcal{N}_{xy1,x}^L) + 2A_{J2(2k)}^i(W_{2,x}, \mathcal{N}_{xy2}^L) \\
& - 2A_{J3(2k)}^i(W_{1,x}, \mathcal{N}_{xy1}^L)] + [A_{IJ2(2k)}^i(W_2, \mathcal{N}_{yy1}^L) - A_{IJ3(2k)}^i(W_1, \mathcal{N}_{yy1}^L) \\
& - A_{J22(2k)}^i(W_1, \mathcal{N}_{yy2}^L) - A_{J23(2k)}^i(W_2, \mathcal{N}_{yy1}^L)] \left(\frac{\pi}{R}\right)^2 \\
& + \left(\frac{\pi}{R}\right)^2 [-A_{IJ2(2k)}^i(W_2+W_2^0, \mathcal{N}_{yy1}^\pi) - A_{IJ3(2k)}^i(W_1+W_1^0, \mathcal{N}_{yy2}^\pi) \\
& - A_{J22(2k)}^i(W_1+W_1^0, \mathcal{N}_{yy2}^\pi) - A_{J23(2k)}^i(W_2+W_2^0, \mathcal{N}_{yy1}^\pi)] \\
& + \frac{\delta_1}{R} [-A_{2(2k)}^i(U_1, \mathcal{N}_{xy2,x}^\pi + \mathcal{N}_{xy2,x}^L) - A_{3(2k)}^i(U_2, \mathcal{N}_{xy1,x}^\pi + \mathcal{N}_{xy1,x}^L) \\
& - A_{2(2k)}^i(U_{1,x}, \mathcal{N}_{xy2}^\pi + \mathcal{N}_{xy2}^L) - A_{3(2k)}^i(U_{2,x}, \mathcal{N}_{xy1}^\pi + \mathcal{N}_{xy1}^L)] \\
& + \frac{\delta_1 \pi}{R^2} [A_{I2(2k)}^i(U_1, \mathcal{N}_{yy1}^\pi + \mathcal{N}_{yy1}^L) - A_{I3(2k)}^i(U_2, \mathcal{N}_{yy2}^\pi + \mathcal{N}_{yy2}^L)] \\
& + A_{2(2k)}^i(W_{1,xx}+W_{1,xx}^0, \mathcal{N}_{xx2}^\pi) + A_{3(2k)}^i(W_{2,xx}+W_{2,xx}^0, \mathcal{N}_{xx1}^\pi) \\
& + A_{2(2k)}^i(W_{1,xx}, \mathcal{N}_{xx2}^L) + A_{3(2k)}^i(W_{2,xx}, \mathcal{N}_{xx1}^L) \quad (A-159d)
\end{aligned}$$

According to Eqs A-119 subject to the constraint of Eq A-120, there exist $6k + 3$ unknown functions of position. These are the displacement coefficients $u_{1i}(x)$, $v_{1i}(x)$, $w_{1i}(x)$ for $i = 0, 1, 2 \dots k$, and $u_{2i}(x)$, $v_{2i}(x)$, $w_{2i}(x)$ for $i = 1, 2, 3 \dots k$. Note that if one can solve for the displacement components the response of the system is fully characterized (deformation approach).

Next, the Galerkin procedure is employed in the circumferential direction. The vanishing of the Galerkin integrals leads to $(6k + 3)$ nonlinear algebraic equations in the $(6k + 3)$ unknowns. These equations are:

$$n_{xx1i,x} + \frac{in}{R} n_{xy2i} + n_{xx1i,x}^L + n_{xy2i}^L \frac{in}{R} = -n_{xx1i,x}^n - \frac{in}{R} n_{xy2i}^n$$

$$\xi_{ii}^1 + \xi_{iiL}^2 + \xi_{iiL}^3 + \xi_{iin}^2 + \xi_{iin}^3 = 0$$

$$\eta_{ii,x}^1 + \eta_{iiL}^2 + \eta_{iiL}^3 + \eta_{iin}^2 + \eta_{iin}^3 = -g_{ii}$$

$$\text{for } i = 0, 1, 2, \dots, k$$

$$n_{xx2i,x} - \frac{in}{R} n_{xy1i} + n_{xx2i,x}^L - \frac{in}{R} n_{xy1i}^L = \frac{in}{R} n_{xy1i}^n - n_{xx2i,x}^n$$

$$\xi_{2i}^1 + \xi_{2iL}^2 + \xi_{2iL}^3 + \xi_{2in}^2 + \xi_{2in}^3 = 0$$

$$\eta_{2i,x}^1 + \eta_{2iL}^2 + \eta_{2iL}^3 + \eta_{2in}^2 + \eta_{2in}^3 = -g_{2i}$$

$$\text{for } i = 1, 2, \dots, k$$

(A-160)

Next, the generalized Newton's method (Ref. 38) is used to reduce the nonlinear field equations to a sequence of linear systems. This procedure is similar as the one in section II.2. Because the final set of equations, Eqs A-160, contains n 's, ξ 's and η 's, and because these are in turn functions of other parameters, then Eq A-72 will be applied to all of the elements, needed in deriving the iteration equations. In so doing, only the nonlinear terms need be considered. Thus,

$$\begin{aligned} (t_{x1i}^n)^{m+1} &= A_{1(k)}^i(w_{1,x}^m, w_{1,x}^{m+1}) + A_{4(k)}^i(w_{2,x}^m, w_{2,x}^{m+1}) \\ &\quad - \frac{1}{2} \{ A_{1(k)}^i(w_{1,x}^m, w_{1,x}^m) + A_{4(k)}^i(w_{2,x}^m, w_{2,x}^m) \} \end{aligned} \quad (A-161)$$

$$\begin{aligned} (t_{x2i}^n)^{m+1} &= A_{2(k)}^i(w_{1,x}^m, w_{2,x}^{m+1}) + A_{3(k)}^i(w_{2,x}^m, w_{1,x}^{m+1}) \\ &\quad - \frac{1}{2} \{ A_{2(k)}^i(w_{1,x}^m, w_{2,x}^m) + A_{3(k)}^i(w_{2,x}^m, w_{1,x}^m) \} \end{aligned} \quad (A-162)$$

$$\begin{aligned}
(t_{y1i}^n)^{m+1} = & \frac{n^2}{R^2} [A_{IJ4(k)}^i(w_1^m, w_2^{m+1}) + A_{IJ1(k)}^i(w_2^m, w_3^{m+1})] \\
& + \frac{\delta_1}{R^2} [A_{1(k)}^i(v_1^m, v_1^{m+1}) + A_{4(k)}^i(v_2^m, v_2^{m+1})] \\
& + \frac{\delta_1 n}{R^2} [A_{J4(k)}^i(w_1^m, v_2^{m+1}) + A_{I4(k)}^i(v_2^m, w_1^{m+1}) \\
& - A_{J1(k)}^i(w_2^m, v_1^{m+1}) - A_{I1(k)}^i(v_1^m, w_2^{m+1})] \\
& - \frac{1}{2} \frac{n^2}{R^2} [A_{IJ4(k)}^i(w_1^m, w_1^m) + A_{IJ1(k)}^i(w_2^m, w_2^m)] \\
& - \frac{\delta_1}{2R^2} [A_{1(k)}^i(v_1^m, v_1^m) + A_{4(k)}^i(v_2^m, v_2^m)] \\
& + \frac{\delta_1 n}{R^2} [A_{J4(k)}^i(w_1^m, v_2^m) - A_{J1(k)}^i(w_2^m, v_1^m)] \quad (A-163)
\end{aligned}$$

$$\begin{aligned}
(t_{y2i}^n)^{m+1} = & -\frac{n^2}{R^2} [A_{IJ2(k)}^i(w_2^m, w_1^{m+1}) + A_{IJ3(k)}^i(w_1^m, w_2^{m+1})] \\
& + \frac{\delta_1}{R^2} [A_3^i(v_2^m, v_1^{m+1}) + A_{2(k)}^i(v_1^m, v_2^{m+1})] \\
& + \frac{\delta_1 n}{R^2} [A_{J3(k)}^i(w_1^m, v_1^{m+1}) + A_{I2(k)}^i(v_1^m, w_1^{m+1}) \\
& - A_{J2(k)}^i(w_2^m, v_2^{m+1}) - A_{I3(k)}^i(v_2^m, w_2^{m+1})] \\
& + \frac{1}{2} \frac{n^2}{R^2} [A_{IJ2(k)}^i(w_2^m, w_1^m) + A_{IJ3(k)}^i(w_1^m, w_2^m)] \\
& - \frac{\delta_1}{2R^2} [A_3^i(v_2^m, v_1^m) + A_{2(k)}^i(v_1^m, v_2^m)] \\
& - \frac{\delta_1 n}{R^2} [A_{J3(k)}^i(w_1^m, v_1^m) - A_{J2(k)}^i(w_2^m, v_2^m)] \quad (A-164)
\end{aligned}$$

$$\begin{aligned}
(t_{xyi}^n)^{m+1} = & \frac{n}{R} [A_{J1(k)}^i(w_2^m, w_{1,x}^{m+1}) - A_{J4(k)}^i(w_1^m, w_{2,x}^{m+1}) \\
& + A_{I1(k)}^i(w_{1,x}^m, w_2^{m+1}) - A_{I4(k)}^i(w_{2,x}^m, w_1^{m+1})] \\
& - \frac{\delta_1}{R} [A_{1(k)}^i(v_1^m, w_{1,x}^{m+1}) + A_{4(k)}^i(v_2^m, w_{2,x}^{m+1}) \\
& + A_{1(k)}^i(w_{1,x}^m, v_1^{m+1}) + A_{4(k)}^i(w_{2,x}^m, v_2^{m+1})]
\end{aligned}$$

$$\begin{aligned}
& -\frac{\eta}{2R} [A_{J1(K)}^i(W_2^m, W_{1,X}^m) - A_{J4(K)}^i(W_1^m, W_{2,X}^m) \\
& - A_{I4(K)}^i(W_{2,X}^m, W_1^m) + A_{I1(K)}^i(W_{1,X}^m, W_2^m)] \\
& + \frac{\delta_1}{R} [A_{1(K)}^i(v_1^m, W_{1,X}^m) + A_{4(K)}^i(v_2^m, W_{2,X}^m)]
\end{aligned} \tag{A-165}$$

$$\begin{aligned}
(t_{xy2i})^\eta &= \frac{\eta}{R} [A_{J2(K)}^i(W_2^m, W_{2,X}^m) - A_{J3(K)}^i(W_1^m, W_{1,X}^{m+1}) \\
& - A_{I2(K)}^i(W_{1,X}^m, W_1^{m+1}) + A_{I3(K)}^i(W_{2,X}^m, W_2^{m+1})] \\
& - \frac{\delta_1}{R} [A_{3(K)}^i(v_2^m, W_{1,X}^{m+1}) + A_{2(K)}^i(v_1^m, W_{2,X}^{m+1}) \\
& + A_{2(K)}^i(W_{1,X}^m, v_2^{m+1}) + A_{3(K)}^i(W_{2,X}^m, v_1^{m+1})] \\
& - \frac{\eta}{2R} [A_{J1(K)}^i(W_2^m, W_{1,X}^m) - A_{J4(K)}^i(W_1^m, W_{2,X}^m) \\
& - A_{I4(K)}^i(W_{2,X}^m, W_1^m) + A_{I1(K)}^i(W_{1,X}^m, W_2^m)] \\
& + \frac{\delta_1}{R} [A_{1(K)}^i(v_1^m, W_{1,X}^m) + A_{4(K)}^i(v_2^m, W_{2,X}^m)]
\end{aligned} \tag{A-166}$$

$$\begin{aligned}
(t_{x1i,x})^{m+1} &= A_{1(K)}^i(W_{1,xx}^m, W_{1,X}^{m+1}) + A_{1(K)}^i(W_{1,X}^m, W_{1,xx}^{m+1}) \\
& + A_{4(K)}^i(W_{2,xx}^m, W_{2,X}^{m+1}) + A_{4(K)}^i(W_{2,X}^m, W_{2,xx}^{m+1}) \\
& - \frac{1}{2} [A_{1(K)}^i(W_{1,xx}^m, W_{1,X}^m) + A_{4(K)}^i(W_{2,xx}^m, W_{2,X}^m) \\
& + A_{1(K)}^i(W_{1,X}^m, W_{1,xx}^m) + A_{4(K)}^i(W_{2,X}^m, W_{2,xx}^m)]
\end{aligned} \tag{A-167}$$

$$\begin{aligned}
(t_{x2i,x})^{m+1} &= A_{2(K)}^i(W_{1,xx}^m, W_{2,X}^{m+1}) + A_{2(K)}^i(W_{1,X}^m, W_{2,xx}^{m+1}) \\
& + A_{3(K)}^i(W_{2,xx}^m, W_{1,X}^{m+1}) + A_{3(K)}^i(W_{2,X}^m, W_{1,xx}^{m+1}) \\
& - \frac{1}{2} [A_{2(K)}^i(W_{1,xx}^m, W_{2,X}^m) + A_{2(K)}^i(W_{1,X}^m, W_{2,xx}^m) \\
& + A_{3(K)}^i(W_{2,xx}^m, W_{1,X}^m) + A_{3(K)}^i(W_{2,X}^m, W_{1,xx}^m)]
\end{aligned} \tag{A-168}$$

$$\begin{aligned}
(t_{y i, x}^m)^{m+1} = & \frac{\eta^2}{R^2} [A_{IJ4(k)}^i(w_{1,x}^m, w_1^{m+1}) + A_{IJ4(k)}^i(w_1^m, w_{1,x}^{m+1}) \\
& + A_{IJ1(k)}^i(w_{2,x}^m, w_2^{m+1}) + A_{IJ1(k)}^i(w_2^m, w_{2,x}^{m+1})] \\
& + \frac{\delta_1}{R^2} [A_{1(k)}^i(v_{1,x}^m, v_{1,x}^{m+1}) + A_{4(k)}^i(v_{2,x}^m, v_2^{m+1}) \\
& + A_{1(k)}^i(v_1^m, v_{1,x}^{m+1}) + A_{4(k)}^i(v_2^m, v_{2,x}^{m+1})] \\
& + \frac{\delta_1 \eta}{R^2} [A_{J4(k)}^i(w_{1,x}^m, v_2^{m+1}) + A_{J4(k)}^i(w_1^m, v_{2,x}^{m+1}) \\
& + A_{I4(k)}^i(v_{2,x}^m, w_1^{m+1}) + A_{I4(k)}^i(v_2^m, w_{1,x}^{m+1}) \\
& - A_{J1(k)}^i(w_{2,x}^m, v_2^{m+1}) - A_{J1(k)}^i(w_2^m, v_{1,x}^{m+1}) \\
& - A_{I1(k)}^i(v_{1,x}^m, w_2^{m+1}) - A_{I1(k)}^i(v_1^m, w_{2,x}^{m+1})] \\
& - \frac{1}{2} \frac{\eta^2}{R^2} [A_{IJ4(k)}^i(w_{1,x}^m, w_1^m) + A_{IJ4(k)}^i(w_1^m, w_{1,x}^m) \\
& + A_{IJ1(k)}^i(w_{2,x}^m, w_2^m) + A_{IJ1(k)}^i(w_2^m, w_{2,x}^m)] \\
& - \frac{\delta_1}{2R^2} [A_{1(k)}^i(v_{1,x}^m, v_1^m) + A_{4(k)}^i(v_{2,x}^m, v_2^m) \\
& + A_{1(k)}^i(v_1^m, v_{1,x}^m) + A_{4(k)}^i(v_2^m, v_{2,x}^m)] \\
& - \frac{\delta_1 \eta}{R^2} [A_{J4(k)}^i(w_{1,x}^m, v_2^m) + A_{J4(k)}^i(w_1^m, v_{2,x}^m) \\
& + A_{I4(k)}^i(v_{2,x}^m, w_1^{m+1}) + A_{I4(k)}^i(v_2^m, w_{1,x}^{m+1}) \\
& - A_{J1(k)}^i(w_{2,x}^m, v_2^{m+1}) - A_{J1(k)}^i(w_2^m, v_{1,x}^{m+1}) \\
& - A_{I1(k)}^i(v_{1,x}^m, w_2^m) - A_{I1(k)}^i(v_1^m, w_{2,x}^m)] \quad (A-169)
\end{aligned}$$

$$\begin{aligned}
(t_{y2i,x}^{\eta})^{\eta+1} = & -\left(\frac{\eta}{R}\right)^2 [A_{IJ2(K)}^i(W_{2,x}^{\eta}, W_1^{\eta+1}) + A_{IJ2(K)}^i(W_2^{\eta}, W_{1,x}^{\eta+1}) \\
& + A_{IJ3(K)}^i(W_{1,x}^{\eta}, W_2^{\eta+1}) + A_{IJ3(K)}^i(W_1^{\eta}, W_{2,x}^{\eta+1})] \\
& + \frac{\delta_1}{R^2} [A_{3(K)}^i(v_{2,x}^{\eta}, v_1^{\eta+1}) + A_{2(K)}^i(v_{1,x}^{\eta}, v_2^{\eta+1}) \\
& + A_{3(K)}^i(v_2^{\eta}, v_{1,x}^{\eta+1}) + A_{2(K)}^i(v_1^{\eta}, v_{2,x}^{\eta+1})] \\
& + \frac{\delta_1 \eta}{R^2} [A_{J3(K)}^i(W_{1,x}^{\eta}, v_1^{\eta+1}) + A_{J3(K)}^i(W_1^{\eta}, v_{1,x}^{\eta+1}) \\
& + A_{I2(K)}^i(v_{1,x}^{\eta}, W_1^{\eta+1}) + A_{I2(K)}^i(v_1^{\eta}, W_{1,x}^{\eta+1}) \\
& - A_{J2(K)}^i(W_{2,x}^{\eta}, v_2^{\eta+1}) - A_{J2(K)}^i(W_2^{\eta}, v_{2,x}^{\eta+1}) \\
& - A_{I3(K)}^i(v_{2,x}^{\eta}, W_2^{\eta+1}) - A_{I3(K)}^i(v_2^{\eta}, W_{2,x}^{\eta+1})] \\
& - \frac{\delta_1}{2R^2} [A_{3(K)}^i(v_{2,x}^{\eta}, v_1^{\eta}) + A_{2(K)}^i(v_{1,x}^{\eta}, v_2^{\eta}) \\
& + A_{3(K)}^i(v_2^{\eta}, v_{1,x}^{\eta}) + A_{2(K)}^i(v_2^{\eta}, v_{2,x}^{\eta})] \\
& - \frac{\delta_1 \eta}{R^2} [A_{J3(K)}^i(W_{1,x}^{\eta}, v_1^{\eta}) + A_{J3(K)}^i(W_1^{\eta}, v_{1,x}^{\eta}) \\
& + A_{I3(K)}^i(v_{1,x}^{\eta}, W_1^{\eta}) + A_{I2(K)}^i(v_1^{\eta}, W_{1,x}^{\eta}) \\
& - A_{J2(K)}^i(W_{2,x}^{\eta}, v_2^{\eta}) - A_{J2(K)}^i(W_2^{\eta}, v_{2,x}^{\eta}) \\
& - A_{I3(K)}^i(v_{2,x}^{\eta}, W_2^{\eta}) - A_{I3(K)}^i(v_2^{\eta}, W_{2,x}^{\eta})] \\
& + \frac{1}{2} \left(\frac{\eta}{R}\right)^2 [A_{IJ2(K)}^i(W_{2,x}^{\eta}, W_1^{\eta}) + A_{IJ2(K)}^i(W_2^{\eta}, W_{1,x}^{\eta}) \\
& + A_{IJ3(K)}^i(W_{1,x}^{\eta}, W_2^{\eta}) + A_{IJ3(K)}^i(W_1^{\eta}, W_{2,x}^{\eta})] \quad (A-170)
\end{aligned}$$

$$\begin{aligned}
(t_{xyil,x}^n)^{m+1} = & \frac{n}{R} [A_{J1(K)}^i(w_{2,x}^m, w_{1,x}^{m+1}) + A_{J1(K)}^i(w_2^m, w_{1,xx}^{m+1}) \\
& - A_{J4(K)}^i(w_{1,x}^m, w_{2,x}^{m+1}) - A_{J4(K)}^i(w_1^m, w_{2,xx}^{m+1}) \\
& + A_{I1(K)}^i(w_{1,xx}^m, w_2^{m+1}) + A_{I1(K)}^i(w_{1,x}^m, w_{2,x}^{m+1}) \\
& - A_{I4(K)}^i(w_{2,xx}^m, w_1^{m+1}) - A_{I4(K)}^i(w_{2,x}^m, w_{1,x}^{m+1})] \\
& - \frac{\delta_1}{R} [A_{1(K)}^i(v_{1,x}^m, w_{1,x}^{m+1}) + A_{1(K)}^i(v_1^m, w_{1,xx}^{m+1}) \\
& + A_{4(K)}^i(v_{2,x}^m, w_{2,x}^{m+1}) + A_{4(K)}^i(v_2^m, w_{2,xx}^{m+1}) \\
& + A_{1(K)}^i(w_{1,xx}^m, v_2^{m+1}) + A_{1(K)}^i(w_{1,x}^m, v_{1,x}^{m+1}) \\
& + A_{4(K)}^i(w_{2,xx}^m, v_2^{m+1}) + A_{4(K)}^i(w_{2,x}^m, v_{2,x}^{m+1})] \\
& - \frac{n}{2R} [A_{J1(K)}^i(w_{2,xx}^m, w_{1,x}^m) + A_{J1(K)}^i(w_2^m, w_{1,xx}^m) \\
& - A_{J4(K)}^i(w_{1,x}^m, w_{2,x}^m) - A_{J4(K)}^i(w_1^m, w_{2,xx}^m) \\
& + A_{I1(K)}^i(w_{1,xx}^m, w_2^m) + A_{I1(K)}^i(w_{2,x}^m, w_{1,x}^m)] \\
& - \frac{\delta_1}{R} [A_{1(K)}^i(v_{1,x}^m, w_{1,x}^m) + A_{1(K)}^i(v_1^m, w_{1,xx}^m) \\
& + A_{4(K)}^i(v_{2,x}^m, w_{2,x}^m) + A_{4(K)}^i(v_2^m, w_{2,xx}^m) \\
& + A_{1(K)}^i(w_{1,xx}^m, v_1^m) + A_{1(K)}^i(w_{1,x}^m, v_{1,x}^m) \\
& + A_{4(K)}^i(w_{2,xx}^m, v_2^m) + A_{4(K)}^i(w_{2,x}^m, v_{2,x}^m)] \\
& + \frac{n}{2R} [A_{I4(K)}^i(w_{2,xx}^m, v_2^m) + A_{I4(K)}^i(w_{2,x}^m, v_{2,x}^m)] \quad (A-171)
\end{aligned}$$

$$\begin{aligned}
(t_{xy2i,x}^m)^{m+1} = & \frac{\eta}{R} [A_{J2(k)}^i(W_{2,x}^m, W_{2,x}^{m+1}) + A_{J2(k)}^i(W_2^m, W_{2,xx}^{m+1}) \\
& - A_{J3(k)}^i(W_{1,x}^m, W_{1,x}^{m+1}) - A_{J3(k)}^i(W_1^m, W_{1,xx}^{m+1}) \\
& - A_{I2(k)}^i(W_{1,xx}^m, W_1^{m+1}) - A_{I2(k)}^i(W_{1,x}^m, W_{1,x}^{m+1}) \\
& + A_{I3(k)}^i(W_{2,xx}^m, W_2^{m+1}) + A_{I3(k)}^i(W_{2,x}^m, W_{2,x}^{m+1})] \\
& - \frac{\delta_1}{R} [A_{3(k)}^i(U_{2,x}^m, W_{1,x}^{m+1}) + A_{3(k)}^i(U_2^m, W_{1,xx}^{m+1}) \\
& + A_{2(k)}^i(U_{1,x}^m, W_{2,x}^{m+1}) + A_{2(k)}^i(U_1^m, W_{2,xx}^{m+1}) \\
& + A_{2(k)}^i(W_{1,xx}^m, U_2^{m+1}) + A_{2(k)}^i(W_{1,x}^m, U_{2,x}^{m+1}) \\
& + A_{3(k)}^i(W_{2,xx}^m, U_1^{m+1}) + A_{3(k)}^i(W_{2,x}^m, U_{1,x}^{m+1})] \\
& - \frac{\eta}{2R} [A_{J2(k)}^i(W_{2,x}^m, W_{2,x}^m) + A_{J2(k)}^i(W_2^m, W_{2,xx}^m) \\
& - A_{J3(k)}^i(W_{1,x}^m, W_{1,x}^m) - A_{J3(k)}^i(W_1^m, W_{1,xx}^m) \\
& - A_{I2(k)}^i(W_{1,xx}^m, W_1^m) - A_{I2(k)}^i(W_{1,x}^m, W_{1,xx}^m) \\
& + A_{I3(k)}^i(W_{2,xx}^m, W_2^m) + A_{I3(k)}^i(W_{2,x}^m, W_{2,x}^m)] \\
& + \frac{\delta_1}{R} [A_{3(k)}^i(U_{2,x}^m, W_{1,x}^m) + A_{3(k)}^i(U_2^m, W_{1,xx}^m) \\
& + A_{2(k)}^i(U_{1,x}^m, W_{2,x}^m) + A_{2(k)}^i(U_1^m, W_{2,xx}^m) \\
& + A_{2(k)}^i(W_{1,xx}^m, U_2^m) + A_{2(k)}^i(W_{1,x}^m, U_{2,x}^m) \\
& + A_{3(k)}^i(W_{2,xx}^m, U_1^m) + A_{3(k)}^i(W_{2,x}^m, U_{1,x}^m)]
\end{aligned} \tag{A-172}$$

$$\begin{aligned}
(t_{x1,xx}^n)^{m+1} &= A_{1(k)}^i(w_{1,xxx}^m, w_{1,x}^{m+1}) + 2A_{1(k)}^i(w_{1,xx}^m, w_{1,xx}^{m+1}) + A_{1(k)}^i(w_{1,x}^m, w_{1,xxx}^{m+1}) \\
&+ A_{4(k)}^i(w_{2,xxx}^m, w_{2,x}^{m+1}) + 2A_{4(k)}^i(w_{2,xx}^m, w_{2,xx}^{m+1}) + A_{4(k)}^i(w_{2,x}^m, w_{2,xxx}^{m+1}) \\
&- \frac{1}{2} [A_{1(k)}^i(w_{1,xxx}^m, w_{1,x}^m) + 2A_{1(k)}^i(w_{1,xx}^m, w_{1,xx}^m) + A_{1(k)}^i(w_{1,x}^m, w_{1,xxx}^m) \\
&+ A_{4(k)}^i(w_{2,xxx}^m, w_{2,x}^m) + 2A_{4(k)}^i(w_{2,xx}^m, w_{2,xx}^m) + A_{4(k)}^i(w_{2,x}^m, w_{2,xxx}^m)] \quad (A-173)
\end{aligned}$$

$$\begin{aligned}
(t_{x2,xx}^n)^{m+1} &= A_{2(k)}^i(w_{1,xxx}^m, w_{2,x}^{m+1}) + 2A_{2(k)}^i(w_{1,xx}^m, w_{2,xx}^{m+1}) + A_{2(k)}^i(w_{1,x}^m, w_{2,xxx}^{m+1}) \\
&+ A_{3(k)}^i(w_{2,xxx}^m, w_{1,x}^{m+1}) + 2A_{3(k)}^i(w_{2,xx}^m, w_{1,xx}^{m+1}) + A_{3(k)}^i(w_{2,x}^m, w_{1,xxx}^{m+1}) \\
&- \frac{1}{2} [A_{2(k)}^i(w_{1,xxx}^m, w_{2,x}^m) + 2A_{2(k)}^i(w_{1,xx}^m, w_{2,xx}^m) + A_{2(k)}^i(w_{1,x}^m, w_{2,xxx}^m) \\
&+ A_{3(k)}^i(w_{2,xxx}^m, w_{1,x}^m) + 2A_{3(k)}^i(w_{2,xx}^m, w_{1,xx}^m) + A_{3(k)}^i(w_{2,x}^m, w_{1,xxx}^m)] \quad (A-174)
\end{aligned}$$

$$\begin{aligned}
(t_{y1i,xx}^n)^{m+1} &= \frac{\eta^2}{R^2} [A_{IJ4(k)}^i(w_{1,x}^m, w_i^{m+1}) + 2A_{IJ4(k)}^i(w_{1,x}^m, w_{i,x}^{m+1}) + A_{IJ4(k)}^i(w_i^m, w_{1,xx}^{m+1}) \\
&+ A_{IJ1(k)}^i(w_{1,xx}^m, w_2^{m+1}) + 2A_{IJ1(k)}^i(w_{1,x}^m, w_{2,x}^{m+1}) + A_{IJ1(k)}^i(w_i^m, w_{2,xx}^{m+1})] \\
&+ \frac{\delta_1 \eta}{R^2} [A_{1(k)}^i(v_{1,xx}^m, v_i^{m+1}) + 2A_{1(k)}^i(v_{1,x}^m, v_{i,x}^{m+1}) + A_{1(k)}^i(v_i^m, v_{1,xx}^{m+1}) \\
&+ A_{4(k)}^i(v_{2,xx}^m, v_2^{m+1}) + 2A_{4(k)}^i(v_{2,x}^m, v_{2,x}^{m+1}) + A_{4(k)}^i(v_2^m, v_{2,xx}^{m+1})] \\
&+ \frac{\delta_1 \eta}{R^2} [A_{J4(k)}^i(w_{1,xx}^m, v_2^{m+1}) + 2A_{J4(k)}^i(w_{1,x}^m, v_{2,x}^{m+1}) + A_{J4(k)}^i(w_i^m, v_{2,xx}^{m+1}) \\
&+ A_{I4(k)}^i(v_{2,xx}^m, w_i^{m+1}) + 2A_{I4(k)}^i(v_{2,x}^m, w_{i,x}^{m+1}) + A_{I4(k)}^i(v_2^m, w_{i,xx}^{m+1}) \\
&- A_{J1(k)}^i(w_{2,x}^m, v_i^{m+1}) - 2A_{J1(k)}^i(w_{2,x}^m, v_{i,x}^{m+1}) - A_{J1(k)}^i(w_2^m, v_{i,xx}^{m+1}) \\
&- A_{I1(k)}^i(v_{1,xx}^m, w_2^{m+1}) - 2A_{I1(k)}^i(v_{1,x}^m, w_{2,x}^{m+1}) - A_{I1(k)}^i(v_i^m, w_{2,xx}^{m+1})] \\
&- \frac{\eta^2}{2R^2} [A_{IJ4(k)}^i(w_{1,xx}^m, w_i^m) + 2A_{IJ4(k)}^i(w_{1,x}^m, w_{i,x}^m) + A_{IJ4(k)}^i(w_i^m, w_{1,xx}^m) \\
&+ A_{IJ1(k)}^i(w_{2,xx}^m, w_2^m) + 2A_{IJ1(k)}^i(w_{2,x}^m, w_{2,x}^m) + A_{IJ1(k)}^i(w_2^m, w_{2,xx}^m)]
\end{aligned}$$

$$\begin{aligned}
& -\frac{\delta_1}{2R^2} [A_{1(k)}^i(u_{1,xx}^m, u_1^m) + 2A_{1(k)}^i(u_{1,x}^m, u_{1,x}^{m+1}) + A_{1(k)}^i(u_1^m, u_{1,xx}^{m+1}) \\
& \quad + A_{4(k)}^i(u_{2,xx}^m, u_2^m) + 2A_{4(k)}^i(u_{2,x}^m, u_{2,x}^m) + A_{4(k)}^i(u_2^m, u_{2,xx}^m)] \\
& -\frac{\delta_1 \eta}{R^2} [A_{J4(k)}^i(w_{1,xx}^m, u_2^m) + 2A_{J4(k)}^i(w_{1,x}^m, u_{2,x}^m) + A_{J4(k)}^i(w_1^m, u_{2,xx}^m) \\
& \quad + A_{I4(k)}^i(u_{2,xx}^m, w_1^m) + 2A_{I4(k)}^i(u_{2,x}^m, w_{1,x}^m) + A_{I4(k)}^i(u_2^m, w_{1,xx}^m) \\
& \quad - A_{J1(k)}^i(w_{2,xx}^m, u_1^m) - 2A_{J1(k)}^i(w_{2,x}^m, u_{1,x}^m) - A_{J1(k)}^i(w_2^m, u_{1,xx}^m) \\
& \quad - A_{I1(k)}^i(u_{1,xx}^m, w_2^{m+1}) - 2A_{I1(k)}^i(u_{1,x}^m, w_{2,x}^m) - A_{I1(k)}^i(u_1^m, w_{2,xx}^m)] \quad (A-175)
\end{aligned}$$

$$\begin{aligned}
(t_{y2i,xx}^m)^{m+1} = & -(\frac{\eta}{R})^2 [A_{IJ2(k)}^i(w_{2,xx}^m, w_1^{m+1}) + 2A_{IJ2(k)}^i(w_{2,x}^m, w_{1,x}^{m+1}) + A_{IJ2(k)}^i(w_2^m, w_{1,xx}^{m+1}) \\
& + A_{IJ3(k)}^i(w_{1,xx}^m, w_2^{m+1}) + 2A_{IJ3(k)}^i(w_{1,x}^m, w_{2,x}^{m+1}) + A_{IJ3(k)}^i(w_1^m, w_{2,xx}^{m+1})] \\
& + \frac{\delta_1}{R} [A_{3(k)}^i(u_{2,xx}^m, u_1^{m+1}) + 2A_{3(k)}^i(u_{2,x}^m, u_{1,x}^{m+1}) + A_{3(k)}^i(u_2^m, u_{1,xx}^{m+1}) \\
& + A_{2(k)}^i(u_{1,xx}^m, u_2^{m+1}) + 2A_{2(k)}^i(u_{1,x}^m, u_{2,x}^{m+1}) + A_{2(k)}^i(u_1^m, u_{2,xx}^{m+1})] \\
& + \frac{\delta_1 \eta}{R^2} [A_{J3(k)}^i(w_{1,xx}^m, u_1^{m+1}) + 2A_{J3(k)}^i(w_{1,x}^m, u_{1,x}^{m+1}) + A_{J3(k)}^i(w_1^m, u_{1,xx}^{m+1}) \\
& + A_{I2(k)}^i(u_{1,xx}^m, w_1^{m+1}) + 2A_{I2(k)}^i(u_{1,x}^m, w_{1,x}^{m+1}) + A_{I2(k)}^i(u_1^m, w_{1,xx}^{m+1}) \\
& - A_{J2(k)}^i(w_{2,xx}^m, u_2^{m+1}) - 2A_{J2(k)}^i(w_{2,x}^m, u_{2,x}^{m+1}) - A_{J2(k)}^i(w_2^m, u_{2,xx}^{m+1}) \\
& - A_{I3(k)}^i(u_{2,xx}^m, w_2^{m+1}) - 2A_{I3(k)}^i(u_{2,x}^m, w_{2,x}^{m+1}) - A_{I3(k)}^i(u_2^m, w_{2,xx}^{m+1})] \\
& + \frac{1}{2}(\frac{\eta}{R})^2 [A_{IJ2(k)}^i(w_{2,xx}^m, w_1^m) + 2A_{IJ2(k)}^i(w_{2,x}^m, w_{1,x}^m) + A_{IJ2(k)}^i(w_2^m, w_{1,xx}^m) \\
& + A_{IJ3(k)}^i(w_{1,xx}^m, w_2^m) + 2A_{IJ3(k)}^i(w_{1,x}^m, w_{2,x}^m) + A_{IJ3(k)}^i(w_1^m, w_{2,xx}^m)] \\
& - \frac{\delta_1}{2R} [A_{3(k)}^i(u_{2,xx}^m, u_1^m) + 2A_{3(k)}^i(u_{2,x}^m, u_{1,x}^m) + A_{3(k)}^i(u_2^m, u_{1,xx}^m) \\
& + A_{2(k)}^i(u_{1,xx}^m, u_2^m) + 2A_{2(k)}^i(u_{1,x}^m, u_{2,x}^m) + A_{2(k)}^i(u_1^m, u_{2,xx}^m)]
\end{aligned}$$

$$\begin{aligned}
& -\frac{\delta_1 \eta}{R^2} [A_{J3(K)}^i(W_{1,xx}^m, U_1^m) + 2A_{J3(K)}^i(W_{1,x}^m, U_{1,x}^m) + A_{J3(K)}^i(W_1^m, U_{1,xx}^m) \\
& + A_{J2(K)}^i(U_{1,xx}^m, W_1^m) + 2A_{J2(K)}^i(U_{1,x}^m, W_{1,x}^m) + A_{J2(K)}^i(U_1^m, W_{1,xx}^m) \\
& - A_{J2(K)}^i(W_{2,xx}^m, U_2^m) - 2A_{J2(K)}^i(W_{2,x}^m, U_{2,x}^m) - A_{J2(K)}^i(W_2^m, U_{2,xx}^m) \\
& - A_{J3(K)}^i(U_{2,xx}^m, W_2^m) - 2A_{J3(K)}^i(U_{2,x}^m, W_{2,x}^m) - A_{J3(K)}^i(U_2^m, W_{2,xx}^m)] \quad (A-176)
\end{aligned}$$

$$\begin{aligned}
(t_{xy|1,xx})^{m+1} &= \frac{\eta}{R} [A_{J1(K)}^i(W_{2,xy}^m, W_{1,x}^m) + 2A_{J1(K)}^i(W_{2,x}^m, W_{1,xx}^m) + A_{J1(K)}^i(W_2^m, W_{1,xxx}^m) \\
& - A_{J4(K)}^i(W_{1,xx}^m, W_{2,x}^{m+1}) + 2A_{J4(K)}^i(W_{1,x}^m, W_{2,xx}^{m+1}) - A_{J4(K)}^i(W_1^m, W_{2,xxx}^m) \\
& + A_{J1(K)}^i(W_{1,xxx}^m, W_2^{m+1}) + 2A_{J1(K)}^i(W_{1,xx}^m, W_{2,x}^{m+1}) + A_{J1(K)}^i(W_{1,x}^m, W_{2,xx}^{m+1}) \\
& - A_{J4(K)}^i(W_{2,xxx}^m, W_1^{m+1}) - 2A_{J4(K)}^i(W_{2,xx}^m, W_{1,x}^{m+1}) - A_{J4(K)}^i(W_{2,x}^m, W_{1,xx}^{m+1})] \\
& - \frac{\delta_1}{R} [A_{1(K)}^i(U_{1,xx}^m, W_{1,x}^{m+1}) + 2A_{1(K)}^i(U_{1,x}^m, W_{1,xx}^{m+1}) + A_{1(K)}^i(U_1^m, W_{1,xxx}^{m+1}) \\
& + A_{4(K)}^i(U_{2,xx}^m, W_{2,x}^{m+1}) + 2A_{4(K)}^i(U_{2,x}^m, W_{2,xx}^{m+1}) + A_{4(K)}^i(U_2^m, W_{2,xxx}^{m+1}) \\
& + A_{10(K)}^i(W_{1,xxx}^m, U_1^{m+1}) + 2A_{1(K)}^i(W_{1,xx}^m, U_{1,x}^{m+1}) + A_{1(K)}^i(W_{1,x}^m, U_{1,xx}^{m+1}) \\
& + A_{4(K)}^i(W_{2,xxx}^m, U_2^{m+1}) + 2A_{4(K)}^i(W_{2,xx}^m, U_{2,x}^{m+1}) + A_{4(K)}^i(W_{2,x}^m, U_{2,xx}^{m+1})] \\
& - \frac{\eta}{2R} [A_{J1(K)}^i(W_{2,xx}^m, W_{1,x}^m) + 2A_{J1(K)}^i(W_{2,x}^m, W_{1,xx}^m) + A_{J1(K)}^i(W_2^m, W_{1,xxx}^m) \\
& - A_{J4(K)}^i(W_{1,xx}^m, W_{2,x}^m) - 2A_{J4(K)}^i(W_{1,x}^m, W_{2,xx}^m) + A_{J4(K)}^i(W_1^m, W_{2,xxx}^m) \\
& + A_{J1(K)}^i(W_{1,xxx}^m, W_2^m) + 2A_{J1(K)}^i(W_{1,xx}^m, W_{2,x}^m) + A_{J1(K)}^i(W_{1,x}^m, W_{2,xx}^m)]
\end{aligned}$$

$$-A_{I4(k)}^i(w_{2,xx}^m, w_1^m) - 2A_{I4(k)}^i(w_{2,xx}^m, w_{1,x}^m) - A_{I4(k)}^i(w_{2,x}^m, w_{1,xx}^m)]$$

$$+ \frac{\delta_1}{R} [A_{1(k)}^i(v_{1,xx}^m, w_{1,x}^m) + 2A_{1(k)}^i(v_{1,x}^m, w_{1,xx}^m) + A_{1(k)}^i(v_1^m, w_{1,xxx}^m)$$

$$+ A_{4(k)}^i(v_{2,xx}^m, w_{2,x}^m) + 2A_{4(k)}^i(v_{2,x}^m, w_{2,xx}^m) + A_{4(k)}^i(v_2^m, w_{2,xxx}^m)$$

$$+ A_{1(k)}^i(w_{1,xxx}^m, v_1^m) + 2A_{1(k)}^i(w_{1,xx}^m, v_{1,x}^m) + A_{1(k)}^i(w_{1,x}^m, v_{1,xx}^m)$$

$$+ A_{4(k)}^i(w_{2,xxx}^m, v_2^m) + 2A_{4(k)}^i(w_{2,xx}^m, v_{2,x}^m) + A_{4(k)}^i(w_{2,x}^m, v_{2,xx}^m)] \quad (A-177)$$

$$(t_{xy2i,xx}^m)^{m+1} = \frac{n}{R} [A_{J2(k)}^i(w_{2,xx}^m, w_{2,x}^{m+1}) + 2A_{J2(k)}^i(w_{2,x}^m, w_{2,xx}^{m+1}) + A_{J2(k)}^i(w_2^m, w_{2,xxx}^{m+1})$$

$$- A_{J3(k)}^i(w_{1,xx}^m, w_{1,x}^{m+1}) - 2A_{J3(k)}^i(w_{1,x}^m, w_{1,xx}^{m+1}) - A_{J3(k)}^i(w_1^m, w_{1,xxx}^{m+1})$$

$$- A_{I2(k)}^i(w_{1,xxx}^m, w_1^{m+1}) - 2A_{I2(k)}^i(w_{1,xx}^m, w_{1,x}^{m+1}) - A_{I2(k)}^i(w_{1,x}^m, w_{1,xx}^{m+1})$$

$$+ A_{I3(k)}^i(w_{2,xxx}^m, w_2^{m+1}) + 2A_{I3(k)}^i(w_{2,xx}^m, w_{2,x}^{m+1}) + A_{I3(k)}^i(w_{2,x}^m, w_{2,xx}^{m+1})]$$

$$- \frac{\delta_1}{R} [A_{3(k)}^i(v_{2,xx}^m, w_{2,x}^{m+1}) + 2A_{3(k)}^i(v_{2,x}^m, w_{2,xx}^{m+1}) + A_{3(k)}^i(v_2^m, w_{2,xxx}^{m+1})$$

$$+ A_{2(k)}^i(v_{1,xx}^m, w_{2,x}^{m+1}) + 2A_{2(k)}^i(v_{1,x}^m, w_{2,xx}^{m+1}) + A_{2(k)}^i(v_1^m, w_{2,xxx}^{m+1})$$

$$+ A_{2(k)}^i(w_{1,xxx}^m, v_2^{m+1}) + 2A_{2(k)}^i(w_{1,xx}^m, v_{2,x}^{m+1}) + A_{2(k)}^i(w_{1,x}^m, v_{2,xx}^{m+1})$$

$$+ A_{3(k)}^i(w_{2,xxx}^m, v_1^{m+1}) + 2A_{3(k)}^i(w_{2,xx}^m, v_{1,x}^{m+1}) + A_{3(k)}^i(w_{2,x}^m, v_{1,xx}^{m+1})]$$

$$- \frac{n}{2R} [A_{J2(k)}^i(w_{2,xx}^m, w_{2,x}^m) + 2A_{J2(k)}^i(w_{2,x}^m, w_{1,xx}^m) + A_{J2(k)}^i(w_2^m, w_{1,xxx}^m)$$

$$- A_{J3(k)}^i(w_{1,xx}^m, w_{1,x}^m) - 2A_{J3(k)}^i(w_{1,x}^m, w_{1,xx}^m) - A_{J3(k)}^i(w_1^m, w_{1,xxx}^m)]$$

$$\begin{aligned}
& - A_{I2(K)}^i (W_{1,XXX}^m, W_1^m) - 2 A_{I2(K)}^i (W_{1,XX}^m, W_{1,X}^m) - A_{I2(K)}^i (W_{1,X}^m, W_{1,XX}^m) \\
& + A_{I3(K)}^i (W_{2,XXX}^m, W_2^m) + 2 A_{I3(K)}^i (W_{2,XX}^m, W_{2,X}^m) + A_{I3(K)}^i (W_{2,X}^m, W_{2,XX}^m) \\
& + \frac{\delta_1}{R} [A_{3(K)}^i (U_{2,XX}^m, W_{1,X}^m) + 2 A_{3(K)}^i (U_{2,X}^m, W_{1,XX}^m) + A_{3(K)}^i (U_2^m, W_{1,XXX}^m) \\
& + A_{2(K)}^i (U_{1,XX}^m, W_{2,X}^m) + 2 A_{2(K)}^i (U_{1,X}^m, W_{2,XX}^m) + A_{2(K)}^i (U_1^m, W_{2,XXX}^m) \\
& + A_{2(K)}^i (W_{1,XXX}^m, U_2^m) + 2 A_{2(K)}^i (W_{1,XX}^m, U_{2,X}^m) + A_{2(K)}^i (W_{1,X}^m, U_{2,XX}^m) \\
& + A_{3(K)}^i (W_{2,XXX}^m, U_1^m) + 2 A_{3(K)}^i (W_{2,XX}^m, U_{1,X}^m) + A_{3(K)}^i (W_{2,X}^m, U_{1,XX}^m)] \quad (A-178)
\end{aligned}$$

where m is the number of the iteration step.

Substitution of Eqs A-161- A-178 into Eqs A-149 and A-150 one may obtain the iteration equations for the nonlinear part of the stress and moment resultant vectors $(\{n_1^n\}_i$ and $\{n_2^n\}_i)$. In so doing, new symbols are introduced and defined. The part of the t's or n's that is linearized (linear) with respect to the iteration parameters (containing u^{m+1} , v^{m+1} & w^{m+1}) is denoted by superscript L next to n, i.e. $\{t_{1L}^{nL}\}$. The part that only depends on the value of the parameters at the previous step (u^m , v^m , w^m), is denoted by superscript n next to n, i.e. $\{t_{1L}^{nn}\}$.

$$\begin{aligned}
\{n_1^n\}_i^{m+1} &= \begin{bmatrix} \bar{A} & \bar{B} \\ \bar{B} & \bar{D} \end{bmatrix} (\{t_{1L}^{nL}\}^{m+1} + \{t_{1L}^{nn}\}^m) \\
&= \{n_1^{nL}\}_i^{m+1} + \{n_1^{nn}\}_i^m \quad (A-179)
\end{aligned}$$

$$\begin{aligned}
\{n_2^n\} &= \begin{bmatrix} \bar{A} & \bar{B} \\ \bar{B} & \bar{D} \end{bmatrix} (\{t_{2L}^{nL}\}^{m+1} + \{t_{2L}^{nn}\}^m) \\
&= \{n_2^{nL}\}_i^{m+1} + \{n_2^{nn}\}_i^m \quad (A-180)
\end{aligned}$$

$$\begin{aligned}\left\{ \mathcal{N}_{1,X}^n \right\}_i^{m+1} &= \begin{bmatrix} \bar{A} & \bar{B} \\ \bar{B} & \bar{D} \end{bmatrix} \left(\left\{ t_{1i,X}^{nL} \right\}^{m+1} + \left\{ t_{1i,X}^{nn} \right\}^m \right) \\ &= \left\{ \mathcal{N}_{1,X}^{nL} \right\}_i^{m+1} + \left\{ \mathcal{N}_{1,X}^{nn} \right\}_i^m\end{aligned}\quad (A-181)$$

$$\begin{aligned}\left\{ \mathcal{N}_{2,X}^n \right\}_i^{m+1} &= \begin{bmatrix} \bar{A} & \bar{B} \\ \bar{B} & \bar{D} \end{bmatrix} \left(\left\{ t_{2i,X}^{nL} \right\}^{m+1} + \left\{ t_{2i,X}^{nn} \right\}^m \right) \\ &= \left\{ \mathcal{N}_{2,X}^{nL} \right\}_i^{m+1} + \left\{ \mathcal{N}_{2,X}^{nn} \right\}_i^m\end{aligned}\quad (A-182)$$

$$\begin{aligned}\left\{ \mathcal{N}_{1,XX}^n \right\}^{m+1} &= \begin{bmatrix} \bar{A} & \bar{B} \\ \bar{B} & \bar{D} \end{bmatrix} \left(\left\{ t_{1i,XX}^{nL} \right\}^{m+1} + \left\{ t_{1i,XX}^{nn} \right\}^m \right) \\ &= \left\{ \mathcal{N}_{1,XX}^{nL} \right\}^{m+1} + \left\{ \mathcal{N}_{1,XX}^{nn} \right\}^m\end{aligned}\quad (A-183)$$

$$\begin{aligned}\left\{ \mathcal{N}_{2,XX}^n \right\}^{m+1} &= \begin{bmatrix} \bar{A} & \bar{B} \\ \bar{B} & \bar{D} \end{bmatrix} \left(\left\{ t_{2i,XX}^{nL} \right\}^{m+1} + \left\{ t_{2i,XX}^{nn} \right\}^m \right) \\ &= \left\{ \mathcal{N}_{2,XX}^{nL} \right\}^{m+1} + \left\{ \mathcal{N}_{2,XX}^{nn} \right\}^m\end{aligned}\quad (A-184)$$

In a very similar manner, the nonlinear terms of the equilibrium equations are also linearized by Newton's method:

$$\begin{aligned}\xi_{in}^2 &= -\frac{i\eta}{R}(\mathcal{N}_{yy1i}^{nL} + \mathcal{N}_{yy1i}^{nn}) + \mathcal{N}_{xy2i,X}^{nL} + \mathcal{N}_{xy2i,X}^{nn} + \frac{\delta_1}{R}(\mathcal{M}_{xy2i,X}^{nL} + \mathcal{M}_{xy2i,X}^{nn}) \\ &\quad - \frac{i\eta}{R^2}\delta_1(\mathcal{M}_{yy1i}^{nL} + \mathcal{M}_{yy1i}^{nn}) + \frac{\delta_1}{R^2}\mathcal{N}(A_{J1(u)}^i(W_2^m, \mathcal{N}_{yy1}^{m+1}) + A_{J1(u)}^i(W_2^{m+1}, \mathcal{N}_{yy1}^m) \\ &\quad - A_{J1(u)}^i(W_2^m, \mathcal{N}_{yy1}^m) - A_{J4(u)}^i(W_1^{m+1}, \mathcal{N}_{yy2}^m) - A_{J4(u)}^i(W_1^m, \mathcal{N}_{yy2}^{m+1}) + A_{J4(u)}^i(W_1^m, \mathcal{N}_{yy2}^m) \\ &\quad - \frac{\delta_1}{R^2}[A_{1(u)}^i(V_1^{m+1}, \mathcal{N}_{yy1}^m) + A_{1(u)}^i(V_1^m, \mathcal{N}_{yy1}^{m+1}) + A_{1(u)}^i(V_1^m, \mathcal{N}_{yy1}^m)]\end{aligned}$$

$$\begin{aligned}
& + A_{4(k)}^i (V_2^{m+1}, \mathcal{N}_{yy2}^m) + A_{4(k)}^i (V_2^m, \mathcal{N}_{yy2}^{m+1}) - A_{4(k)}^i (V_2^m, \mathcal{N}_{yy2}^m) \\
& + \frac{\delta_1}{R} [A_{1(k)}^i (W_{1,x}^{m+1}, \mathcal{N}_{xy1}^m) + A_{1(k)}^i (W_{1,x}^m, \mathcal{N}_{xy1}^{m+1}) - A_{1(k)}^i (W_{1,x}^m, \mathcal{N}_{xy1}^m) \\
& + A_{4(k)}^i (W_{2,x}^{m+1}, \mathcal{N}_{xy2}^m) + A_{4(k)}^i (W_{2,x}^m, \mathcal{N}_{xy2}^{m+1}) - A_{4(k)}^i (W_{2,x}^m, \mathcal{N}_{xy2}^m)] \quad (A-185)
\end{aligned}$$

$$\begin{aligned}
\Sigma_{2in}^2 = & -\frac{i\mathcal{N}}{R} (\mathcal{N}_{yy1i}^{nL} + \mathcal{N}_{yy1i}^{nn}) + \mathcal{N}_{xy2i,x}^{nL} + \mathcal{N}_{xy2i,x}^{nn} + \frac{\delta_1}{R} (\mathcal{M}_{xy2i,x}^{nL} + \mathcal{M}_{xy2i,x}^{nn}) \\
& - \frac{i\mathcal{N}}{R} \delta_1 (\mathcal{M}_{yy1i}^{nL} + \mathcal{M}_{yy1i}^{nn}) + \frac{\delta_1 \mathcal{N}}{R^2} [A_{J2(k)}^i (W_2^{m+1}, \mathcal{N}_{yy2}^m) + A_{J2(k)}^i (W_2^m, \mathcal{N}_{yy2}^{m+1}) \\
& - A_{J2(k)}^i (W_2^m, \mathcal{N}_{yy2}^m) + A_{J3(k)}^i (W_1^{m+1}, \mathcal{N}_{yy1}^m) + A_{J3(k)}^i (W_1^m, \mathcal{N}_{yy1}^{m+1}) \\
& - A_{J3(k)}^i (W_1^m, \mathcal{N}_{yy1}^m)] - \frac{\delta_1}{R^2} [A_{3(k)}^i (V_2^{m+1}, \mathcal{N}_{yy1}^m) + A_{3(k)}^i (V_2^m, \mathcal{N}_{yy1}^{m+1}) \\
& - A_{3(k)}^i (V_2^m, \mathcal{N}_{yy1}^m) + A_{2(k)}^i (V_1^{m+1}, \mathcal{N}_{yy2}^m) + A_{2(k)}^i (V_1^m, \mathcal{N}_{yy2}^{m+1}) - A_{2(k)}^i (V_1^m, \mathcal{N}_{yy2}^m)] \quad (A-186)
\end{aligned}$$

$$\begin{aligned}
\Sigma_{in}^3 = & \frac{\delta_1 \mathcal{N}}{R^2} [A_{J1(2k)}^i (W_2^0, \mathcal{N}_{yy1}^{nL}) + A_{J1(2k)}^i (W_2^0, \mathcal{N}_{yy1}^{nn}) + A_{J1(2k)}^i (W_2^m, \mathcal{N}_{yy1}^{nn}) \\
& - A_{J4(2k)}^i (W_1^m, \mathcal{N}_{yy2}^{nn}) - A_{J4(2k)}^i (W_1^0, \mathcal{N}_{yy2}^{nL}) - A_{J4(2k)}^i (W_1^0, \mathcal{N}_{yy2}^{nn}) \\
& - \frac{\delta_1}{R^2} [A_{1(2k)}^i (V_1^m, \mathcal{N}_{yy1}^{nn}) + A_{4(2k)}^i (V_2^m, \mathcal{N}_{yy2}^{nn})] \\
& + \frac{\delta_1}{R} [A_{1(2k)}^i (W_{1,x}^0, \mathcal{N}_{xy1}^{nn}) + A_{1(2k)}^i (W_{1,x}^0, \mathcal{N}_{xy1}^{nn}) + A_{1(2k)}^i (W_{1,x}^m, \mathcal{N}_{xy1}^{nn}) \\
& + A_{4(2k)}^i (W_{2,x}^0, \mathcal{N}_{xy2}^{nn}) + A_{4(2k)}^i (W_{1,x}^0, \mathcal{N}_{xy1}^{nn}) + A_{4(2k)}^i (W_{2,x}^m, \mathcal{N}_{xy2}^{nn})] \\
& + \frac{\delta_1 \mathcal{N}}{R^2} [A_{J1(2k)}^i (W_2^{m+1}, \mathcal{N}_{yy1}^{Lm}) + A_{J1(2k)}^i (W_2^m, \mathcal{N}_{yy1}^{Lm+1}) - A_{J1(2k)}^i (W_2^m, \mathcal{N}_{yy1}^{Lm}) \\
& - A_{J4(2k)}^i (W_1^m, \mathcal{N}_{yy2}^{Lm+1}) - A_{J4(2k)}^i (W_1^{m+1}, \mathcal{N}_{yy2}^{Lm}) + A_{J4(2k)}^i (W_1^m, \mathcal{N}_{yy2}^{Lm})] \\
& - \frac{\delta_1}{R^2} [A_{1(2k)}^i (V_1^{m+1}, \mathcal{N}_{yy1}^{Lm}) + A_{1(2k)}^i (V_1^m, \mathcal{N}_{yy1}^{Lm+1}) - A_{1(2k)}^i (V_1^m, \mathcal{N}_{yy1}^{Lm}) \\
& + A_{4(2k)}^i (V_2^{m+1}, \mathcal{N}_{yy2}^{Lm}) + A_{4(2k)}^i (V_2^m, \mathcal{N}_{yy2}^{Lm+1}) - A_{4(2k)}^i (V_2^m, \mathcal{N}_{yy2}^{Lm})] \\
& + \frac{\delta_1}{R} [A_{1(2k)}^i (W_{1,x}^{m+1}, \mathcal{N}_{xy1,x}^{Lm}) + A_{1(2k)}^i (W_{1,x}^m, \mathcal{N}_{xy1,x}^{Lm+1}) - A_{1(2k)}^i (W_{1,x}^m, \mathcal{N}_{xy1,x}^{Lm})
\end{aligned}$$

$$+ A_{4(2K)}^i(W_{yx}^{m+1}, n_{xy2}^{Lm}) + A_{4(2K)}^i(W_{2,x}^m, n_{xy2}^{Lm+1}) - A_{4(2K)}^i(W_{2,x}^m, n_{xy2}^{Lm})] \quad (A-187)$$

$$\begin{aligned} \xi_{2in}^3 = & \frac{\delta_1 n}{R^2} [-A_{J3(2K)}^i(W_1^m, n_{yy1}^{nn}) - A_{J3(2K)}^i(W_1^0, n_{yy1}^{nL}) - A_{J3(2K)}^i(W_1^0, n_{yy1}^{nn}) \\ & + A_{J2(2K)}^i(W_2^m, n_{yy2}^{nn}) + A_{J2(2K)}^i(W_2^0, n_{yy2}^{nL}) + A_{J2(2K)}^i(W_2^0, n_{yy2}^{nn})] \\ & - \frac{\delta_1}{R^2} [A_{2(2K)}^i(v_1^m, n_{yy2}^{nn}) + A_{3(2K)}^i(v_2^m, n_{yy1}^{nn})] \\ & + \frac{\delta_1}{R} [A_{3(2K)}^i(W_{2,x}^m, n_{xy1}^{nn}) + A_{3(2K)}^i(W_{2,x}^0, n_{xy1}^{nL}) + A_{3(2K)}^i(W_{2,x}^0, n_{xy1}^{nn}) \\ & + A_{2(2K)}^i(W_{1,x}^m, n_{xy2}^{nn}) + A_{2(2K)}^i(W_{1,x}^0, n_{xy2}^{nL}) + A_{2(2K)}^i(W_{1,x}^0, n_{xy2}^{nn})] \\ & + \frac{\delta_1 n}{R^2} [-A_{J3(2K)}^i(W_1^{m+1}, n_{yy1}^{Lm}) - A_{J3(2K)}^i(W_1^m, n_{yy1}^{Lm+1}) + A_{J3(2K)}^i(W_1^m, n_{yy1}^{Lm}) \\ & + A_{J2(2K)}^i(W_2^{m+1}, n_{yy2}^{Lm}) + A_{J2(2K)}^i(W_2^m, n_{yy2}^{Lm+1}) - A_{J2(2K)}^i(W_2^m, n_{yy2}^{Lm})] \\ & - \frac{\delta_1}{R^2} [A_{2(2K)}^i(v_1^{m+1}, n_{yy2}^{Lm}) + A_{2(2K)}^i(v_1^m, n_{yy2}^{Lm+1}) - A_{2(2K)}^i(v_1^m, n_{yy2}^{Lm}) \\ & + A_{3(2K)}^i(v_2^{m+1}, n_{yy1}^{Lm}) + A_{3(2K)}^i(v_2^m, n_{yy1}^{Lm+1}) - A_{3(2K)}^i(v_2^m, n_{yy1}^{Lm})] \\ & + \frac{\delta_1}{R} [A_{3(2K)}^i(W_{2,x}^{m+1}, n_{xy1}^{Lm}) + A_{3(2K)}^i(W_{2,x}^m, n_{xy1}^{Lm+1}) - A_{3(2K)}^i(W_{2,x}^m, n_{xy1}^{Lm}) \\ & + A_{2(2K)}^i(W_{1,x}^{m+1}, n_{xy2}^{Lm}) + A_{2(2K)}^i(W_{1,x}^m, n_{xy2}^{Lm+1}) - A_{2(2K)}^i(W_{1,x}^m, n_{xy2}^{Lm})] \quad (A-188) \end{aligned}$$

$$\begin{aligned} \eta_{iin}^2 = & m_{xxii,xx}^{nL} + m_{xxii,xx}^{nn} + 2\left(\frac{in}{R}\right)(m_{xy2i,x}^{nL} + m_{xy2i,x}^{nn}) - \left(\frac{in}{R}\right)^2(m_{yyii}^{nL} + m_{yyii}^{nn}) \\ & - \frac{1}{R}(n_{yyii}^{nL} + n_{yyii}^{nn}) + \frac{n}{R} [A_{J1(K)}^i(W_2^{m+1}, n_{xy1,x}^m) + A_{J1(K)}^i(W_2^m, n_{xy1,x}^{m+1}) \\ & - A_{J1(K)}^i(W_2^m, n_{xy,x}^m) - A_{J4(K)}^i(W_1^{m+1}, n_{xy1,x}^{m+1}) - A_{J4(K)}^i(W_1^m, n_{xy2,x}^{m+1}) + A_{J4(K)}^i(W_1^m, n_{xy2,x}^m)] \\ & + \left(\frac{n}{R}\right)^2 [A_{IJ1(K)}^i(W_2^m, n_{yy2}^m) + A_{IJ4(K)}^i(W_1^{m+1}, n_{yy1}^m) - A_{IJ4(K)}^i(W_1^m, n_{yy1}^m)] \\ & + A_{IJ4(K)}^i(W_1^{m+1}, n_{yy1}^m) + A_{IJ4(K)}^i(W_1^m, n_{yy1}^{m+1}) - A_{IJ4(K)}^i(W_1^m, n_{yy1}^m)] \\ & + \frac{\delta_1}{R} [-A_{1(K)}^i(v_1^{m+1}, n_{xy1,x}^m) - A_{1(K)}^i(v_1^m, n_{xy1,x}^{m+1}) + A_{1(K)}^i(v_1^m, n_{xy1,x}^m)] \end{aligned}$$

$$\begin{aligned}
& -A_{4(k)}^i(v_2^{m+1}, n_{xy2,x}^m) - A_{4(k)}^i(v_2^m, n_{xy2,x}^{m+1}) + A_{4(k)}^i(v_2^m, n_{xy2,x}^m) \\
& + \frac{\delta_1 \eta}{R^2} [-A_{I1(k)}^i(v_1^{m+1}, n_{yy2}^m) - A_{I1(k)}^i(v_1^m, n_{yy2}^{m+1}) + A_{I1(k)}^i(v_1^m, n_{yy2}^m) \\
& + A_{I4(k)}^i(v_2^{m+1}, n_{yy1}^m) + A_{I4(k)}^i(v_2^m, n_{yy1}^{m+1}) - A_{I4(k)}^i(v_2^m, n_{yy1}^m) \\
& + A_{I(k)}^i(w_{1,xx}^{m+1}, n_{xx1}^m) + A_{I(k)}^i(w_{1,xx}^m, n_{xx1}^{m+1}) - A_{I(k)}^i(w_{1,xx}^m, n_{xx1}^m) \\
& + A_{4(k)}^i(w_{2,xx}^{m+1}, n_{xx2}^m) + A_{4(k)}^i(w_{2,xx}^m, n_{xx2}^{m+1}) - A_{4(k)}^i(w_{2,xx}^m, n_{xx2}^m) \\
& + \frac{2\eta}{R} [A_{J1(k)}^i(w_{2,x}^{m+1}, n_{xy1}^m) + A_{J1(k)}^i(w_{2,x}^m, n_{xy1}^{m+1}) - A_{J1(k)}^i(w_{2,x}^m, n_{xy1}^m) \\
& - A_{J4(k)}^i(w_{1,x}^{m+1}, n_{xy2}^m) - A_{J4(k)}^i(w_{1,x}^m, n_{xy2}^{m+1}) + A_{J4(k)}^i(w_{1,x}^m, n_{xy2}^m) \\
& + (\frac{\eta}{R})^2 [-A_{J21(k)}^i(w_1^{m+1}, n_{yy1}^m) - A_{J21(k)}^i(w_1^{m+1}, n_{yy1}^m) + A_{J21(k)}^i(w_1^m, n_{yy1}^m) \\
& - A_{J24(k)}^i(w_2^{m+1}, n_{yy2}^m) - A_{J24(k)}^i(w_2^m, n_{yy2}^{m+1}) + A_{J24(k)}^i(w_2^m, n_{yy2}^m) \\
& + \frac{\delta_1 \eta}{R^2} [-A_{J1(k)}^i(v_2^{m+1}, n_{yy1}^m) - A_{J1(k)}^i(v_2^m, n_{yy1}^{m+1}) + A_{J1(k)}^i(v_2^m, n_{yy1}^m) \\
& + A_{J4(k)}^i(v_1^{m+1}, n_{yy2}^m) + A_{J4(k)}^i(v_1^m, n_{yy2}^{m+1}) - A_{J4(k)}^i(v_1^m, n_{yy2}^m)] \quad (A-189)
\end{aligned}$$

$$\begin{aligned}
\eta_{2in}^2 &= m_{xx2i,xx}^{nL} + m_{xx2i,xx}^{nn} - 2(\frac{i\eta}{R})(m_{xy1i,x}^{nL} + m_{xy2i,x}^{nn}) \\
& - (\frac{i\eta}{R})^2 (m_{yy2i}^{nL} + m_{yy2i}^{nn}) - \frac{1}{R} (\eta_{yy2}^{nL} + \eta_{yy2}^{nn}) \\
& + (\frac{\eta}{R}) [A_{J2(k)}^i(w_2^{m+1}, n_{xy2,x}^m) + A_{J2(k)}^i(w_2^m, n_{xy2,x}^{m+1}) - A_{J2(k)}^i(w_2^m, n_{xy2,x}^m) \\
& - A_{J3(k)}^i(w_1^{m+1}, n_{xy2,x}^m) - A_{J3(k)}^i(w_1^m, n_{xy2,x}^{m+1}) + A_{J3(k)}^i(w_1^m, n_{xy2,x}^m) \\
& + (\frac{\eta}{R})^2 [-A_{IJ2(k)}^i(w_2^{m+1}, n_{yy1}^m) - A_{IJ2(k)}^i(w_2^m, n_{yy1}^{m+1}) + A_{IJ2(k)}^i(w_2^m, n_{yy1}^m) \\
& - A_{IJ3(k)}^i(w_1^{m+1}, n_{yy2}^m) - A_{IJ3(k)}^i(w_1^m, n_{yy2}^{m+1}) + A_{IJ3(k)}^i(w_1^m, n_{yy2}^m) \\
& + \frac{\delta_1}{R} [-A_{2(k)}^i(v_1^{m+1}, n_{xy2,x}^m) - A_{2(k)}^i(v_1^m, n_{xy2,x}^{m+1}) + A_{2(k)}^i(v_1^m, n_{xy2,x}^m)
\end{aligned}$$

$$\begin{aligned}
& -A_{3(K)}^i(v_2^{m+1}, n_{xy1,x}^m) - A_{3(K)}^i(v_2^m, n_{xy1,x}^{m+1}) + A_{3(K)}^i(v_2^m, n_{xy1,x}^m) \\
& + \frac{\delta_1 \eta}{R} [A_{I2(K)}^i(v_1^{m+1}, n_{yy1}^m) + A_{I2(K)}^i(v_1^m, n_{yy1}^{m+1}) - A_{I2(K)}^i(v_1^m, n_{yy1}^m) \\
& \quad + A_{I3(K)}^i(v_2^{m+1}, n_{yy2}^m) + A_{I3(K)}^i(v_2^m, n_{yy2}^{m+1}) - A_{I3(K)}^i(v_2^m, n_{yy2}^m)] \\
& + A_{2(K)}^i(w_{1,xx}^{m+1}, n_{xx2}^m) + A_{2(K)}^i(w_{1,xx}^m, n_{xx2}^{m+1}) - A_{2(K)}^i(w_{1,xx}^m, n_{xx2}^m) \\
& + A_{3(K)}^i(w_{2,xx}^{m+1}, n_{xx1}^m) + A_{3(K)}^i(w_{2,xx}^m, n_{xx1}^{m+1}) - A_{3(K)}^i(w_{2,xx}^m, n_{xx1}^m) \\
& + \frac{\delta_2 \eta}{R} [A_{J2(K)}^i(w_{2,x}^{m+1}, n_{xy1}^m) + A_{J2(K)}^i(w_{2,x}^m, n_{xy1}^{m+1}) - A_{J2(K)}^i(w_{2,x}^m, n_{xy1}^m) \\
& \quad - A_{J3(K)}^i(w_{1,x}^{m+1}, n_{xy1}^m) - A_{J3(K)}^i(w_{1,x}^m, n_{xy1}^{m+1}) + A_{J3(K)}^i(w_{1,x}^m, n_{xy1}^m)] \\
& + \frac{\delta_1}{R} [-A_{2(K)}^i(v_{1,x}^{m+1}, n_{xy2}^m) - A_{2(K)}^i(v_{1,x}^m, n_{xy2}^{m+1}) + A_{2(K)}^i(v_{1,x}^m, n_{xy2}^m) \\
& \quad - A_{3(K)}^i(v_{2,x}^{m+1}, n_{xy1}^m) - A_{3(K)}^i(v_{2,x}^m, n_{xy1}^{m+1}) + A_{3(K)}^i(v_{2,x}^m, n_{xy1}^m)] \\
& + \left(\frac{\eta}{R}\right)^2 [-A_{J22(K)}^i(w_1^{m+1}, n_{yy2}^m) - A_{J22(K)}^i(w_1^m, n_{yy2}^{m+1}) + A_{J22(K)}^i(w_1^m, n_{yy2}^m) \\
& \quad - A_{J23(K)}^i(w_2^{m+1}, n_{yy1}^m) - A_{J23(K)}^i(w_2^m, n_{yy1}^{m+1}) + A_{J23(K)}^i(w_2^m, n_{yy1}^m)] \\
& + \frac{\delta_2 \eta}{R} [-A_{J2(K)}^i(v_2^{m+1}, n_{yy2}^m) - A_{J2(K)}^i(v_2^m, n_{yy2}^{m+1}) + A_{J2(K)}^i(v_2^m, n_{yy2}^m) \\
& \quad + A_{J3(K)}^i(v_1^{m+1}, n_{yy1}^m) + A_{J3(K)}^i(v_1^m, n_{yy1}^{m+1}) - A_{J3(K)}^i(v_1^m, n_{yy1}^m)] \quad (A-190)
\end{aligned}$$

$$\begin{aligned}
\eta_{lin}^3 = \frac{\eta}{R} [& A_{J1(2K)}^i(w_2^m, n_{xy1,x}^{\pi m}) + A_{J1(2K)}^i(w_2^0, n_{xy1,x}^{\pi L}) + A_{J1(2K)}^i(w_2^0, n_{xy1,x}^{\pi \pi}) \\
& - A_{J4(2K)}^i(w_1^m, n_{xy2,x}^{\pi m}) - A_{J4(2K)}^i(w_1^0, n_{xy2,x}^{\pi L}) - A_{J4(2K)}^i(w_1^0, n_{xy2,x}^{\pi \pi}) \\
& - 2A_{J4(2K)}^i(w_{1,x}^m, n_{xy2}^{\pi m}) - 2A_{J4(2K)}^i(w_{1,x}^0, n_{xy2}^{\pi L}) - 2A_{J4(2K)}^i(w_{1,x}^0, n_{xy2}^{\pi \pi}) \\
& + A_{J1(K)}^i(w_2^{m+1}, n_{xy1,x}^{\pi m}) + A_{J1(K)}^i(w_2^m, n_{xy1,x}^{\pi L}) - A_{J1(K)}^i(w_2^m, n_{xy1,x}^{\pi m}) \\
& - A_{J4(K)}^i(w_1^{m+1}, n_{xy2,x}^{\pi m}) - A_{J4(K)}^i(w_1^m, n_{xy2,x}^{\pi L}) + A_{J4(K)}^i(w_1^m, n_{xy2,x}^{\pi m})
\end{aligned}$$

$$\begin{aligned}
& + 2 A_{J1(2K)}^i (W_{2,x}^{m+1}, n_{xy1}^{Lm}) + 2 A_{J1(2K)}^i (W_{2,x}^m, n_{xy1}^{Lm+1}) - 2 A_{J1(2K)}^i (W_{2,x}^m, n_{xy1}^{Lm}) \\
& - 2 A_{J4(2K)}^i (W_{1,x}^{m+1}, n_{xy2}^{Lm}) - 2 A_{J4(2K)}^i (W_{1,x}^m, n_{xy2}^{Lm+1}) + 2 A_{J4(2K)}^i (W_{1,x}^m, n_{xy2}^{Lm}) \} \\
& + \left(\frac{n}{R}\right)^2 \{ A_{IJ1(2K)}^i (W_2^m, n_{yy2}^{nm}) + A_{IJ1(2K)}^i (W_2^0, n_{yy2}^{nL}) + A_{IJ1(2K)}^i (W_2^0, n_{yy2}^{nn}) \\
& + A_{IJ4(2K)}^i (W_1^m, n_{yy1}^{nm}) + A_{IJ4(2K)}^i (W_1^0, n_{yy1}^{nL}) + A_{IJ4(2K)}^i (W_1^0, n_{yy1}^{nn}) \\
& - A_{J21(2K)}^i (W_1^m, n_{yy1}^{nm}) - A_{J21(2K)}^i (W_1^0, n_{yy1}^{nL}) - A_{J21(2K)}^i (W_1^0, n_{yy1}^{nn}) \\
& - A_{J24(2K)}^i (W_2^m, n_{yy2}^{nm}) - A_{J24(2K)}^i (W_2^0, n_{yy2}^{nL}) - A_{J24(2K)}^i (W_2^0, n_{yy2}^{nn}) \\
& + A_{IJ1(2K)}^i (W_2^{m+1}, n_{yy2}^{Lm}) + A_{IJ1(2K)}^i (W_2^m, n_{yy2}^{Lm+1}) - A_{IJ1(2K)}^i (W_2^m, n_{yy2}^{Lm}) \\
& + A_{IJ4(2K)}^i (W_1^{m+1}, n_{yy1}^{Lm}) + A_{IJ4(2K)}^i (W_1^m, n_{yy1}^{Lm+1}) - A_{IJ4(2K)}^i (W_1^m, n_{yy1}^{Lm}) \\
& - A_{J21(2K)}^i (W_1^{m+1}, n_{yy1}^{Lm}) - A_{J21(2K)}^i (W_1^m, n_{yy1}^{Lm+1}) + A_{J21(2K)}^i (W_1^m, n_{yy1}^{Lm}) \\
& + A_{J24(2K)}^i (W_2^{m+1}, n_{yy2}^{Lm}) - A_{J24(2K)}^i (W_2^m, n_{yy2}^{Lm+1}) + A_{J24(2K)}^i (W_2^m, n_{yy2}^{Lm}) \} \\
& + \frac{\delta_1 n}{R} \{ -A_{1(2K)}^i (v_1^m, n_{xy1,x}^{nm}) - A_{4(2K)}^i (v_2^m, n_{xy2,x}^{nm}) - A_{1(2K)}^i (v_{1,x}^m, n_{xy1}^n) \\
& - A_{4(2K)}^i (v_{2,x}^m, n_{xy2}^{nm}) - A_{1(2K)}^i (v_1^{m+1}, n_{xy1,x}^{Lm}) - A_{1(2K)}^i (v_1^m, n_{xy1,x}^{Lm+1}) \\
& + A_{1(2K)}^i (v_1^m, n_{xy1,x}^{Lm}) - A_{4(2K)}^i (v_{2,x}^{m+1}, n_{xy2}^{Lm}) - A_{4(2K)}^i (v_2^m, n_{xy2}^{Lm}) \\
& + A_{4(2K)}^i (v_2^m, n_{xy2}^{Lm}) - A_{1(2K)}^i (v_{1,x}^{m+1}, n_{xy1}^{Lm}) - A_{1(2K)}^i (v_{1,x}^m, n_{xy1}^{Lm+1}) \\
& + A_{1(2K)}^i (v_{1,x}^m, n_{xy1}^{Lm}) - A_{4(2K)}^i (v_{2,x}^{m+1}, n_{xy2}^{Lm}) - A_{4(2K)}^i (v_{2,x}^m, n_{xy2}^{Lm+1}) \\
& + A_{4(2K)}^i (v_{2,x}^m, n_{xy2}^{Lm}) \} \\
& + \frac{\delta_1 n}{R^2} \{ -A_{I1(2K)}^i (v_1^m, n_{yy2}^{nm}) + A_{I4(2K)}^i (v_2^m, n_{yy1}^{nm}) - A_{J1(2K)}^i (v_2^m, n_{yy1}^{nm}) \\
& + A_{J4(2K)}^i (v_1^m, n_{yy2}^{nm}) - A_{I1(2K)}^i (v_1^{m+1}, n_{yy2}^{Lm}) - A_{I1(2K)}^i (v_1^m, n_{yy2}^{Lm+1})
\end{aligned}$$

$$\begin{aligned}
& + A_{I1(2K)}^i (U_1^m, n_{yy2}^{Lm}) + A_{I4(2K)}^i (U_2^{m+1}, n_{yy1}^{Lm}) + A_{I4(2K)}^i (U_2^m, n_{yy1}^{Lm+1}) \\
& + A_{I4(2K)}^i (U_2^m, n_{yy1}^{Lm}) - A_{J1(2K)}^i (U_2^{m+1}, n_{yy1}^{Lm}) - A_{J1(2K)}^i (U_2^m, n_{yy1}^{Lm+1}) \\
& + A_{J1(2K)}^i (U_2^m, n_{yy1}^{Lm}) + A_{J4(2K)}^i (U_1^{m+1}, n_{yy2}^{Lm}) + A_{J4(2K)}^i (U_1^m, n_{yy2}^{Lm+1}) \\
& + A_{J4(2K)}^i (U_1^m, n_{yy2}^{Lm})] \\
& + A_{I1(2K)}^i (W_{1,xx}^m, n_{xx1}^{nm}) + A_{I1(2K)}^i (W_{1,xx}^0, n_{xx1}^{nL}) + A_{I1(2K)}^i (W_{1,xx}^0, n_{xx1}^{nn}) \\
& + A_{I4(2K)}^i (W_{2,xx}^m, n_{xx2}^{nm}) + A_{I4(2K)}^i (W_{2,xx}^0, n_{xx2}^{nL}) + A_{I4(2K)}^i (W_{2,xx}^0, n_{xx2}^{nn}) \\
& + A_{I1(2K)}^i (W_{1,xx}^{m+1}, n_{xx1}^{Lm}) + A_{I1(2K)}^i (W_{1,xx}^m, n_{xx1}^{Lm+1}) - A_{I1(2K)}^i (W_{1,xx}^m, n_{xx1}^{Lm}) \\
& + A_{I4(2K)}^i (W_{2,xx}^{m+1}, n_{xx2}^{Lm}) + A_{I4(2K)}^i (W_{2,xx}^m, n_{xx2}^{Lm+1}) - A_{I4(2K)}^i (W_{2,xx}^m, n_{xx2}^{Lm}) \quad (A-191)
\end{aligned}$$

$$\begin{aligned}
\eta_{2in}^3 = \frac{\eta}{R} [& A_{J2(2K)}^i (W_2^m, n_{xy2,x}^{nm}) + A_{J2(2K)}^i (W_2^0, n_{xy2,x}^{nL}) + A_{J2(2K)}^i (W_2^0, n_{xy2,x}^{nn}) \\
& - A_{J3(2K)}^i (W_1^m, n_{xy1,x}^{nm}) - A_{J3(2K)}^i (W_1^0, n_{xy1,x}^{nL}) - A_{J3(2K)}^i (W_1^0, n_{xy1,x}^{nn}) \\
& + 2 A_{J2(2K)}^i (W_{2,x}^m, n_{xy2}^{nm}) + 2 A_{J2(2K)}^i (W_{2,x}^0, n_{xy2}^{nL}) + 2 A_{J2(2K)}^i (W_{2,x}^0, n_{xy2}^{nn}) \\
& - 2 A_{J3(2K)}^i (W_{1,x}^m, n_{xy1}^{nm}) - 2 A_{J3(2K)}^i (W_{1,x}^0, n_{xy1}^{nL}) - 2 A_{J3(2K)}^i (W_{1,x}^0, n_{xy1}^{nn}) \\
& + A_{J2(2K)}^i (W_2^{m+1}, n_{xy2,x}^{Lm}) + A_{J2(2K)}^i (W_2^m, n_{xy2,x}^{Lm+1}) - A_{J2(2K)}^i (W_2^m, n_{xy2,x}^{Lm}) \\
& - A_{J3(2K)}^i (W_1^{m+1}, n_{xy1,x}^{Lm}) - A_{J3(2K)}^i (W_1^m, n_{xy1,x}^{Lm+1}) + A_{J3(2K)}^i (W_1^m, n_{xy1,x}^{Lm}) \\
& + 2 A_{J2(2K)}^i (W_{2,x}^{m+1}, n_{xy2}^{Lm}) + 2 A_{J2(2K)}^i (W_{2,x}^m, n_{xy2}^{Lm+1}) - 2 A_{J2(2K)}^i (W_{2,x}^m, n_{xy2}^{Lm}) \\
& - 2 A_{J3(2K)}^i (W_{1,x}^{m+1}, n_{xy1}^{Lm}) - 2 A_{J3(2K)}^i (W_{1,x}^m, n_{xy1}^{Lm+1}) + 2 A_{J3(2K)}^i (W_{1,x}^m, n_{xy1}^{Lm})] \\
& + \left(\frac{\eta}{R}\right)^2 [- A_{IJ2(2K)}^i (W_2^m, n_{yy1}^{nm}) - A_{IJ2(2K)}^i (W_2^0, n_{yy1}^{nL}) - A_{IJ2(2K)}^i (W_2^0, n_{yy1}^{nn}) \\
& - A_{IJ3(2K)}^i (W_1^m, n_{yy2}^{nm}) - A_{IJ3(2K)}^i (W_1^0, n_{yy2}^{nL}) - A_{IJ3(2K)}^i (W_1^0, n_{yy2}^{nn})
\end{aligned}$$

$$\begin{aligned}
& -A_{J22(2K)}^i(W_1^m, n_{yy2}^{nm}) - A_{J22(2K)}^i(W_1^0, n_{yy2}^{nL}) - A_{J22(2K)}^i(W_1^0, n_{yy2}^{nn}) \\
& - A_{J23(2K)}^i(W_2^m, n_{yy1}^{nm}) - A_{J23(2K)}^i(W_2^0, n_{yy1}^{nL}) - A_{J23(2K)}^i(W_2^0, n_{yy1}^{nn}) \\
& - A_{IJ2(2K)}^i(W_2^{m+1}, n_{yy1}^{Lm}) - A_{IJ2(2K)}^i(W_2^m, n_{yy1}^{Lm+1}) - A_{IJ2(2K)}^i(W_2^m, n_{yy1}^{Lm}) \\
& - A_{IJ3(2K)}^i(W_1^{m+1}, n_{yy2}^{Lm}) - A_{IJ3(2K)}^i(W_1^m, n_{yy2}^{Lm+1}) + A_{IJ3(2K)}^i(W_1^m, n_{yy2}^{Lm}) \\
& - A_{J22(2K)}^i(W_1^{m+1}, n_{yy2}^{Lm}) - A_{J22(2K)}^i(W_1^m, n_{yy2}^{Lm+1}) + A_{J22(2K)}^i(W_1^m, n_{yy2}^{Lm}) \\
& - A_{J23(2K)}^i(W_2^{m+1}, n_{yy1}^{Lm}) - A_{J23(2K)}^i(W_2^m, n_{yy1}^{Lm+1}) + A_{J23(2K)}^i(W_2^m, n_{yy1}^{Lm})] \\
& + \frac{\delta_1}{R} [-A_{2(2K)}^i(U_1^m, n_{xy2,x}^{nm}) - A_{2(2K)}^i(U_1^{m+1}, n_{xy2,x}^{Lm}) - A_{2(2K)}^i(U_1^m, n_{xy2,x}^{Lm+1}) \\
& + A_{2(2K)}^i(U_1^m, n_{xy2,x}^{Lm}) - A_{3(2K)}^i(U_2^m, n_{xy1,x}^{nm}) - A_{3(2K)}^i(U_2^{m+1}, n_{xy1,x}^{Lm}) \\
& - A_{3(2K)}^i(U_2^m, n_{xy1,x}^{Lm+1}) + A_{3(2K)}^i(U_2^m, n_{xy1,x}^{Lm}) \\
& - A_{2(2K)}^i(U_{1,x}^m, n_{xy2}^{nm}) - A_{2(2K)}^i(U_{1,x}^{m+1}, n_{xy2}^{Lm}) - A_{2(2K)}^i(U_{1,x}^m, n_{xy2}^{Lm+1}) \\
& + A_{2(2K)}^i(U_{1,x}^m, n_{xy2}^{nm}) - A_{3(2K)}^i(U_{2,x}^m, n_{xy1}^{nm}) - A_{3(2K)}^i(U_{2,x}^{m+1}, n_{xy1}^{Lm}) \\
& - A_{3(2K)}^i(U_{2,x}^m, n_{xy1}^{Lm+1}) + A_{3(2K)}^i(U_{2,x}^m, n_{xy1}^{Lm})] \\
& + \frac{\delta_1 n}{R} [A_{I2(2K)}^i(U_1^m, n_{yy1}^{nm}) + A_{I2(2K)}^i(U_1^{m+1}, n_{yy1}^{Lm}) + A_{I2(2K)}^i(U_1^m, n_{yy1}^{Lm+1}) \\
& - A_{I2(2K)}^i(U_1^m, n_{yy1}^{Lm}) - A_{I3(2K)}^i(U_2^m, n_{yy2}^{nm}) - A_{I3(2K)}^i(U_2^{m+1}, n_{yy2}^{Lm}) \\
& - A_{I3(2K)}^i(U_2^m, n_{yy2}^{Lm+1}) + A_{I3(2K)}^i(U_2^m, n_{yy2}^{Lm})] \\
& + A_{2(2K)}^i(W_{1,xx}^m, n_{xx2}^{nm}) + A_{2(2K)}^i(W_{1,xx}^0, n_{xx2}^{nL}) + A_{2(2K)}^i(W_{1,xx}^0, n_{xx2}^{nn}) \\
& + A_{3(2K)}^i(W_{2,xx}^m, n_{xx1}^{nm}) + A_{3(2K)}^i(W_{2,xx}^0, n_{xx1}^{nL}) + A_{3(2K)}^i(W_{2,xx}^0, n_{xx1}^{nn}) \\
& + A_{2(2K)}^i(W_{1,xx}^{m+1}, n_{xx2}^{Lm}) + A_{2(2K)}^i(W_{1,xx}^m, n_{xx2}^{Lm+1}) - A_{2(2K)}^i(W_{1,xx}^m, n_{xx2}^{Lm}) \\
& + A_{3(2K)}^i(W_{2,xx}^{m+1}, n_{xx1}^{Lm}) + A_{3(2K)}^i(W_{2,xx}^m, n_{xx1}^{Lm+1}) - A_{3(2K)}^i(W_{2,xx}^m, n_{xx1}^{Lm}) \quad (A-192)
\end{aligned}$$

After linearization the equilibrium equations, Eqs A-160, can be written in matrix form

$$\begin{aligned}
 & [C_{12}]\{n_{1,xx}\} + [C_{11}]\{n_{1,x}\} + [C_{10}]\{n_1\} + [E_{12}]\{n_{1,xx}^L\} + [E_{11}]\{n_{1,x}^L\} \\
 & + [E_{10}]\{n_{1,x}^L\} + [B_{12}]\{n_{1,xx}^{nL}\} + [B_{11}]\{n_{1,x}^{nL}\} + [B_{10}]\{n_1^{nL}\} + [C_{22}]\{n_{2,xx}\} \\
 & + [C_{21}]\{n_{2,x}\} + [C_{20}]\{n_2\} + [E_{22}]\{n_{2,xx}^L\} + [E_{21}]\{n_{2,x}^L\} + [E_{20}]\{n_2^L\} \\
 & + [B_{22}]\{n_{2,xx}^{nL}\} + [B_{21}]\{n_{2,x}^{nL}\} + [B_{20}]\{n_2^{nL}\} + [A_{12}]\{X_{,xx}\} + [A_{11}]\{X_{,x}\} \\
 & + [A_{10}]\{X\} = \{g\}
 \end{aligned} \tag{A-193}$$

where

$$\{n_1\}^T = \{n_{xx1i}, n_{yy1i}, n_{xy1i}, m_{xx1i}, m_{yy1i}, m_{xy1i}\}^{m+1}$$

$$\{n_2\}^T = \{n_{xx2i}, n_{yy2i}, n_{xy2i}, m_{xx2i}, m_{yy2i}, m_{xy2i}\}^{m+1}$$

$$\{X\}^T = \{u_{1i}, v_{1i}, w_{1i}, u_{2i}, v_{2i}, w_{2i}\}^{m+1}$$

$$\{n_1^L\}^T = \{n_{xx1i}^L, n_{yy1i}^L, n_{xy1i}^L, m_{xx1i}^L, m_{yy1i}^L, m_{xy1i}^L\}^{m+1}$$

$$\{n_2^L\}^T = \{n_{xx2i}^L, n_{yy2i}^L, n_{xy2i}^L, m_{xx2i}^L, m_{yy2i}^L, m_{xy2i}^L\}^{m+1}$$

$$\{n_1^{nL}\}^T = \{n_{xx1i}^{nL}, n_{yy1i}^{nL}, n_{xy1i}^{nL}, m_{xx1i}^{nL}, m_{yy1i}^{nL}, m_{xy1i}^{nL}\}^{m+1}$$

$$\{n_2^{nL}\}^T = \{n_{xx2i}^{nL}, n_{yy2i}^{nL}, n_{xy2i}^{nL}, m_{xx2i}^{nL}, m_{yy2i}^{nL}, m_{xy2i}^{nL}\}^{m+1}$$

In Eqs A-145 A-150 $\{e\}$, $\{t^1\}$ and $\{t^n\}$ can be written as:

$$\{e_{1i}\} = [k1_1]\{X_{,x}\} + [k1_0]\{X\}$$

$$\{e_{2i}\} = [k2_1]\{X_{,x}\} + [k2_0]\{X\}$$

$$\{t_i^L\} = [k1_i^L]\{X_{,x}\} + [k1_0^L]\{X\}$$

$$\begin{aligned}
\{t_2^L\} &= [K2_1^L]\{X_{,x}\} + [K2_0^L]\{X\} \\
\{t_1^n\} &= [K1_1^n]\{X_{,x}\} + [K2_0^n]\{X\} \\
\{t_{1,x}^n\} &= [K1_{2x}^n]\{X_{,xx}\} + [K1_{1x}^n]\{X_{,x}\} + [K1_{0x}^n]\{X\} \\
\{t_{2,x}^n\} &= [K2_{3x}^n]\{X_{,xxx}\} + [K2_{2x}^n]\{X_{,xx}\} + [K2_{1x}^n]\{X_{,x}\} + [K2_{0x}^n]\{X\} \\
\{t_{1,xx}^n\} &= [K1_{3xx}^n]\{X_{,xxx}\} + [K1_{2xx}^n]\{X_{,xx}\} + [K1_{1xx}^n]\{X_{,x}\} + [K1_{0xx}^n]\{X\} \\
\{t_{2,xx}^n\} &= [K2_{3xx}^n]\{X_{,xxx}\} + [K2_{2xx}^n]\{X_{,xx}\} + [K2_{1xx}^n]\{X_{,x}\} + [K1_{0xx}^n]\{X\} \quad (A-194)
\end{aligned}$$

Substitute of Eqs A-145-A-150, and A-194 into Eq A-193 yields a matrix equation which only contain the vector of unknown, $\{x\}$

$$[R4]\{X_{,xxx}\} + [R3]\{X_{,xx}\} + [R2]\{X_{,x}\} + [R1]\{X_{,x}\} + [R0]\{X\} = \{g\} \quad (A-195)$$

As in the case of W-F formulation transformation equation are introduced in order to reduce the order of the linear equations.

$$\{\eta\} = \{X_{,xx}\}$$

By this transformation, Eq A-195 can be written in the following form:

$$[R]\begin{Bmatrix} X_{,xx} \\ \eta_{,xx} \end{Bmatrix} + [S]\begin{Bmatrix} X_{,xx} \\ \eta_{,x} \end{Bmatrix} + [T]\begin{Bmatrix} X \\ \eta \end{Bmatrix} = \{G\} \quad (A-196)$$

A.3.5 Boundary Condition

Boundary condition A-117 can be presented in the following form

Either

$$N_{xx} = \bar{N}_{xx}$$

$$N_{xy}^* = \bar{N}_{xy}^*$$

$$Q^* = \bar{Q} + \bar{M}_{xy,y}$$

$$M_{xx} = \bar{M}_{xx}$$

Or

$$u = \text{Const.}$$

$$v = \text{Const.}$$

$$w = 0$$

$$w_{,x} = 0$$

$$(A-117a)$$

where

$$N_{xy}^* = N_{xy} + \delta \frac{M_{xy}}{R}$$

$$Q^* = N_{xx}(W_{,x} + W_{,x}^0) + N_{xy}(W_{,y} + W_{,y}^0) - \frac{N_{xy}}{R} U \delta_1 + M_{xx,x} + 2M_{xy,y} \quad (A-197)$$

Obviously, the boundary condition can be written in matrix form (at $x = 0, L$)

$$[\Omega I] \begin{Bmatrix} N_{xy} \\ N_{xy}^* \\ Q^* \\ M_{xx} \end{Bmatrix} + [\lambda I] \begin{Bmatrix} U \\ V \\ W \\ W_{,x} \end{Bmatrix} = \{Bg\} \quad (A-198)$$

where the form of $[\Omega I]$ and $[\lambda I]$ depends on the type of boundary conditions.

The stress and moment results, and the displacements are represented in series form.

$$[\Omega I] \begin{Bmatrix} \sum_{i=0}^{2K} [\bar{n}_{xx}^1 \cos \frac{iny}{R} + \bar{n}_{xx}^2 \sin \frac{iny}{R}] \\ \sum_{i=0}^{2K} [\bar{n}_{xy}^{*1} \cos \frac{iny}{R} + \bar{n}_{xy}^{*2} \sin \frac{iny}{R}] \\ \sum_{i=0}^{2K} [Q^{*1} \cos \frac{iny}{R} + Q^{*2} \sin \frac{iny}{R}] \\ \sum_{i=0}^{2K} [\bar{m}_{xx}^1 \cos \frac{iny}{R} + \bar{m}_{xx}^2 \sin \frac{iny}{R}] \end{Bmatrix} + [\lambda I] \begin{Bmatrix} \sum_{i=0}^K [U_{1i} \cos \frac{iny}{R} + U_{2i} \sin \frac{iny}{R}] \\ \sum_{i=0}^K [V_{1i} \cos \frac{iny}{R} + V_{2i} \sin \frac{iny}{R}] \\ \sum_{i=0}^K [W_{1i} \cos \frac{iny}{R} + W_{2i} \sin \frac{iny}{R}] \\ \sum_{i=0}^K [W_{1i,x} \cos \frac{iny}{R} + W_{2i,x} \sin \frac{iny}{R}] \end{Bmatrix} = \{Bg\} \quad (A-199)$$

After applying the Galerkin Procedure, the boundary conditions can be written as:

$$[\Omega] \begin{Bmatrix} \bar{n}_{xxi}^1 \\ \bar{n}_{xyi}^{*1} \\ \bar{Q}_i^{*1} \\ \bar{m}_{xxi}^1 \\ \bar{n}_{xxi}^2 \\ \bar{n}_{xyi}^{*2} \\ \bar{Q}_i^{*2} \\ \bar{m}_{xxi}^1 \end{Bmatrix} + [\lambda] \begin{Bmatrix} u_i \\ v_i \\ w_i \\ w_{i,x} \\ u_{2i} \\ v_{2i} \\ w_{2i} \\ w_{2i,x} \end{Bmatrix} = \{e\} \quad i = 0, \dots, k \quad (A-200)$$

where

$$\begin{aligned} \bar{n}_{xxi}^1 &= n_{xx1i} + n_{xx1i}^L + n_{xx1i}^n \\ \bar{n}_{xxi}^2 &= n_{xx2i} + n_{xx2i}^L + n_{xx2i}^n \\ \bar{n}_{xyi}^{*1} &= n_{xy1i} + n_{xy1i}^L + n_{xy1i}^n + \frac{\delta_1}{R} (m_{xy1i} + m_{xy1i}^L + m_{xy1i}^n) \\ \bar{n}_{xyi}^{*2} &= n_{xy2i} + n_{xy2i}^L + n_{xy2i}^n + \frac{\delta_1}{R} (m_{xy2i} + m_{xy2i}^L + m_{xy2i}^n) \\ \bar{Q}_i^{*1} &= \bar{m}_{xx1,x}^1 + 2 \frac{i n}{R} \bar{m}_{xy}^2 + A_{1(2K)}^i (w_{1,x} + w_{1,x}^0, \bar{n}_{xx}^1) + A_{4(2K)}^i (w_{2,x} + w_{2,x}^0, \bar{n}_{xx}^2) \\ &\quad + \frac{n}{R} [A_{J1(2K)}^i (w_2 + w_2^0, \bar{n}_{xy}^1) - A_{J4(2K)}^i (w_1 + w_1^0, \bar{n}_{xy}^2)] \\ &\quad - \frac{\delta_1}{R} [A_{1(2K)}^i (v_1, \bar{n}_{xy}^1) + A_{4(2K)}^i (v_2, \bar{n}_{xy}^2)] \\ \bar{Q}_i^{*2} &= \bar{m}_{xx2,x}^2 - 2 \frac{i n}{R} \bar{m}_{xy}^1 + A_{2(2K)}^i (w_{1,x} + w_{1,x}^0, \bar{n}_{xx}^2) + A_{3(2K)}^i (w_{2,x} + w_{2,x}^0, \bar{n}_{xx}^1) \\ &\quad + \frac{n}{R} [A_{J2(2K)}^i (w_2 + w_2^0, \bar{n}_{xy}^2) - A_{J3(2K)}^i (w_1 + w_1^0, \bar{n}_{xy}^1)] \\ &\quad - \frac{\delta_1}{R} [A_{2(2K)}^i (v_1, \bar{n}_{xy}^2) + A_{3(2K)}^i (v_2, \bar{n}_{xy}^1)] \\ \bar{m}_{xxi}^1 &= m_{xx1i} + m_{xx1i}^L + m_{xx1i}^n \\ \bar{m}_{xxi}^2 &= m_{xx2i} + m_{xx2i}^L + m_{xx2i}^n \end{aligned} \quad (A-201)$$

Using the similar procedure as used in section II, Eqs A-200 can be linearized and written in matrix form:

$$[\Omega]\{N^B\} + [\lambda]\{X^B\} = [\Omega] (\{N_B\} + \{N_B^L\} + \{N_B^{NL}\} + \{N_B^{NN}\}) + [\lambda]\{X^B\} \\ = \{e\}$$

$$\text{or } [\Omega] (\{N_B\} + \{N_B^L\} + \{N_B^{NL}\}) + [\lambda]\{X^B\} = \{e\} - [\Omega]\{N_B^{NN}\} \quad (A-202)$$

where

$$\{N_B\} = \begin{Bmatrix} \bar{n}_{xx}^1 \\ \bar{n}_{xy}^1 \\ \bar{Q}_{xy}^{*1} \\ \bar{m}_{xy}^1 \\ \bar{n}_{xx}^2 \\ \bar{n}_{xy}^{*2} \\ \bar{Q}_{xy}^{*2} \\ \bar{m}_{xx}^2 \end{Bmatrix}$$

Substituting of Eqs A-145-A-150, A-194 into Eqs A-202 yields the following form for the boundary conditions

$$[DB] \begin{Bmatrix} \{X\} \\ \{h\} \end{Bmatrix} + [DC] \begin{Bmatrix} \{X\} \\ \{h\} \end{Bmatrix} = \begin{Bmatrix} \{e\} - [\Omega]\{N_B^{NN}\} \\ 0 \end{Bmatrix} \\ = \{BG\} \quad (A-203)$$

A.3.6 Solution Methodology - Finite Difference Equations

The linearized iteration equations (equilibrium) assume the form

$$[R] \begin{Bmatrix} \{X_{,xx}\} \\ \{h_{,xx}\} \end{Bmatrix} + [S] \begin{Bmatrix} \{X_{,x}\} \\ \{h_{,x}\} \end{Bmatrix} + [T] \begin{Bmatrix} \{X\} \\ \{h\} \end{Bmatrix} = \{G\} \quad (A-196)$$

Note that the true number of unknown is $(6k + 3)$. These are u_{1i}, v_{1i}, w_{1i} ($i = 1, 2, \dots, k$) and u_{2i}, v_{2i}, w_{2i} ($i = 1, 2, \dots, k$) [see Eqs (119)]. For convenience though the number of unknown is treated as $(6k + 6)$ with u_{20}, v_{20} & w_{20} existing for the count, but subject to the constraint $u_{20} = v_{20} = w_{20} = 0$. Thus with the transformation, $\{\eta\} = \{X_{,xx}\}$, the number of unknowns is $(12k + 12)$.

The equilibrium equation, Eqs A-196, are next cast into finite difference form, by employing the usual central difference formula. Thus at each node point j , the equations become (in matrix form)

$$\begin{aligned} & \left(\frac{1}{h^2} [R]^{(j)} + \frac{1}{2h} [S]^{(j)} \right) \begin{Bmatrix} \{X\} \\ \{h\} \end{Bmatrix}^{(j+1)} + \left(-\frac{1}{2h^2} [R]^{(j)} + [T]^{(j)} \right) \begin{Bmatrix} \{X\} \\ \{h\} \end{Bmatrix}^{(j)} \\ & + \left(\frac{1}{h^2} [R]^{(j)} - \frac{1}{2h} [S]^{(j)} \right) \begin{Bmatrix} \{X\} \\ \{h\} \end{Bmatrix}^{(j-1)} = \{G\}^{(j)} \end{aligned} \quad (A-204)$$

At each end one fictitious point is used. This requires $(12k + 12)$ additional equations at each end ($j = 1$ and N ; the fictitious points are denoted by $j = 0$ and $j = N + 1$). These additional equations come from the boundary conditions.

Paradoxically, the number of boundary equations is $(8k + 8)$ at each end. Note that these are either natural $(8k + 8)$ through the Galerkin (procedure) or kinematic $(8k + 8, u_{1i} = u_{2i} = 0, v_{1i} = v_{2i} = 0, w_{1i} = w_{2i} = 0 \text{ \& } w_{1i,x} = w_{2i,x} = 0 \text{ for } i = 0, 1, 2, \dots, k)$. This necessitates the requirement of $(4k + 4)$ additional conditions at each boundary.

The additional boundary terms are given below and they only involve $u_{1i,xx}, u_{2i,xx}, v_{1i,xx}, v_{2i,xx}$ at each boundary. Their existence derivatives with respect to x of the displacement components u and v in the equilibrium equations. On the other hand, regardless of whether or not the boundary conditions are natural or kinematic, they do not contain second derivatives of u and v with respect to x .

$$\bar{\eta}_1 u_{1i,xx} \left(\begin{smallmatrix} j=0 \\ \text{or} \\ j=N+1 \end{smallmatrix} \right) + \bar{\eta}_2 u_{1i,xx} \left(\begin{smallmatrix} j=1 \\ \text{or} \\ j=N \end{smallmatrix} \right) + \bar{\eta}_3 u_{1i,xx} \left(\begin{smallmatrix} j=2 \\ \text{or} \\ j=N-1 \end{smallmatrix} \right) = 0$$

$$\bar{\eta}_1 v_{1i,xx} \left(\begin{smallmatrix} j=0 \\ \text{or} \\ j=N+1 \end{smallmatrix} \right) + \bar{\eta}_2 v_{1i,xx} \left(\begin{smallmatrix} j=1 \\ \text{or} \\ j=N \end{smallmatrix} \right) + \bar{\eta}_3 v_{1i,xx} \left(\begin{smallmatrix} j=2 \\ \text{or} \\ j=N-1 \end{smallmatrix} \right) = 0$$

$$\bar{\eta}_1 u_{2i,xx} \left(\begin{smallmatrix} j=0 \\ \text{or} \\ j=N+1 \end{smallmatrix} \right) + \bar{\eta}_2 u_{2i,xx} \left(\begin{smallmatrix} j=1 \\ \text{or} \\ j=N \end{smallmatrix} \right) + \bar{\eta}_3 u_{2i,xx} \left(\begin{smallmatrix} j=2 \\ \text{or} \\ j=N-1 \end{smallmatrix} \right) = 0$$

$$\bar{\eta}_1 v_{2i,xx} \left(\begin{smallmatrix} j=0 \\ \text{or} \\ j=N+1 \end{smallmatrix} \right) + \bar{\eta}_2 v_{2i,xx} \left(\begin{smallmatrix} j=1 \\ \text{or} \\ j=N \end{smallmatrix} \right) + \bar{\eta}_3 v_{2i,xx} \left(\begin{smallmatrix} j=2 \\ \text{or} \\ j=N-1 \end{smallmatrix} \right) = 0 \quad (A-205)$$

Where the constant $\bar{\eta}_1$, $\bar{\eta}_2$ and $\bar{\eta}_3$ are assigned to achieve certain goals (in generating some results $\bar{\eta}_1 = 1$, $\bar{\eta}_2 = -2$ and $\bar{\eta}_3 = 1$ are used, which implies that a derivative at a boundary is obtained in a forward manner).

Note that Eqs A-205 are the additional $(4k + 4)$ boundary terms and that these equations are incorporated in the matrix form shown in Eqs A-203. This means that [DB] and [DC] are square matrices, $[(12k + 12) \text{ by } (12k + 12)]$. These boundary equations, Eqs A-203, are also cast into finite difference form.

$$\frac{1}{2h} [DB]^j \begin{Bmatrix} \{X\} \\ \{h\} \end{Bmatrix}^{j+1} + [DC]^j \begin{Bmatrix} \{X\} \\ \{h\} \end{Bmatrix}^j - \frac{1}{2h} [DB]^j \begin{Bmatrix} \{X\} \\ \{h\} \end{Bmatrix}^{j-1} = \{BG\}^j \quad (A-206)$$

where $j = 1$ or N .

A.3.7 Total Potential & End Shortening

The expression for the total potential for a supported (ss-i, cc-i) cylindrical shell is given by

$$\begin{aligned} U_T = & \frac{1}{2} \int_0^{2\pi R} \int_0^L [N_{xx} \epsilon_{xx}^0 + N_{yy} \epsilon_{yy}^0 + N_{xy} \epsilon_{xy}^0 \\ & + M_{xx} \kappa_{xx} + M_{yy} \kappa_{yy} + 2M_{xy} \kappa_{xy}] dx dy \\ & + \int_0^{2\pi R} [-\bar{N}_{xx} u - \bar{N}_{xy} v + \bar{M}_{xx} w_{,x}] \Big|_0^L dy \\ & - \int_0^{2\pi R} \int_0^L g w dx dy \end{aligned} \quad (A-207)$$

or

$$\begin{aligned}
U_T = & \frac{1}{2} \int_0^L \mathcal{N}_{xx0}' \epsilon_{xx0}' + \mathcal{N}_{yy0}' \epsilon_{yy0}' + \mathcal{N}_{xy0}' \gamma_{xy0}' + \mathcal{M}_{xx0}' \kappa_{xx0}' \\
& + \mathcal{M}_{yy0}' \kappa_{yy0}' + 2 \mathcal{M}_{xy0}' \kappa_{xy0}' + \frac{1}{2} \sum_{i=1}^{2K} \left(\mathcal{N}_{xxi}' \epsilon_{xxi}' + \mathcal{N}_{yyi}' \epsilon_{yyi}' \right. \\
& + \mathcal{N}_{xyi}' \gamma_{xyi}' + \mathcal{N}_{xxi}^2 \epsilon_{xxi}^2 + \mathcal{N}_{yyi}^2 \epsilon_{yyi}^2 + \mathcal{N}_{xyi}^2 \gamma_{xyi}^2 \\
& + \mathcal{M}_{xxi}' \kappa_{xxi}' + \mathcal{M}_{yyi}' \kappa_{yyi}' + 2 \mathcal{M}_{xyi}' \kappa_{xyi}' + \mathcal{M}_{xxi}^2 \kappa_{xxi}^2 \\
& \left. + \mathcal{M}_{yyi}^2 \kappa_{yyi}^2 + 2 \mathcal{M}_{xyi}^2 \kappa_{xyi}^2 \right) dx \\
& + 2\pi R \left(-\mathcal{N}_{xx0}^{1\ell} u_0^{1\ell} + \mathcal{N}_{xx0}^{10} u_0^{10} - \mathcal{N}_{xy0}^{1\ell} v_0^{1\ell} + \mathcal{N}_{xy0}^{10} v_0^{10} \right. \\
& \left. + \mathcal{M}_{xx0}^{1\ell} w_0^{1\ell} - \mathcal{M}_{xx0}^{10} w_{0,y}^{10} \right)
\end{aligned} \tag{A-208}$$

where

$$\begin{Bmatrix} \mathcal{N}_{xxi}' \\ \mathcal{N}_{yyi}' \\ \mathcal{N}_{xyi}' \\ \mathcal{M}_{xxi}' \\ \mathcal{M}_{yyi}' \\ \mathcal{M}_{xyi}' \end{Bmatrix} = \{ \mathcal{N}_1 \}_i + \{ \mathcal{N}_1^L \}_i + \{ \mathcal{N}_1^N \}_i$$

$$\begin{Bmatrix} \mathcal{N}_{xxi}^2 \\ \mathcal{N}_{yyi}^2 \\ \mathcal{N}_{xyi}^2 \\ \mathcal{M}_{xxi}^2 \\ \mathcal{M}_{yyi}^2 \\ \mathcal{M}_{xyi}^2 \end{Bmatrix} = \{ \mathcal{N}_2 \}_i + \{ \mathcal{N}_2^L \}_i + \{ \mathcal{N}_2^N \}_i$$

$$\begin{Bmatrix} \epsilon_{xvi}^1 \\ \epsilon_{yvi}^1 \\ \gamma_{xyi}^1 \\ \kappa_{xxi}^1 \\ \kappa_{yyi}^1 \\ 2\kappa_{xyi}^1 \end{Bmatrix} = \{\epsilon_{1i}\} + \{t_{1i}^L\} + \{t_{1i}^N\}$$

$$\begin{Bmatrix} \epsilon_{xvi}^2 \\ \epsilon_{yvi}^2 \\ \gamma_{xyi}^2 \\ \kappa_{xxi}^2 \\ \kappa_{yyi}^2 \\ 2\kappa_{xyi}^2 \end{Bmatrix} = \{\epsilon_{2i}\} + \{t_{2i}^L\} + \{t_{2i}^N\}$$

and $n_{xxi}^{1\ell}$, $n_{xxi}^{1\ell}$, $m_{xxi}^{1\ell}$, $u_i^{1\ell}$, $v_i^{1\ell}$, $w_i^{1\ell}$ are the values at $x = \ell$, n_{xxi}^{10} , n_{xxi}^{10} , m_{xxi}^{10} , u_i^{10} , v_i^{10} , w_i^{10} are the values at $x = 0$

APPENDIX B

COMPUTER PROGRAM

B.1 w, F-Formulation

B.2 u, v, w-Formulation

Flow charts and program listing, for both formulations, will be made available upon request. (Write to Professor G. J. Simitses).

APPENDIX C

MODIFICATION AND GENERALIZATION OF POTTER'S METHOD.

The behavior of several structural configurations is often fully described by a set of linear algebraic equations. In general, when these linear equations are put in matrix form, they can be partitioned as shown in Fig. B-1.

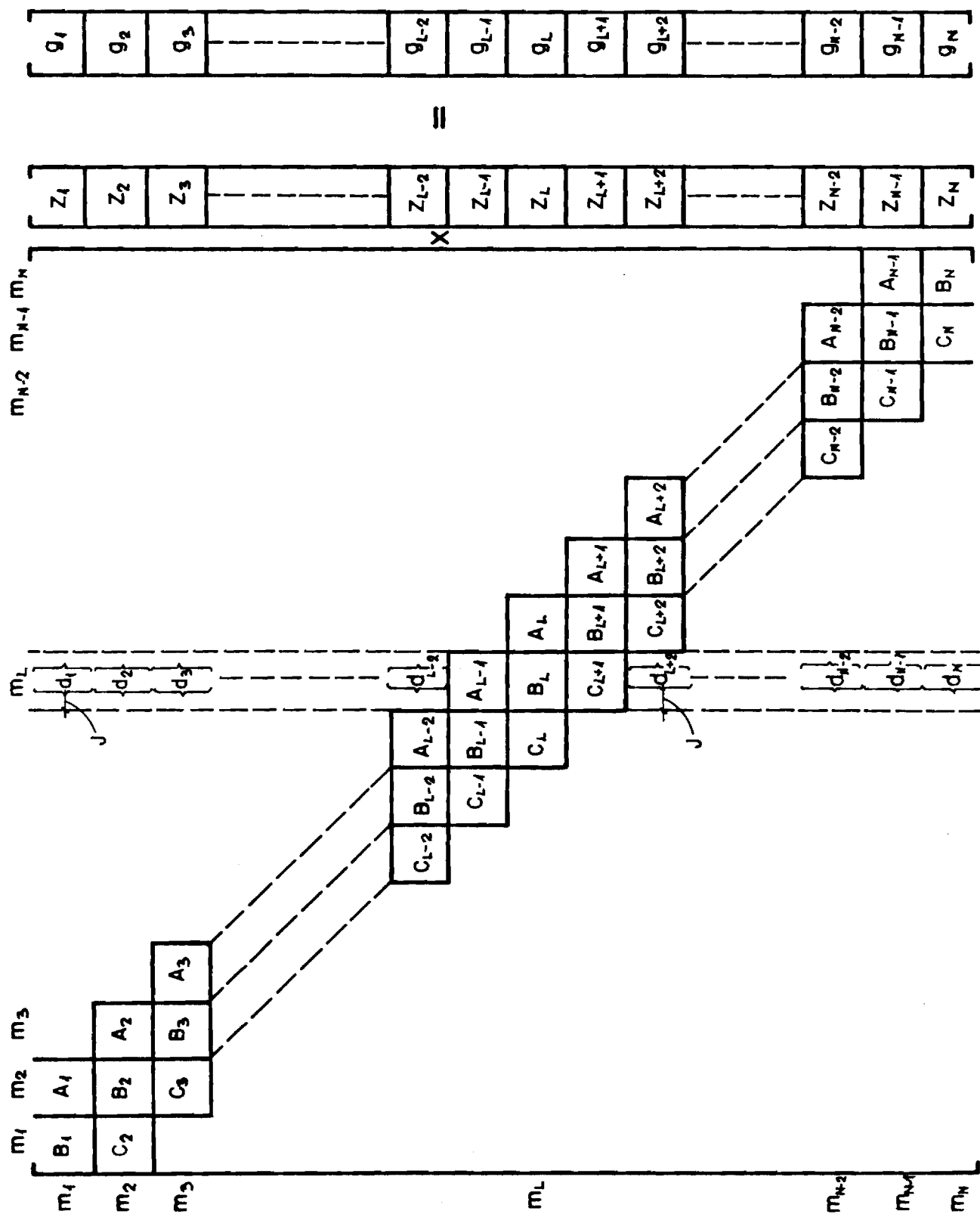
The blank spaces in the coefficient matrix are zeroes and $[C_i]$, $[B_i]$ and $[A_i]$ are matrices of orders m_i by m_{i-1} , m_i by m_i and m_i by m_{i+1} respectively Z_i is the vector of unknowns, each of order m_i by one and there are N such vectors. Let Z_L be the common unknown vector. Moreover, g_i is also a vector of order m_i by one and d_i is a vector of order m_i by one, which includes the coefficients of the common unknown.

Note that the presence of vectors d_i make the whole coefficient matrix nonbanding and irregular. If, on the other hand, the d_i -vectors do not exist then the coefficient matrix is identical to that of Ref C-1. In this case, the matrix is a banded tridiagonal matrix with zeroes everywhere and with, at most, three submatrices banded along the diagonal as shown on Fig. C-1. Therefore, the present case is a bit more general than that of Ref C-1. The solution procedure, though, is basically the same on that of Ref. C-1.

C.1 Description of the Algorithm

The explicit form of the system of linear equations of Fig. C.1 is given by

$$[B_i]\{Z_i\} + [A_i]\{Z_i\} + \{d_i\} Z_L(j) = \{g_i\}$$



$$[C_i]\{z_{i-1}\} + [B_i]\{z_i\} + [A_i]\{z_{i+1}\} + \{d_i\} z_L(j) = \{g_i\}$$

with $i = 2, 3, \dots, N-1$

$$[C_i]\{z_{i-1}\} + [B_i]\{z_i\} + [A_i]\{z_{i+1}\} = \{g_i\}$$

with $i = L-1, L, L+1$

$$[C_N]\{z_{N-1}\} + [B_N]\{z_N\} + \{d_N\} z_L(j) = \{g_N\} \quad (C-1)$$

Note that $z_L(j)$ is one element of the common unknown vector z_L (see Fig C.1).

A short description of the solution procedure is next outlined.

By using Gaussian elimination for the first $(L-2)$ matrix equations, one may find the equivalent set of equations, which is

$$\{z_i\} + [P_i]\{z_{i+1}\} + \{E_i\} z_L(j) = \{X_i\} \quad i = 1, 2, \dots, L-2 \quad (C-2)$$

where

$$[P_i] = [B_i]^{-1}[A_i] \quad ; \quad \{E_i\} = [B_i]^{-1}\{d_i\}$$

$$\{X_i\} = [B_i]^{-1}\{g_i\} \quad (C-3)$$

and

$$[P_i] = [[B_i] - [C_i][P_{i-1}]]^{-1}[A_i]$$

$$\begin{aligned}
\{E_i\} &= \{[B_i] - [C_i][P_{i-1}]\}^{-1} \{ \{d_i\} - [C_i]\{E_{i-1}\} \} \\
\{X_i\} &= \{[B_i] - [C_i][P_{i-1}]\}^{-1} \{ \{g_i\} - [C_i]\{X_{i-1}\} \} \\
&\quad \text{for } i = 2, 3, \dots, L-2
\end{aligned} \tag{C-4}$$

Note that the order of the various matrices is as follows:

$$[C_i] \quad m_i \text{ by } m_{i-1}$$

$$[B_i] \quad m_i \text{ by } m_i$$

$$[A_i] \quad m_i \text{ by } m_{i+1}$$

$$[P_i] \quad m_i \text{ by } m_{i+1}$$

$\{z_i\}$, $\{g_i\}$, $\{d_i\}$, $\{X_i\}$ and $\{E_i\}$ are all m_i by 1

Next, for $i = L-1, L$, and $L+1$ the equivalent equations are:

$$\begin{aligned}
\{Z_{i-1}\} + [P_{i-1}]\{Z_i\} &= \{X_{i-1}\} \\
&\quad \text{for } i = L-1, L, L+1
\end{aligned} \tag{C-5}$$

where, for $i = L-1$

$$\begin{aligned}
[P_i] &= \{[B_i] - [C_i][P_{i-1}]\}^{-1} \{[A_i] - [C_i][\bar{E}_{i-1}]\} \\
\{X_i\} &= \{[B_i] - [C_i][P_{i-1}]\}^{-1} \{ \{g_i\} - [C_i]\{X_{i-1}\} \}
\end{aligned} \tag{C-6}$$

with

$$[\bar{E}_{i-1}] = \begin{bmatrix} \overleftarrow{\quad} \overrightarrow{\quad} \\ 0 \quad \{E_{i-1}\} \quad 0 \end{bmatrix} \quad (C-7)$$

Note that $[\bar{E}_{i-1}]$ is an m_{i-1} by m_{i+1} matrix (defined, as shown, for convenience). and for $i = L, L + 1$

$$[P_i] = ([B_i] - [C_i][P_{i-1}])^{-1} [A_i]$$

$$\{X_i\} = ([B_i] - [C_i][P_{i-1}])^{-1} (\{g_i\} - [C_i]\{X_{i-1}\}) \quad (C-8)$$

Finally, for $i = L + 2, L + 3, \dots, N$, before writing the equivalent equations, $\{d_i\}$ is eliminated from each matrix equation. The elimination is accomplished by multiplying $\{d_i\}$ with the appropriate terms of matrix $[P_L]$. This leads to a matrix with only one nonzero column (vector), as shown below

$$[\{d_i\} \oplus [P_L]] = \begin{bmatrix} 0 & \begin{Bmatrix} d_{i(1)} P_L(L,1) \\ d_{i(2)} P_L(L,2) \\ \vdots \\ d_{i(m_i)} P_L(L,m_i) \end{Bmatrix} & 0 \end{bmatrix} \quad (C-9)$$

$\overleftarrow{\quad} \overrightarrow{\quad}$
 i

Note that the symbol \oplus is introduced to define the operation that leads to the matrix of Eq (C-9).

Similarly, the symbol \odot is introduced to define an operation that leads to a column matrix.

$$\{V_i\} \odot \{V_i\} = \begin{Bmatrix} V_1(1) & V_2(1) \\ V_1(2) & V_2(2) \\ \vdots & \vdots \\ V_1(N_i) & V_2(N_i) \end{Bmatrix} \quad (C-10)$$

With these definitions one may now write the equivalent equations for $i = L+2, L+3, \dots, N-1$. These are

$$\{Z_i\} + [P_i]\{Z_{i+1}\} = \{X_i\} \quad (C-11)$$

where

$$[P_i] = \left[[B_i] - [\bar{C}_i][P_{i-1}] \right]^{-1} [A_i] \quad (C-12)$$

$$\{X_i\} = \left[[B_i] - [\bar{C}_i][P_{i-1}] \right]^{-1} (\{\bar{g}_i\} - [\bar{C}_i]\{X_{i-1}\}) \quad (C-13)$$

with

$$[\bar{C}_i] = [C_i] - (-1)^{i-L-2} \{d_i\} \oplus [P_L][P_{L+1}] \dots [P_{i-2}] \quad (C-14)$$

and

$$\begin{aligned} \{g_i\} = \{g_i\} - \{d_i\} \odot (\{X_i\} - [P_i]\{X_{i+1}\} + [P_L][P_{L+1}]\{X_{L+2}\} \\ - [P_L][P_{L+1}][P_{L+2}]\{X_{L+3}\} + \dots + (-1)^{i-L-2}[P_L] \dots [P_{i-3}]\{X_{i-2}\}) \end{aligned} \quad (C-15)$$

Finally, for $i = N$

$$\{Z_N\} = \{X_N\} \quad (C-16)$$

where $\{X_N\}$ is given by Eq (C-13) with $i=N$. The recurrence formulae for backward substitution, in order to calculate $Z_{N-1}, Z_{N-2}, \dots, Z_2$, and Z_1 are

$$\begin{aligned} \{Z_N\} &= \{X_N\} \\ \{Z_i\} &= \{X_i\} - [P_i]\{Z_{i+1}\} ; i = N-1, N-2, \dots, L-1 \\ \{Z_i\} &= \{X_i\} - [P_i]\{Z_{i+1}\} - [E_i] Z_L(i) ; i = L-2, L-3, \dots, 2, 1 \end{aligned} \quad (C-17)$$

C.2 Determininant Calculation

In each step of the inversion process, one must calculate the corresponding determinant e_i , namely

$$e_1 = \det [B_1]$$

$$e_i = \det [\{B_i\} - \{C_i\}[P_{i-1}]] ; i = 2, 3, \dots, L+2$$

$$e_i = \det [\{B_i\} - \{\bar{C}_i\}[P_{i-1}]] ; i = L+2, L+3, \dots, N \quad (C-18)$$

Thus the determinant, D, of the entire coefficient matrix of the system can easily be computed by

$$D = \prod_{i=1}^N e_i \quad (C-19)$$

Reference

- C.1 Tene y. Epstein M., and Sheinman I. "A generalization of potters method"
Computer & Structures vol. 4 pp. 1099-1103 1974.

Appendix D

INSTABILITY OF LAMINATED CYLINDERS IN TORSION

by

D. Shaw[†] and G. J. Simitse^{††}
School of Engineering Science and Mechanics
Georgia Institute of Technology, Atlanta, Georgia

Introduction

A Galerkin-type solution, for the buckling analysis of a perfect geometry, laminated, circular, cylindrical thin shell subjected to pure torsion, is presented. The torsion is applied through the reference surface, which is the midsurface of the laminate and the boundaries are classical simple supports (SS-3). The analysis is based on Donnell-type nonlinear kinematic relations and linearly elastic material behavior. It is assumed that a primary state exists and that it is axisymmetric. This primary state can be obtained by solving the field equations. Through perturbation of the governing field equation a set of (linearized) buckling equations is obtained, along with the related boundary conditions. A Galerkin procedure is employed for solving the buckling equations. Thus, the problem is reduced to an eigen-boundary-value problem. Critical torsional loads are obtained for several Boron/Epoxy configurations of symmetric, antisymmetric and asymmetric stacking. In addition, approximate buckling modes are established for both positive and negative torsion.

[†]Graduate Research Assistant
^{††}Professor

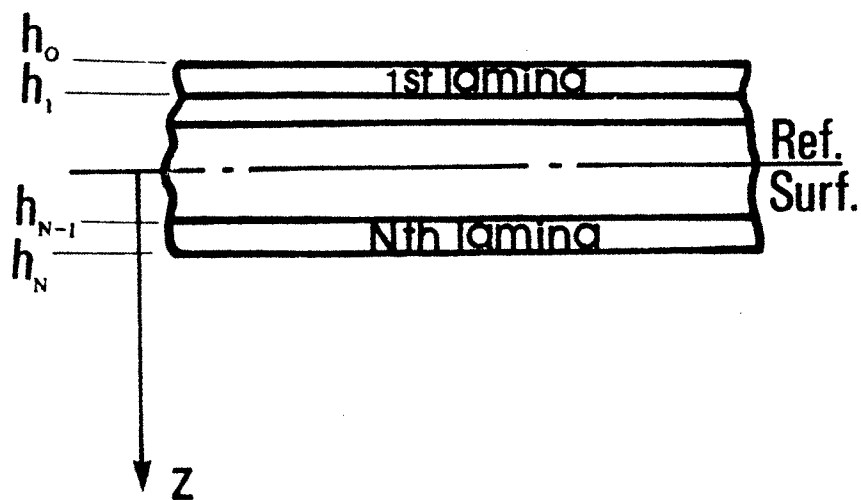
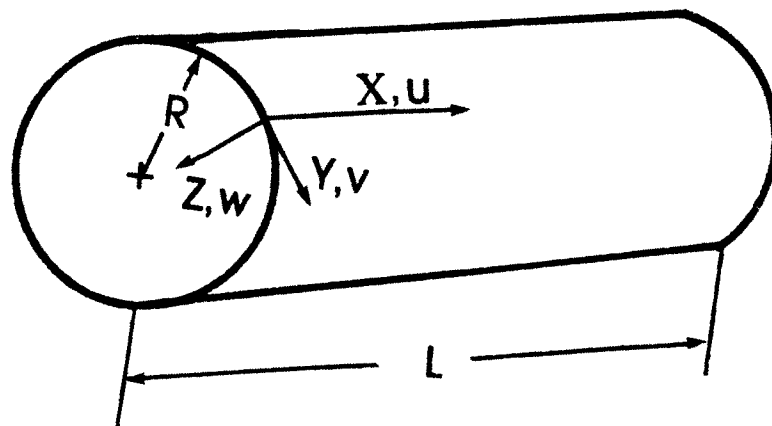


Fig.D.1 Geometry and Sign Convention

Governing Equations and Solution Procedure

The geometry and sign convention are shown on Fig. 1. The torsion is positive if applied clockwise at the right end ($x = L$) and counter-clockwise at the left end ($x = 0$). The governing equations for a general laminated circular cylindrical shell, with or without orthogonal stiffeners, without geometric imperfections, and subjected to a pure torsion, consist of two coupled partial nonlinear differential equations in the transverse displacement component $w(x,y)$ and an Airy stress (resultant) function, $F(x,y)$. One of the equations characterizes transverse equilibrium and the other in-plane compatibility. These equations are taken from [D.1] by setting $\bar{N}_{xx} = q = w^0(x,y) = 0$, where \bar{N}_{xx} denotes the uniform axial compression, q lateral pressure and $w^0(x,y)$ an initial geometric imperfection. The two equations are

Equilibrium:

$$\begin{aligned} & b_{11}F_{,yyxx} + b_{21}F_{,xxxx} - b_{31}F_{,xxxy} + d_{11}w_{,xxxx} + d_{12}w_{,xxzz} + 2d_{13}w_{,xxxy} \\ & + 2b_{13}F_{,xyyy} + 2b_{23}F_{,xxxy} + 2b_{33}F_{,xxxy} + 2d_{31}w_{,xxxy} + 2d_{32}w_{,xyyy} + 4d_{33}w_{,xxxy} \\ & + b_{12}F_{,yyyy} + b_{22}F_{,xxxy} - b_{32}F_{,xyyy} + d_{21}w_{,xxxy} + d_{22}w_{,yyyy} + 2d_{23}w_{,xyyy} \\ & + \frac{1}{R}F_{,xx} + F_{,yy}w_{,xx} + 2\bar{N}_{xy}w_{,xy} - 2F_{,xy}w_{,xy} + F_{,xx}w_{,yy} = 0 \end{aligned} \quad (D-1)$$

Compatibility:

$$\begin{aligned} & a_{11}F_{,yyyy} + a_{12}F_{,xxxy} - a_{13}F_{,xyyy} + b_{11}w_{,xxxy} + b_{12}w_{,yyyy} + 2b_{13}w_{,xyyy} \\ & + a_{12}F_{,xxxy} + a_{22}F_{,xxxx} - a_{23}F_{,xxxy} + b_{21}w_{,xxxx} + b_{22}w_{,xxxy} + 2b_{23}w_{,xxxy} \\ & - a_{13}F_{,xyyy} - a_{23}F_{,xxxy} + a_{33}F_{,xxxy} - b_{31}w_{,xxxy} - b_{32}w_{,xyyy} - 2b_{33}w_{,xxxy} = \\ & - \frac{w_{,xx}}{R} + w_{,xy}w_{,xy} - w_{,xx}w_{,yy} \end{aligned} \quad (D-2)$$

where

$$\begin{aligned} [a_{ij}] &= [A_{ij}]^{-1} ; \quad [b_{ij}] = [A_{ij}]^{-1} [B_{ij}] \\ [d_{ij}] &= [B_{ij}] [b_{ij}] - [D_{ij}] \end{aligned} \quad (D-3)$$

and $[A_{ij}]$, $[B_{ij}]$ and $[D_{ij}]$ are the extensional, coupling and flexural stiffnesses appearing in the usual lamination theory.

The expressions for the simply supported boundary conditions (SS - 3) are given below in terms of w and F (at $x = 0, L$).

$$\begin{aligned} w &= 0 ; \quad F_{,yy} = 0 ; \\ b_{21}F_{,xx} + d_{11}w_{,xx} + 2d_{13}w_{,xy} - b_{31}F_{,xy} &= -b_{31}\bar{N}_{xy} ; \\ a_{22}F_{,xx} - a_{23}F_{,xy} + b_{21}w_{,xx} + 2b_{23}w_{,xy} &= -a_{23}\bar{N}_{xy} . \end{aligned} \quad (D-4)$$

where \bar{N}_{xy} is the applied torsional stress resultant. For more details see [C.1].

It is assumed that, under the action of pure torsion, a primary state exists, which is axisymmetric (all three reference surface displacement components, u , v and w , are independent of the circumferential coordinate y). Note that for symmetric construction (regular angle-ply or cross-ply with odd number of plies, for example) a membrane state exists and, therefore, the above is not an assumption. How reasonable this assumption is depends on the nature and magnitude of the coupling stiffnesses $[B_{ij}]$. Primary state quantities are denoted by tilda. With this assumption, the field equation becomes

$$b_{21}\hat{F}_{,xxxx} + d_{11}\hat{w}_{,xxxx} + \hat{F}_{,xx}/R = 0 \quad (D-5)$$

$$a_{22}\hat{F}_{,xxxx} + b_{21}\hat{w}_{,xxxx} + \hat{w}_{,xx}/R = 0 \quad (D-6)$$

Moreover, the expression for the reference surface hoop strain ϵ_{yy}^o is given by

$$\begin{aligned} \epsilon_{yy}^o &= -\hat{w}/R \\ &= a_{22}\hat{F}_{,xx} + a_{23}\bar{N}_{xy} + b_{21}\hat{w}_{,xx} \end{aligned} \quad (D-7)$$

These three equations, Eqs. D-5, D-5 and D-7, are employed to eliminate \hat{F} and thus there is only a single field equation. This resulting equation is:

$$\left(d_{11} - \frac{b_{21}^2}{a_{22}}\right) \hat{w}_{,xxxx} + 2 \frac{b_{21}}{a_{22}R} \hat{w}_{,xx} - \frac{\hat{w}}{a_{22}R^2} = \frac{a_{23}}{a_{22}R} \bar{N}_{xy} \quad (D-8)$$

The general solutions for \hat{w} and consequently [from Eq. D-7] for $\hat{F}_{,xx}$ become

$$\begin{aligned} \hat{w} &= B_1 \sinh \lambda_1 \left(x - \frac{L}{2}\right) \sin \lambda_2 \left(x - \frac{L}{2}\right) \\ &+ B_2 \cosh \lambda_1 \left(x - \frac{L}{2}\right) \cos \lambda_2 \left(x - \frac{L}{2}\right) - R a_{23} \bar{N}_{xy} \end{aligned} \quad (D-9)$$

$$\begin{aligned} \hat{F}_{,xx} &= \frac{-1}{a_{22}} (b_{21}B_2(\lambda_1^2 - \lambda_2^2) + 2 b_{21}B_1\lambda_1\lambda_2 + \\ &+ \frac{B_2}{R}) \cosh \lambda_1 \left(x - \frac{L}{2}\right) \cos \lambda_2 \left(x - \frac{L}{2}\right) \\ &- \frac{1}{a_{22}} (b_{21}B_1(\lambda_1^2 - \lambda_2^2) - 2 b_{21}B_2\lambda_1\lambda_2 + \\ &+ \frac{B_1}{R}) \sinh \lambda_1 \left(x - \frac{L}{2}\right) \sin \lambda_2 \left(x - \frac{L}{2}\right) \end{aligned} \quad (D-10)$$

$$\lambda_1 = \left\{ \frac{1}{2} \left[a_{22} R^2 \left(\frac{b_{21}^2}{a_{22}} - d_{11} \right) \right]^{-\frac{1}{2}} + \frac{1}{2} \left(\frac{b_{21}}{a_{22} R} \right) \left(d_{11} - \frac{b_{21}^2}{a_{22}} \right)^{-\frac{1}{2}} \right\}^{\frac{1}{2}}$$

$$\lambda_2 = \left\{ \frac{1}{2} \left[a_{22} R^2 \left(\frac{b_{21}^2}{a_{22}} - d_{11} \right) \right]^{\frac{1}{2}} - \frac{1}{2} \left(\frac{b_{21}}{a_{22} R} \right) \left(d_{11} - \frac{b_{21}^2}{a_{22}} \right)^{-\frac{1}{2}} \right\}^{\frac{1}{2}} \quad (D-11)$$

The constants B_1 and B_2 can be obtained by making use of the boundary conditions, Eqs. D.4.

Next, the buckling equations are obtained through a perturbation of the nonlinear governing equations. The dependent variables, w and F , are replaced by the sum of the primary state parameters, \hat{w} and \hat{F} , and small additional quantities, w^1 and F^1 , necessary to represent the buckled state. Moreover, the related boundary conditions for the buckling equations are also obtained in the same manner. Note that since the additional quantities can be made small as one wishes, only the linear terms in w^1 and F^1 are retained.

The buckling equations and related boundary conditions are:

$$\begin{aligned} & b_{21} F_{,xxxx}^1 + (2b_{23} - b_{31}) F_{,xxxxy}^1 + (b_{11} - 2b_{33} + b_{22}) F_{,xxxyy}^1 + (2b_{13} - b_{32}) F_{,xyyy}^1 \\ & + b_{12} F_{,yyyy}^1 + d_{11} w_{,xxxx}^1 + (2d_{31} + 2d_{13}) w_{,xxxxy}^1 + (d_{12} + 4d_{33} + d_{21}) w_{,xxxyy}^1 \\ & + (2d_{32} + 2d_{23}) w_{,xyyy}^1 + d_{22} w_{,yyyy}^1 + \frac{F_{,xx}^1}{R} + \hat{F}_{,xx} w_{,yy}^1 \\ & + \hat{w}_{,xx} F_{,yy}^1 + 2\bar{N}_{xy} w_{,xy}^1 = 0 \end{aligned} \quad (D-12)$$

$$\begin{aligned} & a_{22} F_{,xxxx}^1 - 2a_{23} F_{,xxxxy}^1 + (2a_{12} + a_{33}) F_{,xxxyy}^1 - 2a_{13} F_{,xyyy}^1 + a_{11} F_{,yyyy}^1 \\ & + b_{21} w_{,xxxx}^1 + (2b_{23} - b_{31}) w_{,xxxxy}^1 + (b_{11} - 2b_{33} + b_{22}) w_{,xxxyy}^1 \end{aligned}$$

$$+ (2b_{13} - b_{32})w_{,xyyy}^1 + b_{12}w_{,yyyy}^1 + \frac{w_{,xx}^1}{R} + \hat{w}_{,xx} w_{,yy}^1 = 0 \quad (D-13)$$

$$\begin{aligned} \text{at } w = 0 ; \quad & b_{21}F_{,xx}^1 + b_{31}F_{,xy}^1 + d_{11}w_{,xx}^1 + 2d_{13}w_{,xy}^1 = 0 ; \\ x = 0, L \quad & F_{,yy} ; \quad a_{22}F_{,xx}^1 + a_{23}F_{,xy}^1 + b_{12}w_{,xx}^1 + 2b_{23}w_{,xy}^1 = 0 . \end{aligned} \quad (D-14)$$

The Galerkin procedure is employed for both equations. The following approximate series is used for generating the Galerkin integrals. Note that the boundary conditions are satisfied by each term in the series.

$$\begin{aligned} w^1 &= \sum_{n=1}^N \sum_{i=1}^M (A_{in} \cos \frac{ny}{R} + B_{in} \sin \frac{ny}{R}) \left[\frac{L}{i\pi} \sin \frac{i\pi x}{L} - \frac{L}{(i+2)\pi} \sin \frac{(i+2)\pi x}{L} \right] \\ F^1 &= \sum_{n=1}^N \sum_{i=1}^M (C_{in} \cos \frac{ny}{R} + D_{in} \sin \frac{ny}{R}) \left[\frac{L}{i\pi} \sin \frac{i\pi x}{L} - \frac{L}{(i+2)\pi} \sin \frac{(i+2)\pi x}{L} \right] \end{aligned} \quad (D-15)$$

Substitution of the above expressions, Eqs. D.15, into the buckling equations results into a set of systems of linear homogeneous algebraic equations in A_{in} , B_{in} , C_{in} and D_{in} for each n (decoupled with respect to n). Assuming that the lowest eigenvalue corresponds to the critical load, $\bar{N}_{xy_{cr}}$, a computer program has been written to this effect. The Georgia Tech high speed digital computer CDC - CYBER - 170/760 is used for generating data. Note that a minimization with respect to n is performed in order to find the lowest eigenvalue.

Numerical Results and Conclusions

The geometries considered in the investigation represent variations of the one report in D.2. Each lamina is orthotropic (Boron/Epoxy; AVCO 5505) with the following properties:

$$E_{11} = 2.0690 \times 10^8 \text{ kN/m}^2 \text{ (30} \times 10^6 \text{ psi.)} ; \mu = 0.21 ;$$

$$E_{22} = 0.1862 \times 10^8 \text{ kN/m}^2 \text{ (2.7} \times 10^6 \text{ psi.)} ; R = 190.5 \text{ cm (7.5 in.)} ;$$

$$G_{12} = 0.04482 \times 10^8 \text{ kN/m}^2 \text{ (0.65} \times 10^6 \text{ psi)} ; L = 381 \text{ cm (15 in.)} ;$$

$$h_{\text{ply}} = 0.013462 \text{ cm. (0.0053 in.)} \quad (\text{D-16})$$

$$(h_{\text{ply}} = h_k - h_{k-1} \text{ for } k = 1, 2, 3, 4 ; \text{ four plies})$$

Five different stacking combinations of the four-ply laminate comprise the various geometries, I - i, i = 1, 2, -- 5. These are

$$\text{I - 1} : 45^\circ / -45^\circ / -45^\circ / 45^\circ$$

$$\text{I - 2} : 45^\circ / -45^\circ / 45^\circ / -45^\circ$$

$$\text{I - 3} : -45^\circ / 45^\circ / -45^\circ / 45^\circ$$

(D-17)

$$\text{I - 4} : 90^\circ / 60^\circ / 30^\circ / 0^\circ$$

$$\text{I - 5} : 0^\circ / 30^\circ / 60^\circ / 90^\circ$$

where the first number denotes the orientation of the fibers of the outermost ply with respect to x, and the last of the innermost. A pure torsion is applied through the midsurface of the four-ply laminate.

Some of the generated results are shown on Table D.1. For each geometry, the critical torsion (for both positive and negative application; clockwise and counterclockwise at the end $x = L$), the minimizing value of n (full number of circumferential waves), and the values of the coefficients A_{in} and B_{in} (normalized with respect to B_{2n}) are shown. Note that the A_{in} and B_{in} when substituted into the first of Eqs. D.15, yields the buckling mode. It was concluded that $M = 5$ suffices for determining critical loads.

Table D-1. Numerical Results

Geo.	Minimizing n	\bar{N}_{xy} in N/m (lbs./in.)	A ₂	B ₁	A ₂	B ₂	A ₃	B ₃	A ₄	B ₄	A ₅	B ₅
I-1	12	6987 (39.90)	-0.3353	0.	0.	1.0	0.7520	0.	0.	0.2038	0.3439	0.
	9	-13220 (-75.50)	0.7627	-0.1954	0.2561	1.0	0.0980	-0.0251	0.1185	0.4626	0.0225	0.0058
I-2	10	9534 (54.45)	-0.5830	0.	0.	1.0	0.1696	0.	0.	0.4230	0.1023	0.
	10	-9454 (-53.99)	0.5804	0.	0.	1.0	-0.1753	0.	0.	0.4218	-0.1063	0.
I-3	10	9454 (53.99)	-0.5830	0.	0.	1.0	-0.1753	0.	0.	0.4218	-0.1063	0.
	10	-9534 (54.45)	0.5804	0.	0.	1.0	0.1696	0.	0.	0.4230	0.1023	0.
I-4	13	8597 (49.01)	-0.3290	0.0226	0.0685	1.0	0.7107	0.0487	0.0189	0.2759	0.4182	-0.028
	12	-7790 (-44.59)	0.3431	0.	0.	1.0	0.7355	0.	0.	0.10374	-0.2708	0.
I-5	13	13082 (74.71)	-0.4035	-0.0062	0.0153	1.0	0.5681	0.0087	0.0056	0.3666	0.3994	0.006
	12	-7846 (-44.81)	0.3413	0.0183	0.0536	1.0	-0.8158	-0.0437	0.0010	0.0184	-0.263	-0.014

Note that Geometry I - 1 is symmetric (with respect to the midsurface), Geometries I-2 and I-3 antisymmetric, and Geometries I-4 and I-5 asymmetric. For the symmetric geometry (I-1), the positive direction critical torsion is 6987 N/m (39.9 lbs./in.), while the negative critical torsion is 13,220 N/m (75.5 lbs./in.). The respective reported D-2 experimental values are 4640 N/m (26.5 lbs./in.) for the positive direction and 11,508 N/m (65.72 lbs./in.) for the negative. This suggests that the geometric imperfection in the tested cylinder D-2 is such that the configuration is more sensitive to it, when loaded in the positive direction, than in the negative (the ratio of the experimental to theoretical value is 0.664 for the former and 0.87 for the latter). The difference in response is understandable, because of the anisotropy. The antisymmetric geometries, I-2 and I-3, yield the same response when loaded opposite to each other. Note that the positive direction critical load for I-2 is the same as the negative direction critical load for I-3 (the same is true for the buckling mode). Also, observe that the two (\pm direction) critical loads are very close (9534 N/m. and 9454 N/m.). This is due to the fact that the extensional, $[A_{ij}]$, and flexural, $[D_{ij}]$, stiffness have the same form as if the shell were isotropic. The difference from isotropy is the existence of some small (in value) terms in the coupling, $[B_{ij}]$, stiffnesses.

Finally, for the asymmetric configurations, I-4 and I-5 the response is completely different when each geometry is loaded in the positive and in the negative direction. Although the $[A_{ij}]$ and $[D_{ij}]$ stiffnesses, for the two configurations, are the same and only the signs are different in the $[B_{ij}]$ stiffness, the geometries behave (radically) differently. The only similarity is that the number of full waves, n , is approximately the same (12 and 13).

Acknowledgement

This work is sponsored by the Air Force Office of Scientific Research, Department of the Air Force, under Grant No. AFOSR-81-0227. This financial support is gratefully acknowledged.

References

- D.1 Sheinman, I., Shaw, D., and Simitzes, G. J., "Nonlinear Analysis of Axially-Loaded Laminated Cylindrical Shells". Proceedings of the Symposium on Advances and Trends in Structural and Solid Mechanics. Washington, D. C., October 4-7, 1982.
- D.2 Wilkins, D. J., and Love, T. S., "Combined Compression-Torsion Tests of Laminated Composite Cylindrical Shells", AIAA/ASME/SAE 15th Structures, Structural Dynamics and Materials Conference, Las Vegas, Nevada, 1974, AIAA Paper No. 74-379.

REFERENCES

1. Tennyson, R.C., "Buckling of Laminated Composite Cylinders: a Review," *Composites*, Jan. 1975, pp. 17-24.
2. March, H.W. et al. "Buckling of Thin-Walled Polywood Cylinders in Torsion," Forest Products Lab., Madison, Wisc Report 1529, June, 1945.
3. Schenell, W. and Bruhl, C. "Die Langsgedruckte Orthotrope Kreiszyylinder-schale bei Innendruck," Zeitschrift Flugwiss, Vol. 7, 1959.
4. Thielemann, W.F., Schenell, W. and Fischer, G., "Buckling and Postbuckling Behaviour of Orthotropic Circular Cylindrical Shells Subjected to Combined Axial and Internal Pressure," Zeitschrift Flugwiss 8, 1960.
5. Hess, T.E. "Stability of Orthotropic Cylindrical Shells under Combined Loading," J. American Rocket Society 31, No. 2, Feb. 1961.
6. Cheng, S. and Ho. B.P.C., "Stability of Heterogeneous Aeolotropic Cylindrical Shells Under Combined Loading", AIAA Journal 1, No. 4, April, 1963.
7. Ho. B.P.C. and Cheng, S. "Some Problems in Stability of Heterogeneous Aeolotropic Cylindrical Shells Under Combined Loading", AIAA Journal 1, No. 7, July 1963.
8. Jones, R.M. and Hennemann, J.C.F., "Effect of Prebuckling Deformations on Buckling of Laminate Composite Circular Cylindrical Shells," Proceedings of AIAA 19th Structures, Structural Dynamics and Material Conference, Bethesda, Md., April 1978.
9. Jones, R.M. and Morgan, H.S., "Buckling and Vibration of Cross-Ply Laminated Circular Cylindrical Shell", AIAA Journal Vol. 13, May 1975.
10. Hirano, Y., "Buckling of Angle-Ply Laminated Circular Cylindrical Shells" J. of Applied Mechanics, Vol. 46, March 1979.
11. Tasi, J., "Effect of Heterogeneity on the Stability of Composite Cylindrical Shells Under Axial Compression", AIAA Journal 4, No. 6, June 1966.
12. Martin, R.E. and Drew, D.D., "A Batdorf Type Modified Equation for the Stability Analysis of Anisotropic Cylindrical Shells," Texas A & M University, Tech. Report No. 10, March 1969.
13. Chao, T.L. "Minimum Weight Design of Stiffened Fiber Composite Cylinders," USAF, WPAFB Tech. Report AFML-TR-69-251, Sept. 1969.
14. Jones, R.M., "Buckling of Circular Cylindrical Shells With Multiple Orthotropic Layers and Eccentric Stiffeners" AIAA Journal 6, No. 12, Dec. 1968.
15. Terebushko, O.I., "Stability of Stiffened and Anisotropic Shells, "Trons. of 7th All-Union Conference on Theory of Plates and Shells, Dnepropetrovsk, Ukranian SSR, Sept. 1969.

16. Chang, L.K. and Card, M.F., "Thermal Buckling Analysis for Stiffened Orthotropic Cylindrical Shells," NASA TN-D-6332, 1971.
17. Chehill, D.S. and Cheng, S. "Elastic Buckling of Composite Cylindrical Shells Under Torsion", Journal of Spacecraft and Rockets 5, No. 8, August 1968.
18. Tennyson, R.C. and Muggeridge, D.B., "Buckling of Laminated Anisotropic Imperfect Circular Cylinder Under Axial Compression," Journal of Spacecraft and Rockets, Vol. 10, No. 2, Feb. 1973.
19. Booton, M. and Tennyson, R.C., "Buckling of Imperfect Anisotropic Circular Cylinders Under Combined Loading." AIAA Journal, Vol. 17, No. 3, March 1979.
20. Herakovich, C. "Theroetical-Experimental Correlation for Buckling of Composite Cylinders Under Combined Loads," NASA CR-157359, July 1978.
21. Tripp, L.L., Tamekuni, M., and Viswanathan, A.V., "User's Manual - BUCLASP2: A Computer Program for Instability Analysis of Biaxially Loaded Composite Stiffened Panels and Other Structures," NASA CR-112, 226, 1973 (prepared by the Boeing Co. for Langley Research Center) [BUCLASP 2].
22. Wittrick, W. H., and Williams, F. W., "Buckling and Vibration of Anisotropic or Isotropic Plate Assemblies Under Combined Loadings," International J. Mech. Science, Vol. 16, No. 4, April 1974, pp. 209-239 [VIPASA].
23. Bushnell, D., "Stress Stability and Vibration of Complex Shells of Revolution. Analysis and User's Manual for BOSOR 3", Lockheed Missiles and Space Company Report N-5J-69-1, Sept. 1969, Palo Alto, California. [BOSOR 3].
24. Stanton, E.L., and McGovern, D. J., "The Application of Gradient Minimization Methods and Higher Order Discrete Elements to Shell Buckling and Vibration Eigen-value Problems," McDonnell-Douglas Astronautics Paper WD 1406, Sept. 1970 [DEBACUL].
25. Haisler, W.E., Stricklin, J.A., and Von Riesenmann, W.A., "DYNAPLAS- A Finite Element Program for the Dynamic Elastic-Plastic Analysis of Stiffened Shells of Revolution," TEES RPT-72-27, Department of Aerospace Engineering, Texas A & M University, College Station, Texas, December 1972. [DYNAPLAS].
26. Zudans, Z., "Input Map and User's Guide for the FELAP 8 Computer Program," Franklin Institute Research Laboratories, Jan. 1971 (Proprietary Document) [FELAP 8].
27. Huffington, N.J., Jr., "Large Deflection Elasto-plastic Response of Shell Structures," Ballistic Research Laboratories BRL R 1515, Aberdeen Proving Grounds, Maryland, Nov. 1970 [REPSIL].

28. Anderson, J.S., Fulton, R.E., Heard, W.L., Jr., and Walz, I.E., "Stress, Buckling and Vibration Analysis of Shells of Revolution", J. Computer & Structures, Vol. 1, 1971, pp. 157-192 [SALORS].
29. Ball, R.E., "A Program for the Nonlinear Static and Dynamic Analysis of Arbitrarily Loaded Shells of Revolution," J. Computers and Structures, Vol. 2, 1972, pp. 141-162 [SATANS].
30. Prince, N., "SHELL-3D-The Structural Analysis of Arbitrary Three-Dimensional Thin Shells, Part I: Analytical Development and Part II: Program User's Manual for SHELL 9," Gulf General Atomic, Inc., Report GA-10130, July 1970 [SHELL 9].
31. Almroth, B.O. et al. "Collapse Analysis for Shells of General Shape; Volume II. - User's Manual for the STAGS -A. Computer Code". Technical Report AFFDL-TR 71-8, Air Force Flight Dynamics Laboratory, Wright-Patterson AF Base, Ohio, 1973. [STAGS].
32. Hartung, F.G., "An Assessment of Current Capability for Computer Analysis of Shell Structures," Technical Report AFFDL-TR-71-54, Air Force Flight Dynamics Laboratory, Wright-Patterson AF Base, Ohio, 1971.
33. Donnell, L.H. "Stability of Thin-Walled Tubes under Torsion", NACA Technical Report 479, Washington, D.C., 1933.
34. Sanders J.L., "Nonlinear Theories for Thin Shells," Quart. Appl. Math. Vol. 21. 1963.
35. Jones, R.M., Mechanics of Composite Materials, McGraw-Hill Book Co., Inc., New York, 1975.
36. Sheinman, I. and Simites, G.J., "Buckling Analysis Geometrically Imperfect Stiffened Cylinders Under Axial Compression," AIAA Journal, Vol. 15, No. 3. 1977.
37. Simites, G.J., and Sheinman, I., "Dynamic Stability of Structures: Application to Frames, Cylindrical Shells and Other Systems" Technical Report AFWAL-TR-81-3155, Wright-Patterson Air Force Base, Ohio, February 1982.
38. Thurston, G.A., "Newton's Method Applied to Problems in Nonlinear Mechanics," J. Appl. Mech., Vol. 32, No. 2, 1965.
39. Simites, G.J., "Effect of Static Preloading on the Dynamic Stability of Structures", Proceedings of the AIAA/ASME/ASCE/AHS 23rd Structures, Structural Dynamics and Materials Conference, Part 2, New Orleans, Louisiana, 1982, pp 299-307.
40. Hoff, N.J., and Bruce, V.G., "Dynamic Analysis of the Buckling of Laterally Loaded Flat Arches" J. Math and Phys., Vol. 32, 1954, pp. 276-288.

41. Hsu, C.S. "Stability of Shallow Arches Against Snap-Through under Timewise Step Loads" J. Appl. Mech., Vol. 25, No. 1, 1968, pp 31-39.
42. Simites, G.J., "On the Dynamic Buckling of Shallow Spherical Caps", J. Appl. Mech. Vol. 41, No. 1, 1974, pp. 298-300.
43. Tene, Y. Epstein, M., and Sheinman I., "A Generalization of Potter's Method" Computers and Structures, Vol. 4, 1974, pp. 1099-1103.
44. Wilkins, D.J. and Love, T.S., "Combined Compression-Torsion Buckling Tests of Laminated Composite Cylindrical Shells," Proceedings AIAA 15th Structures, Structural Dynamics and Materials Conference, Las Vegas, Nevada, April 1974.
45. Simites, G.J. and Sheinman, I. "Axially-Loaded, Imperfect, Cylindrical Shells" in Stability in the Mechanics of Continua, Ed. by F.H. Schroeder, Springer-Verlag, Berlin, 1982, pp 113-122.
46. Simites, G.J., and Sheinman, I., "Dynamic Buckling of Shell Structures: Concepts and Applications" Acta Astronautica, Vol. 1, No. 3, 1982, pp 179-182; also Paper IAF-81-391, XXXIInd Int's Astronautical Federation Congress, Rome, Italy, September 1981.
47. Hoff, N.J. "The Perplexing Behavior of Thin Circular Cylindrical Shells in Axial Compression" Israel J. of Technology, Vol. 4, No. 1, 1966, pp. 1-28.
48. Simites, G.J., and Cole, R.T., "General Instability of Eccentrically Stiffened Thin Spherical Shells Under Pressure", J. Appl. Mech., Vol. 37, No. 4, 1970, pp. 1165-1168.

ANALYSIS OF THE NONLINEAR LARGE DEFORMATION BEHAVIOR OF COMPOSITE CYLINDRICAL SHELLS*

**George J. Simitzes
Izhak Sheinman
and
Dein Shaw**



**School of Engineering Science and Mechanics
GEORGIA INSTITUTE OF TECHNOLOGY
A Unit of the University System of Georgia
Atlanta, Georgia 30332**

Qualified requestors may obtain additional copies from the Defense Documentation Center, all others should apply to the National Technical Information Service.

REPORT DOCUMENTATION PAGE		READ INSTRUCTIONS BEFORE COMPLETING FORM
1. REPORT NUMBER AFOSR TR-	2. GOVT ACCESSION NO.	3. RECIPIENT'S CATALOG NUMBER
4. TITLE (and Subtitle) ANALYSIS OF THE NONLINEAR LARGE DEFORMATION BEHAVIOR OF COMPOSITE CYLINDRICAL SHELLS		5. TYPE OF REPORT & PERIOD COVERED Final June 30, 1982 - June 30, 1983
		6. PERFORMING ORG. REPORT NUMBER
7. AUTHOR(s) George J. Simitzes Izhak Sheinman and Dein Shaw		8. CONTRACT OR GRANT NUMBER(s) AFOSR 81-0227
9. PERFORMING ORGANIZATION NAME AND ADDRESS Georgia Institute of Technology School of Engineering Science and Mechanics 225 North Ave., N.W. Atlanta, GA 30332		10. PROGRAM ELEMENT, PROJECT, TASK AREA & WORK UNIT NUMBERS 612300 2307/B1 61102F
11. CONTROLLING OFFICE NAME AND ADDRESS Air Force Office of Scientific Research/NA Bldg. 410 Bolling AFB, D.C. 20332		12. REPORT DATE 1983
		13. NUMBER OF PAGES 88
14. MONITORING AGENCY NAME & ADDRESS (if different from Controlling Office)		15. SECURITY CLASS. (of this report) Unclassified
		15a. DECLASSIFICATION/DOWNGRADING SCHEDULE
16. DISTRIBUTION STATEMENT (of this Report) Approved for public release; distribution unlimited		
17. DISTRIBUTION STATEMENT (of the abstract entered in Block 20, if different from Report)		
18. SUPPLEMENTARY NOTES		
19. KEY WORDS (Continue on reverse side if necessary and identify by block number) Composite Cylinders Axial Compression Laminated Shells Torsion Stability Nonlinear Shell Theories Stiffened Shells		
20. ABSTRACT (Continue on reverse side if necessary and identify by block number) The governing equations for the nonlinear analysis of imperfect, stiffened, laminated, circular, cylindrical, thin shells, subjected to uniform axial compression and torsion, and supported in various ways, are derived and presented. Two types of formulations have been developed; one (w,F-Formulation) is based Donnell-type nonlinear kinematic relations; and the other (u,v,w - formulation) is based on Sanders'-type of nonlinear kinematic relations (small strains, moderate rotations about in-plane axes).		

A solution methodology is developed and presented. Numerical results are generated for certain special geometries, and these serve as bench marks for the solution scheme. Parametric studies are performed for composite cylinders. The scope of these studies is to assess the effect of (a) geometric imperfections (b) lamina stacking, and (c) length to radius ratio. The solution scheme is also tested by comparing theoretical predictions (critical loads based on the developed methodology) to experimentally obtained results.

ANALYSIS OF THE NONLINEAR LARGE DEFORMATION
BEHAVIOR OF COMPOSITE CYLINDRICAL SHELLS*

by

George J. Simitzes⁺, Dein Shaw⁺⁺

and

Izhak Sheinmann⁺⁺⁺

Georgia Institute of Technology

*This work was supported by the United States Air Force Office of Scientific Research under Grant AFOSR-81-0227

⁺Professor of Engineering Science and Mechanics

⁺⁺Postdoctoral Fellow, School of Engineering Science and Mechanics

⁺⁺⁺Visiting Scholar; on leave from Israel Institute of Technology, Haifa, Israel

Qualified requestors may obtain additional copies from the Defense Documentation Center, all others should apply to the National Technical Information Service.

Conditions of Reproduction

Reproduction, translation, publication, use and disposal in whole or in part for the United States Government is permitted.

TABLE OF CONTENTS

	<u>Page</u>
NOMENCLATURE	ii
SUMMARY	iv
CHAPTER	
I. INTRODUCTION	
II. MATHEMATICAL FORMULATION	
AND SOLUTION	
III. RESULTS AND DISCUSSION; u,v,w - FORMULATION	
III.1 Description of Structural Geometry	
III.2 Numerical Results	
III.3 Comparison with Experimental Data	
III.4 Concluding Remarks	
IV. ADDITIONAL RESULTS; w,F - FORMULATION	
IV.1 Description of Geometry	
IV.2 Discussion of Results	
IV.3 Comparison with Experimental Data	
IV.4 Concluding Remarks	
V. CONCLUSIONS AND RECOMMENDATIONS	
REFERENCES	

NOMENCLATURE

A_x, A_y	=	Stiffener Cross-Sectional Areas
A_{ij}	=	$\sum_{k=1}^N \bar{Q}_{ij}^k (z_k - z_{k-1})$
B_{ij}	=	$\frac{1}{2} \sum_{k=1}^N \bar{Q}_{ij}^k (z_k^2 - z_{k-1}^2)$
D_{ij}	=	$\frac{1}{3} \sum_{k=1}^N \bar{Q}_{ij}^k (z_k^3 - z_{k-1}^3)$
$E_{11}, E_{22}, G_{12}, \nu_{12}$	=	Orthotropic Material Engineering Constants
E_x, E_y	=	Young's Moduli for Stiffener Material
e_x, e_y	=	Stiffener Eccentricities
F	=	Airy Stress Function
h	=	Shell Thickness
h_n, h_o	=	z-Coordinate of Extreme Surfaces of the Shell
I_{x_c}, I_{y_c}	=	Second Moments of Stiffener Areas
L	=	Length of Shell
ℓ_x, ℓ_y	=	Stiffener Spacings
M_{xx}, M_{xy}, M_{yy}	=	Moment Resultants
N_{xx}, N_{xy}, N_{yy}	=	Stress Resultants
$\bar{N}_{xx}, \bar{N}_{xy}$	=	Applied Stress Resultants
\bar{Q}_{ij}	=	Material Elastic Constant
R	=	Radius of Shell
u, v, w	=	Displacement Components
w^0	=	Initial Geometric Imperfection

NOMENCLATURE (Continued)

x, y, z	= Coordinates
Z	= Batdorf Curvature Parameter
δ_1	= 0 for Donnell's Approximation = 1 for Sanders' Approximation
$\epsilon_{xx}^0, \epsilon_{xy}^0, \epsilon_{yy}^0$	= Reference Surface Strain Components
θ	= Angle Between the Strong Orthotropic Direction and the x-axis
$\kappa_{xx}, \kappa_{yy}, \kappa_{xy}$	= Changes of Curvatures and Torsion of Reference Surface
ξ	= Imperfection Amplitude Parameter
$\sigma_{xx}, \sigma_{yy}, \sigma_{xy}$	= Stress Components
φ_x, φ_y	= Rotations About In-plane Axes x and y

SUMMARY

Imperfect, laminated, circular, cylindrical, thin shells supported in various ways and subjected to a uniform axial compression and torsion (individually applied or in combination) are analyzed. The analysis is based on nonlinear kinematic relations, linearly elastic material behavior, and the usual lamination theory. The laminate consists of orthotropic laminae, which typically characterize fiber reinforced composites. Two types of formulation have been developed; one is referred to as the w, F -formulation, based on Donnell-type of kinematic relations. The governing equations consist of the transverse equilibrium equation and the in-plane compatibility equation. These two equations are expressed in terms of the transverse displacement, w , and an airy stress resultant function, F . The other, referred to as the u, v, w -formulation, is based on Sanders'-type of kinematic relations. The governing equations for this case consist of the three equilibrium equations. These three equations are expressed in terms of two in-plane displacement components u, v , and the transverse displacement component, w . Donnell's type of shell theory approximation can be treated as a special case in the u, v, w -formulation.

Some results are generated for certain geometries (isotropic and laminated) and these serve as bench marks for the solution scheme (both formulations). Results are also generated for composite cylinders by changing several parameters. The scope of these parametric studies is to establish the effect of geometric imperfections, lamina stacking, and length to radius ratio. Moreover, theoretically computed critical conditions are compared to experimentally obtained results.

CHAPTER I

INTRODUCTION

Shell configurations of various constructions (metallic with or without stiffeners, laminated, plastic etc.) have been widely used as structural elements, for many decades. These configurations, in many cases, are primarily designed to withstand destabilizing loads, which are applied individually or in combination. Various linear and nonlinear shell theories (based on different approximations of the kinematic relations) have been employed in attempting to predict critical loads, as well as, pre- and post-buckling behavior of perfect and imperfect shell configurations.

One of the simplest shell theories is that, which is based on the Donnell (1) approximation (or Mushtari-Vlasov-Donnell approximation) for both, linear and nonlinear kinematic relations. Donnell's equations have been widely used in the solution of problems of stability and equilibrium.

From time to time, because of the approximate nature and because of the extreme simplicity of Donnell's equations, doubt has been raised as to their accuracy. Hoff (2) in 1955 gave the range of some basic parameters of perfect, thin, circular, cylindrical shells, for which solutions to Donnell's and Flügge's (3) equations are approximately equal. Moreover, Dym (4) in 1973 compared buckling results obtained from Donnell's equations with those obtained from Koiter-Budiansky (5,6) equations for thin, circular, perfect cylinders in uniform axial compression. Furthermore, Simites and Aswani (7) compared critical loads for the entire range of radius to thickness and length to radius ratios and for various load behaviors (during the buckling process) for a laterally loaded thin cylindrical shell

by employing several linear shell theories; Koiter-Budiansky (5,6), Sanders (8), Flügge (3) and Donnell (1).

Other comparisons of the linear version of the various shell theories have been reported by Toda (9), Koga and Endo (10), Microys and Schwaighofer (11, 12) and Akeju (13). All of the above investigations deal with isotropic thin cylindrical shells except for Ref. 12, which deals with an orthotropic cylindrical shell.

The only investigation that has any nonlinear flavor is the study of El Naschie and Hosni (14), but even this deals only with initial post-buckling behavior and for an infinitely long thin cylinder (thin ring).

The present report gives a comparison between critical loads for imperfect, thin, cylindrical shells (limit point loads) of isotropic and composite construction, under uniform axial compression for two shell theories, that of Sanders (8) and that of Donnell (1). The intention here is to identify the parameters which affect the accuracy of critical conditions established through Donnell equations, by comparing them to those established by Sanders equations. The implication here is that the Sanders equations, which are typical of the more accurate nonlinear shell equations (5,6,7), should yield accurate results, while the Donnell equations are viewed as approximate and therefore less accurate.

This report is a continuation of Ref. 15. In Ref. 15 the following are presented: 1) the mathematical formulation and derivation of the governing equations, based on Donnell-type (1) non-linear kinematic relations, and presented in terms of the transverse displacement component, w , and an Airy stress (resultant) function, F , defined in the text; this is called the w, F - formulation; 2) the mathematical formulation and deriva-

tion of the governing equations, base on Sanders-type (8) nonlinear kinematic relations and presented in terms of the three displacement components, u , v and w ; the kinematic relations used correspond to small strains, small rotations about the normal, but moderate rotations about in-plane axes; this is called the u,v,w -formulation, and the Donnell's kinematic relations are included in the Sanders relations, therefore this formulation covers both cases (Donnell is a special case of the Sanders equations); 3) solution schemes for both formulations; the solution methodology for the w , F -formulation includes the capability of obtaining post-limit point behavior, while the solution scheme for the u,v,w - formulation refers only to pre-limit point behavior (but nonlinear) including the estimation of critical conditions (limit point loads); moreover, the flow chart and listing of the respective computer codes are presented in the appendices of Ref. 15;4) several numerical results, generated with two objectives in mind, (a) some serve as bench marks for the solution schemes, and (b) some limited parametric studies are performed in order to assess effects of boundary conditions, of load eccentricity and of lamina stacking sequence for axially-loaded laminated cylindrical shells. Furthermore, some limited studies are performed for torsion. For both load cases, the imperfection sensitivity of the configuration is assessed; all of these results were obtained by employing the w,F -formulation.

In this report, additional results, obtained by the w,F -formulation, are presented. The objective here is to compare theoretical predictions with experimental results. Moreover, results (critical conditions), obtained by the u,v,w -formulation are presented. The objective here is to

establish which parameters affect the accuracy of Donnell-type of equations. This is accomplished by comparing Donnell-theory results with Sanders-theory results, the implication being here that the Sanders-theory results are closer to being exact. This is done for axially-loaded, imperfect shells of isotropic, orthotropic and laminated construction. These studies are necessary in order to establish the acceptability of the parametric studies (conclusions of) presented in Ref. 15. Finally, since the reported studies are not complete, proper recommendations are offered.

CHAPTER II

MATHEMATICAL FORMULATION AND SOLUTION

The mathematical formulation and a concise description of the solution scheme, for the u,v,w -formulation are presented in this chapter. The geometry and sign convention are shown on Figs. 1 and 2. The configuration consists of a laminate, which is orthogonally and eccentrically (in general) stiffened by closely spaced stiffeners (in the axial and hoop directions of the cylinder).

In this formulation (u,v,w), two distinctly different kinematic relations (different shell theories) are employed. One is due to Sanders (8) and one due to Donnell (1). In the case of Sanders' equations it is assumed that the reference surface strains are small, the rotation about the normal is negligibly small and the rotations about in-plane axes are moderate.

II.1 Kinematic Relations

The Sanders kinematic relations are based on the assumption of a perfect reference surface (in our case perfectly circular, cylindrical surface). These kinematic relations are modified to include the effect of a small initial geometric imperfection, $w^0(x,y)$.

Let $w^0(x,y)$ be measured from the perfectly cylindrical surface of the laminated shell. Let $w(x,y)$ denote the transverse displacement component of material points on the reference surface and be measured from the undeformed surface. It is positive outward (see Fig. 1) and the midsurface of the laminate is taken to be the reference surface (for convenience; the choice is arbitrary). Let $u(x,y)$ and $v(x,y)$ be the in-plane displacement

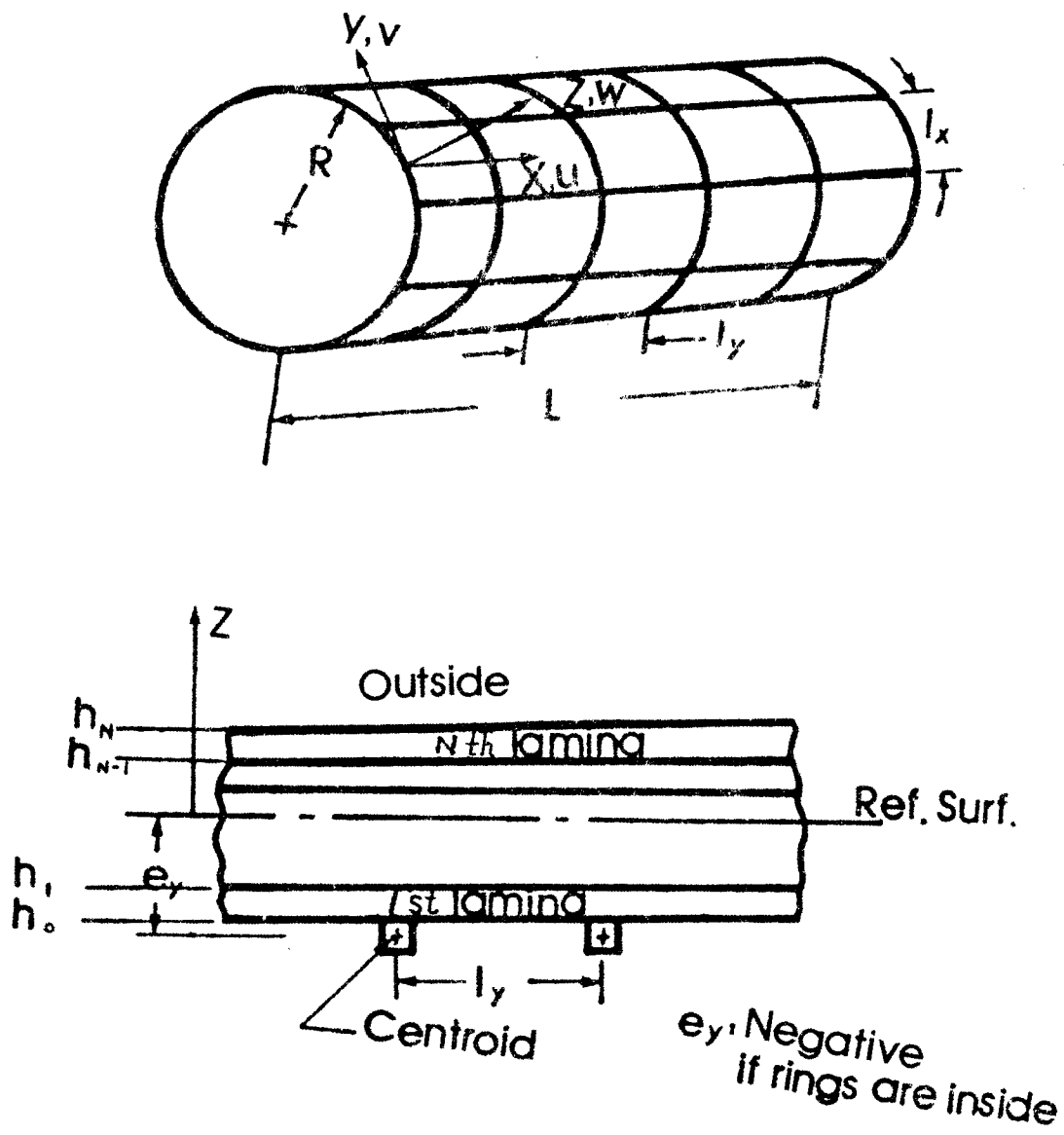
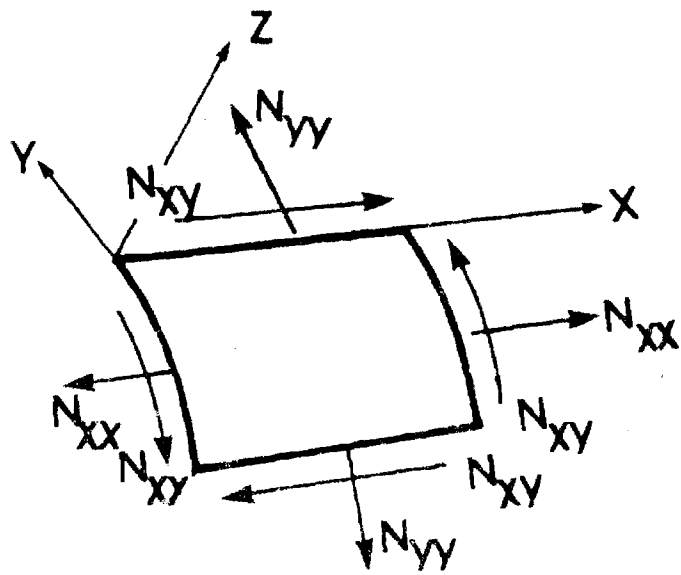
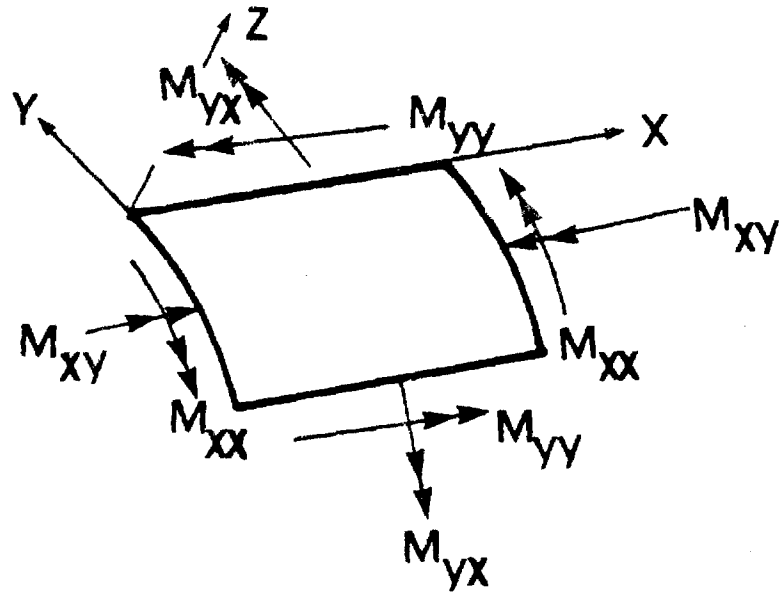


Fig. 1 Geometry and Sign Convention



Stress Resultants



Moment Resultants

Fig. 2. Stress and Moment Resultants
(Right Hand Rule)

components (see Fig. 1). The kinematic or strain-displacement relations are:

$$\epsilon_{xx} = \epsilon_{xx}^0 + z \kappa_{xx}; \quad \epsilon_{yy} = \epsilon_{yy}^0 + z \kappa_{yy}; \quad \gamma_{xy} = \gamma_{xy}^0 + 2z \kappa_{xy} \quad (1)$$

where

$$\left. \begin{aligned} \epsilon_{xx}^0 &= u_{,x} + \frac{1}{2} w_{,x}^2 + w_{,x} w_{,x}^0 \\ \epsilon_{yy}^0 &= v_{,y} + \frac{w}{R} + \frac{1}{2} w_{,y}^2 + w_{,y} w_{,y}^0 + \frac{\delta_1}{2} \left[\frac{v^2}{R^2} - 2 \frac{v}{R} (v_{,y} + w_{,y}^0) \right] \\ \gamma_{xy}^0 &= u_{,y} + v_{,x} + w_{,x} w_{,y} + v_{,x}^0 w_{,y} + w_{,x} w_{,y}^0 - \delta_1 \left[\frac{v}{R} (w_{,y} + w_{,y}^0) \right] \end{aligned} \right\} \quad (2)$$

$$\phi_x = -w_{,x} \quad ; \quad \phi_y = -w_{,y} + \delta_1 \left(\frac{v}{R} \right) \quad (3)$$

$$\kappa_{xx} = -w_{,xx}; \quad \kappa_{yy} = -w_{,yy} + \delta_1 \left(\frac{v_{,y}}{R} \right); \quad \kappa_{xy} = -w_{,xy} + \frac{\delta_1}{2} \left(\frac{v_{,x}}{R} \right) \quad (4)$$

where

$$\delta_1 = \begin{cases} 1 & \text{for Sanders kinematic relations} \\ 0 & \text{for Donnell kinematic relations} \end{cases} \quad (5)$$

II.2 Stress-Strain Relations

The smeared technique (Refs. 16 and 17) is used for the orthogonal stiffeners and the usual lamination theory for the laminate (see Ref. 18). Each lamina is assumed to be orthotropic and the directions of orthotropy make an angle θ with respect to the reference axes x and y . Note that if the orthotropic axis are denoted by "1" and "2", θ is the angle between axes "1" and x , measured counterclockwise from the x -axis.

The stress-strain relations for each lamina are transformed to the xy-axes (18). Moreover, the stress-strain relations for the closely spaced orthogonal and eccentric stiffeners are written on the basis of the assumptions (see Ref. 16) that (i) the stiffeners do not carry shear but only normal stresses, (ii) the stiffeners are torsionally weak and (iii) the stiffener-laminate connection is monolithic. The stiffener eccentricities are positive if the stiffeners are placed on the outer side of the laminate (in the positive z-direction).

Next, the usual stress and moment resultants are defined and their relations to the reference surface (midsurface of the laminate) strains and changes in curvature and torsion are obtained. These are (in matrix form)

$$\begin{Bmatrix} N_{xx} \\ N_{yy} \\ N_{xy} \\ M_{xx} \\ M_{yy} \\ M_{xy} \end{Bmatrix} = \begin{bmatrix} \bar{A}_{11} & \bar{A}_{12} & \bar{A}_{13} & \bar{B}_{11} & \bar{B}_{12} & \bar{B}_{13} \\ \bar{A}_{12} & \bar{A}_{22} & \bar{A}_{23} & \bar{B}_{12} & \bar{B}_{22} & \bar{B}_{23} \\ \bar{A}_{13} & \bar{A}_{23} & \bar{A}_{33} & \bar{B}_{13} & \bar{B}_{23} & \bar{B}_{33} \\ \bar{B}_{11} & \bar{B}_{12} & \bar{B}_{13} & \bar{D}_{11} & \bar{D}_{12} & \bar{D}_{13} \\ \bar{B}_{12} & \bar{B}_{22} & \bar{B}_{23} & \bar{D}_{12} & \bar{D}_{22} & \bar{D}_{23} \\ \bar{B}_{13} & \bar{B}_{23} & \bar{B}_{33} & \bar{D}_{13} & \bar{D}_{23} & \bar{D}_{33} \end{bmatrix} \begin{Bmatrix} \epsilon_{xx}^0 \\ \epsilon_{yy}^0 \\ \gamma_{xy}^0 \\ \kappa_{xx} \\ \kappa_{yy} \\ 2\kappa_{xy} \end{Bmatrix} \quad (6)$$

where

$$[\bar{A}_{ij}] = [A_{ij}] + \begin{bmatrix} \frac{E_x A_x}{l_x} & 0 & 0 \\ 0 & \frac{E_y A_y}{l_y} & 0 \\ 0 & 0 & 0 \end{bmatrix} \quad (7)$$

$$[\bar{B}_{ij}] = [B_{ij}] + \begin{bmatrix} E_x A_x e_x / l_x & 0 & 0 \\ 0 & E_y A_y e_y / l_y & 0 \\ 0 & 0 & 0 \end{bmatrix} \quad (8)$$

$$[\bar{D}_{ij}] = [D_{ij}] + \begin{bmatrix} E_x (I_{x_c} + e_x^2 A_x) / l_x & 0 & 0 \\ 0 & E_y (I_{y_c} + e_y^2 A_y) / l_y & 0 \\ 0 & 0 & 0 \end{bmatrix} \quad (9)$$

and A_{ij} , B_{ij} and D_{ij} are the usual stiffnesses employed in lamination theory (18). Furthermore, E_x and E_y are Young's moduli for the stringer and ring material, A_x and A_y stiffener cross sectional areas, l_x and l_y stiffener spacings, e_x and e_y stiffener eccentricities, and I_{x_c} and I_{y_c} second moment of stiffener areas about centroidal axes.

II.3 Equilibrium Equations and Boundary Conditions

The governing equations are derived for an orthogonally and eccentrically stiffened, laminated, imperfect, thin, circular cylindrical shell, subjected to eccentric in-plane loads and uniform external constant-directional pressure. This is done in order to have a set of equations, which can easily be specialized to and accommodate the following constructions and geometries: perfect or imperfect metallic (isotropic) with or without stiffening; and laminates of symmetric, antisymmetric or completely asymmetric lamina stacking. The nonlinear field equations (equilibrium) and related boundary conditions are derived from the principle of the stationary value of the total potential. These equations are:

$$N_{xx,x} + N_{xy,y} = 0$$

}

$$\begin{aligned}
& N_{xy,x} + N_{yy,y} - \delta_1 \left[\frac{N_{yy}}{R} \left(\frac{v}{R} - w_{,x} - w_{,x}^0 \right) + \frac{N_{xy}}{R} (w_{,x} + \right. \\
& \left. w_{,x}^0) + (M_{xy,x} + M_{yy,y})/R \right] = 0 \\
& [N_{xx}(w_{,x} + w_{,x}^0)]_{,x} + [N_{xy}(w_{,y} + w_{,y}^0)]_{,x} + [N_{xy}(w_{,x} + w_{,x}^0)]_{,y} \\
& + [N_{yy}(w_{,y} + w_{,y}^0)]_{,y} - \frac{N_{yy}}{R} - \frac{\delta_1}{R} [(N_{xy}v)_{,x} + (N_{yy}v)_{,y}] \\
& + M_{xx,x} + 2M_{xy,xy} + M_{yy,yy} + q = 0
\end{aligned} \quad (10)$$

The boundary conditions at $x = 0$ and L are either natural (force and moments prescribed) or kinematic

Either

$$N_{xx} = -\bar{N}_{xx}$$

$$N_{xy} + \delta_1 M_{xy}/R = \bar{N}_{xy} + \delta_1 \bar{M}_{xy}/R$$

$$N_{xx}(w_{,x} + w_{,x}^0) + N_{xy}(w_{,y} + w_{,y}^0 - \delta_1 \frac{v}{R})$$

$$+ M_{xx,x} + 2M_{xy,y} = \bar{Q}_x + \bar{M}_{xy,y}$$

$$M_{xx} = \bar{M}_{xx}$$

Or

$$u = 0$$

$$v = 0$$

$$w = 0$$

$$w_{,x} = 0$$

(11)

Note that the "bar" quantities denote applied forces and moments.

II.4 A Solution Methodology

The solution procedure consists of several steps, which are outlined herein with brevity (for details see Ref. 15). These steps are:

(1) A separated form is assumed for the three dependent variables $u(x,y)$, $v(x,y)$ and $w(x,y)$ [displacement components].

$$\begin{aligned} u(x,y) &= \sum_{i=0}^k \left[u_{1i}(x) \cos \frac{iny}{R} + u_{2i}(x) \sin \frac{iny}{R} \right] \\ v(x,y) &= \sum_{i=0}^k \left[v_{1i}(x) \cos \frac{iny}{R} + v_{2i}(x) \sin \frac{iny}{R} \right] \\ w(x,y) &= \sum_{i=0}^k \left[w_{1i}(x) \cos \frac{iny}{R} + w_{2i}(x) \sin \frac{iny}{R} \right] \end{aligned} \quad (12)$$

Note that since $\sin \frac{(0)ny}{R} = 0$ the functions $u_{20}(x)$, $v_{20}(x)$, and $w_{20}(x)$ do not enter into the solution scheme, and thus the number of independent and unknown functions of position x is $(6k + 3)$.

The known imperfection $w^0(x,y)$ can also be expressed in a form similar to $w(x,y)$. In this case $w_{1i}^0(x)$ and $w_{2i}^0(x)$ are known (taken as known) functions of position.

(2) The expressions for the displacement components are substituted into the kinematic relations, Eqs. (2) and (4). Because of the nonlinearity of the in-plane strain-displacement equations, this substitution yields double summations for the trigonometric functions. These double summations involve products of sines and cosines in all four possible combinations (sine - sine, cosine - cosine, sine-cosine and cosine - sine). Use of trigonometric identities involving products changes the double summation to single summation of either sine or cosine terms but with twice as many terms.

Through this step, all strain components (stretching and bending) can be expressed in terms of sines and cosines of iny/R . Some of the sums go from $i = 0$ to $i = k$ and some from $i = 0$ to $i = 2k$. Note that the coefficients of the sine and cosine terms involve linear and nonlinear combinations of the $(6k + 3)$ dependent functions, u_{1i} , u_{2i} , v_{1i} , v_{2i} , w_{1i} and w_{2i} .

(3) The above separated expressions for the in-plane strains, and changes in curvature and torsion are then substituted into the constitutive equations, Eqs. (6). Since these equations relate the stress and moment resultants to the stretching (ϵ_{ij} 's) and bending (κ_{ij} 's) strains in a linear manner, then use of Eqs. (6) yields single sums of sines and cosines of iny/R , similar to those for strains.

(4) Once steps (2) and (3) are completed, the obtained separated expressions for the stress and moment resultants, along with the assumed expressions for the displacement components (u , v and w) are substituted into the equilibrium equations, Eqs. (10).

Note that some of the stress resultants are multiplied by either some displacement components or their gradients. Because of this one obtains products of sums (of sines and cosines) and some sums go from $i = 0$ to $i = k$ (for the N_{ij} 's). Using a procedure similar to the one outlined in step (2), these products of sums are changed to a single sum and the highest upper limit of the summation is $3k$ (the single sums go from $i = 0$ to $i = 3k$). The boundary conditions, Eqs. (11) can also be expressed in term of the dependent variables, following the above procedure.

(5) The Galerkin procedure is then employed, in the circumferential direction. The vanishing of the Galerkin integrals leads to $(6k + 3)$ unknown functions of position x , $u_{1i}(x)$, $v_{1i}(x)$, $w_{1i}(x)$ for $i = 0, 1, 2 \dots k$, and $u_{2i}(x)$, $v_{2i}(x)$ and $w_{2i}(x)$ for $i = 1, 2, \dots k$.

(6) Next, the generalized Newton's method (19, 17), applicable to differential equations, is used to reduce the nonlinear field equations and boundary conditions to a sequence of linearized systems. The linearized iteration equations are derived based on the conjecture that the solution to the nonlinear set can be achieved by small corrections to an approximate solution. The small corrections or the values of the variables at the $(m + 1)$ th step, in terms of the values at the closely spaced m th state, can be obtained by solving the linearized differential equations. The linearization of a typically nonlinear term (product of X and Y), in the differential equations, is shown below.

$$\begin{aligned}
 X^{m+1} Y^{m+1} &= (X^m + dX^m)(Y^m + dY^m) \\
 &= X^m Y^m + X^m dY^m + Y^m dX^m + dX^m dY^m + X^m Y^m - X^m Y^m \\
 &= X^m (Y^m + dY^m) + Y^m (X^m + dX^m) - X^m Y^m \\
 &= X^m Y^{m+1} + X^{m+1} Y^m - X^m Y^m
 \end{aligned} \tag{13}$$

(7) The order of the linearized differential equations is reduced from four to two by a simple transformation. If the vector of all the unknowns is denoted by $[x]$ (in matrix form) then

$$\{x\} = (u_{1i}^{m+1}, u_{2i}^{m+1}, v_{1i}^{m+1}, v_{2i}^{m+1}, w_{1i}^{m+1}, w_{2i}^{m+1})^T \tag{14}$$

For convenience the number of unknowns is taken as $(6k + 6)$ subject to the constraint

$$u_{20} = v_{20} = w_{20} = 0 \tag{15}$$

The iteration equations can be written in matrix form as

$$[R4]\{x_{,xxx}\} + [R3]\{x_{,xx}\} + [R2]\{x_{,x}\} + [R1]\{x_x\} + [R0]\{x\} = \{g\} \quad (16)$$

By introducing the transformation

$$\{\eta\} = \{x_{,xx}\} \quad (17)$$

only in connection with the third and fourth derivatives, the iteration equations, Eqs. (16), become

$$[R] \begin{Bmatrix} \{x_{,xxx}\} \\ \{\eta_{,xx}\} \end{Bmatrix} + [S] \begin{Bmatrix} \{x_{,x}\} \\ \{\eta_{,x}\} \end{Bmatrix} + [T] \begin{Bmatrix} \{x\} \\ \{\eta\} \end{Bmatrix} = \{G\} \quad (18)$$

where $[R]$, $[S]$, and $[T]$ are $12(k + 1)$ by $12(k + 1)$ square matrices, with elements involving values of the variables at the mth step [see Eq. (14)] plus other known parameters. $\{G\}$ is a $12(k + 1)$ by one matrix with known elements.

Moreover, the boundary terms are also put in matrix form

$$[DB] \begin{Bmatrix} \{x_{,xx}\} \\ \{\eta_{,xx}\} \end{Bmatrix} + [DC] \begin{Bmatrix} \{x\} \\ \{\eta\} \end{Bmatrix} = \{BG\} \quad (19)$$

The details can be found in Ref. 15.

(8) The linearized iteration equations, Eqs. (18) are next cast into finite difference form by employing the usual central difference formula. At each end of the cylindrical shell (boundaries $x = 0$ and $x = L$) one fictitious point is used. The required additional equations are provided by the boundary terms, Eqs. (19), and some auxiliary equations, which are also cast in finite difference form.

(9) Finally, the total potential is expressed in terms of the dependent functions and, at each level of the applied loading, its value is computed by numerical integration.

In closing, a computer program has been written to compute the response of the shell at each level of the applied loading. Initially, at a low value of the loading, the solution is estimated through the use of the linear axisymmetric equations. Then, the iteration equations are employed, and by step increasing the loading the complete response (up to the limit point) (20) is obtained.

Several results are obtained by employing this formulation (u, v, w) and are discussed, in detail, in the next chapter.

CHAPTER III

RESULTS AND DISCUSSION; U,V,W - FORMULATION

Numerical results are generated for the u,v,w - formulation, by employing two different digital computers: (a) the interactive computer IBM 43/31 at the Technion Computer Center and (b) the VAX 11/780 of the GTICES (Georgia Tech integrated Computer Engineering System) Systems Laboratory of the School of Civil Engineering.

III.1 Description of Structural Geometry.

Three basic configurations are used in generating results. They consist of an isotropic cylinder, an orthotropic one and a laminated one. All configurations are imperfect, and the imperfection shape is either symmetric or (virtually) axisymmetric. The laminated geometry is the one employed in (21). The properties for each configuration are given separately.

Isotropic Geometry

The isotropic geometry consists of a thin imperfect cylindrical shell with the following dimensions and properties

$$E = 7.24 \times 10^7 \text{ kN/m}^2 (10.5 \times 10^6 \text{ psi}) ; \nu = 0.30$$

$$R = 10.16 \text{ cm (4 in.)} ; 1 \leq L/R \leq 10 ;$$

$$188.7 \leq R/h \leq 1000.0$$

As seen from the data above, the cylinder length, L, and the shell thickness, h, are varied in order to cover the range of practical interest.

Orthotropic Geometry

The properties of the orthotropic configuration are (given in terms of axes "1" and "2").

$$E_{11} = 2.069 \times 10^8 \text{ kN/m}^2 \text{ (} 30 \times 10^6 \text{ psi)} ; \nu_{12} = 0.21$$

$$E_{22} = 0.1862 \times 10^8 \text{ kN/m}^2 \text{ (} 2.7 \times 10^6 \text{ psi)} ; G_{12} = 0.0448 \times 10^8 \text{ kN/m}^2 \text{ (} 0.65 \times 10^6 \text{ psi)}$$

$$h = 0.05385 \text{ cm (} 0.0212 \text{ in.)} ; R = 10.16 \text{ cm (} 4 \text{ in.) or } 19.05 \text{ cm (} 7.5 \text{ in.)}$$

$$\text{and } 1 \leq L/R \leq 10.$$

If θ is the angle between the orthotropic axis "1" and the reference axis x, both 0° and 90° configurations are employed, herein.

Laminated Geometry

For the laminated geometry, a four-ply laminate is employed. The orthotropic lamina properties are the same as those given for the orthotropic geometry. The total thickness of the laminate and that of each ply are

$$h_{\text{tot}} = 0.05385 \text{ cm. (} 0.0212 \text{ in.) and}$$

$$h_k - h_{k-1} = 0.013462 \text{ cm. (} 0.0053 \text{ in.)}$$

Furthermore, $R = 19.05 \text{ cm (} 7.5 \text{ in.)}$ and

$$L/R = 2, 5, 10.$$

The stacking sequence is

$$I - 1: - 45^\circ / +45^\circ / +45^\circ / -45^\circ$$

where the first number denotes the orientation of the outermost ply with respect to the x-axis, and the last of the innermost. Note that I-1 is a symmetric geometry (with respect to the reference surface - midsurface).

Imperfection Shapes

Two imperfection shapes are used in the study, one which is symmetric and one which is virtually axisymmetric.

$$\text{symmetric: } w^0(x,y) = \zeta h \sin \frac{\pi x}{L} \cos \frac{\pi y}{R} \quad (20)$$

$$\text{axisymmetric: } w^0(x,y) = \zeta h \left(\cos \frac{2\pi x}{L} - 0.1 \sin \frac{\pi x}{L} \cos \frac{\pi y}{R} \right) \quad (21)$$

where ζ is a measure of the imperfection amplitude. Note that for the symmetric imperfection $\zeta = w_{\max}^0/h$, while for the (almost) axisymmetric one, $\zeta = w_{\max}^0/1.1h$.

III.2 Numerical Results

For all geometries considered, results are obtained for classical simply supported (SS-3) boundary conditions, Eqs. (22), and zero load eccentricity. The load case considered is uniform axial compression. The primary emphasis in the numerical studies is to establish which (design) parameters influence the accuracy of the Donnell-type of shell approximation and establish the range of these parameters for which the accuracy is acceptable (by comparison to the Sanders-type approximation).

$$\begin{aligned} N_{xx}(0,y) &= -\bar{N}_{xx} ; v(0,y) = w(0,y) = M_{xx}(0,y) = 0 \\ N_{xx}(L,y) &= -\bar{N}_{xx} ; v(L,y) = w(L,y) = M_{xx}(L,y) = 0 \end{aligned} \quad (22)$$

Numerical results were generated by employing two different computers:

- (a) the interactive computer IBM 43/31 at the Technion (Israel Institute of Technology) Computer Center and b) the VAX 11/780 of the GTICES (Georgia Tech Integrated Computer Engineering System) Systems Laboratory of the School of Civil Engineering.

The results for each geometry are presented and discussed separately.

Isotropic Geometry

The results are presented (in part) graphically on Fig. 3 and in tabular form on Table 1. On Table 1, the geometry, as well as the computed critical loads ($N_{xx,c} = 0.606 Eh^2/R$ and N_{xx}^l : limit point loads), the corresponding wave number, n , and the imperfection amplitude parameter ξ are presented.

One observation is that the discrepancy between critical loads obtained from the two different shell theory approximations (Sanders and Donnell), is primarily affected by L/R and there is a small effect of R/h . Note that as L/R increases the difference between the two results increases. Moreover, for the same L/R there is a small R/h effect. As R/h decreases the difference increases. The combined effect is shown on Fig. 3 by plotting ρ versus the square root of the Batdorf curvature parameter, Z , defined by

$$Z = \frac{L^2}{Rh} \sqrt{1 - \nu^2}$$

Furthermore, the obtained results substantiate the contention (2) that the Donnell approximation is dependent on the wave number, n . Clearly, from Table 1, if $n > 4$ the two theories yield the same critical load (within one percent), but for $n \leq 4$ the computed difference can be as large as ten percent.

Finally, from Fig. 3, one can see that the imperfection sensitivity decreases with increasing values for the curvature parameter. This is so because, for the same value of the imperfection amplitude parameter, ξ , the

TABLE 1. CRITICAL LOADS (ISOTROPIC GEOMETRY) ;
SS-3; AXISYMMETRIC IMPERFECTION

Case	R cm(in.)	L/R	R/h	$\bar{N}_{xx_{cl}}$ kN/cm (lbs/in.)	$\rho = \frac{\bar{N}_{xx}}{\bar{N}_{xx_{cl}}}$		n: wave No.		ξ Imp. Ampl.	$\frac{1}{Z^2}$
					Sanders	Donnell	Sanders	Donnell		
1	10.16(4)	1	1000.0	4.457 (25.45)	0.652	0.652	13	13	0.5	30.9
2	10.16(4)	1	1000.0	4.457 (25.45)	0.446	0.446	13	13	1.0	30.9
3	10.16(4)	1	250.0	71.319 (407.23)	0.246	0.248	8	8	1.0	15.4
4	10.16(4)	5	250.0	71.319 (407.23)	0.703	0.719	4	4	1.0	77.2
5	10.16(4)	10	250.0	71.319 (407.23)	0.790	0.831	3	3	1.0	154.4
6	10.16(4)	2	188.7	125.208 (714.94)	0.395	0.396	6	6	1.0	26.8
7	10.16(4)	5	188.7	125.208 (714.94)	0.652	0.677	4	4	1.0	67.1
8	10.16(4)	10	188.7	125.208 (714.94)	0.753	0.830	3	3	1.0	134.2

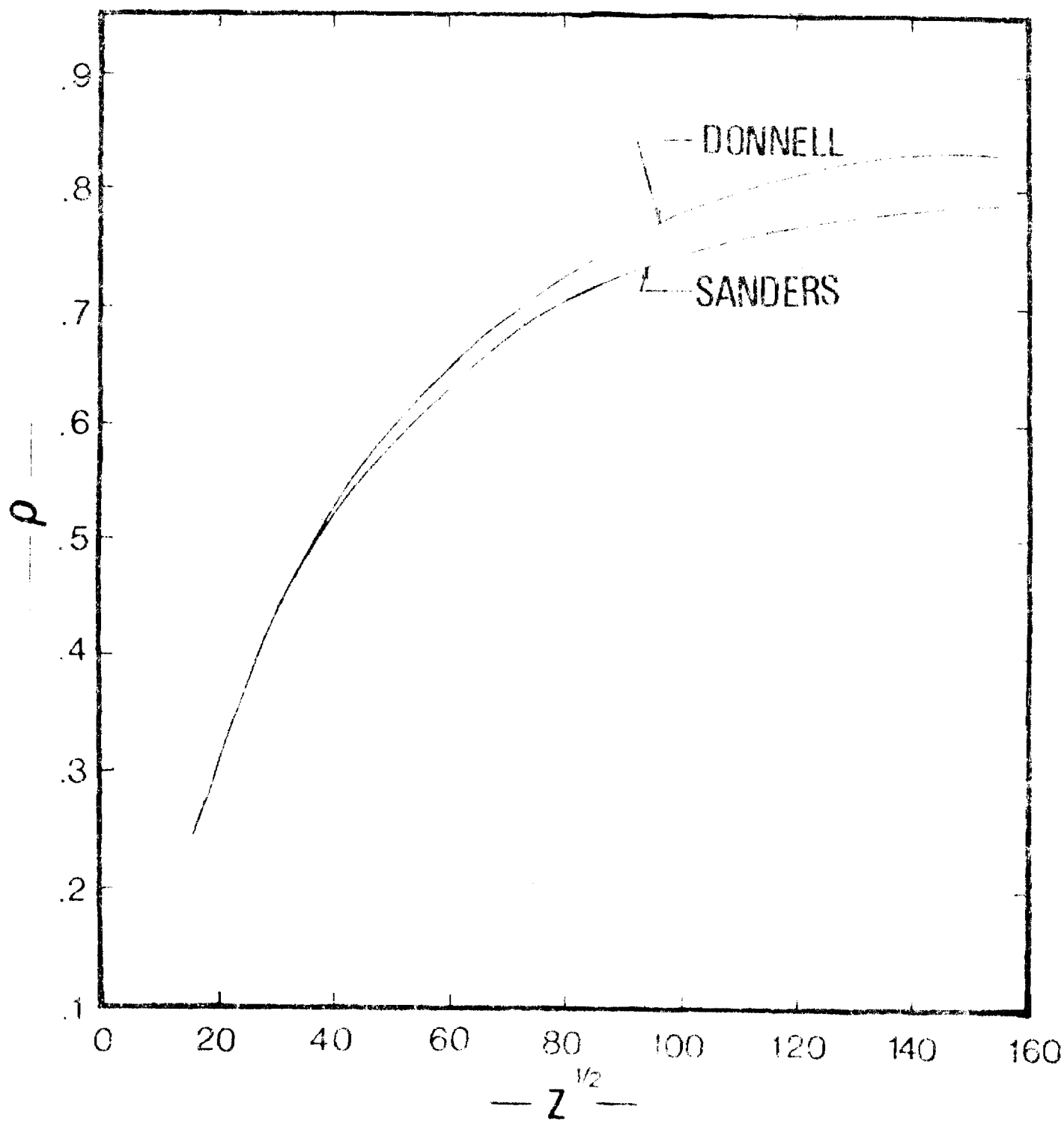


Fig. 3. Load Parameter, ρ ($= \bar{N}_{xx}^l / \bar{N}_{xx_{cl}}$) vs. Curvature

Parameter (Isotropic Geometry; SS-3, Axisym. Imp.)

computed limit point value approaches the classical value (ρ increases) as Z increases. Please note that the curves on Fig. 3 are drawn from points corresponding to different L/R and R/h values.

In closing, it is worth mentioning that Hoff and Soong (22) plotted similar results for perfect isotropic cylinders (using linear theory), but for the SS-1 boundary condition, i.e.,

$$\text{at } x = 0, L: N_{xx} = -\bar{N}_{xx}, N_{xy} = 0, w = 0 \text{ and } M_{xx} = 0 \quad (23)$$

Their (22) results show that the two approximations yield very close critical loads (linear theory eigen-values).

Orthotropic Geometry

The orthotropic geometries and their properties are described in the previous section. The numerical results are presented in tabular form, Tables 2 and 3, and graphically in Figs. 4 and 5.

Table 2 contains results for various orthotropic configurations with a virtually axisymmetric imperfection and $\beta = 1$ [see Eq. (21)]. The first column denotes the angle that the strong direction makes with the x -axis. The next three columns describe the geometry. The classical value is estimated from the data of Ref. 23 (see Fig. 10c of this reference; D_k/D_θ is assumed to be one). The value of \bar{N}_{xx} should only be considered an approximation used as a weighting function. This classical value, which is based on a linear eigenvalue approach is independent of the R/L ratio (this is also true for isotropic geometries). The data of Table 2 are plotted on Fig. 4. Through the plots one may assess better the effect of certain parameters. Fig. 4 shows plots of ρ (the ratio of the limit point load to the classical load) versus $\sqrt{L^2/Rh}$, which is similar to the Batdorf

curvature parameter for isotropic construction, for both shell approximations and separately for the two angles that the strong direction makes with the x-axis. It is seen from Fig. 4 that the behavior is similar to that of the isotropic geometry (see Fig. 3), but it is more pronounced for the 90° -curves than it is for the 0° -curves. In other words, when the strong axis is in the x-direction, the Donnell approximation is accurate (within 6%) even for large values of the curvature parameter (for $L^2/Rh \leq 20,000$). For the 90° -curves the trend is the same, but the Donnell approximation yields less accurate results even for small values of the curvature parameter. Note that, as in the isotropic case, the effect of L/R is the predominant one, while the effect of R/h is negligibly small. Moreover, note that part of the effect due to the construction (orthotropic) is buried in the weighting parameter $\bar{N}_{xx_{cl}}$, because $\bar{N}_{xx_{cl}}$ is dependent upon the E_{xx}/E_{yy} ratio. Finally, it is worth mentioning that, regardless of the approximation (Sanders or Donnell), when the strong direction is along the x-axis the configuration is more sensitive to the initial imperfection than when the strong direction is in the hoop direction (ρ for 0° is smaller than ρ for 90° , everything else being equal).

Similar results are presented on Table 3 and Fig. 5, with the same observations. The main difference here is that the imperfection is symmetric and the R/h ratio is constant. It is stressed again that the classical critical load is approximate in nature (taken from data of Ref. 23) and thus the critical load parameter ρ -values should be considered as qualitative rather than quantitative.

TABLE 2: CRITICAL CONDITIONS FOR ORTHOTROPIC GEOMETRIES

$$[w^0 = h \left(\cos \frac{2\pi x}{L} - 0.1 \sin \frac{\pi x}{L} \cos \frac{\pi y}{R} \right)]$$

θ Angle of Strong Direction	R/h	L/R	$(L^2/Rh)^{1/2}$	$\frac{\bar{N}_{xx}^l}{N_{xx}}$ lbs/in.		$\frac{F_{N_{xx}}^*}{N_{xx}^{cl}}$ lbs in	$\rho = \frac{\bar{N}_{xx}^l}{N_{xx}^{cl}}$	
				Sanders (Wave No.)	Donnell (Wave No.)		Sanders	Donnell
0°	188.7	2	27.5	92(7)	92(7)	487	0.189	0.189
0°	↓	5	68.7	222(5)	229(5)	↓	0.456	0.470
0°	↓	10	137.4	265(4)	283(5)	↓	0.544	0.581
90°	↓	2	27.5	230(10)	260(11)	481	0.478	0.541
90°	↓	1	13.7	157(6)	159(6)	↓	0.326	0.331
0°	353.8	2	37.6	69(8)	69(8)	270	0.256	0.256
0°	↓	5	94.0	132(6)	-	↓	0.489	-
90°	↓	2	37.6	127(7)	144(6)	262	0.485	0.550
90°	↓	1	18.8	108(7)	111(7)	↓	0.412	0.424

*Values estimated (calculated) from data of Ref. 23.

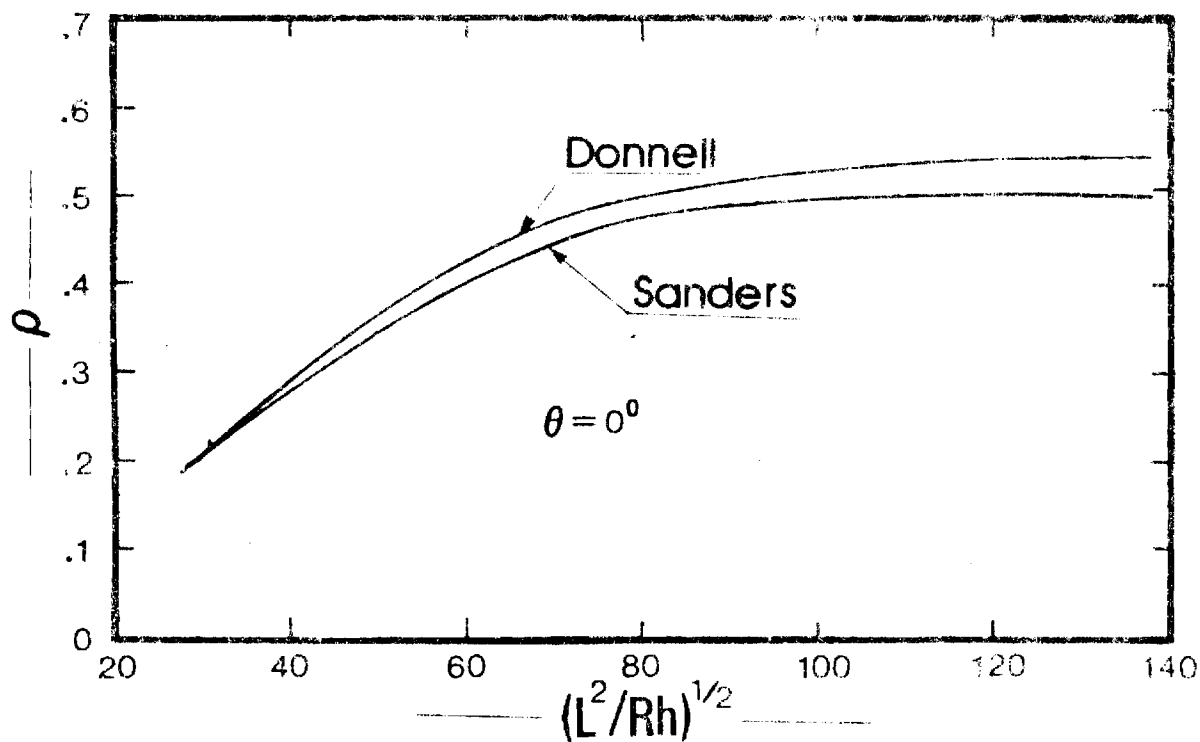
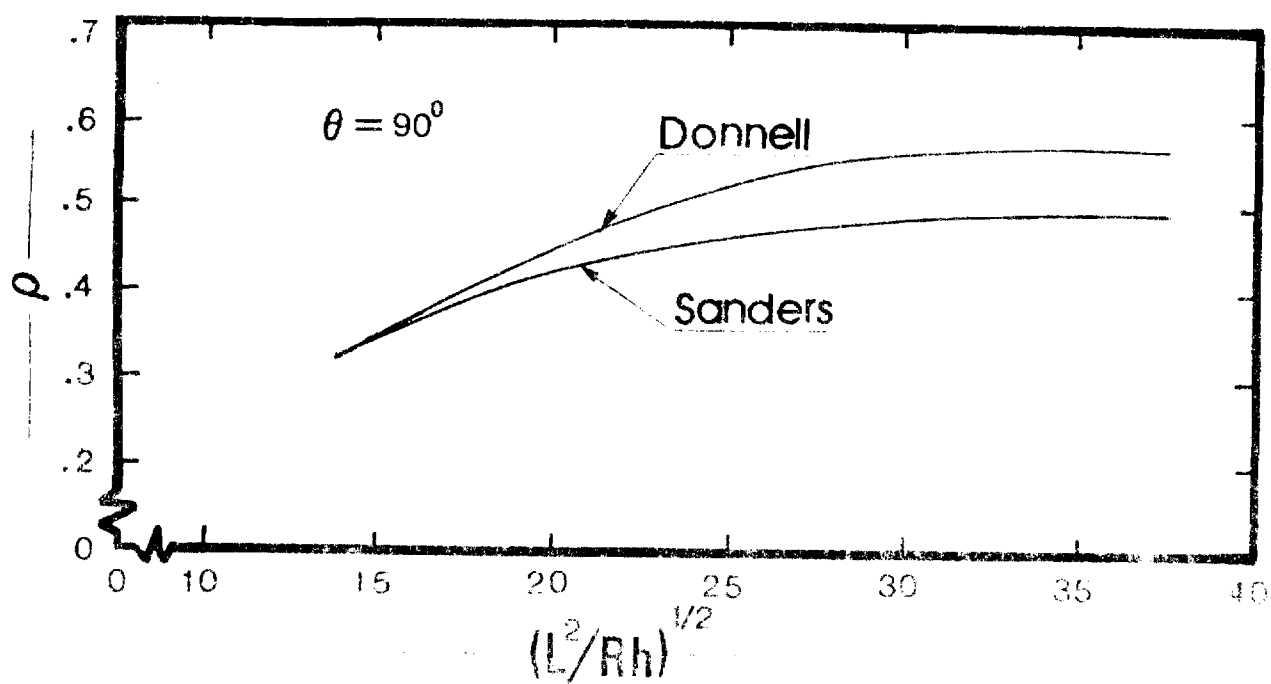


Fig. 4. Load Parameter ρ ($= \bar{N}_{xx}^l / \bar{N}_{xx_{cl}}$) vs. $(L^2/Rh)^{1/2}$

(Orthotropic Geometry; SS-3; Axisym. Imp.)

TABLE 3. CRITICAL CONDITIONS FOR ORTHOTROPIC GEOMETRIES

$$(w^0 = h \sin \frac{\pi x}{L} \cos \frac{\pi y}{R})$$

θ Angle of Strong Direction	R/h	L/R	$(L^2/RH)^{1/2}$	\bar{N}_{xx}^l in lbs/in.		$\bar{N}_{xx}^*_{cl}$ lbs/in	$\rho = \bar{N}_{xx}^l / \bar{N}_{xx}^*_{cl}$	
				Sanders (Wave No.)	Donnell (Wave No.)		Sanders	Donnell
0°	353.8	2	37.6	85(9)	85(9)	270	0.315	0.315
0°	↓	5	94.0	125(6)	130(6)	↓	0.463	0.481
0°		10	188.0	155(4)	165(4)	↓	0.574	0.611
90°		2	37.6	145(5)	152(5)	262	0.553	0.580
90°		5	94.0	195(4)	215(4)	↓	0.744	0.821
90°		10	188.0	212(3)	271(3)	↓	0.809	1.034

*Values estimated from data of Ref. 23.

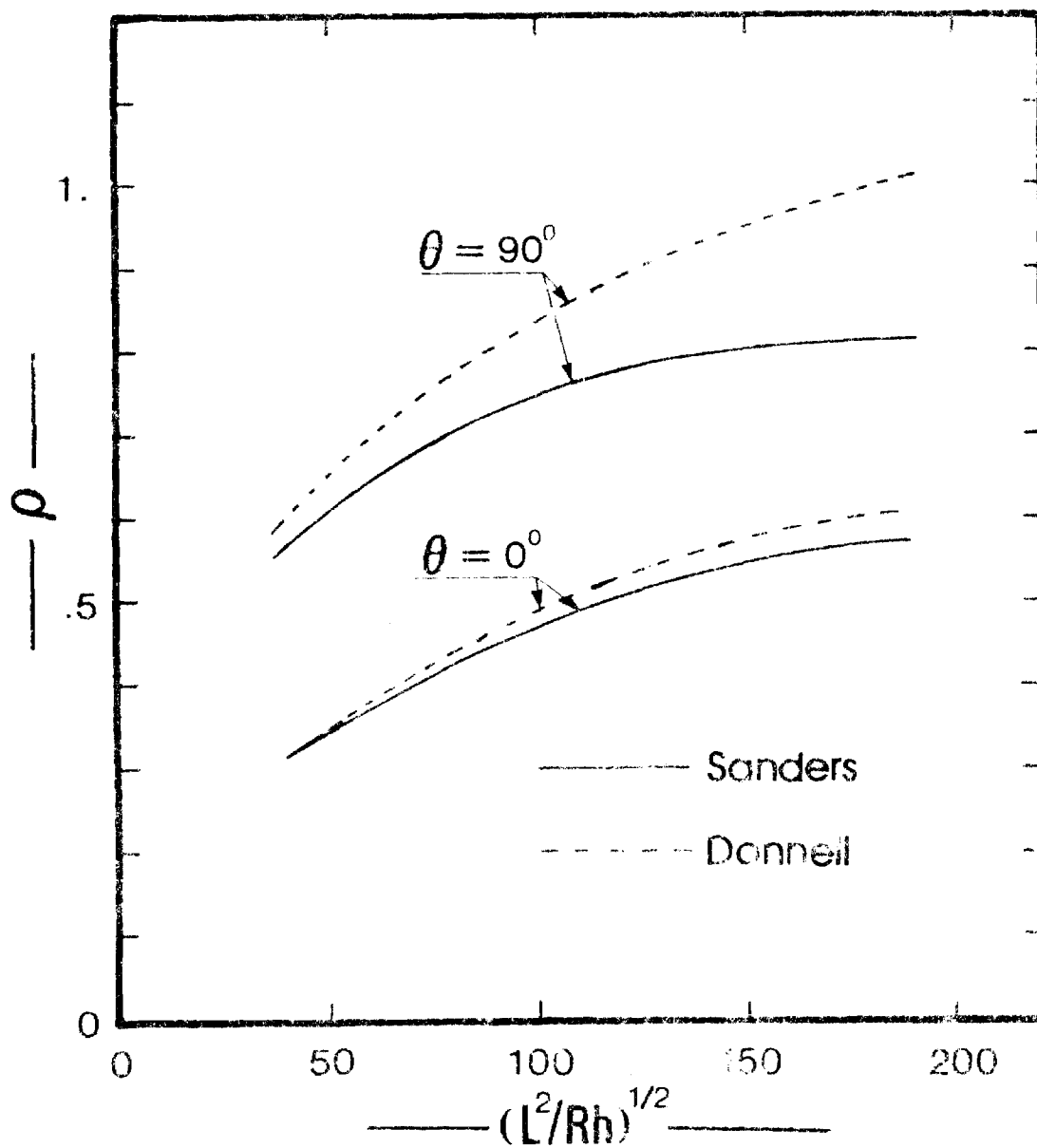


Fig. 5. Load Parameter ρ ($= \bar{N}_{xx}^l / \bar{N}_{xx_{cl}}$) vs. $(L^2/Rh)^{1/2}$
(Orthotropic Geometry; SS-3; Sym. Imp.)

Laminated Geometry

For this geometry, the symmetric imperfection shape, Eq. (20), and the geometric and material properties are presented in a previous article.

This geometry is taken from (21) in which experimental results are reported for $L/R = 2$. Note also that because of the stacking (symmetric and $\pm 45^\circ$), the resulting configuration has $B_{ij} = 0$, and in-plane (A_{ij}) and bending (D_{ij}) stiffness parameters that are similar to an isotropic configuration.

For this geometry results are generated for several ξ -values (imperfection sensitivity study) and three values of L/R (2,5,10).

The results are presented in tabular (Table 4) and graphical form (Fig. 6).

As seen from Table 4, the trend is the same as for the isotropic geometry. For $L/R = 2$ the two shell theory approximations yield the same critical load for all values of the imperfection amplitude parameter, but different for higher values of L/R . Moreover, the wave number for $L/R = 2$ is six, while for $L/R = 5$ is four, and for $L/R = 10$ is three. The similarity in behavior between the isotropic and the laminated geometries is primarily attributed to the fact that for the laminated geometry $B_{ij} = 0$, $A_{11} = A_{22}$ and $D_{11} = D_{22}$, which makes the elements of the A_{ij} and D_{ij} matrices be similar to the elements of an isotropic configuration.

One important difference is that the critical load for the corresponding perfect laminated geometry appears to be heavily dependent upon the value of L/R (observation made by extrapolation of the curves in Fig. 6). Finally, it is seen from Fig. 6 that the laminated geometry, regardless of the shell theory, becomes more sensitive to initial geometric

imperfections as L/R increases. For $L/R \pm 2$ the curve is rather flat but for $L/R = 10$, the curve drops rapidly. These observations are made on the basis of the generated results (limited), and they should not be generalized.

TABLE 4. CRITICAL LOADS (LAMINATED GEOMETRY)

Critical Load, kN/cm (lbs/in)									
ξ	$L/R = 2$			$L/R = 5$			$L/R = 10$		
	Sanders	n	Donnell	Sanders	n	Donnell	Sanders	n	Donnell
0.5	22.767 (130.00)	6	22.767 (130.00)	25.744 (147.00)	4	26.444 (151.00)	43.783 (250.00)	3	63.047 (360.00)
1.0	20.665 (118.00)	6	21.103 (120.50)	22.767 (130.00)	4	24.518 (140.00)	33.275 (190.00)	3	45.534 (260.00)
2.0	17.368 (98.60)	6	17.391 (99.30)	19.264 (110.30)	4	21.366 (122.00)	26.270 (150.00)	3	35.902 (205.00)

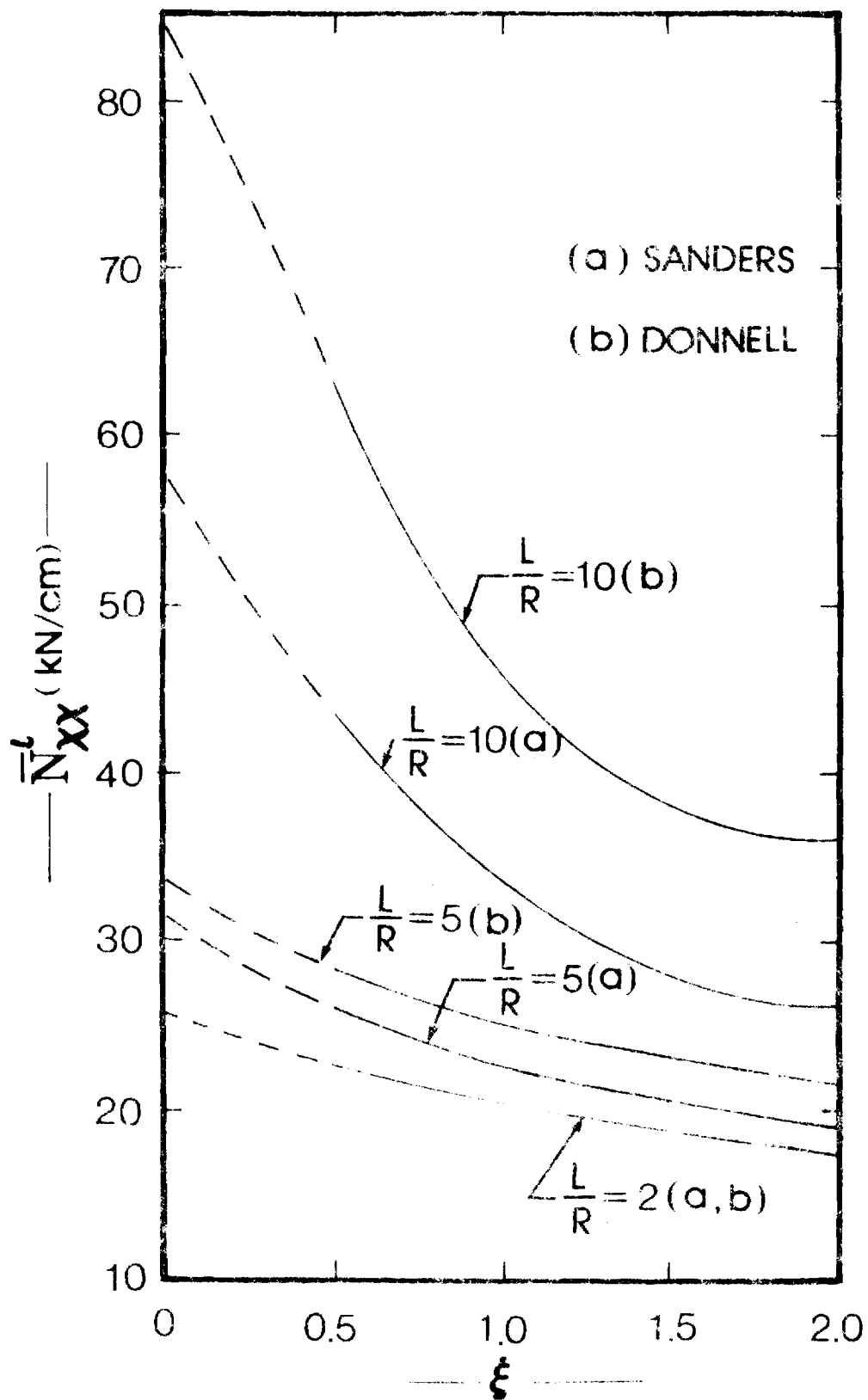


Fig. 6. Critical Loads for the Laminated Geometry
(SS-3; Symmetric Imp.)

CHAPTER IV

ADDITIONAL RESULTS; w,F - FORMULATION

In addition to the results reported in Chapter III, certain parametric studies were performed by employing the w,F-formulation (Ref. 15). These studies include assessment of imperfection sensitivity and of the effect of lamina stacking on the critical conditions of four-and six-ply laminated cylinders under axial compression and torsion (individually applied). These geometries represent variations of two symmetric geometries reported in Ref. 21. Moreover, the effect of L/R-ratios on critical loads is assessed for the four-ply and the six-ply geometries. In all of these studies the load eccentricity is taken to be zero and the boundaries are simply supported (SS-3). The geometries employed in the parametric studies and the results are next presented, separately.

IV. 1 Description of Geometry

Two basic laminated configurations are used in generating results. They consist of four-ply laminates, I-i, using various stacking sequences, and of six-ply laminates, II-i with different stacking sequences. For both groups five stacking sequences ($i = 1, 2, \dots, 5$) are employed.

First, the common properties of the orthotropic laminae (Boron/Epoxy; AVCO 5505) are:

$$\begin{aligned} E_{11} &= 2.0690 \times 10^8 \text{ kN/m}^2 \text{ (30} \times 10^6 \text{ psi)} \\ E_{22} &= 0.1862 \times 10^8 \text{ kN/m}^2 \text{ (2.7} \times 10^6 \text{ psi)} \\ G_{12} &= 0.0448 \times 10^8 \text{ kN/m}^2 \text{ (0.65} \times 10^6 \text{ psi)} \end{aligned} \quad \nu_{12} = 0.21 \quad (24)$$

Furthermore ,

$$R = 19.05 \text{ cm (7.5 in.)}$$

and the length, L , is varied so that

$$L/R = 1, 3 \text{ and } 5.$$

The ply thicknesses ($h_k - h_{k-1}$) and the total laminate thickness for each group is:

$$\text{I-i; } h_k - h_{k-1} = 0.013462 \text{ cm (0.0053 in.)} \quad (25a)$$

$$h = 4(h_k - h_{k-1}) = 0.05385 \text{ cm. (0.0212 in.)}$$

$$\text{and II-i; } h_k - h_{k-1} = 0.008975 \text{ cm (0.003533 in.)} \quad (25b)$$

$$h = 6(h_k - h_{k-1}) = 0.05385 \text{ cm (0.0212 in.)}$$

Note that for both groups (I-i and II-i), the radius to thickness ratio is 353.77 ($=R/h$).

For each group the five stacking combinations are denoted by I-i or II-i, $i = 1, 2, \dots, 5$ and they correspond to

$$\text{I-1} = 45^\circ/-45^\circ/-45^\circ/45^\circ; \text{ I-2: } 45^\circ/-45^\circ/45^\circ/-45^\circ; \quad (26a)$$

$$\text{I-3} = -[\text{I-2}]; \text{ I-4: } 90^\circ/60^\circ/30^\circ/0^\circ; \text{ I-5: } 0^\circ/30^\circ/60^\circ/90^\circ$$

$$\text{II-1: } 0^\circ/45^\circ/-45^\circ/-45^\circ/45^\circ/0^\circ$$

$$\text{II-2: } -45^\circ/45^\circ/-45^\circ/45^\circ/-45^\circ/45^\circ/45^\circ$$

$$\text{II-3} = -[\text{II-2}]$$

$$\text{II-4 : } -90^\circ/72^\circ/54^\circ/36^\circ/18^\circ/0^\circ$$

$$\text{II-5 : } 0^\circ/18^\circ/36^\circ/54^\circ./72^\circ/90^\circ$$

(26b)

Where the first number denotes the orientation of the fibers (strong orthotropic direction) of the outermost ply with respect to the x-axis, and the last of the innermost. Note that in the u,v,w -formulation, geometry I-1 (same as in this chapter) is listed as $-45^\circ/45^\circ/45^\circ/-45^\circ$. This is so because the system of reference axes used in the u,v,w -formulation (see Fig. 1) is different from the one employed in the

w,F-formulation (see Ref. 15) [the x-axis is the same as shown on Fig. 1, but the y-and z-axes are opposite from those shown on Fig. 1].

Geometries I-1 and II-1 are symmetric with respect to the midsurface and they are identical to those employed in Ref. 21. Geometries I-2,3 and II-2,3 denote antisymmetric, regular ($h_k - h_{k-1} = \text{constant}$) angle-ply laminates. Finally, geometries, I-4,5 and II-4,5 are completely asymmetric with respect to the midsurface.

Two load cases are considered and for each load case different imperfection shapes are employed. These are:

(α) for uniform axial compression

(a) for geometries I-i ($i = 1, 2 \dots 5$)

$$w^0(x,y) = \frac{1}{2} h \sin \frac{\pi x}{L} \cos \frac{\pi y}{R} \quad (27)$$

(b) for geometries III-i ($i = 1, 2, \dots 5$)

$$w^0(x,y) = \frac{1}{2} h \left(-\cos \frac{2\pi x}{L} + 0.1 \sin \frac{\pi x}{L} \cos \frac{\pi y}{R} \right) \quad (28)$$

Note that the first one, Eq. (27) denotes a symmetric shape, while the second one, Eq. (28), an (almost) axisymmetric shape.

(β) for torsion

(a) for $L/R = 1$

$$\begin{aligned} \text{I-i: } w^0(x,y) = 0.6235383 \frac{1}{2} h & \left[\left(\sin \frac{\pi x}{L} - \frac{1}{3} \sin \frac{3\pi x}{L} \right) \cos \frac{\pi y}{R} \right. \\ & \left. + \left(\sin \frac{2\pi x}{L} - \frac{1}{2} \sin \frac{4\pi x}{L} \right) \sin \frac{\pi y}{R} \right] \end{aligned} \quad (29a)$$

$$\begin{aligned} \text{II-i: } w^0(x,y) = \frac{1}{2} h & \left[-0.583133 \left(\sin \frac{\pi x}{L} - \frac{1}{3} \sin \frac{3\pi x}{L} \right) \cos \frac{\pi y}{R} \right. \\ & \left. + 0.647926 \left(\sin \frac{2\pi x}{L} - \frac{1}{2} \sin \frac{4\pi x}{L} \right) \sin \frac{\pi y}{R} \right] \end{aligned} \quad (29b)$$

(b) for $L/R = 2$ and both groups

$$\begin{aligned} w^0(x,y) = \frac{1}{2} h & \left[-0.536769 \left(\sin \frac{\pi x}{L} - \frac{1}{3} \sin \frac{3\pi x}{L} \right) \cos \frac{\pi y}{R} \right. \\ & \left. + 0.670961 \left(\sin \frac{2\pi x}{L} - \frac{1}{2} \sin \frac{4\pi x}{L} \right) \sin \frac{\pi y}{R} \right] \end{aligned} \quad (30)$$

(c) for $L/R = 5$ and both groups

$$w^0(x,y) = \frac{1}{8} h \left[-0.417060 \left(\sin \frac{\pi x}{L} - \frac{1}{3} \sin \frac{3\pi x}{L} \right) \cos \frac{\pi y}{R} \right. \\ \left. + 0.694444 \left(\sin \frac{2\pi x}{L} - \frac{1}{2} \sin \frac{4\pi x}{L} \right) \sin \frac{\pi y}{R} \right. \\ \left. + 0.833333 \left(\frac{1}{3} \sin \frac{3\pi x}{L} - \frac{1}{5} \sin \frac{5\pi x}{L} \right) \cos \frac{\pi y}{R} \right] \quad (31)$$

For this load case (torsion), the imperfection shape is taken to be similar to the linear theory buckling mode (see Ref. 15). These shapes, Eqs. (29), (30), and (31), represent some average of the modes of the various configurations (the modes are very similar for all configurations).

IV.2 Discussion of Results

The results for all configurations are presented both graphically and in tabular form. Each group through, is discussed separately.

Table 5 presents critical loads (limit point loads-uniform axial compression) for geometries I-i and three values of L/R (1,2 and 5). The imperfection shape for this group is symmetric, Eq. (27), and the amplitude parameter is varied from a small number up to two ($w^0_{max}/h = \frac{2}{8}$). The values obtained from the w,F -formulation differ slightly from those obtained by the u,v,w -formulation (see Table 4). The difference is not caused by the two different formulations (both based on Donnell equations), but it is attributed to the fact that the load step in the u,v,w -formulation is larger than in the w,F -formulation. This is so, because it is much more expensive (in time and money) to run the program for the former formulation. It is seen from Figs. 7-9 that, for $L/R = 1$ and small values for $\frac{2}{8}$ ($\frac{2}{8} < 0.75$), the weakest configuration corresponds to I-2,3 (regular antisymmetric angle-ply laminate), while the strongest configuration is the

TABLE 5. CRITICAL LOADS; UNIFORM AXIAL
COMPRESSION (I-i GEOMETRIES)

Geometry	ξ	\bar{N}_{xx}^l in lbs/in (wave No. at Limit Pt.)		
		L/R = 1	L/R = 2	L/R = 5
I - 1	0.05	-	145.6 (6)	-
	0.10	130.7 (9)	-	153.7 (4)
	0.50	118.9 (9)	136.0 (6)	147.7 (4)
	1.00	104.5 (9)	123.0 (6)	135.9 (4)
	2.00	67.1 (9)	98.3 (6)	121.0 (4)
I - 2,3	0.05	-	138.8 (6)	-
	0.10	126.7 (9)	-	145.3 (4)
	0.50	115.1 (9)	130.0 (6)	140.2 (4)
	1.00	98.6 (9)	118.7 (6)	129.0 (4)
	2.00	61.3 (9)	92.2 (6)	111.4 (4)
I-4	0.01	-	243.1 (8)	-
	0.05	-	232.0 (8)	245.4 (5)
	0.10	189.9 (12)	-	-
	0.50	130.7 (11)	178.0 (8)	211.5 (5)
	1.00	86.8 (11)	137.2 (8)	187.7 (5)
	2.00	46.1 (10)	90.0 (8)	153.4 (5)
I-5	0.05	-	233.3 (8)	292.9 (5)
	0.10	183.3 (11)	-	-
	0.50	146.3 (11)	191.0 (8)	268.3 (5)
	1.00	97.5 (12)	150.0 (8)	239.0 (5)
	2.00	48.0 (11)	109.5 (8)	194.0 (5)

Symmetric Imperfection

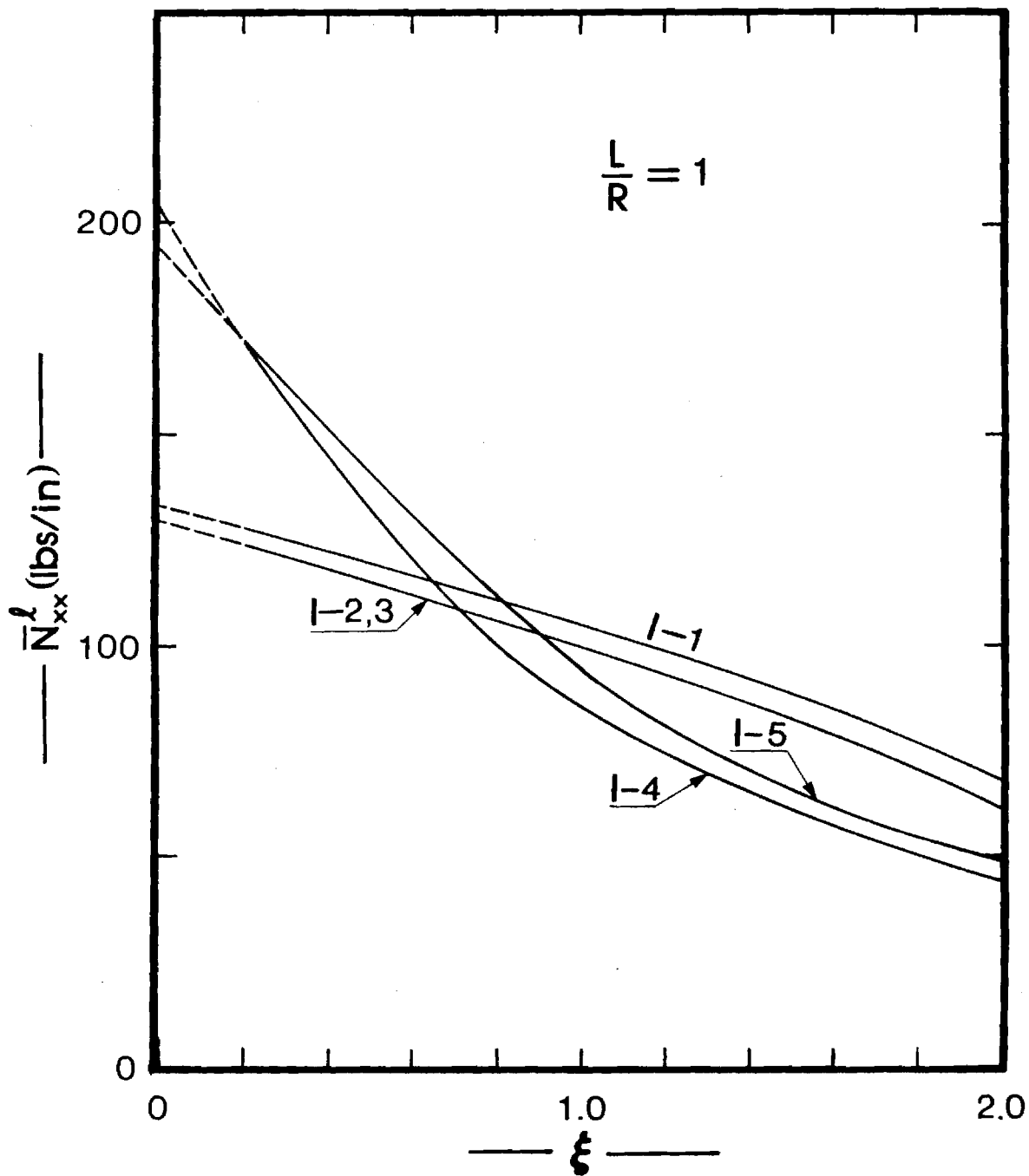


Fig. 7. Critical Conditions for I-i Geometries;
Uniform Axial Compression; $L/R = 1$
(SS-3; Symmetric Imp.)

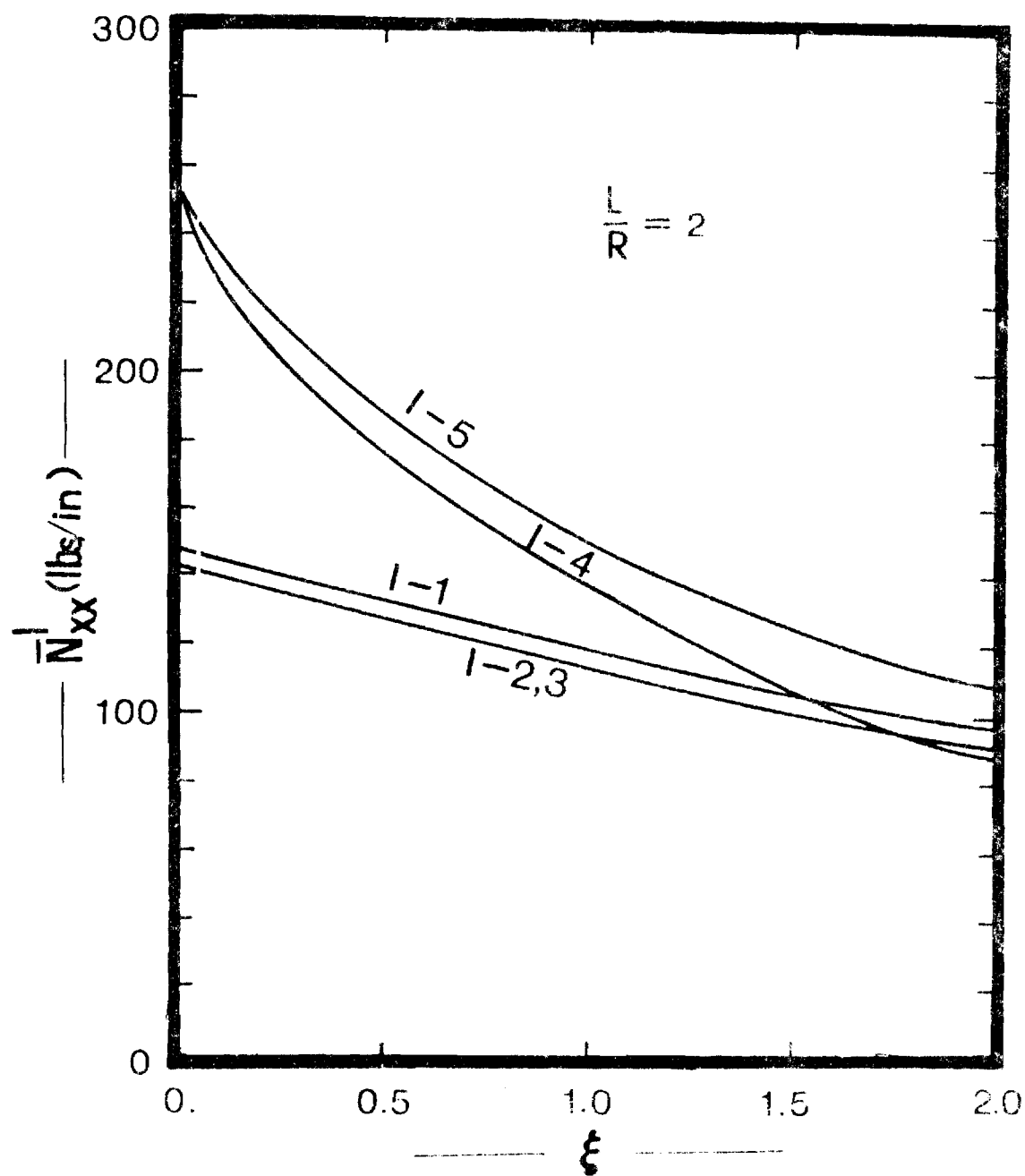


Fig. 8 Critical Conditions for I-i Geometries;
Uniform Axial Compression; $L/R = 2$
(SS-3; Symmetric Imp.)

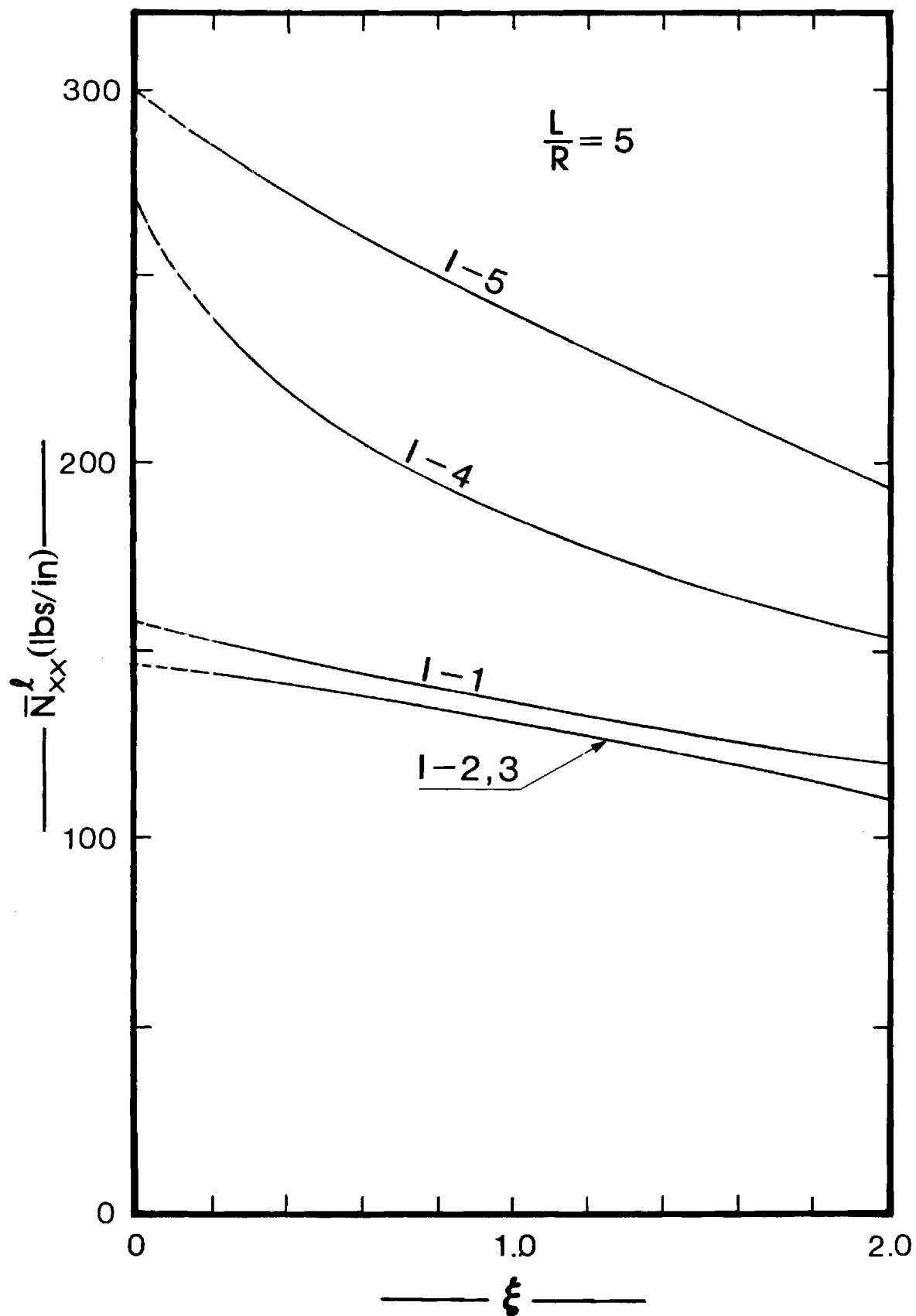


Fig. 9. Critical Conditions for I-i Geometries;
Uniform Axial Compression; $L/R = 5$
(SS-3; Symmetric Imp.)

asymmetric I-5 (except for a very small range of extremely small ξ - values). But, as L/R increases, I-2,3 yields the weakest configurations for virtually all ξ -values. Moreover, for $L/R > 2$ the order of going from the weakest to the strongest configuration is I-2,3, I-1,I-4 and I-5. Note that asymmetric stacking may be compared to eccentric positioning of the orthogonal stiffeners in metallic shells.

Table 6 presents critical loads (uniform compression) for geometries II-i. The results are similar to those for group I (geometries I-i) but with one exception; geometry II-1 is among the strong configurations, while I-1 is among the weak configurations, especially for higher L/R ratios (see Figs. 10-12 and 7-9). The reason for this is that the II-1 geometry has 0° plies on the outside and inside of the laminate, which increases its stiffness in the axial direction.

The results, for this group, are also presented graphically on Figs. 10-12. Fig. 10 contains results for $L/R = 1$. No results are reported (limit points could not be found) for $\xi > 1.0$. This implies, that for this L/R value and $\xi > 1$ the load-deflection curve does not exhibit limit point instability, but only stable response. For $L/R \geq 2$, the picture changed and limit points are found. Note from the three figures, Figs. 10-12, that as L/R increases the imperfection sensitivity of all configurations decreases (the curves do not fall as sharply as they do for $L/R = 1$).

It is worth noticing that for $L/R \leq 2$, there are many crossings of the curves and it is not easy to identify the strongest or the weakest configuration (which is ξ -dependent). On the other hand, at $L/R = 5$, the strongest configuration is II-5 and the order of going from the strongest to the weakest is, II-5 , II-1 , II-4 , II-2,3. As expected, the $\pm 45^\circ$

TABLE 6. CRITICAL LOADS; UNIFORM AXIAL
COMPRESSION (II-i GEOMETRIES)

Geometry	ξ	N_{xx}^{ℓ} in lbs/in. (wave No. at Limit Pt)		
		L/R = 1	L/R = 2	L/R = 5
II-1	0.10	231.7 (12)	244.86 (8)	255.6 (5)
	0.50	120.9 (11)	171.3 (8)	219.4 (5)
	1.00	63.4 (10)	112.5 (8)	182.7 (5)
	2.00	-	58.4 (7)	128.2 (5)
II - 2,3	0.10	133.5 (9)	140.5 (6)	150.8 (4)
	0.50	120.7 (9)	134.6 (6)	147.8 (4)
	1.00	87.2 (9)	114.1 (6)	136.2 (4)
	2.00	44.7 (8)	72.6 (6)	111.4 (4)
II - 4	0.10	177.7 (10)	211.3 (8)	227.0 (5)
	0.50	101.7 (10)	157.0 (7)	199.3 (5)
	1.00	57.9 (10)	108.7 (7)	171.0 (5)
	2.00	-	56.8 (7)	128.8 (5)
II-5	0.10	173.5 (11)	199.5	275.0 (5)
	0.50	124.0 (10)	191.3	261.7 (5)
	1.00	66.7 (10)	139.0	227.9 (5)
	2.00		70.4 (7)	168.4 (5)

Axisymmetric Imperfection

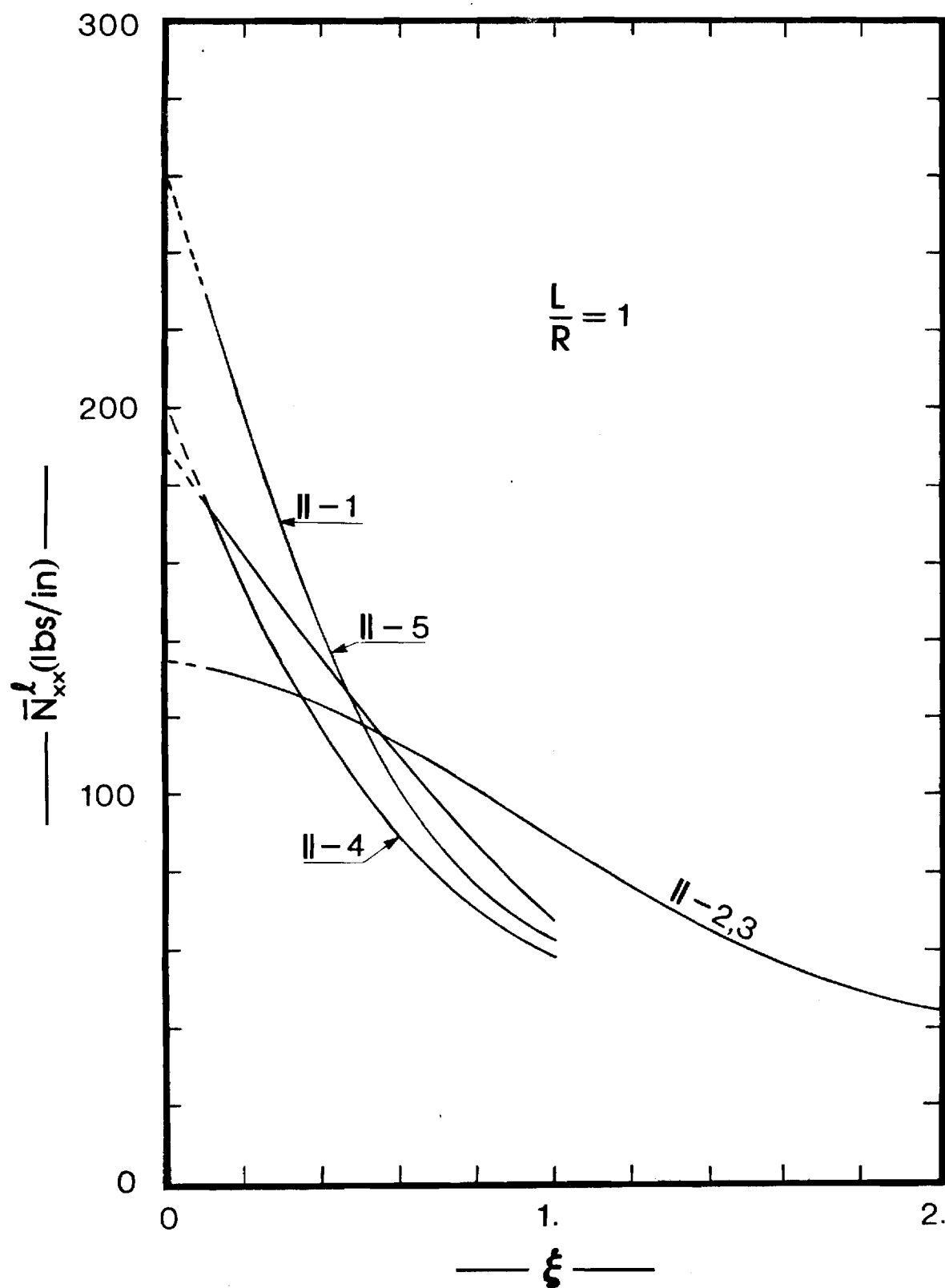


Fig. 10. Critical Conditions for II-i Geometries;
Uniform Axial Compression; $L/R = 1$
(SS-3; Axisymmetric Imp.)

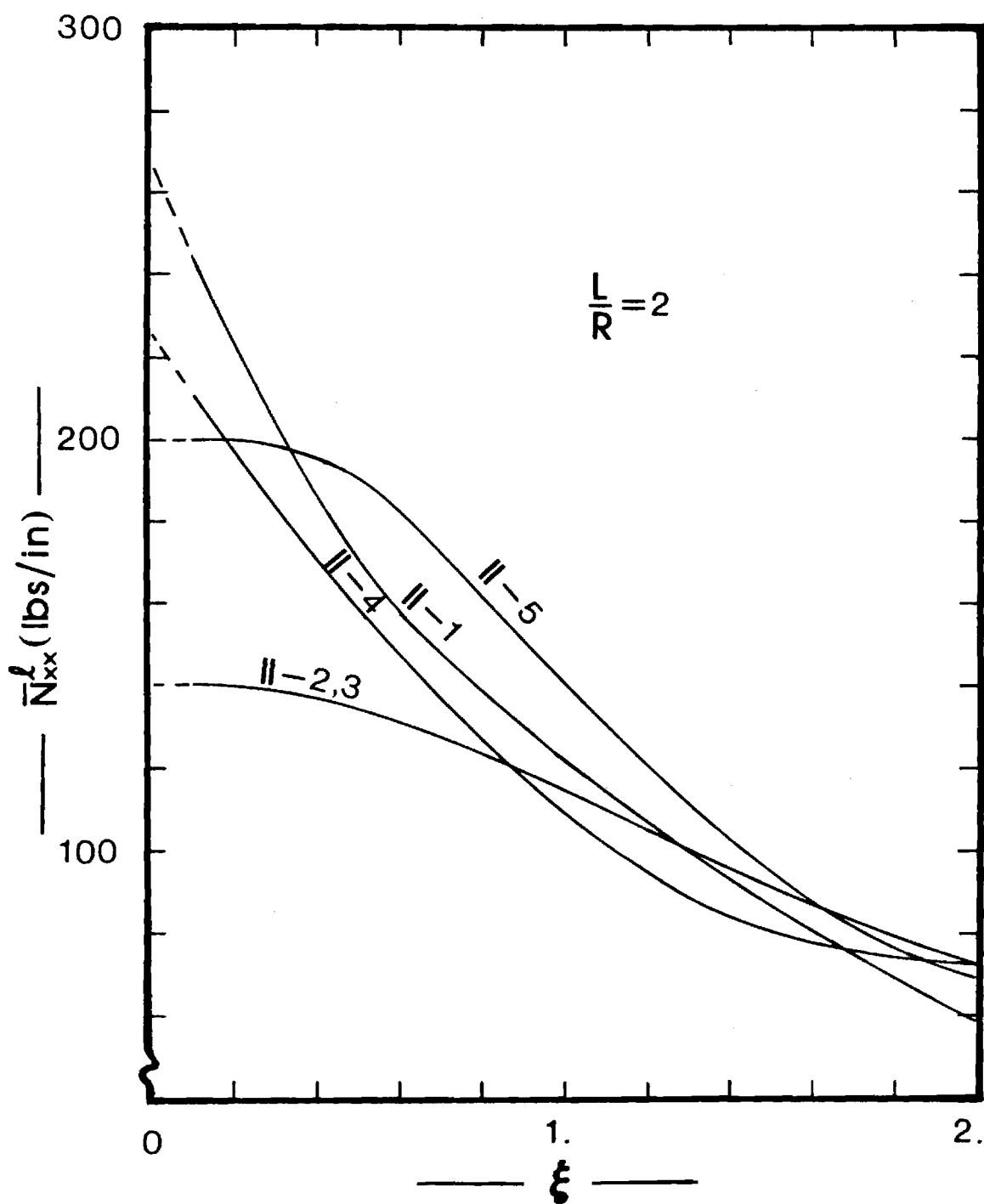


Fig. 11. Critical Conditions for II-i Geometries;
Uniform Axial Compression; $L/R = 2$
(SS-3; Axisymmetric Imp.)

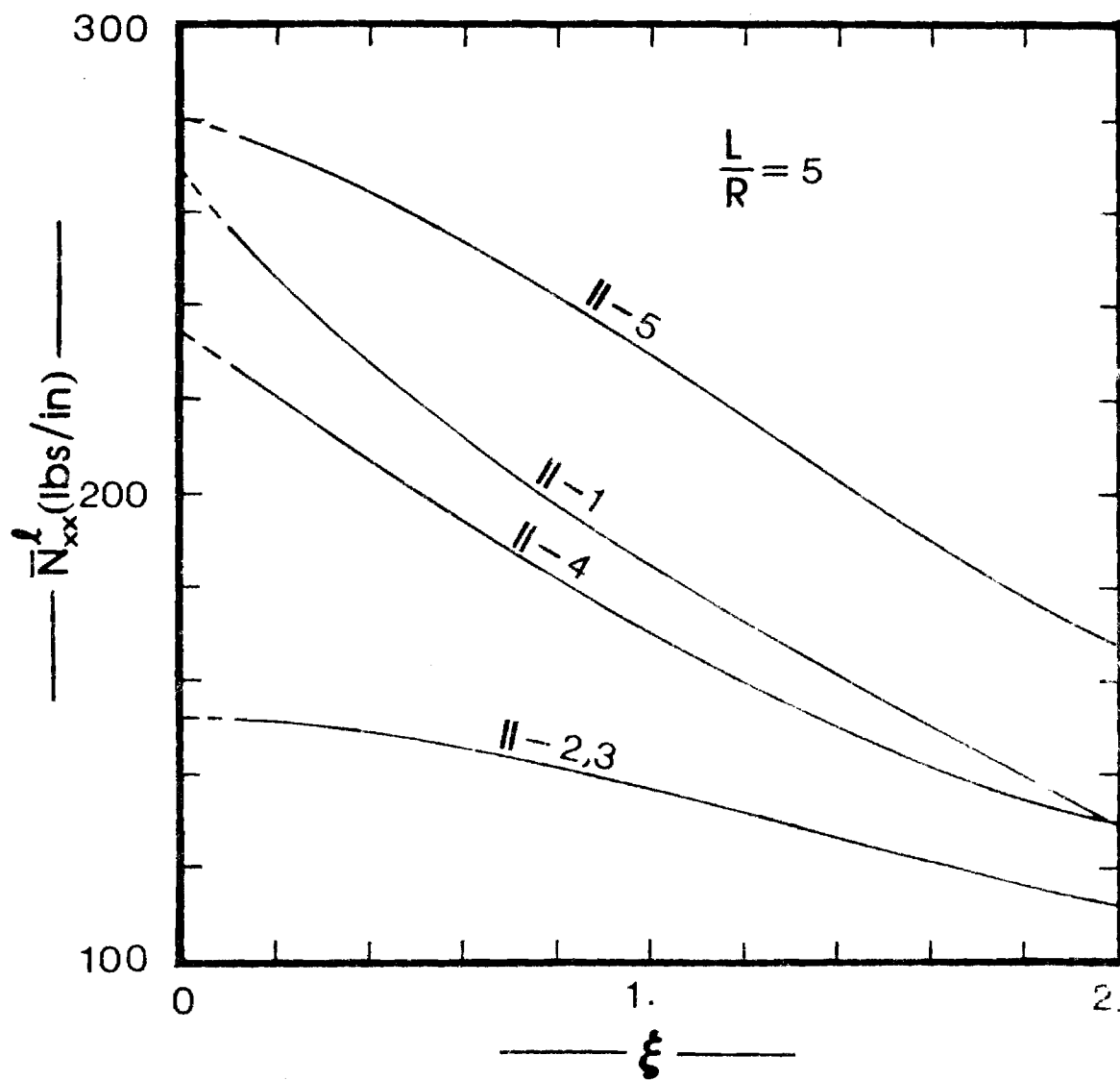


Fig. 12. Critical Conditions for II-i Geometries
 Uniform Axial Compression; $L/R = 5$
 (SS-3; Axisymmetric Imp.)

antisymmetric laminate is not the best layup for resisting axial compression.

Table 7 presents critical loads for geometries I-i subjected to torsion. The results are also presented graphically on Figs. 13-15. The reader is reminded that the imperfection shape for this load case is similar to the linear theory eigenmode (see Ref. 15) and it is L/R -dependent. Regardless of the shape, the imperfection parameter, ξ , is equal to w_{\max}/h . For all L/R values the I-1 geometry seems to be the weakest one. On the other hand, geometry I-5 yields the strongest configuration. For $L/R = 1$ the I-2,3 configurations seem strong, but as L/R increases they become weaker by comparison to the asymmetric configurations. If torsion were to be reversed the strength of the I-2,3 configurations would remain unchanged (the role of I-2 and I-3 would be interchanged), while the asymmetric configurations could change for the worse. The reason for this expectation is that for positive torsion, tension is expected along a direction making a positive angle with the x-axis (for isotropic construction it would have been $\approx 45^\circ$). The fibers are placed from 0° to 90° or from 90° to 0° in the various layers of I-5 and I-4. Thus, the tensile unidirectional strength of the fibers is utilized. If the torsion is reversed, these same fibers would tend to be in compression and this would imply that I-4 and I-5 are weaker for negative torsion than for positive torsion. Of course no mention is made of the effect of the (negative torsion) imperfection shape. This could be a totally separate study. Along these lines, note that the I-1 geometry (see Ref. 15) is stronger when loaded in the negative direction than in the positive direction, provided that the imperfection shape is similar to the positive torsion buckling mode.

TABLE 7. CRITICAL LOADS; TORSION
(I - i GEOMETRIES)

Geometries	ξ	\bar{N}_{xy}^l in lbs/in (wave No. at Limit Pt.)		
		L/R = 1	L/R = 2	L/R = 5
I - 1	0.1	55.34 (15)	35.32 (11)	21.00 (7)
	0.5	45.36 (15)	31.57 (11)	19.43 (7)
	1.0	43.62 (15)	28.32 (11)	18.01 (7)
I - 2	0.1	78.90 (13)	46.4 (9)	24.91 (6)
	0.3	73.16 (13)	-	-
	0.5	66.36 (13)	41.81 (9)	23.15 (6)
	1.0	-	37.89 (9)	21.57 (6)
I - 3	0.1	79.34 (13)	46.36 (9)	24.84 (5)
	0.3	73.41 (13)	-	-
	0.5	66.50 (13)	41.84 (9)	23.08 (6)
	1.0	-	37.96 (9)	21.51 (6)
I-4	0.1	56.69 (16)	44.18 (12)	29.81 (8)
	0.5	45.91 (15)	38.75 (12)	27.16 (8)
	1.0	39.51 (14)	34.22 (12)	24.74 (8)
I-5	0.1	84.83 (16)	66.49 (12)	42.91 (8)
	0.5	64.20 (16)	56.91 (12)	38.50 (8)
	1.0	46.79 (15)	48.72 (12)	34.27 (8)

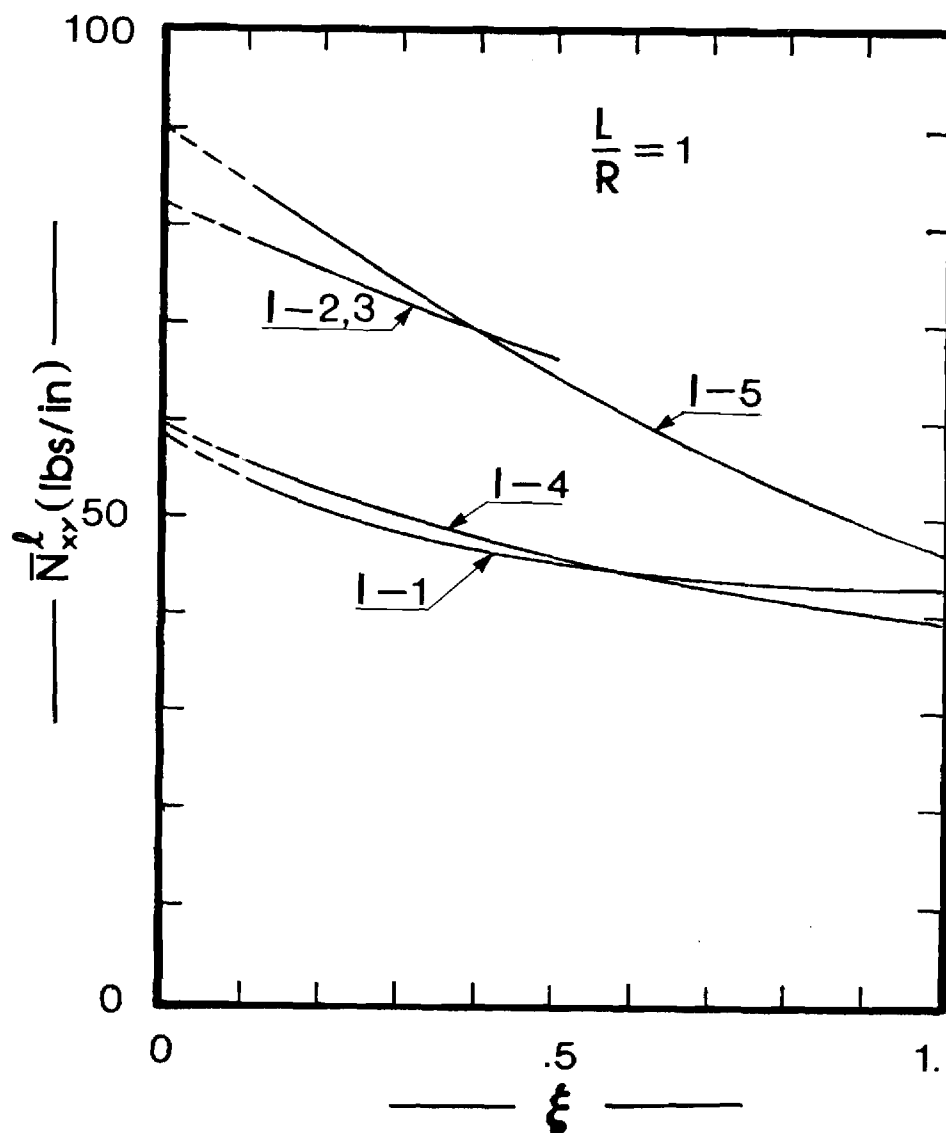


Fig. 13. Critical Conditions for I-i Geometries; Torsion; $L/R = 1$ [(SS-3; Imp. - Eq. (29a))]

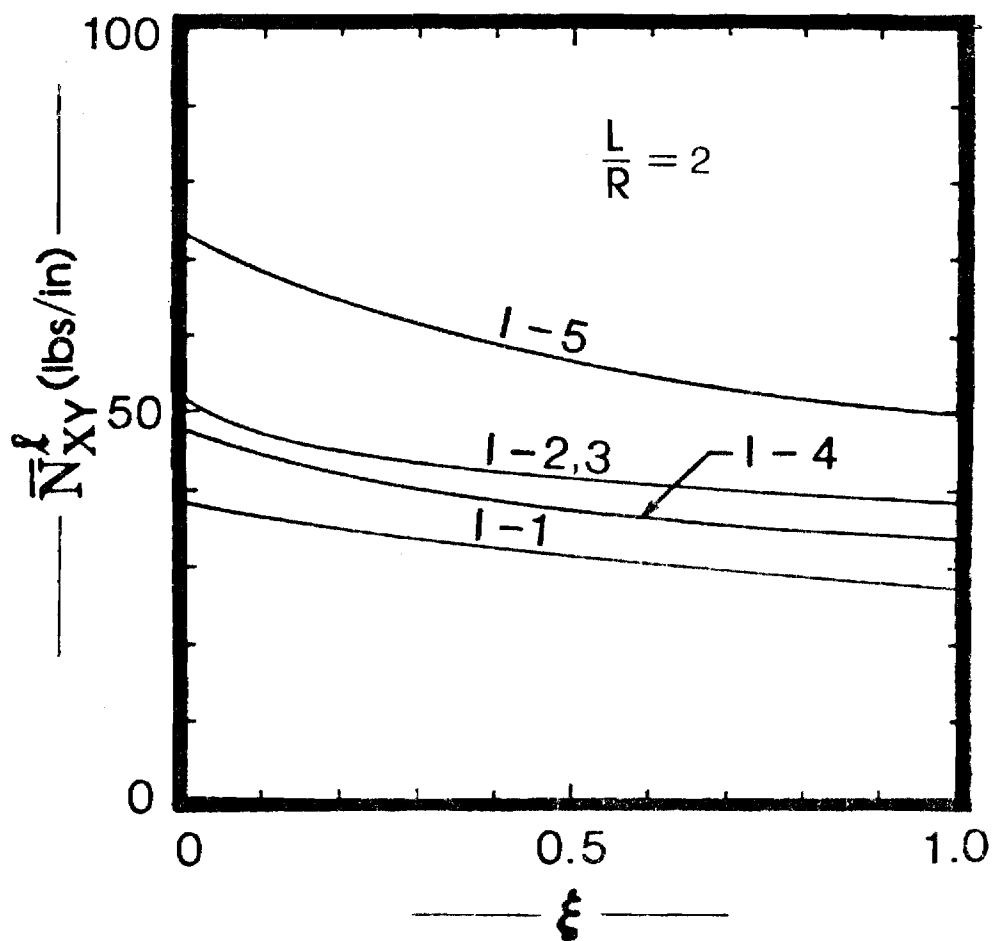


Fig. 14. Critical Conditions for I-i Geometries;
Torsion; $L/R = 2$ [SS-3; Imp. - Eq. (30)].

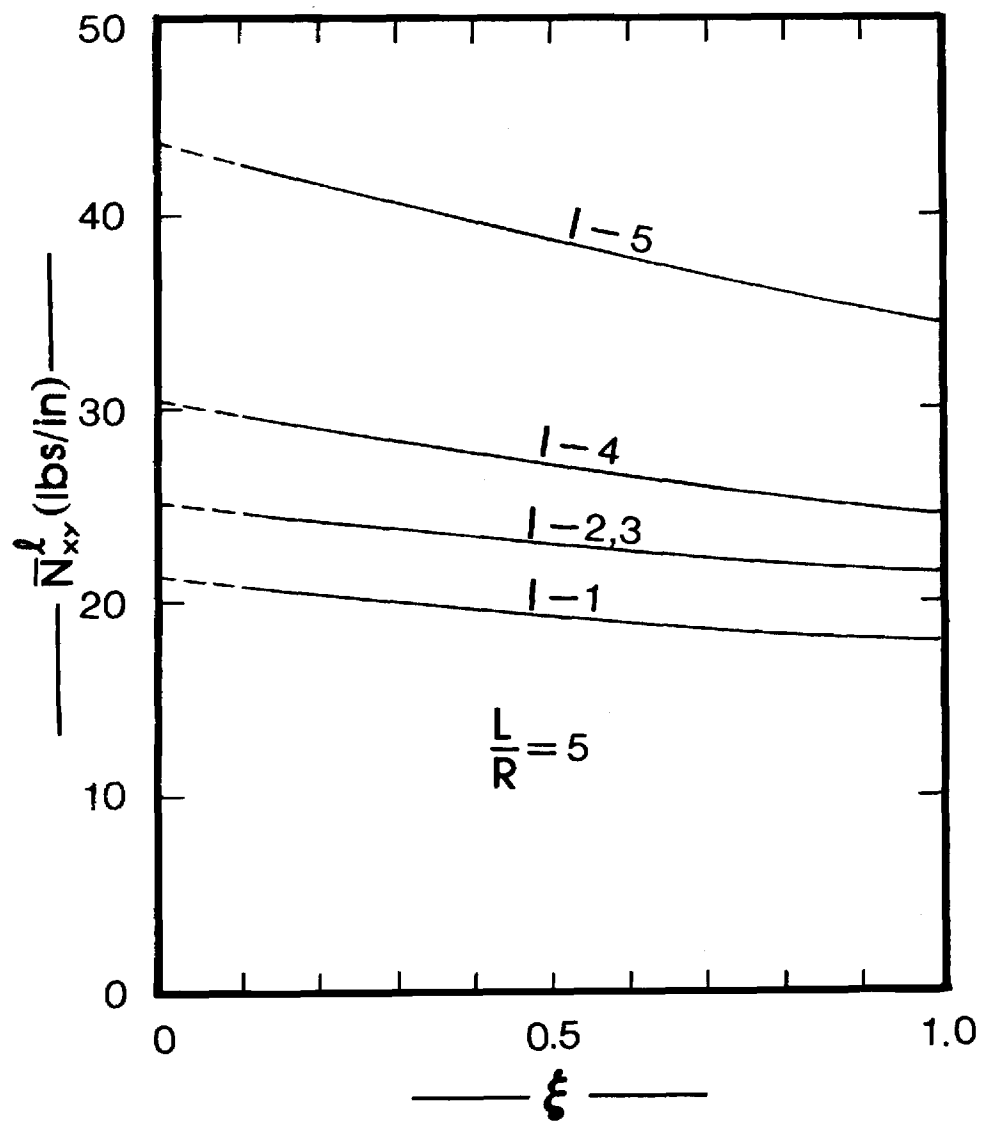


Fig. 15. Critical Conditions for I-i Geometries;
Torsion; $L/R = 5$ [SS-3; Imp. - Eq. (31)]

TABLE 8. CRITICAL LOADS: TORSION
(II-i GEOMETRIES)

Geometry	ξ	N_{xx}^{ℓ} in lbs/in (wave No. at Limit Pt)		
		L/R = 1	L/R = 2	L/R = 5
II-1	0.1	53.54 (18)	38.49 (13)	25.50 (9)
	0.5	43.49 (17)	31.74 (13)	23.10 (9)
	1.0	40.15 (17)	27.17 (13)	20.92 (9)
II-2	0.1	82.46 (14)	48.25 (9)	26.17 (6)
	0.3	73.194 (13)	-	-
	0.4	69.76 (12)	-	-
	0.5	-	42.43 (9)	24.50 (6)
	1.0	-	37.31 (9)	23.00 (6)
II-3	0.1	82.12 (13)	48.25 (9)	26.22 (6)
	0.3	73.07 (13)	-	-
	0.4	69.69 (13)	-	-
	0.5	-	42.45 (9)	24.55 (6)
	1.0	-	37.40 (9)	23.06 (6)
II-4	0.1	57.13 (16)	44.11 (12)	29.69 (8)
	0.5	44.23 (15)	37.73 (12)	27.36 (8)
	1.0	37.46 (15)	32.54 (11)	25.29 (8)
II-5	0.1	81.19 (16)	63.61 (13)	41.96 (8)
	0.5	56.42 (16)	52.33 (12)	38.10 (8)
	1.0	42.23 (14)	41.38 (13)	34.51 (8)

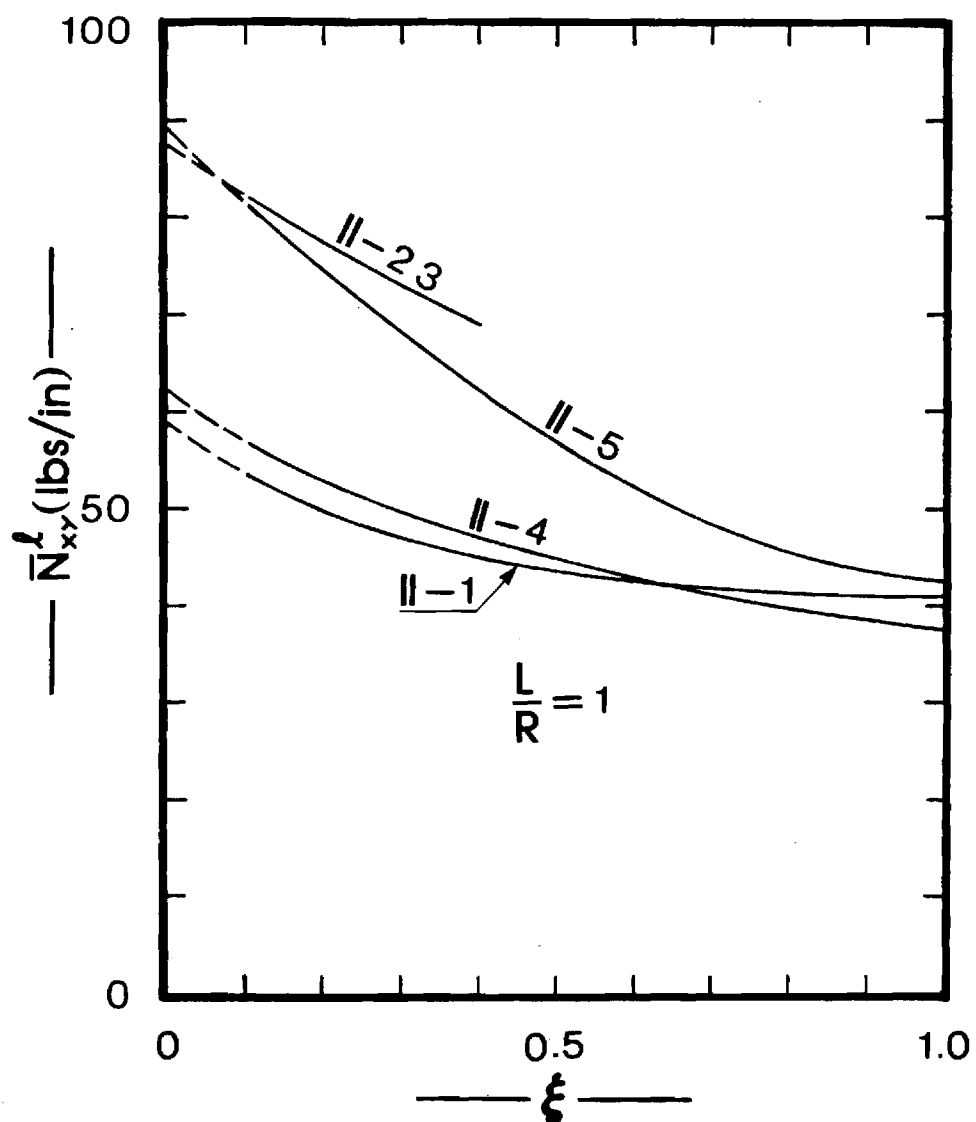


Fig. 16. Critical Conditions for II-i Geometries; Torsion; $L/R = 1$ [SS-3; Imp. - Eq. (29b)]

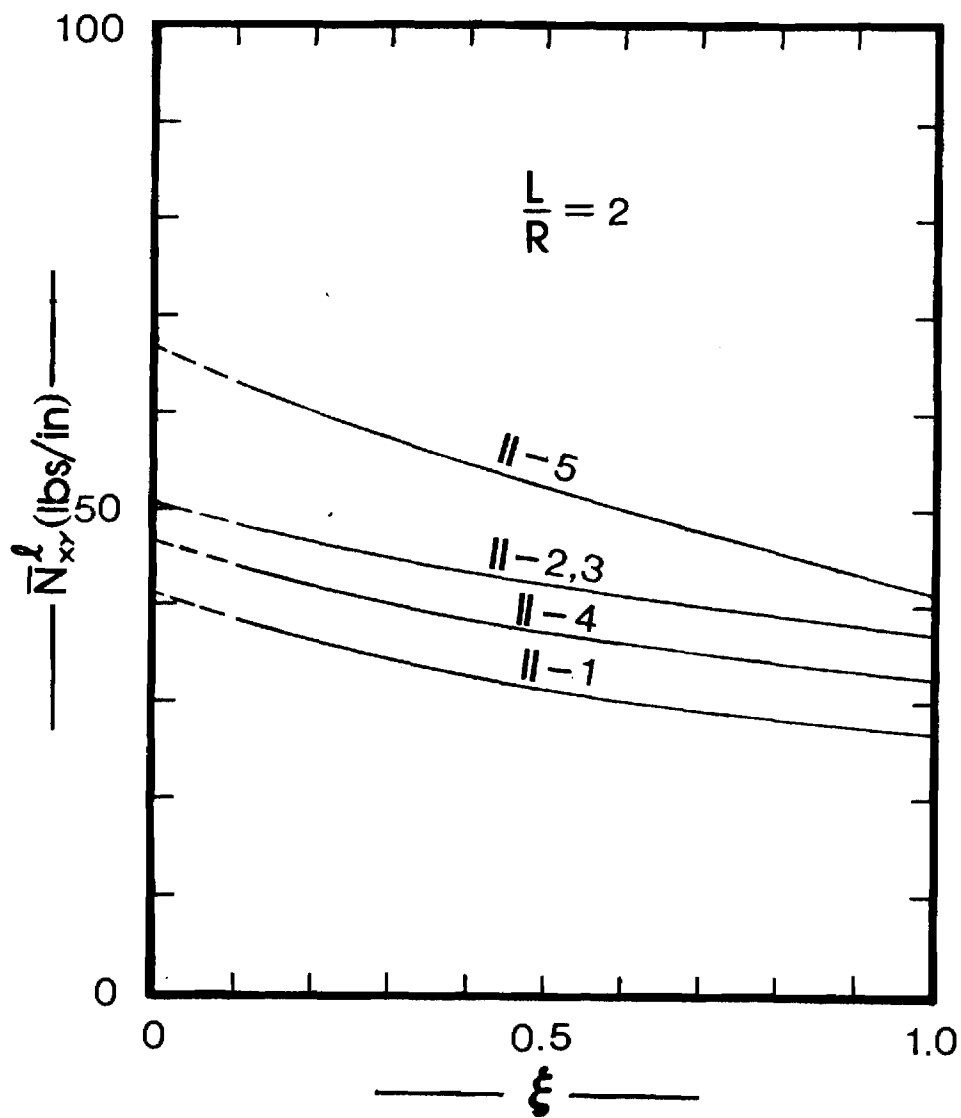


Fig. 17. Critical Conditions for II-i Geometries; Torsion; $L/R = 2$ [SS-3; Imp.- Eq. (30)].

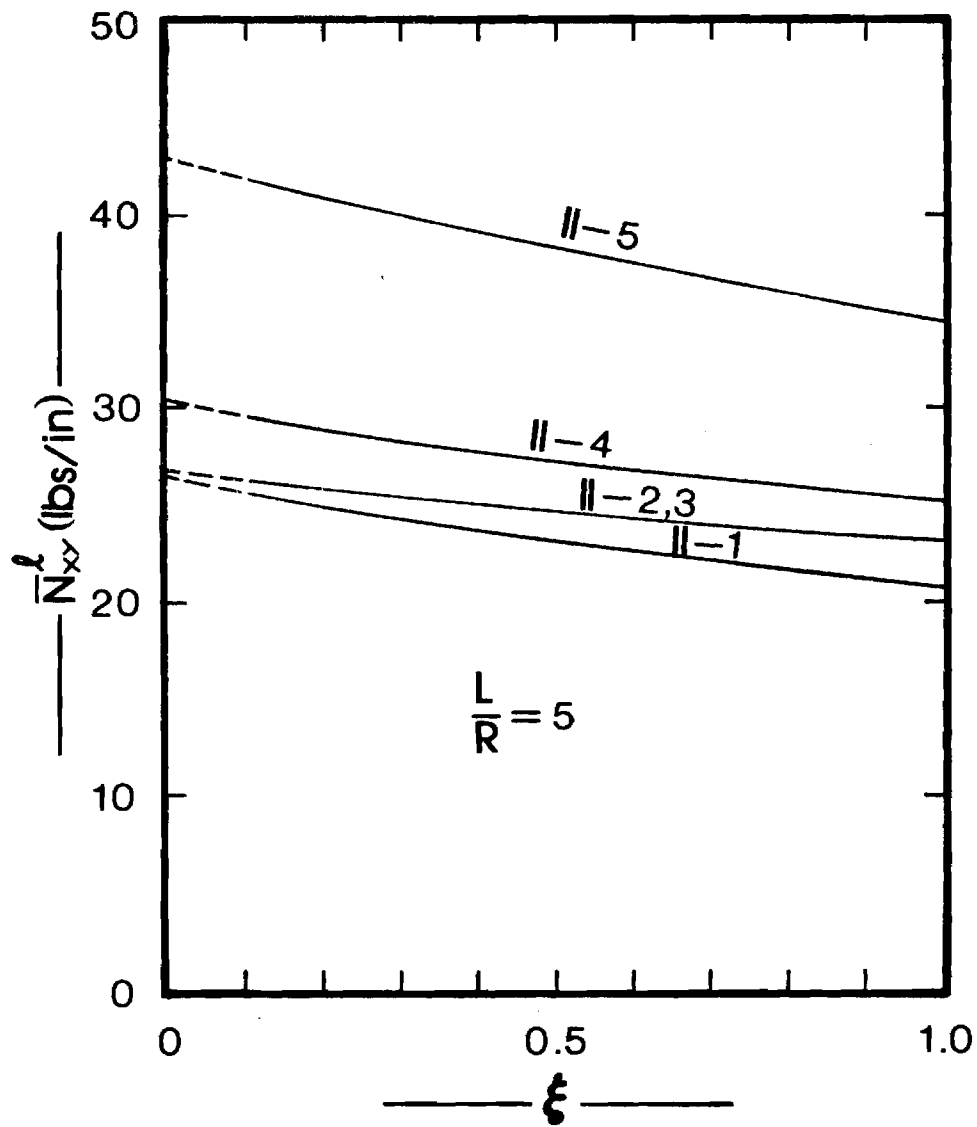


Fig. 18. Critical Conditions for II=i Geometries;
Torsion; $L/R = 5$ [SS-3; Imp. - Eq. (31)].

Table 8 presents critical torques for geometries II-i. The results are also presented graphically on Figs. 16-18. The conclusions are very similar to those for geometries I-i. There is one important observation though derived from the comparison of the two groups. Since both groups have the same total thickness (0.0212 in.) and radius (7.5 in.) use of more layers (from four to six) increases the load carrying capacity for the antisymmetric configurations (II-2,3 versus I-2,3), but it decreases it for the asymmetric configuration II-5 (it can even be said for II-4). The comparison between II-1 and I-1 is not valid, since II-1 contains two 0°-plies (outer and inner), while I-1 has no such plies.

Finally, when the curves (see Figs. 13 and 16) terminate at $\xi = 0.5$, it means that no limit point could be found for higher ξ -values.

Experimental results do exist for some of the configurations discussed in this section (see Ref. 21). These along with other experimental findings are discussed in the next section.

IV.3 Comparison with Experimental Data

The best means for establishing confidence in an analytical method is to compare it with experimental results, obtained by researchers not connected in any manner with those who developed the analytical procedure.

The purpose of the present section is to present such a comparison. The literature was searched and two sets of experimental results are found; (a) those for which the imperfect geometry is described in terms of imperfection shape and amplitude and (b) those for which there is no data describing the initial geometric imperfection. Moreover, the load cases considered are uniform axial compression and torsion, applied either individually or in combination.

The comparison for class (a) (above) is direct, because both the shape and the amplitude of the initial geometric imperfection are known. On the other hand for class (b) geometries, the comparison is made by assuming a shape for the initial geometric imperfection and by varying the amplitude from some small fraction of the total thickness (five or ten percent to approximately 50% of the total thickness). Clearly, for this latter class of imperfect geometries, the comparison is more qualitative.

IV.3.1 Description of Geometry

Experimental results, used herein for comparison with theoretical predictions, are obtained from four sources. The first source is an unpublished paper presented by Professor Shigeo Kobayashi at the AIAA/ASME/ASCE/AHS 23rd SDM Conference in New Orleans in 1982 (Ref. 24). The presentation took place in a "Work in Progress" session (structures). At this presentation the author supplied the audience with an addendum to his abstract which described the experimental results on Graphite-Epoxy Composite cylinders in axial compression. Through this information and private communication that followed, the complete description was secured and is listed herein as Group A. The imperfection amplitude and shape are not known for this group.

The second source (Ref. 25) is a 1976 University of Toronto report in which analytical and experimental results are given for imperfect Glass/Epoxy cylinders subjected to combined loading. Only one set of results is employed herein and it is listed as Group B. Information concerning the imperfection shape and amplitude is provided by the author and listed below. The load case for this group is a combined application of axial compression and torsion.

The third source is a 1974 AIAA Paper (Ref. 21) which presents experimental results for Boron/Epoxy and Graphite/Epoxy imperfect cylinders subjected to axial compression and torsion, applied either individually or in combination. Certain geometries, from this reference are employed herein. These configurations are listed below as Group C. Information is not provided for the imperfection shapes and amplitudes.

Finally, the last source is a 1973 Journal of Spacecraft paper (Ref. 26), which describes experimental and theoretical results on axially-loaded Glass/Epoxy imperfect cylinders. This work was also performed at the University of Toronto under the direction of Professor Tennyson. Three geometries from this source are employed herein and they constitute Group D. The imperfection shape and amplitude are supplied by Ref. 26.

In describing each group, information concerning the following is provided: Load case, number of plies, stacking description and order, material and material properties, ply and laminate thickness, length and radius of the laminate, boundary conditions, and information on the geometric imperfection. Each configuration in a group (if more than one) is listed as case-Li, where i is an integer, and L assumes the letters A, B, C and D (group).

Group A (Kobayashi et al - Ref. 24)

- 1) Load: Uniform Axial Compression
- 2) Material: Graphite/Epoxy
- 3) Material Properties: $E_{11} = 17.40 \times 10^6$ psi;
 $E_{22} = 1.115 \times 10^6$ psi
 $G_{12} = 0.707 \times 10^6$ psi
 $\nu_{12} = 0.32$

- 4) Diameter and Length: $2R = 7.874$ in.; $L = 7.874$ in.
- 5) Boundary Conditions: CC-4 ($u = \bar{u}$, $v = w = w_{,x} = 0$)
- 6) Imperfection: No information. So far, the data are common for all cases.

Case-A1: A three-ply laminate ($90^\circ/-20^\circ/20^\circ$)

$$h_{\text{ply}} = 0.0055 \text{ in.}, h = 0.0165 \text{ in.}$$

Case-A2: A four-ply laminate ($90^\circ/-45^\circ/-45^\circ/0^\circ$)

$$h_{\text{ply}} = 0.0057 \text{ in.}, h = 0.0228 \text{ in.}$$

Case-A3: A six-ply laminate ($90^\circ/90^\circ/30^\circ/-30^\circ/-30^\circ/30^\circ$)

$$h_{\text{ply}} = 0.0059 \text{ in.},$$

$$h = 0.0354 \text{ in.}$$

Note that all three configurations are asymmetric with respect to the midsurface.

The stacking order starts from the outside of the cylinder and moves inward. Thus, in case-A1 the outer ply strong axis (of orthotropy) makes a 90° angle with longitudinal axis of the cylinder; the next ply makes a -20° and the inner one a 20° angle with the longitudinal axis.

Case-A4: There is a fourth configuration in this group, for which all data are the same as A1, A2, and A3 except for the material properties, thickness and the sequence of stacking. For this case,

$$E_{11} = 16.78 \times 10^6 \text{ psi}; E_{22} = 0.922 \times 10^6 \text{ psi};$$

$$G_{12} = .707 \times 10^6 \text{ psi}; \nu_{12} = 0.32$$

$$h_{\text{ply}} = 0.00667 \text{ in.}; h = 0.04 \text{ in. and the stacking sequence for this six-}$$

$$\text{ply laminate is: } (0^\circ/60^\circ/-60^\circ/-60^\circ/60^\circ/0^\circ)$$

Note that, unlike the other three configurations in this group, this laminate is symmetric with respect to the midsurface.

Group B (Booton, Ref. 25)

- 1) Load: Combined Axial Compression and Torsion.
- 2) Material: Glass/Epoxy
- 3) Material Properties: $E_{11} = 6.32 \times 10^6$ psi;
 $E_{22} = 1.74 \times 10^6$ psi;
 $G_{12} = 0.78 \times 10^6$ psi;
 $\nu_{12} = 0.435$.
- 4) Diameter and Length; $2R = 13.2$ in.; $L = 12.4$ in.
- 5) Boundary Conditions: CC-4 ($u = \bar{u}$; $v = w = \bar{w} = 0$).
- 6) Imperfection: $w^0(x,y) = (0.28)(0.27) \cos \frac{17\pi x}{L}$
(w^0 is positive inward; axisymmetric imperfection).

Only one configuration is used for this group.

Thus, case-B1: A three-ply laminate ($45^\circ/0^\circ/-45^\circ$)

$h_{\text{ply}} = 0.009$ in.; $h = 0.027$ in.

Group C (Wilkins et al. - Ref. 21)

- 1) Load: Combined Axial Compression and Torsion
- 2) Material: Boron/Epoxy and Graphite/Epoxy
- 3) Material Properties:

(i) Boron/Epoxy	(ii) Graphite/Epoxy
$E_{11} = 30.0 \times 10^6$ psi	$E_{11} = 2.17 \times 10^6$ psi
$E_{22} = 2.7 \times 10^6$ psi	$E_{22} = 1.44 \times 10^6$ psi

$$G_{12} = 0.65 \times 10^6 \text{ psi} \quad G_{12} = 0.65 \times 10^6 \text{ psi}$$

$$\nu_{12} = 0.21 \quad \nu_{12} = 0.28$$

- 4) Diameter and Length: $2R = 15 \text{ in.}; L = 15 \text{ in.}$
- 5) Boundary Conditions: SS-3 ($N_{xx} = -\bar{N}_{xx}; v = w = M_{xx} = 0$)
- 6) Imperfection: No information

So far, the data are common for all cases.

Case-C1: A four-ply Boron/Epoxy laminate

$$(45^\circ/-45^\circ/-45^\circ/45^\circ) \quad h_{\text{ply}} = 0.0053 \text{ in.}$$

$$h = 0.212 \text{ in.}$$

Case-C2: A six-ply Graphite/Epoxy laminate

$$(0^\circ/45^\circ/-45^\circ/-45^\circ/0^\circ)$$

$$h_{\text{ply}} = 0.0056 \text{ in.}, h = 0.336 \text{ in.}$$

Note that both configurations are symmetric about the laminate midsurface.

As in Group A, the stacking sequence starts from the outside and moves inward.

Group D (Tennyson and Muggeridge, Ref. 26)

- 1) Load: Uniform Axial Compression
- 2) Material: Glass/Epoxy "Skotchply" (XP250)
- 3) Material Properties: The properties are given separately for each configuration.
- 4) Diameter and Length: $2R = 12.5 \text{ in.}, L = 12.45 \text{ in.}$
- 5) Boundary Conditions: CC-4 ($u = \bar{u}; v = w = w_{,x} = 0$).
- 6) Imperfection: $w^0(x,y) = \frac{5}{8} h \cos \frac{\pi x}{L}$

Note that the laminate thickness (h) wave number (m) and imperfection amplitude (ξ) depend on the configurations (case). Furthermore, the imperfection shape for all configurations, is axisymmetric.

The above data are common to all cases

Case-D1: A three-ply Glass/Epoxy laminate ($0^\circ/70^\circ/-70^\circ$)

$$E_{11} = 5.03 \times 10^6 \text{ psi}; E_{22} = 2.58 \times 10^6 \text{ psi};$$

$$G_{12} = 0.837 \times 10^6 \text{ psi}; \nu_{12} = 0.345$$

$$h_1 = h_2 = h_3 = 0.009 \text{ in (} h_i \text{ thickness of each ply;}$$

from outer to inner: 1, 2, 3).

$$h = 0.027 \text{ in.} \quad = 0.0468$$

$$(\xi = w_{\max}^0/h) ; m = 18 \text{ (see the imperfection expression);}$$

Case 1a of Ref. 26.

Case-D2: A three-ply Glass/Epoxy laminate ($45^\circ/-45^\circ/90^\circ$)

$$E_{11} = 6.109 \times 10^6 \text{ psi};$$

$$E_{22} = 2.69 \times 10^6 \text{ psi}; G_{12} = 0.517 \times 10^6 \text{ psi};$$

$$\nu_{12} = 0.317$$

$$h_1 = 0.009 \text{ in}; h_2 = h_3 = 0.0092 \text{ in}; h = 0.274 \text{ in.}$$

$$\xi = 0.034; m = 18; \text{ case 4a of Ref. 26}$$

Case-D3: A three-ply Glass/Epoxy laminate ($30^\circ/90^\circ/30^\circ$)

$$E_{11} = 5.42 \times 10^6 \text{ psi}; E_{22} = 2.6 \times 10^6 \text{ psi};$$

$$G_{12} = 0.687 \times 10^6 \text{ psi}; \nu_{12} = 0.365$$

$$h_1 = h_3 = 0.009 \text{ in.}, h_2 = 0.0093 \text{ in.}; h = 0.0273 \text{ in.}$$

$$\xi = 0.0304; m = 17; \text{ case 11a of Ref. 26.}$$

Note that all three configurations are asymmetric. Moreover, all data are taken from Ref. 26. In Ref. 26, the imperfection (axisymmetric) is given in the form of

$$w^0(x) = \xi h \cos \frac{qx}{R} \quad (32)$$

where the number q is given (Ref. 26). The imperfection expression is changed, herein, to be compatible with Eqs. (12).

The solution methodology described in Ref. 15 is employed to compute critical (limit point) loads which are then compared to the experimental results. This is easily done for the configurations for which the imperfection shape and amplitude are fully described.

For the geometries, for which no information concerning the imperfection is given, the comparison is more qualitative.

IV.3.2. Theoretical Results and Discussion

The theoretical predictions, based on the solution scheme of Ref. 15, and the comparison with the experimental results is discussed separately for each group of configurations.

Group A

Since no information is provided (for this group), concerning the amplitude and shape of imperfection, the comparison is expected to be more qualitative than quantitative. It is assumed that the shape of imperfection is almost axisymmetric and the amplitude of imperfection is varied

from a small fraction of the thickness to almost one thickness of the laminate.

$$w^0(x,y) = -\xi h \left(\cos \frac{2\pi x}{L} + 0.1 \sin \frac{\pi x}{L} \cos \frac{\pi y}{R} \right) \quad (28)$$

Note that $|w_{\max}| = 1.1 \xi h$, where h is the laminate thickness.

Both the theoretical and the experimental results are presented in tabular form (see Table 9).

On Table 9, the buckling load and the observed circumferential wave number are listed on columns two and three (data from Ref. 24). The next three columns contain theoretical results for three values of the imperfection amplitude parameter ξ . For case-A1, the comparison suggests that the maximum imperfection amplitude for the tested geometry might be larger than one laminate thickness. Note that when $\xi = 1$ ($w^0_{\max}/h = 1.1$) the theoretical load is 133.83 lbs/in.

For case A2, the comparison suggests, that the "tested geometry" maximum imperfection amplitude is (approximately) 0.9 h .

Finally, the comparison for the other two cases (A2 and A4) is much better, since it suggests that the maximum imperfection amplitude is 0.4 h . Again, it is stressed, that for this group the comparison is rather qualitative.

Group B

Only one geometry is taken from Ref. 25. According to this reference, the imperfection is axisymmetric and experimental results are reported for a combined application of uniform axial compression and torsion. Moreover, theoretical predictions are reported in Ref. 25, which are obtained by employing a solution scheme that assumes axisymmetric prebuckling behavior and finding bifurcation loads corresponding to asymmetric behavior.

TABLE 9. THEORETICAL AND EXPERIMENTAL RESULTS FOR GROUP A

Geometry	Experimental			Theoretical			
Case-	$\frac{-\ell}{N_{xx}}$	$\frac{\text{lbs.}}{\text{in.}}$	n wave No.	$\frac{-\ell}{N_{xx}}$	$\frac{\text{lbs.}}{\text{in.}}$	n wave No.	ξ :Imp. Amplitude
A1	120.56		10	151.19		12	0.3
				140.55		12	0.5
				133.83		12	1.0
A2	248.46		8	362.30		9	0.1
				294.54		9	0.5
				231.83		9	1.0
A3	802.99		-	945.78		9	0.1
				872.99		9	0.3
				792.91		9	0.5
A4	892.02		-	944.66		10	0.2
				895.38		10	0.3

The present results, along with the theoretical predictions of Ref. 25 and the experimental findings are presented graphically on Fig. 19. It is clearly seen from this figure that the agreement is very good.

Group C

For this particular group there is no information concerning the amplitude and shape of imperfection. It is important then, to employ some shape for the imperfection and vary the imperfection amplitude in order to accomplish some comparison (qualitative) with the experimental results (Ref. 21).

Because the loading consists of both axial compression and torsion, three imperfection shapes are initially employed. First, a virtually axisymmetric imperfection is used, which is characterized by Eq. (28).

The other two shapes, used for the imperfection, correspond to approximations of the linear theory (Ref. 15) buckling modes for positive and negative torsion.

In particular, one of the Appendices of Ref. 15 deals with solutions to the linearized buckling equations for the case of pure torsion. The Galerkin procedure is employed and the following approximate form, for the buckling mode, w^1 , is employed:

$$w^1(x,y) = \sum_{n=0}^N \sum_{m=1}^M \left(A_{mn} \cos \frac{n\pi y}{R} + B_{mn} \sin \frac{n\pi y}{R} \right) \times \quad (33)$$

$$\left[\frac{L}{m\pi} \sin \frac{m\pi x}{L} - \frac{L}{(m+2)\pi} \sin \frac{(m+2)\pi x}{L} \right]$$

Because of orthogonality only one n -value is needed. A ten-term approximation ($m = 5$) is obtained in Ref. 15. By studying the results it

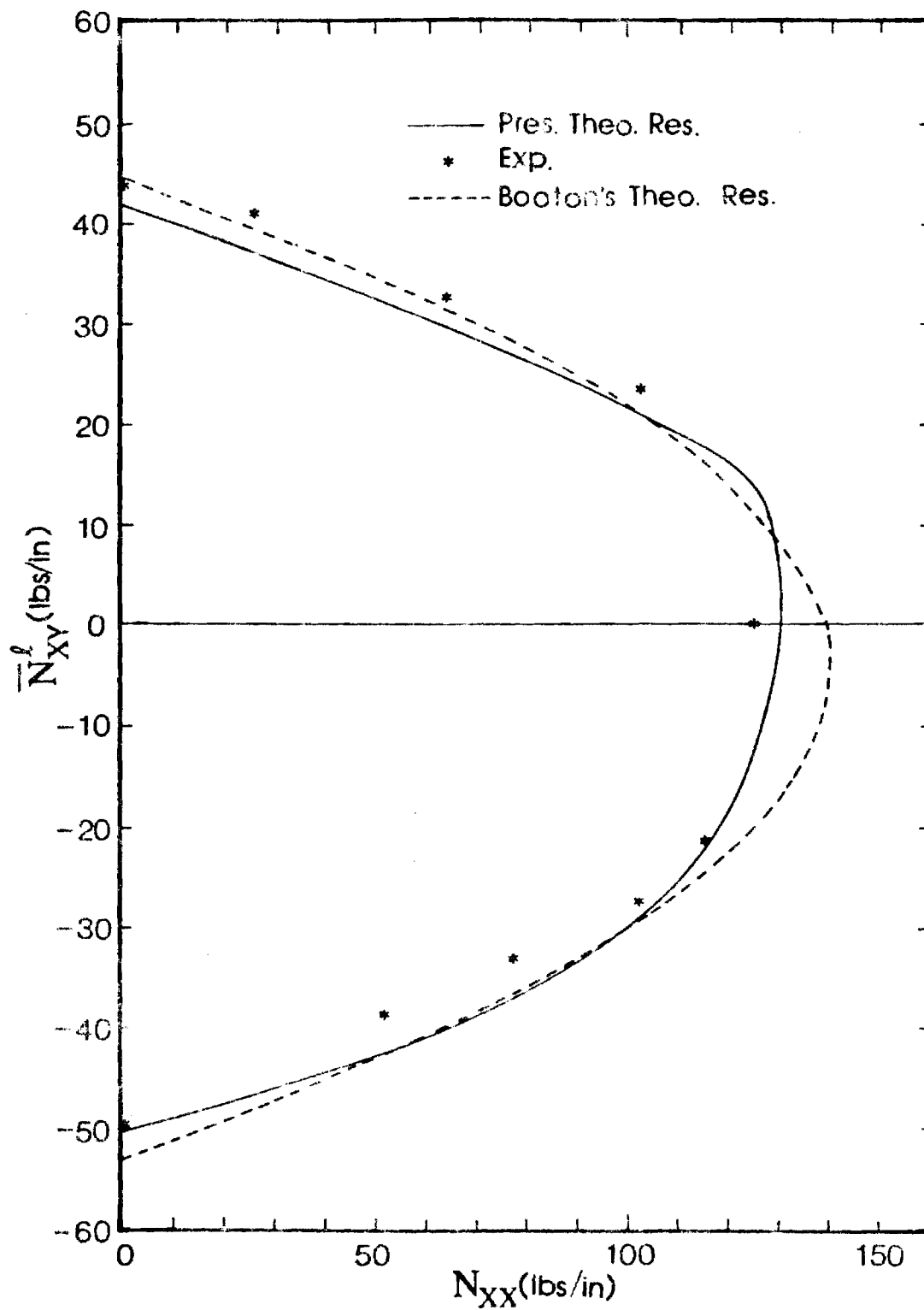


Fig. 19. Critical (Theoretical) and Buckling (Experimental) Loads for Group B

is observed that the linear theory buckling mode is well approximated by two terms. This is accomplished by normalizing all coefficients, in the ten-term approximation, with respect to B_{2n} . A comparison of the order of magnitude of these coefficients yields that all are negligibly small except two. Finally, these two remaining coefficients are adjusted such that the maximum amplitude is $\frac{3}{8}h$. Thus, one two-term approximation is used for positive torsion, $w^0(+)$, and one two-term approximation for negative torsion, $w^0(-)$. These expressions are (applicable to both configurations; cases C1 and C2).

$$w^0(+) = \frac{3}{8}h \left[0.537 \cos \frac{\pi y}{R} \left(\sin \frac{\pi x}{L} - \frac{1}{3} \sin \frac{3\pi x}{L} \right) - 0.671 \sin \frac{\pi y}{R} \left(\sin \frac{2\pi x}{L} - \frac{1}{2} \sin \frac{4\pi x}{L} \right) \right] \quad (34)$$

$$w^0(-) = \frac{3}{8}h \left[0.583 \cos \frac{\pi y}{R} \left(\sin \frac{\pi x}{L} - \frac{1}{3} \sin \frac{3\pi x}{L} \right) + 0.648 \sin \frac{\pi y}{R} \left(\sin \frac{2\pi x}{L} - \frac{1}{2} \sin \frac{4\pi x}{L} \right) \right] \quad (35)$$

Note that, for both expressions (by design)

$$w_{\max}^0 / h = \frac{3}{8} \quad (36)$$

The generated results for each configuration are presented (in part) both in graphical and tabular form. Each configuration is treated separately.

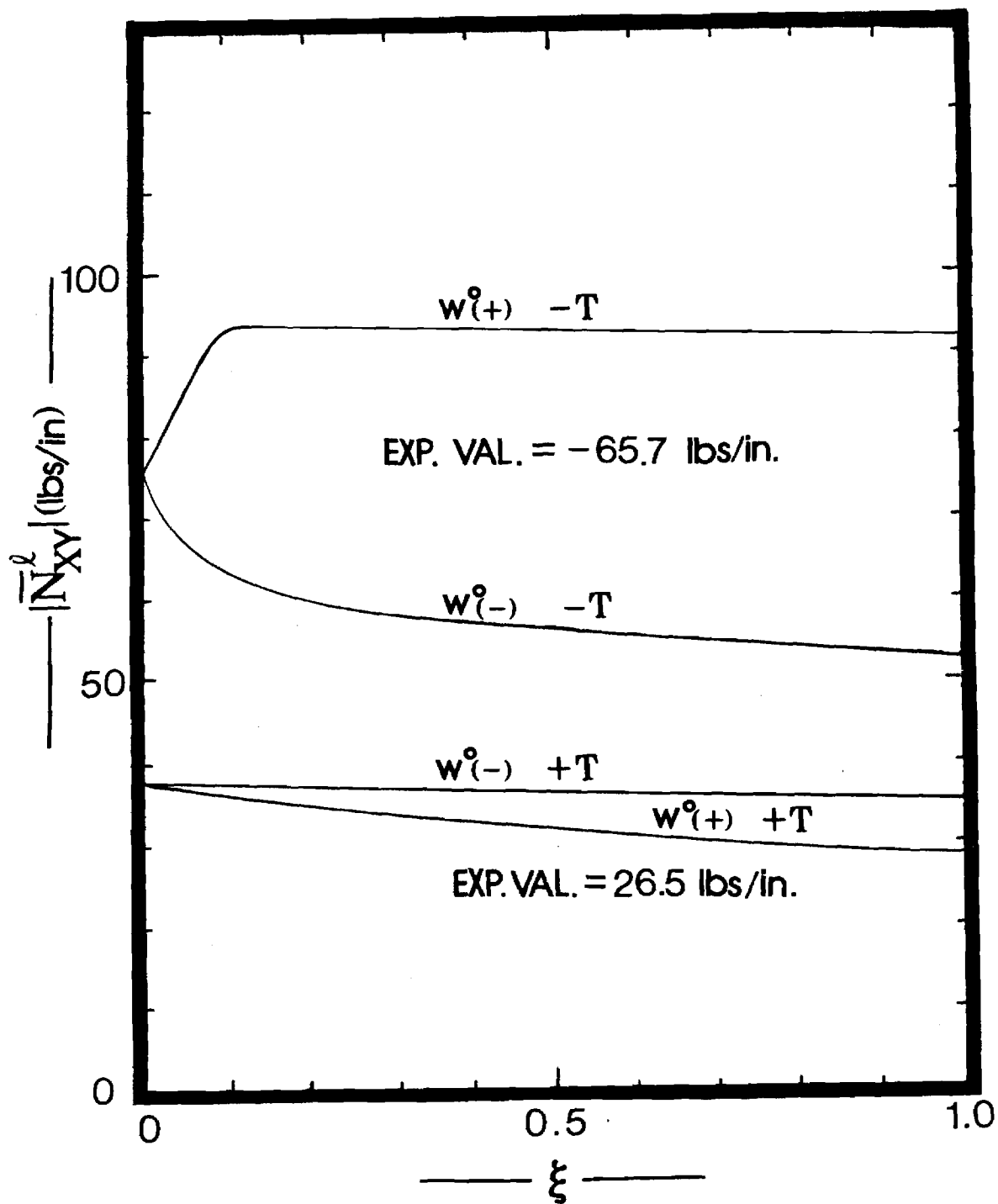


Fig. 20. $|N_{xy}|^l$ vs. ξ (Imp. Ampl. Parameter)

For Two Imp. Shapes [Eqs. (34) and (35)]

Case C-1: For the case of pure torsion, theoretical predictions are generated for the two imperfection shapes, Eqs. (34) and (35), and for positive and negative torsion for each shape. These theoretical predictions are shown as plots of the value of the critical (limit point) torsion $|\bar{N}_{xy}^{\ell}|$, versus the imperfection amplitude parameter, ξ , on Fig. 20. Note that as the imperfection amplitude approaches zero the results corresponding to the two shapes $w^0(+)$ and $w^0(-)$, approach the same value (as they should). Moreover, it is seen that the shape corresponding to Eq. (34) has a stabilizing effect for small values of ξ and for negative torsion.

The experimental values for positive and negative torsion are also listed on Fig. 20. Note that, for positive torsion the experimental value is 26.5 lbs/in, and the comparison with the theoretical result suggests that the imperfection amplitude is a little larger than one laminate thickness. On the other hand, for negative torsion, the experimental value is 65.7 lbs/in. and the comparison suggests that the imperfection amplitude is less than two tenths of the laminate thickness.

In addition, Ref. 21 provides experimentally obtained, buckling interaction curves (\bar{N}_{xx} vs \bar{N}_{xy}) for this geometry. Again since the imperfection is not known, theoretical interaction curves are obtained analytically for two shapes of imperfection. Eqs. (28) and (34) and various values for the imperfections amplitude parameter, ξ . This comparison is for positive torsion and the results are shown graphically on Figs. 21 and 22. The experimental data are shown by the dashed line.

For this case the comparison must be viewed as qualitative rather than quantitative.

Case - C2: For this six-ply symmetric laminate, a qualitative type of comparison is presented only for positive torsion. The results are, in part, presented graphically on Fig. 23 and in tabular form on Table 10.

Table 10 shows theoretical results obtained by the present analysis, for two imperfection amplitude parameter values ($\xi = 0.05$ and $\xi = 0.50$) and the shape characterized by Eq. (34). First, the critical values corresponding to individual application of the loads are obtained and then the interaction curve is completed by assigning values for the applied torsion and finding the corresponding critical (limit point) axial compression. Note that the assigned values for the torsion are smaller than the individually applied critical torsion.

TABLE 10. CRITICAL CONDITIONS FOR CASE - C2

$\xi = 0.05$	\bar{N}_{xx}^{ℓ} lbs/in.	442.6	348.1	232.3	70.32	0
	\bar{N}_{xy}^{ℓ} lbs/in.	0	20	40	60	76.4
	n	13	13	12	13	12
$\xi = 0.50$	\bar{N}_{xx}^{ℓ} lbs/in.	328.3	262.5	70.5	0	-
	\bar{N}_{xy}^{ℓ} lbs/in.	0	15	14	61.4	-
	n	12	14	12	12	

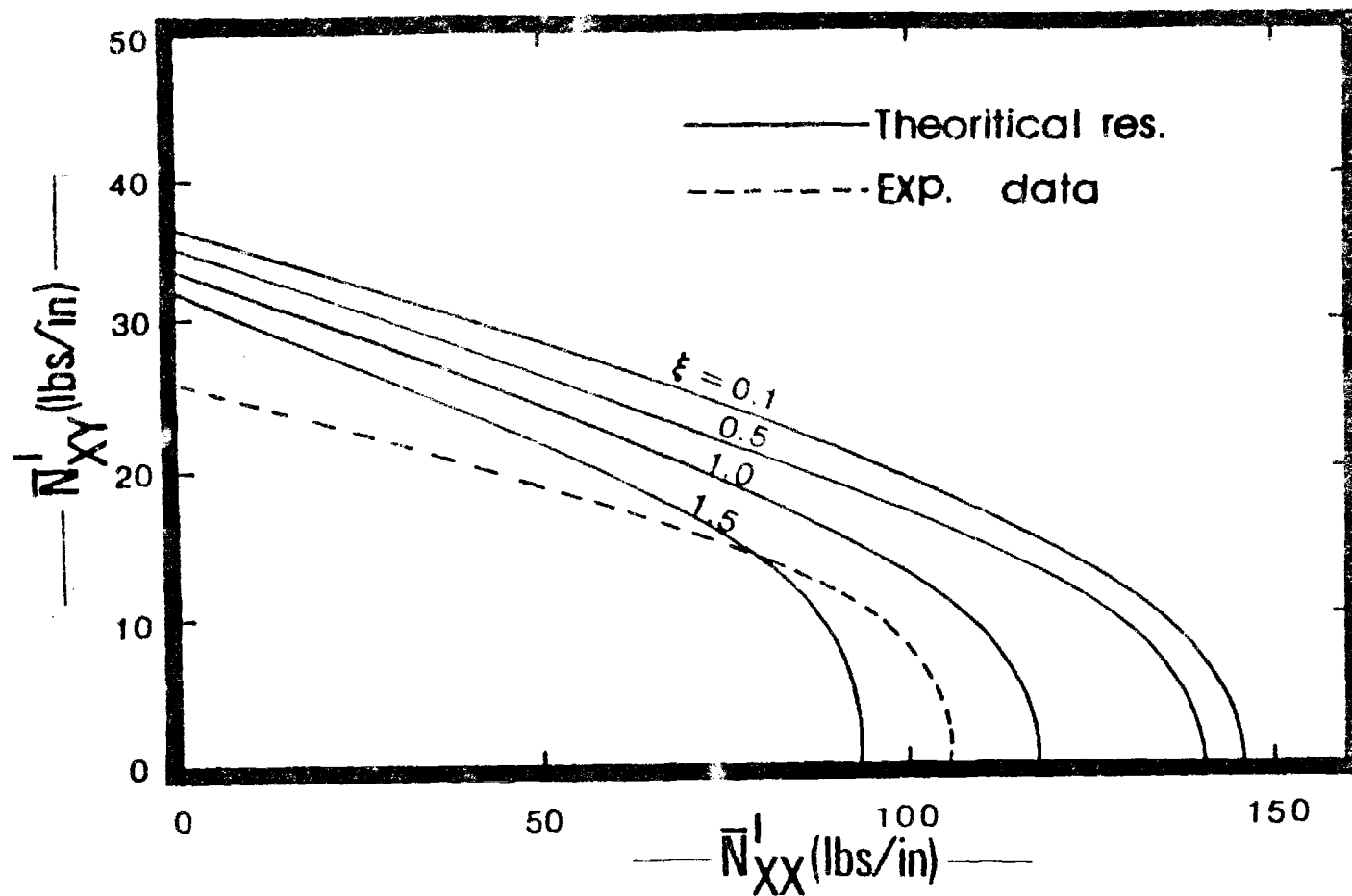


Fig. 21. Critical Interaction Curves
 [Geometry C1(I-1); Axisym. Imp. - Eq. (28)]

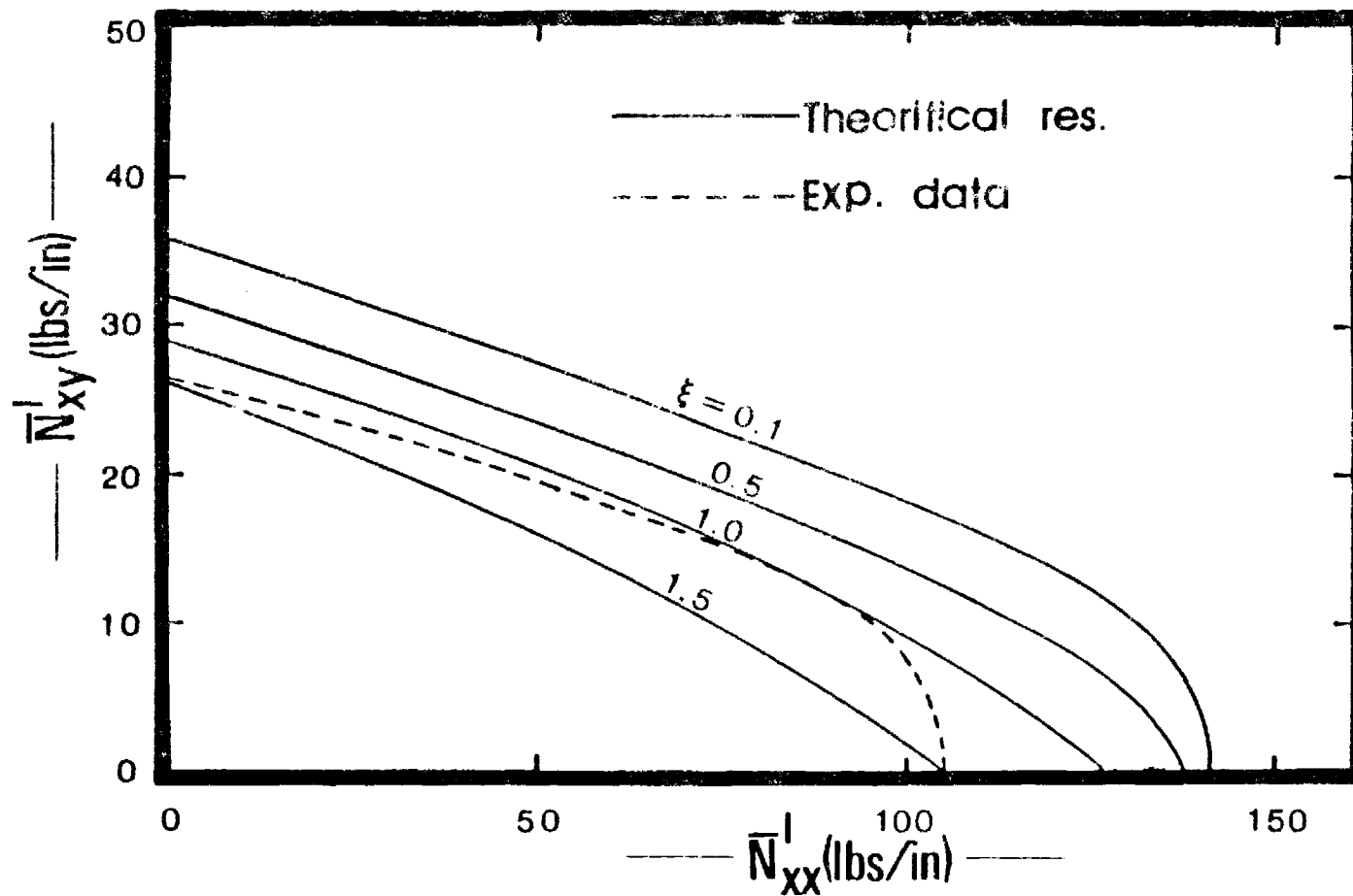


Fig. 22. Critical Interaction Curves
 [Geometry C1 (I-1); Imp. $w^0(+)$ - Eq. (34)]

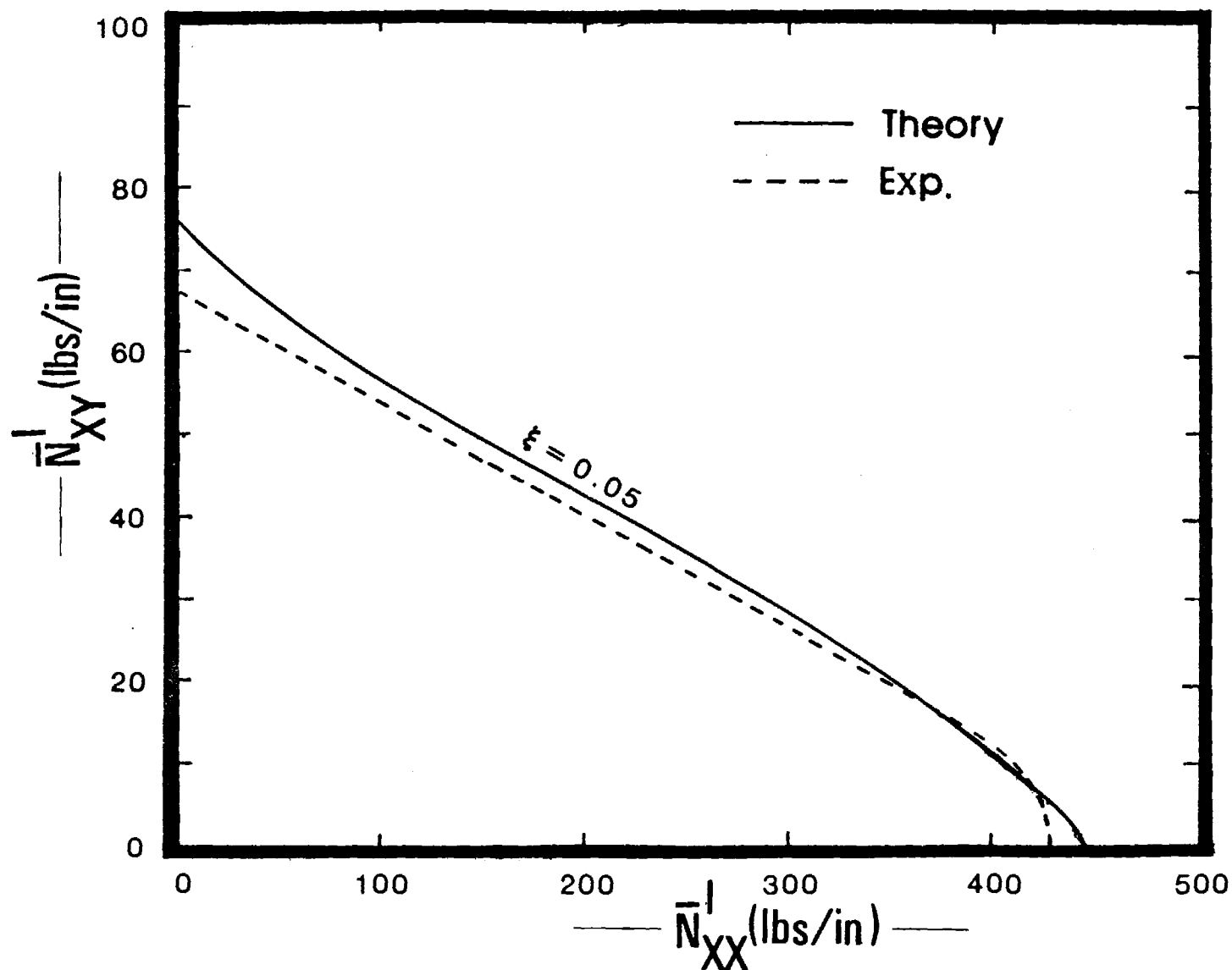


Fig. 23. Critical Interaction Curves

[Geometry C2 (II-1); Imp. $w^0(+)$ - Eq. (34)]

On Fig. 23 the experimental results of Ref. 21, and only the theoretical prediction corresponding to $\xi = 0.05$ are shown. The two curves seem to be very close for the entire range of interest. Thus, the comparison between experimental and theoretical interaction curves seems to be reasonable for this geometry.

Group D

There are several tests reported in Ref. 26. In all of these tests, the imperfection is axisymmetric and theoretical critical loads are reported in Ref. 26, which are obtained by employing a linearized bifurcation analysis. The present methodology is employed and a comparison is made through Table 11. In this table, the geometry, Ref. 26 results, and the present critical loads are listed.

For the first geometry (case-D1), the agreement between experiment (buckling load) and present theory (critical load) is excellent. The theoretical prediction of Ref. 26 is also very good. For the other two geometries (cases - D2 and D3) the agreement seems to be reasonably good (acceptable). For the same reason, the theoretical prediction of Ref. 26 may also be called reasonably good.

TABLE 11. A COMPARISON BETWEEN THEORY AND EXPERIMENT FOR GROUP D

Geometry Case-	Description of Geometry					Ref. 10 Results			Present Results	
	L in.	h in.	R/h	m	δ	Test No.	\bar{N}_{xx} (lbs/in)		$- \frac{\ell}{N_{xx}}$	$\frac{\text{lbs}}{\text{in. n}}$
D1	12.42	0.0270	232	18	0.0468	1a	148.9	153.2	151.2	11
D2	12.45	0.276	267	18	0.0340	4a	142.0	165.1	174.5	11
D3	12.43	0.0273	229	17	0.0304	11a	149.1	185.2	174.3	11

IV.4 Concluding Remarks

The comments of this section are only related to the work reported in Chapter IV.

The limited parametric studies, reported herein, suggest that, in order to resist uniform axial compression effectively, 0° -plies should be placed at the extreme plies of the laminate (I-4,5, II-1,4,5). Clearly the anti-symmetric $\pm 45^\circ$ layup yields a weak configuration for this load case. On the other hand for torsion, an asymmetric layup (of the type considered here, I-4,5 and II-4, 5) can be very efficient for torsion of a specified direction (say positive), but if the torsion is reversed, its efficiency is in doubt. The antisymmetric $\pm 45^\circ$ layup, though, seems to be efficient for torsion, which is expected to be acting in both directions (for different load conditions, of course). The symmetric layup (I-1 and II-1) seems to be the weaker configuration, for torsion (by comparison to all used herein.)

The comparison with experimental results seems to be rather good. When direct comparisons (quantitative) were possible (groups B and D) the agreement was good. The qualitative comparison can also be considered a success. These comparisons definitely increase one's confidence in the theoretical solution scheme.

CHAPTER V

CONCLUSIONS AND RECOMMENDATIONS

On the basis of the generated results and their assessment certain findings can be reported.

First, theoretical solutions schemes have been developed for analyzing the behavior of stiffened, laminated, thin cylindrical shells with initial geometric imperfections, various boundary conditions and subjected to static or suddenly applied destabilizing loads (eccentric and applied individually or in combination). Behavior includes the establishment of critical conditions and post-limit point response. This is true for the w, F -formulation which is based on Donnell-type of kinematic relations. With the u, v, w -formulation (regardless of the character of the kinematic relations) dynamic critical loads cannot be found, since the solution scheme was not carried to the post-limit point response (it was deemed unnecessary to do so, because it is very expensive in time and money and the expected benefits did not justify this extra effort).

Next, by comparing critical static loads obtained from two different sets of nonlinear kinematic relations (Donnell and Sanders) it is seen that for isotropic constructions or laminates with properties and layups that yield properties similar to isotropic construction ($B_{ij} = 0$ $A_{11} = A_{22}$, $D_{11} = D_{22}$, $A_{13} = A_{23} = D_{13} = D_{23} = 0$) the L/R ratio is the only influencing parameter. This means that the two results are virtually the same for small to moderate values of L/R ($L/R \leq 5$), but they differ by as much as 15% at large L/R values ($L/R \geq 10$).

For orthotropic construction the results are similar to the isotropic case, when the strong direction is along the cylinder axis (0° along

x-axis) but they start having significant differences, even for small L/R - values ($L/R \leq 2$), when the strong direction is in the hoop direction (y-axis). This conclusion is based on axial compression. No assessment is made for other load cases and/or other laminate layups ($\pm 45^\circ$ anti-symmetric, asymmetric etc).

It is important (and therefore recommended) to continue this study and (a) establish which design parameters affect the accuracy, when using Donnell-type of kinematic relations, and (b) establish limits or bounds on these parameters inside which the Donnell equations yield accurate results.

Moreover, even through the use of Donnell equations, more parametric studies are needed (of the type, reported in Chapter IV), in order to enhance our understanding of the buckling behavior of laminated shells, and therefore improve our capability of designing efficient laminated shells.

Finally, the comparison between theoretical predictions and experimentally obtained results serves to increase our confidence in the developed solution scheme. Thus, this solution methodology may confidently be used, especially in the preliminary design stage, because it allows a quick and an inexpensively obtained assessment of the effect of various design variables on the load carrying capacity of thin cylindrical shells (when subjected to destabilizing loads).

REFERENCES

1. Donnell, L. H., "Stability of Thin-walled Tubes under Torsion", National Advisory Committee for Aeronautics (NACA), TR-479, Washington, D.C., 1933.
2. Hoff, N. J., "The Accuracy of Donnell's Equations", Journal of Applied Mechanics, Vol. 22, No. 3, 1955, pp. 329-334.
3. Flugge, W., Static und Dynamik der Schalen, Julius Springer, Berlin, p. 118; or see Stresses in Shells, Springer-Verlag, Berlin, 1962.
4. Dym, C. L., "On the Buckling of Cylinders in Axial Compression", Journal of Applied Mechanics, Vol. 40, No. 2, 1973, pp. 565-568.
5. Koiter, W. T., "General Equations of Elastic Stability for Thin Shells", Muster D. ed., Proceedings, Symposium on the Theory of Shells, University of Houston, Houston, Texas, 1967.
6. Budiansky, B. "Notes on Nonlinear Shell Theory", Journal of Applied Mechanics, Vol. 35, No. 2, 1968, pp. 393-401.
7. Simitses, G. J. and Aswani, M., "Buckling of Thin Cylinders under Uniform Lateral Loading", Journal of Applied Mechanics, Vol. 41, no. 3, 1974, pp. 827-829.
8. Sanders, J. L., "Nonlinear Theories of Thin Shells", Quarterly of Applied Mathematics, Vol. 21, 1963, pp. 21-36.
9. Toda, S., "A Note on the Characteristic Roots for Donnell's Linear Buckling Equations", Proceedings of the National Congress for Applied Mechanics, Vol. 28, (November 1978), 1980 (published), pp. 21-31.
10. Koga, T., and Endo, S., "Comparison of Accuracies of Solutions of Linear Shell Theories for Closed Circular Cylinders under Edgewise Loading", Technical Report of National Aerospace Laboratory, Tokyo, NAL TR-SS2T, November, 1978.
11. Microys, H. F., and Schwaighofer, J., "Isotropic Cylindrical Shells under Line Load", Journal of the Engineering Mechanics Division, Proceedings of the American Society of Civil Engineers, Vol. 104, EM2, 1978, pp. 301-317.
12. Schaighofer, J., and Microys, H. F., "Orthotropic Cylindrical Shells under Line Load", Journal of Applied Mechanics, Vol. 46, No. 2, 1979, pp. 356-362.
13. Akeju, T. A. I., "Reduced Thin Shell Equations for Circular Cylinders", Journal of the Engineering Mechanics Division, Proceedings of the American Society of Civil Engineers, Vol. 1979, EMI, 1981, pp. 249-255.

14. El Naschie, M. S., and Hosni, A. F., "A Note on the Accuracy of the Nonlinear Shell Equations in the Postbuckling range", Zeitschrift für Angewandte Mathematik und Mechanik, Vol. 57, No. 11, 1977, pp. 673-674.
15. Simites, G. J., Sheinman, I., and Shaw, D. "Stability of Laminated Composite Shells Subjected to Uniform Axial Compression and Torsion" Interim Scientific Report to the Air Force Office of Scientific Research (Grant No. AFOSR 81-0227), AFOSR TR-82-XXXX, Georgia Institute of Technology, Atlanta, 1982.
16. Baruch, M., and Singer, J., "Effect of Eccentricity of Stiffeners on the General Instability of Stiffened Cylindrical Shells under Hydrostatic Pressure", Journal of Mechanical Engineering Science, Vol. 6, No. 1, 1963, pp. 23-27.
17. Sheinman, I., Shaw, D., and Simites, G. J., "Nonlinear Analysis of Axially-Loaded Laminated Cylindrical Shells", International Journal of Computers and Structures, Vol. 16, No. 1, 1983, pp. 131-137.
18. Jones, R. M., Mechanics of Composite Materials, McGraw-Hill Book Co., Inc., New York, 1975, p. 147.
19. Thurston, G. A., "Newton's Method Applied to Problems in Nonlinear Mechanics" Journal of Applied Mechanics, Vol. 32, 1965, pp. 383-388.
20. Sheinman, I., and Simites, G. J., "Buckling Analysis of Geometrically Imperfect, Stiffened Cylinders under Axial Compression", AIAA Journal, Vol. 15, 1977, pp. 374-382.
21. Wilkins, D. J., and Love, T. S., "Combined Compression Torsion Tests of Laminated Composite Cylindrical Shells", Proceedings of the AIAA/ASME/SAE 15th Structures, Structural Dynamics and Materials Conference, Las Vegas, April 1974, AIAA Paper No. 74-379.
22. Hoff, N. J., and Soong, T. C., "Buckling of Circular Cylindrical Shells in Axial Compression", International Journal of Mechanical Sciences, Vol. 7, 1965, pp. 489-496, (also Stanford University Department of Aeronautics and Astronautics, Report SUDAER No. 204, 1964).
23. Hess, T. E. "Stability of Orthotropic Cylindrical Shells Under Combined Loading" Am. Rocket Society Journal, Vol. 31, No. 2, Feb. 1961, pp. 237-246.
24. Kobayashi, S., Koyama, K., and Seko, H., "Compressive Buckling of Graphite-Epoxy Composite Circular Cylindrical Shells" (Abstract and Supplement of Abstract), Paper presented at the AIAA/ASME/ASCE/AHS 23rd Structures, Structural Dynamics, and Materials Conference, New Orleans May 1982; also private communications.
25. Booton, N., "Buckling of Imperfect Anisotropic Cylinders Under Combined Loading" UTIAS Report No. 203, University of Toronto, August 1976; also Proceedings of AIAA/ASME/ASCE/AHS Structures, Structural Dynamics and Materials Conference, Bethesda, Md.

26. Tennyson, R. C., and Muggeridge, D. B., "Buckling of Laminated Anisotropic Imperfect Circular Cylinders under Axial Compression" J. Spacecraft and Rockets, Vol. 10, No. 2, Feb. 1973, pp. 143-148.